
Why Does Risk Matter More in Recessions than in Expansions?

Discussion Paper no. [2021-11](#)**Martin M. Andreasen, Giovanni Caggiano, Efrem Castelnuovo and Giovanni Pellegrino****Abstract:**

This paper uses a nonlinear vector autoregression and a non-recursive identification strategy to show that an equal-sized uncertainty shock generates a larger contraction in real activity when growth is low (as in recessions) than when growth is high (as in expansions). An estimated New Keynesian model with recursive preferences and approximated to third order around its risky steady state replicates these state-dependent responses. The key mechanism behind this result is that firms display a stronger upward nominal pricing bias in recessions than in expansions, because recessions imply higher inflation volatility and higher marginal utility of consumption than expansions.

Keywords: New Keynesian Model, Nonlinear SVAR, Non-recursive identification, State-dependent uncertainty shock, Risky steady state.

JEL Classification: E32

Martin M. Andreasen: Aarhus University, CREATES, and the Danish Finance Institute. (email: mandreasen@econ.au.dk); Giovanni Caggiano: Monash University and University of Padova. (email: giovanni.caggiano@monash.edu); Efrem Castelnuovo: University of Padova. (email: efrem.castelnuovo@unipd.it); Giovanni Pellegrino: Aarhus University (email: gpellegrino@econ.au.dk).

Why Does Risk Matter More in Recessions than in Expansions?*

Martin M. Andreasen[†] Giovanni Caggiano[‡]

Efrem Castelnuovo[§] Giovanni Pellegrino[¶]

August 2021

Abstract

This paper uses a nonlinear vector autoregression and a non-recursive identification strategy to show that an equal-sized uncertainty shock generates a larger contraction in real activity when growth is low (as in recessions) than when growth is high (as in expansions). An estimated New Keynesian model with recursive preferences and approximated to third order around its risky steady state replicates these state-dependent responses. The key mechanism behind this result is that firms display a stronger upward nominal pricing bias in recessions than in expansions, because recessions imply higher inflation volatility and higher marginal utility of consumption than expansions.

Keywords: New Keynesian Model, Nonlinear SVAR, Non-recursive identification, State-dependent uncertainty shock, Risky steady state.

*We thank Guido Ascari, Nicholas Bloom, Ryan Chahrour, Chris Edmond, Andrea Ferrero, Pablo Guerron-Quintana, Tom Holden, Michel Juillard, Martin Kleim, Sydney Ludvigson, Elmar Mertens, Juan Rubio-Ramirez, Henning Weber and participants to many seminar and conference audiences for their comments. Andreasen and Pellegrino acknowledge funding from the Independent Research Fund Denmark, project number 7024-00020B. Caggiano and Castelnuovo acknowledge financial support by the Australian Research Council (respectively, DP190102802 and DP160102281). .

[†]Aarhus University, CREATES, and the Danish Finance Institute. Email: mandreasen@econ.au.dk.

[‡]Monash University and University of Padova. Email: giovanni.caggiano@monash.edu.

[§]University of Padova. Email: efrem.castelnuovo@unipd.it.

[¶]Aarhus University. Email: gpellegrino@econ.au.dk.

1 Introduction

The Great Recession and the recent COVID-19 pandemic have gone hand-in-hand with spectacular spikes in virtually all measures of US uncertainty (Bloom (2014), Barrero and Bloom (2020)). Following the seminal papers by Bloom (2009) and Fernández-Villaverde et al. (2011), numerous studies have investigated the importance of uncertainty shocks for the business cycle. This paper makes three contributions to this literature. First, using a nonlinear vector autoregressive (VAR) with a non-recursive identification strategy, we show that an equal-sized uncertainty shock generates a larger contraction in real activity when growth is low (as in recessions) than when growth is high (as in expansions). Second, we demonstrate that a dynamic stochastic general equilibrium (DSGE) model approximated to third order around its risky steady state is able to capture such state-dependent responses to an uncertainty shock. In contrast, any state-dependent effects of this shock are absent when using the deterministic steady state for the third-order approximation, as commonly done in the literature. Third, relying on this methodological contribution, we use an estimated New Keynesian model to examine the economic mechanisms behind our new VAR evidence. The results reveal that the traditional aggregate supply (AS) relation implies an upward nominal pricing bias for firms, as emphasized in Fernández-Villaverde et al. (2015), but that this bias is *state-dependent* and essential to understand the asymmetric responses to an uncertainty shock. As a result, our analysis delivers an empirically credible micro-founded model that can be used to study the role of monetary policy for addressing the state-dependent effects of uncertainty shocks across the business cycle.

Let us elaborate on our contributions. First, we estimate a nonlinear VAR using quarterly US data to assess whether an uncertainty shock has real effects that depend on the stance of the business cycle. To allow for potentially state-dependent effects to a shock, we extend the standard VAR by adding quadratic terms that involve the growth rate of real GDP and a proxy for financial uncertainty, which are both endogenous in the VAR. Uncertainty shocks are identified using a non-recursive strategy that combines event, correlation, and sign restrictions following the recent work of Antolín-Díaz and Rubio-Ramírez (2018) and Ludvigson et al. (2019). Our main empirical result is that an uncertainty shock of the same size generates a larger response of real activity during recessions than in expansions. This finding is in line with previous contributions on the nonlinear effects of uncertainty shocks (see, for instance, Caggiano et al. (2014), Alessandri and Mumtaz (2019), Cacciatore and Ravenna (2020)). Importantly, our empirical finding is based on a non-recursive identification strategy, and is therefore not subject to the critique in Ludvigson et al. (2019) of the standard recursive identification scheme

often used to identify exogenous variations in uncertainty.

Our second contribution is methodological and relates to the ability of nonlinear DSGE models to generate state-dependent effects of uncertainty shocks. These models are widely used in the literature to study the economic mechanisms behind the real effects of uncertainty shocks when solved by a third-order approximation around the deterministic steady state, as in Fernández-Villaverde et al. (2011), Born and Pfeifer (2014), Fernández-Villaverde et al. (2015), and Basu and Bundick (2017), among many others. This is a fruitful way to proceed to understand the effects of uncertainty shocks *on average*. However, it does not allow the researcher to investigate the potentially *state-dependent* effects of uncertainty shocks, because only the level of a given variable and terms that are linear in the states are risk-corrected in this approximation (Cacciatore and Ravenna (2020)). One way to address this shortcoming is to apply a fourth-order approximation around the deterministic steady state, because it also corrects terms that are quadratic in the states and hence allows for state-dependent effects of uncertainty shocks, as exploited in Cacciatore and Ravenna (2020) and Diercks et al. (2020). But going beyond a third-order approximation substantially increases the execution time and the memory requirement when solving DSGE models, which may limit the applicability of this solution when the desire is to formally estimate these models. We therefore propose a computationally less demanding alternative by simply moving the approximation point for the third-order approximation to the risky steady state.¹ This long-term equilibrium point is characterized by allowing agents to respond to uncertainty, whereas any effects of uncertainty is absent in the deterministic steady state. The appealing feature of this modification is that all linear *and* nonlinear terms in the approximation are adjusted for risk, enabling us to capture potentially different effects of uncertainty shocks in expansions and recessions. To ensure stability, we also provide a pruned version of this approximation and its closed-form solution for unconditional first and second moments as well as impulse response functions by using the results in Andreasen et al. (2018). Hence, our contribution makes it feasible to estimate nonlinear DSGE models with state-dependent effects of uncertainty shocks using techniques that are commonly applied in the literature.

Building on this methodological contribution, in the third part of the paper we work with a version of the New Keynesian model proposed by Basu and Bundick (2017) and refined in Basu and Bundick (2018) to understand why risk matters more in recessions than in expansions. Key features of this model are recursive preferences as in Epstein and Zin (1989), an uncertainty shock in the disturbance to the household's utility function, and nominal price stickiness as in Rotemberg (1982). We extend the model by consumption habits, the flexible formulation of recursive preferences in Andreasen and Jørgensen

¹Solutions around the risky steady state are discussed in Coeurdacier et al. (2011) for a first-order approximation and in de Groot (2013) for approximations up to second order. However, the methods adopted in these papers to compute approximations around the risky steady state differ from the approach applied in the present paper.

(2020), and cost-push shocks. This model is then estimated by matching stylized unconditional moments jointly with our nonlinear VAR impulse response functions to an uncertainty shock in both recessions and expansions. The estimation results show that this New Keynesian model goes a long way in reproducing the different responses to uncertainty shocks in expansions and recessions. Crucially, these differences in the impulse response functions arise from different initial conditions as captured by different values of the states, which through the model’s endogenous propagation mechanisms make uncertainty shocks more severe in recessions than in expansions. In other words, we do not rely on any form of occasionally binding constraints as in Cacciatore and Ravenna (2020) or an unanticipated switch in the structural parameters attached to different subsamples to generate asymmetric responses to uncertainty shocks. A further investigation of the model reveals that these asymmetries are primarily generated by the nonlinear terms in the aggregate supply (or Phillips) curve that lead firms to set higher nominal prices than what would be optimal without uncertainty. Hence, our results show that in response to an uncertainty shock firms bias their prices upward relatively more in recessions than in expansions, and therefore display a *state-contingent upward nominal pricing bias*. To understand this effect, recall that firms can reset their prices in every period with sticky prices as in Rotemberg (1982) but they face costs when doing so. In this setting, the conditional volatility of inflation affects the current price, because it is optimal for firms to set higher prices after an uncertainty shock to avoid large expensive future increases in prices. That is, firms simply smooth out their pricing bias. Two effects help to make this pricing bias stronger in recessions than expansions. First, inflation volatility is higher in recessions than in expansions. Second, firms discount future profits by the consumption-based stochastic discount factor, which has a higher level in recessions than in expansions due to lower consumption and higher marginal utility when growth is low. This implies that firms assign more weight to future profits in recessions, which also help to increase their pricing bias. We finally show that this explanation of a state-contingent upward nominal pricing bias is consistent with evidence for firms’ price markup, which increases by more in recessions than in expansions following an uncertainty shock.

The rest of this paper is organized as follows. Section 2 provides VAR evidence on the effects of uncertainty shocks, while Section 3 presents an otherwise standard New Keynesian model with recursive preferences. The proposed model solution is described in Section 4, and we discuss our empirical findings for the New Keynesian model in Section 5. Section 6 investigates the key mechanism behind the state-dependent effects of uncertainty shocks. Concluding comments are provided in Section 7.

2 VAR Evidence

This section presents our reduced-form evidence for state-dependent effects of an uncertainty shock. We introduce a nonlinear VAR in Section 2.1, discuss identification in Section 2.2, and present the impulse responses in Section 2.3. Various robustness checks are discussed in Section 2.4, while Section 2.5 presents a simulation study that validates the applied estimation method.

2.1 An Interacted VAR

We consider the vector of macro variables $\mathbf{Y}_t = [\log VXO_t, \log GDP_t, \log C_t, \log I_t, \log H_t, \log P_t, R_t]'$ of dimension $n \times 1$, where VXO_t is the implied volatility index in the stock market (the S&P 100), GDP_t is output, C_t is consumption, I_t is investment, H_t is hours worked, P_t is the price level, and R_t is the policy rate.² The vector \mathbf{Y}_t evolves as specified by the following interacted VAR (IVAR)

$$\mathbf{Y}_t = \boldsymbol{\alpha} + \sum_{j=1}^L \mathbf{A}_j \mathbf{Y}_{t-j} + \sum_{j=1}^L \mathbf{c}_j \log VXO_{t-j} \times \Delta \log GDP_{t-j} + \boldsymbol{\eta}_t, \quad (1)$$

where $\boldsymbol{\alpha}$ and \mathbf{c}_j have dimension $n \times 1$, \mathbf{A}_j has dimension $n \times n$, and the $n \times 1$ vector of residuals $\boldsymbol{\eta}_t \sim \mathcal{IID}(\mathbf{0}, \boldsymbol{\Omega})$. Unlike linear VARs, our IVAR includes the quadratic terms $\log VXO_{t-j} \times \Delta \log GDP_{t-j}$ to capture potentially state-contingent effects of higher uncertainty for various levels of the growth rate in GDP, i.e., $\Delta \log GDP_t \equiv \log(GDP_t/GDP_{t-1})$. We estimate this IVAR with four lags by OLS using quarterly US data from 1962Q3 to 2017Q4.³ Given that the VXO is unavailable before 1986, we follow Bloom (2009) and combine the VXO by the monthly volatility of daily returns in the S&P 500 before 1986. Our sample includes the zero lower bound for the monetary policy rate from 2008Q4 to 2015Q4. Hence, we replace the federal funds rate in this period by the shadow rate of Wu and Xia (2016) to account for unconventional monetary policy. The estimation results clearly favor our IVAR specification against a linear VAR, as we reject the joint null hypothesis of $\mathbf{c}_j = \mathbf{0}$ for $j = \{1, 2, 3, 4\}$ with a likelihood ratio test statistics of 62.0, implying a p -value of 0.0002 in the χ^2_{28} -distribution. Table 1 reports stylized unconditional moments for the growth rates of the four variables in the VAR and IVAR that are related to economic activity. Both models match the empirical means and standard deviations, and hence show no sign of overfitting. We also see that the IVAR is marginally

²The definition of these variables follows the one used by Basu and Bundick (2017) for their VAR.

³Alternatives to the IVAR include the nonlinear factor model in Guerron-Quintana et al. (2021) and the quadratic autoregression in Aruoba et al. (2017) that both are motivated from a second-order pruned perturbation approximation. We prefer the IVAR because it is computationally easier to estimate than the factor model in Guerron-Quintana et al. (2021), which requires the use of a particle filter. To our knowledge, the quadratic autoregression in Aruoba et al. (2017) is currently only developed for univariate time series.

better at generating negative skewness and excess kurtosis than the linear VAR. Thus, the presence of nonlinear terms allow the IVAR to better capture higher order moments of the empirical distribution than implied by the linear VAR.

Table 1: VARs: Unconditional Moments for Economic Activity

This table reports unconditional moments for the growth rate in output, consumption, investment, and hours worked using US data from 1962Q3 to 2017Q4. The corresponding moments in the linear VAR and the IVAR are obtained from 500 simulated time series of the same length as in the empirical sample.

	Data				Linear VAR				IVAR			
	Mean	Std.	Skew.	Kurt.	Mean	Std.	Skew.	Kurt.	Mean	Std.	Skew.	Kurt.
Growth rates:												
Output	0.39	0.81	-0.36	4.75	0.38	0.81	-0.004	3.23	0.38	0.81	-0.02	3.30
Consumption	0.40	0.46	-0.27	4.01	0.39	0.45	-0.09	3.20	0.39	0.45	-0.13	3.20
Investment	0.69	2.06	-1.15	6.70	0.63	2.07	-0.13	3.52	0.64	2.00	-0.26	3.73
Hours worked	0.04	0.66	-0.92	5.18	0.04	0.66	-0.02	3.10	0.04	0.63	-0.26	3.50

2.2 Uncertainty Shocks: Identification Strategy

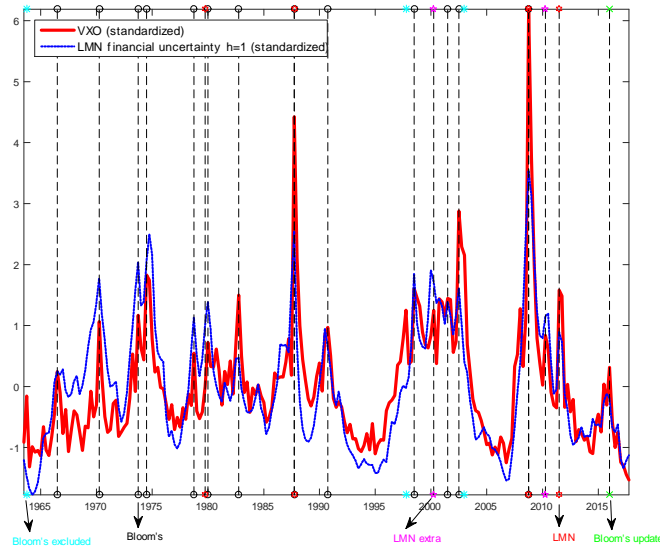
Following Bloom (2009), many contributions in the literature have identified uncertainty shocks by imposing zero-restrictions either on the impact of macroeconomic shocks on uncertainty or on the impact of uncertainty shocks on the business cycle. However, this recursive identification strategy has recently been questioned by Ludvigson et al. (2019), who find a non-zero contemporaneous correlation between uncertainty and the business cycle. We therefore follow Ludvigson et al. (2019) and use a combination of event restrictions and constraints from external variables, which we supplement with sign restrictions to obtain a robust non-recursive identification of uncertainty shocks. To present this alternative, let \mathbf{e}_t denote the structural shocks with zero mean and covariance matrix \mathbf{I}_n . The mapping between the reduced-form residuals $\boldsymbol{\eta}_t$ and the structural shocks \mathbf{e}_t in the IVAR is $\boldsymbol{\eta}_t = \mathbf{B}\mathbf{e}_t$, where $\mathbf{B} = \mathbf{P}\mathbf{Q}$ is of dimension $n \times n$, \mathbf{P} is a lower-triangular Cholesky factor of $\boldsymbol{\Omega}$ with non-negative diagonal elements, and \mathbf{Q} is any orthonormal rotation matrix (i.e., $\mathbf{Q}\mathbf{Q}' = \mathbf{I}_n$) that implies positive diagonal elements of \mathbf{B} . Let \mathcal{B} denote the set that contains the infinitely many solutions of \mathbf{B} that satisfy the $n(n+1)/2$ restrictions implied by the covariance matrix, i.e., $\boldsymbol{\Omega} = \mathbf{B}\mathbf{B}'$. Given that not all of these mathematically acceptable solutions are interesting from an economic standpoint, we impose restrictions to get the subset of economically admissible solutions.⁴

⁴The set \mathcal{B} is constructed using the algorithm in Rubio-Ramírez et al. (2010). First, we initialize \mathbf{B} to be the unique lower-triangular Cholesky factor \mathbf{P} . Then, we rotate \mathbf{B} by drawing $K = 500,000$ random orthogonal matrices \mathbf{Q} . Each rotation is performed by drawing an $n \times n$ matrix \mathbf{M} from a $\mathcal{N}(0, \mathbf{I}_n)$ density. Then, \mathbf{Q} is taken to be the orthonormal matrix in the \mathbf{QR} decomposition of \mathbf{M} . Let $\mathbf{e}_t(\mathbf{B}) =$

The first set of restrictions we impose relate to specific events or narratives following the work of Antolín-Díaz and Rubio-Ramírez (2018) and Ludvigson et al. (2019). In particular, we consider the dates located by Bloom (2009) that coincide with spikes in the financial uncertainty proxy of Ludvigson et al. (2019).⁵ In addition, we also include the events emphasized in Ludvigson et al. (2019) as well as 2000Q2 (collapse of the dot-com bubble) and 2010Q2 (Euro area debt crisis and fears about a global slowdown) with clear spikes in the financial uncertainty proxy of Ludvigson et al. (2019). At each of the dates, we require that realized uncertainty shocks $e_{unc,t}$ exceed their 50th percentile $p(e_{unc,t}, 50)$ across all unconstrained solutions in \mathcal{B} , except on 1987Q4 (Black Monday) and 2008Q4 (collapse of Lehman Brothers) where the uncertainty shock should exceed its 75th percentile as in Ludvigson et al. (2019). The selected dates with spikes in financial uncertainty are plotted in Figure 1.

Figure 1: Spikes in Financial Uncertainty

The red line denotes financial volatility according to the VXO since 1986, and the realized volatility in the S&P 500 before 1986 as in Bloom (2009). The blue line is the measure of financial uncertainty in Ludvigson et al. (2019) for a forecast horizon of one month. Vertical black lines denote the events that are used to identify uncertainty shocks as reported in Table 2.



Our second set of restrictions impose two external constraints on $e_{unc,t}$ following the work of Ludvigson et al. (2019). The first requirement is that the correlation between $e_{unc,t}$ and the stock market return R_t^m must be lower than the median value of this correlation

$\overline{B_t^{-1}\eta_t}$ be the shocks implied by $\mathbf{B} \in \mathcal{B}$ for a given η_t . Then, K different matrices \mathbf{B} imply K different unconstrained shocks $e_t(\mathbf{B}) = \mathbf{B}^{-1}\eta_t$, $t = 1, \dots, T$.

⁵When examining the recent peaks in the VXO, we identify one in 2016Q1, which we also include. Several uncertainty-triggering events occurred right before or during this quarter, e.g., the first increase of the federal funds rate that ended the zero lower bound phase after seven years; fears about China's economic fragility; the policy rate in Japan became negative; and the announcement in February 2016 by the British Prime Minister David Cameron of the Brexit referendum in June that year.

across all unconstrained solutions in \mathcal{B} . In our case, this implies that the correlation between R_t^m and $e_{unc,t}$ must be less than or equal to -0.15 , which is a stronger requirement than imposed in Ludvigson et al. (2019). The motivation for this assumption is the well-known leverage effect, which implies that a negative shock to the stock market (that reduces R_t^m) make firms more leveraged and hence more risky. The second constraint requires that the correlation between $e_{unc,t}$ and the growth rate in the real gold price Δg_t must be higher than the median value of this correlation across all unconstrained solutions in \mathcal{B} . In our case, this means that the correlation between Δg_t and $e_{unc,t}$ must be bigger than or equal to 0.03 , which also is slightly more restrictive than in Ludvigson et al. (2019). The theoretical justification for this constraint is that gold operates as a safe asset among investors, and its price should therefore be positively correlated with uncertainty shocks due to higher demand.

To further sharpen the identification, we require a non-positive response of GDP, investment, consumption, and hours on impact following a positive uncertainty shock, which is consistent with a large number of theoretical and empirical investigations of uncertainty shocks (see, e.g., Bloom (2014) for a survey). As shown in the Online Appendix, these sign restrictions only help to narrow the identified set but have hardly any effect on the median target of the identified set, which we will focus on in our subsequent analysis. For completeness, all the identification restrictions are summarized in Table 2.

2.3 Impulse Response Functions

We quantify the business cycle effects of uncertainty shocks by computing generalized impulse response functions (GIRFs) that account for the nonlinearities introduced by the term $\log VXO_{t-j} \times \Delta \log GDP_{t-j}$ in the IVAR (Koop et al. (1996)). The GIRFs for \mathbf{Y}_t at horizon h to an uncertainty shock of size δ_{unc} in period t is defined as

$$GIRF_{\mathbf{Y}}(h, \delta_{unc}, \boldsymbol{\varpi}_{t-1}) \equiv \mathbb{E}[\mathbf{Y}_{t+h} | \delta_{unc}, \boldsymbol{\varpi}_{t-1}] - \mathbb{E}[\mathbf{Y}_{t+h} | \boldsymbol{\varpi}_{t-1}]. \quad (2)$$

These impulse responses depend on the state of the economy, which is captured by the initial conditions $\boldsymbol{\varpi}_{t-1} \equiv \{\mathbf{Y}_{t-1}, \dots, \mathbf{Y}_{t-L}\}$. We are interested in exploring the effects of an uncertainty shock across the business cycle, and we therefore compute GIRFs when the initial condition for real GDP growth is below its 10th percentile (i.e., deep recessions) and above its 90th percentile (i.e., strong expansions). The results are reported in the left column in Figure 2, which shows the responses for the the median target (MT) model \mathbf{B}_{MT} , which is the solution in \mathcal{B} that delivers the GIRFs with the smallest distance to the median of the impulse responses in the identified set (see Fry and Pagan (2011)). For a positive one-standard deviation uncertainty shock ($\delta_{unc} = 1$), we find the familiar drop in real activity for several quarters after the shock in both recessions and expansions. However, the key focus of the present paper is the finding that this drop in activity

Table 2: Identifying Restrictions for Uncertainty Shocks

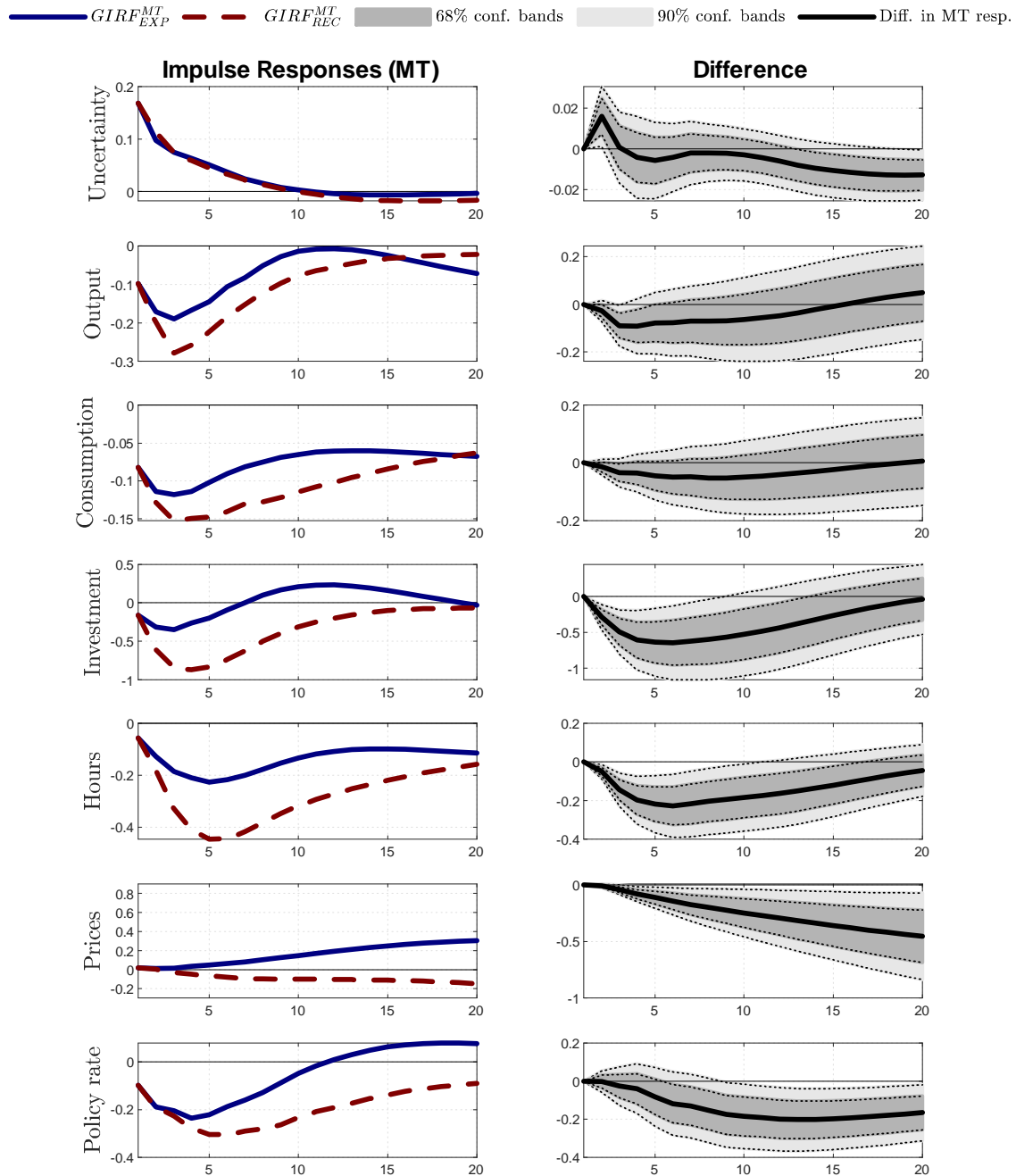
This table summarizes the identifying assumptions for uncertainty shocks in the IVAR. For event restrictions, the notation $\geq p(e_{unc,t}, 50^{th})$ indicates that the uncertainty shock at a given date should exceed the 50th percentile of its distribution. The sources for each of these event constraints are from Bloom (2009) and Ludvigson et al. (2019) (LMN). Excluded dates from Bloom (2009) are 1963Q4 (Assassination of JFK), 1997Q4 (Asian crisis), and 2003Q1 (Iraq invasion).

	Conditions on $e_{unc,t}$	Source
<i>Event Restrictions</i>		
1966Q3: Vietnam buildup	$\geq p(e_{unc,t}, 50^{th})$	Bloom
1970Q2: Cambodia and Kent state	$\geq p(e_{unc,t}, 50^{th})$	Bloom
1973Q4: OPEC I, Arab-Israeli War	$\geq p(e_{unc,t}, 50^{th})$	Bloom
1974Q3: Franklin National	$\geq p(e_{unc,t}, 50^{th})$	Bloom
1978Q4: OPEC II	$\geq p(e_{unc,t}, 50^{th})$	Bloom
1979Q4: Volcker experiment	$\geq p(e_{unc,t}, 50^{th})$	LMN
1980Q1: Afghanistan, Iran hostages	$\geq p(e_{unc,t}, 50^{th})$	Bloom
1982Q4: Monetary policy turning point	$\geq p(e_{unc,t}, 50^{th})$	Bloom
1987Q4: Black Monday	$\geq p(e_{unc,t}, 75^{th})$	Bloom & LMN
1990Q4: Gulf War I	$\geq p(e_{unc,t}, 50^{th})$	Bloom
1998Q3: Russian, LTCM default	$\geq p(e_{unc,t}, 50^{th})$	Bloom
2000Q2: Collapse of the tech bubble	$\geq p(e_{unc,t}, 50^{th})$	LMN extra
2001Q3: 9/11 terrorist attacks	$\geq p(e_{unc,t}, 50^{th})$	Bloom
2002Q3: Worldcom, Enron	$\geq p(e_{unc,t}, 50^{th})$	Bloom
2008Q4: Great recession	$\geq p(e_{unc,t}, 75^{th})$	Bloom & LMN
2010Q2: European debt crisis	$\geq p(e_{unc,t}, 50^{th})$	LMN extra
2011Q3: Debt ceiling crisis	$\geq p(e_{unc,t}, 50^{th})$	LMN
2016Q1: FFR liftoff and China	$\geq p(e_{unc,t}, 50^{th})$	Bloom (update)
<i>External Restrictions</i>		
Stock market return, r_t^m	$\leq p(\text{corr}(e_{unc,t}, r_t^m), 50^{th})$	LMN
Real log difference price of gold, Δg_t	$\geq p(\text{corr}(e_{unc,t}, \Delta g_t), 50^{th})$	LMN
<i>Sign Restrictions on Impact</i>		
GDP	< 0	
Investment	< 0	
Consumption	< 0	
Hours	< 0	

is *larger* and *more persistent* in deep recessions (the red dotted lines) than in strong expansions (the blue lines) although the size of the uncertainty shock is the same. For instance, in recessions the peak responses of output, investment, and hours are -0.28%, -0.87%, and -0.45%, respectively, whereas the corresponding responses in expansions are only -0.19%, -0.35%, and -0.23%. Turning to the nominal side, the responses for prices are slightly positive in expansions and slightly negative in recessions. For the monetary policy rate, we find a clear negative effect of an uncertainty shock, with effects that are stronger in recessions than in expansions.

Figure 2: Nonlinear VAR: Impulse Responses to an Uncertainty Shock

The charts to the left show the median target responses in the IVAR in deep recessions and strong expansions following a positive one-standard deviation uncertainty shock. The charts to the right show the difference between these responses in (deep recessions minus strong expansions) in addition to the 68 and 90 percent confidence interval, which are estimated by a residual-based bootstrap (with 1,000 draws) when conditioning on the median target responses. All responses are shown in percentage deviations, except for the policy rate where changes in percentage points are reported.



The charts to the right in Figure 2 report the distance between the MT responses in recessions relative to the MT responses in expansions, where the shaded gray and

light gray areas report the bootstrapped 68% and 90% confidence intervals, respectively.⁶ These confidence intervals reveal that the different responses in expansions and recessions in general are significant at the 68% level, and for investment, hours, prices, and the policy rate we even have significance at the 90% level.

2.4 Robustness Analysis

In the Online Appendix, we show that our new result is robust to the following modifications and extensions of the IVAR presented above: i) re-estimating the IVAR using data from 1987Q1 to 2017Q4 to only use the official VXO measure and to exclude the Great Inflation period; ii) replacing the shadow rate of Wu and Xia (2016) by the federal funds rate throughout the sample and adding the 10-year Treasury zero-coupon yield to capture effects of quantitative easing and forward guidance; iii) adding a series for realized skewness in the S&P500 to control for skewness shocks as discussed in Salgado et al. (2019); iv) use the purchasing managers index instead of real GDP growth for the interactive term in the IVAR; v) controlling for first-moment financial shocks by including the credit spread between BAA and AAA yields for bonds with more than 20 years to maturity; and vi) defining the expansionary state as episodes where real GDP growth is above its 10th percentile (i.e., outside deep recessions).

2.5 Simulation Evidence

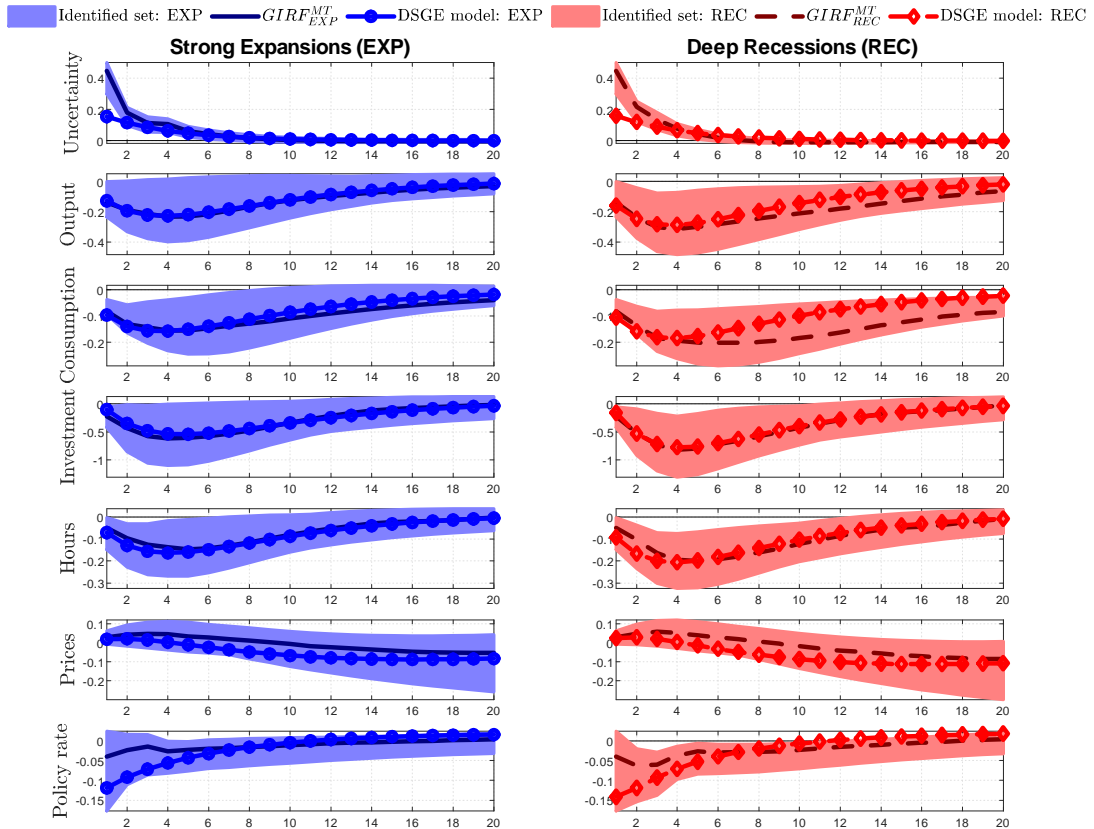
Before proceeding, it is important to test the ability of the IVAR and the non-recursive identification scheme to estimate the effects of uncertainty shocks and capture any state-dependence in these responses. We therefore simulate $\{\mathbf{Y}_t\}_{t=1}^S$ from the DSGE model presented below and estimate the IVAR on this sample using a relatively high value of $S = 3,000$ to sidestep issues related to sampling uncertainty. The adopted identifying assumptions for uncertainty shocks on this simulated sample are similar to those presented above, except for two minor modifications. First, when working with historical data, we locate extreme observations for volatility as periods when spikes in the VXO (i.e., the conditional volatility of the stock market return R_t^m) coincide with spikes in the financial uncertainty proxy of Ludvigson et al. (2019), which is an estimated stochastic volatility process extracted from a rich panel of financial variables. This volatility proxy is not available in our simulated sample, and we therefore replace it by the stochastic volatility process in the DSGE model. This implies that extreme observations for volatility in our

⁶There are two reasons to focus on a single model instead of the entire identified set. First, our goal is to estimate a DSGE model by matching impulse responses and we therefore have to focus on a single set of responses from the IVAR. Second, the confidence bands for the GIRFs can be computed by a standard bootstrap algorithm when focusing on a single model. However, in our Online Appendix, we show that for *all* models belonging to the set \mathcal{B} , the response of real activity to an uncertainty shock is stronger in recessions than in expansions.

simulated sample are episodes when the conditional volatility of R^m and the stochastic volatility shocks both are high and exceed their 50th percentile across all unconstrained solutions in \mathcal{B} . Second, the DSGE model presented below does not include a gold price, and we are therefore unable to include the correlation restriction between the real gold price and uncertainty shocks in the simulation study.

Figure 3: Simulation Exercise for the IVAR: IRFs to an Uncertainty Shock

This figure shows the generalized impulse response functions (GIRFs) in the IVAR to a positive one-standard deviation shock to uncertainty in strong expansions (to the left) and deep recessions (to the right) on a simulated sample of 3,000 draws from the New Keynesian DSGE model using the estimates in column (1) of Table 4. The solid (dashed) lines report the median target impulse responses in strong expansions (deep recessions) when computed as suggested by Fry and Pagan (2011), while the identified sets in the IVAR are denoted by the shaded areas. The marked solid lines denote the true responses in the DSGE model. All responses are shown in percentage deviations, except for the policy rate where changes in percentage points are reported.



The results from this simulation exercise are summarized in Figure 3. Very encouragingly, we find that the identified set for uncertainty shocks in the IVAR (denoted by the shaded areas) nearly always contains the true responses in the DSGE model.⁷ A careful

⁷The exception is for the responses in uncertainty (i.e. VXO), which exceed the true responses in the first couple of periods after the uncertainty shock. Unreported results show that this upward bias is closely

inspection of Figure 3 also shows that the IVAR is able to generate state-dependent effects in the responses, and that they match those in the DSGE model. This is especially the case for investment and hours, where we see large differences between recessions and expansions.⁸

We draw two conclusions from this simulation exercise. First, the non-recursive identifying scheme in the IVAR is sufficiently flexible to capture the responses of uncertainty shocks in our DSGE model. Second, any state-dependence in the responses to uncertainty shocks are well captured by the IVAR in (1). Thus, an important econometric implication of this simulation exercise is that the GIRFs from the IVAR can be used for a direct inference approach when estimating our DSGE model.

3 A New Keynesian Model

This section presents a New Keynesian DSGE model to explain why uncertainty shocks have larger effects in recessions than in expansions. Our starting point is the model by Basu and Bundick (2017) and its refinement in Basu and Bundick (2018). We extend this model along three dimensions. First, external consumption habits are included to capture a hump-shaped response in consumption to an uncertainty shock. Second, the flexible formulation of recursive preferences in Andreasen and Jørgensen (2020) is adopted to keep risk aversion at a low and plausible level. Finally, standard cost-push shocks are introduced to match the comovement between consumption and output across the business cycle. Given that the basic structure of this New Keynesian model is widely known, we only present its crucial parts and defer a full presentation with derivations to the Online Appendix.

3.1 Households

We consider an infinitely lived representative household with recursive preferences as in Epstein and Zin (1989) and Weil (1990). Using the formulation in Rudebusch and Swanson (2012), the value function V_t is given by

$$V_t = \begin{cases} u_t + \beta(\mathbb{E}_t [V_{t+1}^{1-\alpha}])^{\frac{1}{1-\alpha}} & \text{when } u_t > 0 \text{ for all } t \\ u_t - \beta(\mathbb{E}_t [(-V_{t+1})^{1-\alpha}])^{\frac{1}{1-\alpha}} & \text{when } u_t < 0 \text{ for all } t \end{cases}, \quad (3)$$

related to the adopted simulation procedure for the VXO which is $100\sqrt{4\max\{\mathbb{V}_t[R_{t+1}^m], 0.000026\}}$ as suggested by the codes related to Basu and Bundick (2018). By imposing this lower bound for the conditional variance of stock returns $\mathbb{V}_t[R_{t+1}^m]$, we get an upward bias in the IVAR residuals for $\log VXO_t$ and subsequently also an upward bias in the impulse response functions for $\log VXO_t$.

⁸See also the Online Appendix, where we also plot the median target responses.

where u_t is the utility function and $\mathbb{E}_t[\cdot]$ is the conditional expectation in period t . The parameter $\alpha \in \mathbb{R} \setminus \{1\}$ captures households' appetite for the resolution of uncertainty, implying preferences for early (late) resolution of uncertainty if $\alpha > 0$ ($\alpha < 0$) for $u_t > 0$, and vice versa when $u_t < 0$. Andreasen and Jørgensen (2020) further argue that the size of this timing attitude is proportional to α , meaning that numerically larger values of α imply stronger preferences for early (late) resolution of uncertainty.

The expression for households' utility at time t is

$$u_t \equiv a_t^{1-\sigma} \left(\frac{1}{1-\sigma} \left((C_t - bC_{t-1})^\eta (1 - N_t)^{1-\eta} \right)^{1-\sigma} + u_0 \right), \quad (4)$$

which depends on habit-adjusted consumption $C_t - bC_{t-1}$ and leisure $1 - N_t$.⁹ As in Basu and Bundick (2017), a_t is a preference shock that evolves according to the process $a_{t+1} = \rho_a a_t + \sigma_{a,t} \epsilon_{a,t+1}$ where $\epsilon_{a,t+1} \sim \mathcal{NID}(0, 1)$. The process for stochastic volatility $\sigma_{a,t}$ is specified as $\sigma_{a,t+1} = (1 - \rho_\sigma) + \rho_\sigma \sigma_{a,t} + \sigma_\sigma \epsilon_{\sigma,t+1}$, where the innovations in uncertainty $\epsilon_{\sigma,t+1} \sim \mathcal{NID}(0, 1)$ and uncorrelated with $\epsilon_{a,t+1}$ at all leads and lags. The constant u_0 captures utility from government spending and goods produced and consumed within the household. As shown by Andreasen and Jørgensen (2020), the main reason for including u_0 is to separately control the level of the utility function and hence disentangle the timing attitude α from relative risk aversion (RRA), which otherwise are tightly linked in the standard formulation of recursive preferences in Epstein and Zin (1989) and Weil (1990). To see this, note that (3) and (4) imply

$$\text{RRA} = \frac{\eta}{1-b} \left[\sigma + \alpha(1-\sigma) \frac{((C_{ss} - bC_{ss})^\eta (1 - N_{ss})^{1-\eta})^{1-\sigma}}{((C_{ss} - bC_{ss})^\eta (1 - N_{ss})^{1-\eta})^{1-\sigma} + (1-\sigma)u_0} \right],$$

at the deterministic steady state (ss) when accounting for the endogenous labor supply (see Swanson (2018)). Hence, a high timing attitude α does not necessarily imply a high RRA, which is in contrast to the standard case with $u_0 = 0$ where $\text{RRA} = \frac{\eta}{1-b} (\sigma + \alpha(1-\sigma))$.

The household receives labor income W_t for each unit of labor N_t supplied to the intermediate firms. These firms are owned by the household that therefore holds their equity shares S_t , which have the price P_t^E and pay dividends D_t^E . The household also holds one-period real bonds with the gross return R_t^R as issued by the firms, and it holds nominal bonds issued by the government with the gross return R_t .

⁹Following Basu and Bundick (2018), we include $a_t^{1-\sigma}$ instead of a_t in (4) to avoid having an asymptote in the policy function at $\sigma = 1$, as noted by de Groot et al. (2018).

3.2 Firms

The final output Y_t is produced by a representative final good producer using the production function $Y_t = \left(\int_0^1 Y_t(i)^{(\theta_{\mu,t}-1)/\theta_{\mu,t}} di \right)^{\theta_{\mu,t}/(\theta_{\mu,t}-1)}$, where $\theta_{\mu,t}$ captures a time-varying substitution elasticity between the intermediate goods $Y_t(i)$. It is assumed that $\log(\theta_{\mu,t+1}/\theta_{\mu,t}) = \rho_{\theta_{\mu}} \log(\theta_{\mu,t}/\theta_{\mu,t-1}) + \sigma_{\theta_{\mu}} \epsilon_{\theta,t+1}$, where $\epsilon_{\theta,t+1} \sim \mathcal{NID}(0, 1)$. Cost minimization implies that $Y_t(i) = \left[\frac{P_t(i)}{P_t} \right]^{-\theta_{\mu,t}} Y_t$, where $P_t \equiv \left(\int_0^1 P_t(i)^{1-\theta_{\mu,t}} di \right)^{\frac{1}{1-\theta_{\mu,t}}}$ denotes the aggregate price level and $P_t(i)$ is the price of the i th good.

Intermediate firms produce $Y_t(i)$ using the Cobb-Douglas production function with fixed costs, i.e., $Y_t(i) = (K_{t-1}(i)U_t(i))^{\alpha_p} (Z_t N_t(i))^{1-\alpha_p} - \Phi$, where $K_{t-1}(i)$ is the capital stock, $U_t(i)$ is the utilization rate, and Z_t captures productivity shocks as $\log Z_{t+1} = \rho_Z \log Z_t + \sigma_Z \epsilon_{Z,t+1}$ with $\epsilon_{Z,t+1} \sim \mathcal{NID}(0, 1)$. The capital stock evolves as $K_t(i) = \left(1 - \delta(U_t(i)) - \frac{\phi_K}{2} (I_t(i)/K_{t-1}(i) - \delta)^2 \right) K_t(i) + I_t(i)$, where ϕ_K introduces adjustment costs and $I_t(i)$ is investment. The depreciation costs are given by $\delta(U_t(i)) = \delta + \delta_1(U_t(i) - U_{ss}) + \frac{\delta_2}{2}(U_t(i) - U_{ss})^2$. Intermediate firms operate in a market with monopolistic competition and face quadratic adjustment costs as in Rotemberg (1982). The expression for real dividends therefore reads

$$\frac{D_t(i)}{P_t} = \left[\frac{P_t(i)}{P_t} \right]^{1-\theta_{\mu,t}} Y_t - \frac{W_t}{P_t} N_t(i) - I_t(i) - \frac{\phi_P}{2} \left(\frac{P_t(i)}{\Pi_{ss} P_{t-1}(i)} - 1 \right)^2 Y_t$$

where W_t is the wage and Π_{ss} denotes inflation in the deterministic steady state. Each intermediate firm finances a fraction ν of its capital stock by issuing one-period riskless bonds, i.e., $B_t(i) = \nu K_{t-1}(i)$. As a result, the real dividend payments to equity holders are $D_t^E(i)/P_t = D_t(i)/P_t - \nu(K_{t-1}(i) - K_t(i))/R_t^R$.

3.3 Monetary Policy and Stock Market Volatility

The central bank adjusts the nominal interest rate R_t to stabilize inflation around its target Π_{ss} and output growth according to the rule

$$\ln(R_t/R_{ss}) = \zeta_{\Pi} \log(\Pi_t/\Pi_{ss}) + \zeta_{\Delta Y} \log(Y_t/Y_{t-1}), \quad (5)$$

where $\Pi_t \equiv P_t/P_{t-1}$ denotes gross inflation.¹⁰

As in Basu and Bundick (2017), the gross stock market return is defined as $R_t^m = (D_t^E + P_t^E)/P_{t-1}^E$. The model-implied measure for stock market volatility is then given by $VXO_t = 100\sqrt{4 \times \mathbb{V}_t[R_{t+1}^m]}$, where $\mathbb{V}_t[R_{t+1}^m]$ is the quarterly conditional variance of R_{t+1}^m .

¹⁰Unreported results show no evidence of interest rate smoothing in (5) when using the estimator presented in Section 5.1.

3.4 Equilibrium

We focus on the symmetric equilibrium, where all intermediate firms choose the same price $P_t(i) = P_t$, employ the same amount of labor $N_t(i) = N_t$, and choose the same level of capital $K_t(i) = K_t$ and utilization rate $U_t(i) = U_t$. Consequently, all firms have the same cash flows and are financed with the same mix of bonds and equity. The markup of the price in relation to marginal cost is $\mu_t = 1/\Xi_t$, where Ξ_t denotes the marginal cost of producing one additional unit by the intermediate firm.

4 Model Solution

This section derives a third-order approximation to DSGE models around the risky steady state and study some of its implications. Section 4.1 describes a general class of DSGE models that includes the New Keynesian model presented above. The third-order Taylor approximation around the risky steady state is derived in Section 4.2, and we discuss a pruned version of this approximation in Section 4.3. The accuracy and execution time of various approximations are studied in Section 4.4.

4.1 General Model

We consider the class of models where the equilibrium conditions are given by

$$\mathbb{E}_t [\mathbf{f}(\mathbf{y}_{t+1}, \mathbf{y}_t, \mathbf{x}_{t+1}, \mathbf{x}_t)] = \mathbf{0}. \quad (6)$$

The states appear in \mathbf{x}_t with dimension $n_x \times 1$, while the control variables of dimension $n_y \times 1$ are collected in \mathbf{y}_t , with $n \equiv n_x + n_y$. We also let $\mathbf{x}_t \equiv \begin{bmatrix} \mathbf{x}'_{1,t} & \mathbf{x}'_{2,t} \end{bmatrix}'$, where $\mathbf{x}_{1,t}$ refers to the endogenous states and $\mathbf{x}_{2,t}$ to the exogenous states, which evolve as

$$\mathbf{x}_{2,t+1} = \mathbf{h}_2(\mathbf{x}_{2,t}) + \tilde{\boldsymbol{\eta}}\boldsymbol{\epsilon}_{t+1}, \quad (7)$$

where $\boldsymbol{\epsilon}_{t+1} \sim \mathcal{IID}(\mathbf{0}, \mathbf{I}_{n_\epsilon})$, and n_ϵ is the number of elements in the vector of shocks $\boldsymbol{\epsilon}_{t+1}$.¹¹ The assumption that the innovations enter linearly in (7) is without loss of generality, because the state vector may be extended to account for nonlinearities between \mathbf{x}_t and $\boldsymbol{\epsilon}_{t+1}$, as needed when including stochastic volatility in the exogenous states (see Andreasen (2012) for further details). The exact solution to this class of models is given by

$$\mathbf{y}_t = \mathbf{g}(\mathbf{x}_t) \quad (8)$$

¹¹ All eigenvalues of $\partial \mathbf{h}_2(\mathbf{x}_{2,t}) / \partial \mathbf{x}_{2,t}$ must have modulus less than one, implying that trends may only be included if the model after re-scaling has an equivalent representation without trending variables. The procedure of re-scaling a DSGE model with trends is carefully described in King et al. (2002).

$$\mathbf{x}_{t+1} = \mathbf{h}(\mathbf{x}_t) + \boldsymbol{\eta}\boldsymbol{\epsilon}_{t+1} \quad (9)$$

where $\boldsymbol{\eta} \equiv \begin{bmatrix} \mathbf{0} & \tilde{\boldsymbol{\eta}}' \end{bmatrix}'$ has dimension $n_x \times n_\epsilon$. The functions $\mathbf{g}(\cdot)$ and $\mathbf{h}(\cdot)$ are generally unknown and must be approximated.

4.2 A Third-Order Approximation at the Risky Steady State

Let $\mathbf{x}_t = \bar{\mathbf{x}}$ denote the risky steady state. This long-term equilibrium point is characterized by the absence of structural shocks (i.e., $\boldsymbol{\epsilon}_{t+1} = \mathbf{0}$) but agents nevertheless respond to their probability distribution. This makes the risky steady state different from the widely used deterministic steady state, where agents do not respond to the probability distribution of the structural shocks.

The considered third-order approximation around $\bar{\mathbf{x}}$ is given by

$$\begin{aligned} \mathbf{y}_t &= \mathbf{g}(\bar{\mathbf{x}}) + \mathbf{g}_x(\bar{\mathbf{x}})(\mathbf{x}_t - \bar{\mathbf{x}}) + \frac{1}{2}\mathbf{g}_{xx}(\bar{\mathbf{x}})(\mathbf{x}_t - \bar{\mathbf{x}})^{\otimes 2} + \frac{1}{6}\mathbf{g}_{xxx}(\bar{\mathbf{x}})(\mathbf{x}_t - \bar{\mathbf{x}})^{\otimes 3} \\ \mathbf{x}_{t+1} &= \mathbf{h}(\bar{\mathbf{x}}) + \mathbf{h}_x(\bar{\mathbf{x}})(\mathbf{x}_t - \bar{\mathbf{x}}) + \frac{1}{2}\mathbf{h}_{xx}(\bar{\mathbf{x}})(\mathbf{x}_t - \bar{\mathbf{x}})^{\otimes 2} + \frac{1}{6}\mathbf{h}_{xxx}(\bar{\mathbf{x}})(\mathbf{x}_t - \bar{\mathbf{x}})^{\otimes 3} + \boldsymbol{\eta}\boldsymbol{\epsilon}_{t+1}, \end{aligned} \quad (10)$$

where $(\mathbf{x}_t - \bar{\mathbf{x}})^{\otimes 2} \equiv (\mathbf{x}_t - \bar{\mathbf{x}}) \otimes (\mathbf{x}_t - \bar{\mathbf{x}})$ and $(\mathbf{x}_t - \bar{\mathbf{x}})^{\otimes 3} \equiv (\mathbf{x}_t - \bar{\mathbf{x}})^{\otimes 2} \otimes (\mathbf{x}_t - \bar{\mathbf{x}})$. The first-order derivative of $\mathbf{g}(\mathbf{x}_t)$ with respect to \mathbf{x}_t is denoted $\mathbf{g}_x(\bar{\mathbf{x}})$ when evaluated at $\bar{\mathbf{x}}$. A similar notation is used for $\mathbf{h}(\mathbf{x}_t)$ and for higher-order derivatives.¹² The procedure we use to compute the required derivatives of $\mathbf{g}(\cdot)$ and $\mathbf{h}(\cdot)$ is similar to the one applied in Collard and Juillard (2001a) for a simple endowment model and in Collard and Juillard (2001b) for a DSGE model solved by a second-order approximation. Hence, we substitute (8) and (9) into (6) to get

$$\mathbb{E}_t[\mathbf{F}(\mathbf{x}_t, \boldsymbol{\epsilon}_{t+1})] \equiv \mathbb{E}_t[\mathbf{f}(\mathbf{g}(\mathbf{h}(\mathbf{x}_t) + \boldsymbol{\eta}\boldsymbol{\epsilon}_{t+1}), \mathbf{g}(\mathbf{x}_t), \mathbf{h}(\mathbf{x}_t) + \boldsymbol{\eta}\boldsymbol{\epsilon}_{t+1}, \mathbf{x}_t)] = \mathbf{0}. \quad (11)$$

We then compute a third-order Taylor approximation of $\mathbf{F}(\mathbf{x}_t, \boldsymbol{\epsilon}_{t+1})$ at $\mathbf{x}_t = \bar{\mathbf{x}}$ and $\boldsymbol{\epsilon}_{t+1} = \mathbf{0}$. Evaluating the expectations with respect to terms that involve $\boldsymbol{\epsilon}_{t+1}$ and using the method of undetermined coefficients, we obtain the following conditions (derived in our Online Appendix):

$$[\mathbf{F}(\bar{\mathbf{x}}, \mathbf{0})]^i + \frac{1}{2}[\mathbf{F}_{\epsilon\epsilon}(\bar{\mathbf{x}}, \mathbf{0})]_{\phi_1\phi_2}^i [\mathbb{V}[\boldsymbol{\epsilon}_{t+1}]]_{\phi_2}^{\phi_1} + \frac{1}{6}[\mathbf{F}_{\epsilon\epsilon\epsilon}(\bar{\mathbf{x}}, \mathbf{0})]_{\phi_1\phi_2\phi_3}^i [\mathbf{m}_\epsilon^3]_{\phi_2\phi_3}^{\phi_1} = 0 \quad (12)$$

$$[\mathbf{F}_x(\bar{\mathbf{x}}, \mathbf{0})]_{\alpha_1}^i + \frac{3}{6}[\mathbf{F}_{\epsilon\epsilon x}(\bar{\mathbf{x}}, \mathbf{0})]_{\phi_1\phi_2\alpha_3}^i [\mathbb{V}[\boldsymbol{\epsilon}_{t+1}]]_{\phi_2}^{\phi_1} = 0 \quad (13)$$

$$[\mathbf{F}_{xx}(\bar{\mathbf{x}}, \mathbf{0})]_{\alpha_1\alpha_2}^i = 0 \quad (14)$$

$$[\mathbf{F}_{xxx}(\bar{\mathbf{x}}, \mathbf{0})]_{\alpha_1\alpha_2\alpha_3}^i = 0, \quad (15)$$

¹²Note that $\bar{\mathbf{x}}$ is a fixed-point in $\mathbf{h}(\cdot)$, i.e. $\mathbf{h}(\bar{\mathbf{x}}) = \bar{\mathbf{x}}$, and that the ergodic mean $\mathbb{E}[\mathbf{x}_t]$ generally differs from the risky steady state $\bar{\mathbf{x}}$ because $\mathbb{E}[\mathbf{x}_{t+1} - \bar{\mathbf{x}}] = \mathbb{E}\left[\frac{1}{2}\mathbf{h}_{xx}(\bar{\mathbf{x}})(\mathbf{x}_t - \bar{\mathbf{x}})^{\otimes 2} + \frac{1}{6}\mathbf{h}_{xxx}(\bar{\mathbf{x}})(\mathbf{x}_t - \bar{\mathbf{x}})^{\otimes 3}\right] \neq 0$.

where the tensor notation is used with $i = \{1, 2, \dots, n\}$, $\phi_1, \phi_2, \phi_3 = \{1, 2, \dots, n_\epsilon\}$, and $\alpha_1, \alpha_2, \alpha_3 = \{1, 2, \dots, n_x\}$. Also, $\mathbb{V}[\epsilon_{t+1}]$ is the covariance matrix of ϵ_{t+1} (which equals \mathbf{I}_{n_ϵ}), and \mathbf{m}_ϵ^3 with dimensions $n_\epsilon \times n_\epsilon \times n_\epsilon$ contains all third order moments of ϵ_{t+1} . The derivatives of $\mathbf{F}(\mathbf{x}_t, \epsilon_{t+1})$ are denoted with subscripts and evaluated at the risky steady state, e.g., $\mathbf{F}_x(\bar{\mathbf{x}}, \mathbf{0}) = \partial \mathbf{F}(\mathbf{x}_t, \epsilon_{t+1}) / \partial \mathbf{x}_t' |_{\mathbf{x}_t = \bar{\mathbf{x}}, \epsilon_{t+1} = \mathbf{0}}$.

To understand the implications of (12) to (15), let us first consider the case without uncertainty by letting $\mathbb{V}[\epsilon_{t+1}] = \mathbf{0}$ and $\mathbf{m}_\epsilon^3(\epsilon_{t+1}) = \mathbf{0}$ to obtain the certainty equivalence solution. The $n \times 1$ equations in (12) then simplifies to $[\mathbf{F}(\bar{\mathbf{x}}, \mathbf{0})]^i = 0$, implying that $\bar{\mathbf{x}} = \mathbf{x}_{ss}$ and $\bar{\mathbf{y}} = \mathbf{y}_{ss}$. We also have that (13) reduces to $[\mathbf{F}_x(\mathbf{x}_{ss}, \mathbf{0})]_{\alpha_1}^i = 0$, which gives the well-known quadratic system for computing the first-order derivatives $\mathbf{g}_x(\mathbf{x}_{ss})$ and $\mathbf{h}_x(\mathbf{x}_{ss})$, as shown in Schmitt-Grohe and Uribe (2004). Moreover, (14) reduces to $[\mathbf{F}_{xx}(\mathbf{x}_{ss}, \mathbf{0})]_{\alpha_1 \alpha_2}^i = 0$ and (15) to $[\mathbf{F}_{xxx}(\mathbf{x}_{ss}, \mathbf{0})]_{\alpha_1 \alpha_2 \alpha_3}^i = 0$, which are the linear systems exploited by the standard perturbation method to compute the second-order terms $\mathbf{g}_{xx}(\mathbf{x}_{ss})$ and $\mathbf{h}_{xx}(\mathbf{x}_{ss})$ and the third-order terms $\mathbf{g}_{xxx}(\mathbf{x}_{ss})$ and $\mathbf{h}_{xxx}(\mathbf{x}_{ss})$, respectively (see Schmitt-Grohe and Uribe (2004) and Andreasen (2012)). Thus, without uncertainty, the conditions in (12) to (15) are identical to those used by the standard perturbation method to obtain the certainty equivalent part of this approximation.

In the presence of uncertainty, condition (12) still determines $\bar{\mathbf{x}}$ and $\bar{\mathbf{y}}$, but in this case $\bar{\mathbf{x}} \neq \mathbf{x}_{ss}$ and $\bar{\mathbf{y}} \neq \mathbf{y}_{ss}$. Given $(\bar{\mathbf{x}}, \bar{\mathbf{y}})$, condition (13) allows us to determine the first-order derivatives of $\mathbf{g}(\cdot)$ and $\mathbf{h}(\cdot)$ by solving a quadratic system that includes the variance term $\frac{3}{6} [\mathbf{F}_{\epsilon \epsilon x}(\bar{\mathbf{x}}, \mathbf{0})]_{\phi_1 \phi_2 \alpha_3}^i [\mathbb{V}[\epsilon_{t+1}]]_{\phi_2}^{\phi_1}$. This adjustment has two important implications. First, it implies that the first-order derivatives $\mathbf{g}_x(\bar{\mathbf{x}})$ and $\mathbf{h}_x(\bar{\mathbf{x}})$ contain an uncertainty correction for variance risk. Second, the Blanchard-Kahn conditions for getting unique and stable first-order derivatives have to hold for a risk-adjusted version of the model. Hence, uncertainty may contribute to violate or satisfy the Blanchard-Kahn conditions, unlike in the standard perturbation method where these conditions are evaluated at the deterministic steady state. Importantly, the uncertainty correction $\frac{3}{6} [\mathbf{F}_{\epsilon \epsilon x}(\bar{\mathbf{x}}, \mathbf{0})]_{\phi_1 \phi_2 \alpha_3}^i [\mathbb{V}[\epsilon_{t+1}]]_{\phi_2}^{\phi_1}$ is of third order and therefore not present in the second-order approximation around the risky steady state as studied in Collard and Juillard (2001b).

The condition in (14) for the second-order terms $\mathbf{g}_{xx}(\bar{\mathbf{x}})$ and $\mathbf{h}_{xx}(\bar{\mathbf{x}})$ is similar to the one used in the standard perturbation method, except that all derivatives of $\mathbf{F}(\cdot)$, $\mathbf{g}(\cdot)$, and $\mathbf{h}(\cdot)$ are evaluated at the risky steady state. This implies that $\mathbf{g}_{xx}(\bar{\mathbf{x}})$ and $\mathbf{h}_{xx}(\bar{\mathbf{x}})$ contain a correction for uncertainty, which is essential for our analysis, because it enables us to obtain impulse response functions for uncertainty shocks that are state-dependent. Finally, the condition in (15) allows us to determine $\mathbf{g}_{xxx}(\bar{\mathbf{x}})$ and $\mathbf{h}_{xxx}(\bar{\mathbf{x}})$ by solving a linear system, where all derivatives of $\mathbf{F}(\cdot)$, $\mathbf{g}(\cdot)$, and $\mathbf{h}(\cdot)$ are evaluated at the risky steady state. As a result, $\mathbf{g}_{xxx}(\bar{\mathbf{x}})$ and $\mathbf{h}_{xxx}(\bar{\mathbf{x}})$ are also adjusted for uncertainty for the same reasons as mentioned for $\mathbf{g}_{xx}(\bar{\mathbf{x}})$ and $\mathbf{h}_{xx}(\bar{\mathbf{x}})$.¹³ For the New Keynesian model we

¹³Very loosely, one can think of $\mathbf{g}_x(\bar{\mathbf{x}}) \approx \mathbf{g}_x(\mathbf{x}_{ss}) + 0.5 \mathbf{g}_{\sigma \sigma x}(\mathbf{x}_{ss})$ and $\mathbf{h}_x(\bar{\mathbf{x}}) \approx \mathbf{h}_x(\mathbf{x}_{ss}) + 0.5 \mathbf{h}_{\sigma \sigma x}(\mathbf{x}_{ss})$,

consider, nearly all of the uncertainty correction in the higher-order derivatives comes from the risk adjustment in $\mathbf{g}_x(\bar{\mathbf{x}})$ and $\mathbf{h}_x(\bar{\mathbf{x}})$, meaning that a third-order approximation is needed for our model to get visible state-dependence in the impulse response functions for an uncertainty shock.¹⁴

Unfortunately, the moment conditions in (12) to (15) do not imply a recursive structure for computing the required terms in (10). This is because $\mathbf{F}_{\epsilon\epsilon}(\bar{\mathbf{x}}, \mathbf{0})$, $\mathbf{F}_{\epsilon\epsilon x}(\bar{\mathbf{x}}, \mathbf{0})$, and $\mathbf{F}_{\epsilon\epsilon\epsilon}(\bar{\mathbf{x}}, \mathbf{0})$ depend on $(\bar{\mathbf{x}}, \bar{\mathbf{y}})$ and the derivatives of $\mathbf{g}(\cdot)$ and $\mathbf{h}(\cdot)$. We therefore use an iterative procedure, where $\mathbf{F}_{\epsilon\epsilon}(\bar{\mathbf{x}}, \mathbf{0})$, $\mathbf{F}_{\epsilon\epsilon x}(\bar{\mathbf{x}}, \mathbf{0})$, and $\mathbf{F}_{\epsilon\epsilon\epsilon}(\bar{\mathbf{x}}, \mathbf{0})$ are computed using derivatives of $\mathbf{g}(\cdot)$ and $\mathbf{h}(\cdot)$ from the standard perturbation method in the first iteration and afterwards from the previous iteration to recursively solve (12) to (15). Our Online Appendix summarizes this algorithm, which basically iterates on the solution routine for the standard perturbation approximation until convergence (typically with five iterations).¹⁵

4.3 A Pruned State-Space Representation

The system for a standard third-order perturbation approximation obviously reduces to the system in (10) when all derivatives of the \mathbf{g} - and \mathbf{h} -functions with respect to the perturbation parameter are equal to zero. This means that the pruning scheme introduced in Andreasen et al. (2018) can also be applied to (10) with all derivatives of the \mathbf{g} - and \mathbf{h} -functions with respect to \mathbf{x}_t evaluated at $\bar{\mathbf{x}}$ instead of \mathbf{x}_{ss} . The Blanchard-Kahn condition related to (13) ensures that $\mathbf{h}_x(\bar{\mathbf{x}})$ is stable and hence that this pruned approximation is stable. Thus, the closed-form solution for unconditional moments and GIRFs derived in Andreasen et al. (2018) can also be applied to our third order approximation at the risky steady state. This greatly facilitates its use in a formal estimation routine that matches unconditional first and second moments, impulse response functions, or a combination of the two, as considered below in Section 5.

where σ is the perturbation parameter as defined in Schmitt-Grohe and Uribe (2004). In the standard perturbation method, only $\mathbf{g}_x(\mathbf{x}_{ss})$ and $\mathbf{h}_x(\mathbf{x}_{ss})$ are used to compute the higher-order derivatives. In contrast, the procedure we use implies that $\mathbf{g}_x(\mathbf{x}_{ss}) + 0.5\mathbf{g}_{\sigma\sigma x}(\mathbf{x}_{ss})$ and $\mathbf{h}_x(\mathbf{x}_{ss}) + 0.5\mathbf{h}_{\sigma\sigma x}(\mathbf{x}_{ss})$ are used to compute the higher-order derivatives, which therefore include an adjustment for uncertainty.

¹⁴As shown in the Online Appendix, the expressions for $\mathbf{F}_{\epsilon\epsilon}(\bar{\mathbf{x}}, \mathbf{0})$, $\mathbf{F}_{\epsilon\epsilon x}(\bar{\mathbf{x}}, \mathbf{0})$, and $\mathbf{F}_{\epsilon\epsilon\epsilon}(\bar{\mathbf{x}}, \mathbf{0})$ are identical to those provided for $\mathbf{F}_{\sigma\sigma}$, $\mathbf{F}_{\sigma\sigma x}$, and $\mathbf{F}_{\sigma\sigma\sigma}$, respectively, in Schmitt-Grohe and Uribe (2004) and Andreasen (2012), when setting all derivatives of $\mathbf{g}(\cdot)$ and $\mathbf{h}(\cdot)$ with respect to the perturbation parameter σ equal to zero. The conditions in (12) to (15) are therefore easy to implement from existing results and computer packages on the standard perturbation method. In our case, we modify the highly efficient Matlab codes of Binning (2013).

¹⁵The proposed solution in (10) is, strictly speaking, not a perturbation approximation, because it does not perturb a known solution. Instead, it corresponds to a projection approximation that only exploits local properties of the model solution, and it is therefore best characterized as a local projection approximation.

4.4 Accuracy and Execution Time

We evaluate the accuracy of Taylor approximations around the deterministic and risky steady state by computing unit-free Euler-equation errors for the considered New Keynesian model along a simulated sample of 10,000 observations for the states. The two estimated versions of the New Keynesian model presented below in Table 4 are considered for this exercise, where the states are simulated using a standard third-order perturbation approximation, i.e., by a Taylor approximation around the deterministic steady state.

Table 3: Accuracy and Execution Time

Panel \mathcal{A} in this table reports the mean absolute unit-free Euler-equation errors (MAEs) and the root mean squared unit-free Euler-equation errors (RMSEs) in a second-, third-, and fourth-order Taylor approximation around the deterministic steady state, and in a second- and third-order Taylor approximation around the risky steady state. All model equations are included when computing the MAEs and the RMSEs, except for the link-equations related to lagged controls and the equations for the exogenous shocks, where the errors always are zero. The Euler-equations errors are reported in percent and computed using a simulated sample path of 10,000 observations for the states. For each estimated version of the model, the simulated sample path is computed using a third-order Taylor approximation around the deterministic steady state. Conditional expectations in the Euler-equations are evaluated by Gauss-Hermite quadratures using five points per shock, giving a total of $5^4 = 625$ points. The considered model parameters are those reported in Table 4. Panel \mathcal{B} shows the execution time in seconds for obtaining the approximated model solutions and for simulating 10,000 observations using each of the considered approximations. The computations are done on a standard laptop with an Intel(R) Core(TM) i7-7600 CPU processor with 2.80GHz.

		Taylor approximations at deterministic steady state			Taylor approximations at risky steady state	
		2nd	3rd	4th	2nd	3rd
Panel \mathcal{A} : Accuracy (in pct.)						
Benchmark	MAEs	1.19	1.10	0.65	1.06	0.79
	RMSEs	3.26	3.03	2.27	3.10	2.44
Standard EZ	MAEs	1.41	1.22	0.79	1.16	0.87
	RMSEs	3.98	3.44	5.61	3.45	3.44
Panel \mathcal{B} : Execution time (in sec.)						
Benchmark	Model solution	0.03	0.60	12.0	0.45	3.50
	Simulation of of 10,000 observations	0.13	1.04	22.4	0.13	1.04

For the benchmark model, panel \mathcal{A} in Table 3 shows that the standard perturbation method performs fairly well, as the mean absolute Euler errors (MAEs) across all endogenous equations in the model are only 1.19% at second order, 1.10% at third order, and 0.65% at fourth order. We find a similar monotone improvement in accuracy by increasing the approximation order when computing the root mean squared Euler-equation errors (RMSEs), that penalize large errors more heavily than the MAEs. For approximations around the risky steady state, the second-order approximation of Collard and Juillard (2001b) provides a small improvement when compared to the standard perturbation method at second order, as the MAEs falls from 1.19% to 1.06% and the RMSEs

from 3.26% to 3.10%. We see more notable reductions in the Euler errors by using the proposed third-order approximation around the risky steady state, as the MAEs falls from 1.10% to 0.79% and the RMSEs from 3.03% to 2.44% when compared to a third-order approximation around \mathbf{x}_{ss} . Thus, the accuracy of our approximation clearly outperforms the standard perturbation method at third order and is close to providing the same level of accuracy as the fourth-order Taylor approximation around \mathbf{x}_{ss} with a MAE of 0.65 and a RMSE of 2.27.

Table 3 shows that we broadly find the same results for the estimated version of the New Keynesian model with standard Epstein-Zin preferences, i.e., $u_0 = 0$. The only exception is that the RMSEs for the fourth-order Taylor approximation around \mathbf{x}_{ss} is 5.61% and hence higher than both third-order approximations with RMSEs of 3.44%.

The execution time for the various approximations are provided in panel \mathcal{B} of Table 3. The standard third-order perturbation approximation is obtained in just 0.60 seconds, while it takes 12 seconds to compute a fourth-order approximation using the codes of Levintal (2017). The required time for computing our third-order approximation around the risky steady state depends mainly on the number of iterations needed to obtain convergence, but the execution time is typically around 4 seconds. Thus, we get an approximated model solution with state-dependent impulse response functions following an uncertainty shock that is about three times faster than the existing alternative of using a fourth-order approximation. In addition, it is also more costly to use a fourth-order than a third-order approximation when simulating the model. This is illustrated at the bottom of Table 3, where it takes one second to simulate 10,000 observations from a third-order approximation but about 22 seconds when using a fourth-order approximation.

To summarize, the proposed third-order Taylor approximation around the risky steady state delivers a high level of accuracy that is comparable to a fourth-order perturbation approximation but is computationally much more efficient than this fourth order alternative. This is particularly convenient when it comes to estimating DSGE models like ours, where uncertainty shocks are allowed to have state-dependent effects.¹⁶

5 Empirical Results for the New Keynesian Model

This section presents our empirical findings for the New Keynesian model. We introduce the adopted estimation methodology in Section 5.1, and discuss the estimated parameters in Section 5.2 and the model fit in Section 5.3.

¹⁶de Groot (2016) highlights another shortcoming of the third-order Taylor approximation at the deterministic steady state, as none of its terms account for the conditional standard deviation of volatility shocks, i.e. σ_σ . Unreported results show that our third-order Taylor approximation around the risky steady state corrects for σ_σ and hence also addresses this limitation of the standard solution method.

5.1 Estimation Methodology

To describe our estimation approach, let the vector γ contain the structural parameters of the New Keynesian model. As in Basu and Bundick (2017), we estimate γ using two sets of moments. The first set includes the MT responses from the IVAR for the first 20 periods following an uncertainty shock in expansions $\hat{\psi}_{EXP}$ and in recessions $\hat{\psi}_{REC}$ as presented in Section 2. The second source of information is a vector of unconditional sample moments $\hat{\mathbf{m}}_T$, which ensures that the model also matches stylized unconditional properties of the US economy in addition to the conditional moments following an uncertainty shock. These unconditional moments are constructed using the same data as applied to estimate the IVAR. That is, we use inflation, the shadow rate of Wu and Xia (2016), output, investment, consumption, and hours (with the four latter series detrended as in Hamilton (2018)). The included moments are the mean of inflation and the policy rate, as well as the covariances and auto-covariances related to the standard deviations and correlations listed in Table 5. Hence, the adopted estimator is given by

$$\begin{aligned} \hat{\gamma} = \arg \min_{\gamma \in \Gamma} & \left(\hat{\psi}_{EXP} - \psi_{EXP}(\gamma) \right)' \mathbf{V}_{EXP}^{-1} \left(\hat{\psi}_{EXP} - \psi_{EXP}(\gamma) \right) + \\ & \left(\hat{\psi}_{REC} - \psi_{REC}(\gamma) \right)' \mathbf{V}_{REC}^{-1} \left(\hat{\psi}_{REC} - \psi_{REC}(\gamma) \right) + \\ & \Lambda \left(\hat{\mathbf{m}}_T - \mathbf{m}(\gamma) \right)' \mathbf{W}^{-1} \left(\hat{\mathbf{m}}_T - \mathbf{m}(\gamma) \right), \end{aligned} \quad (16)$$

where \mathbf{V}_{EXP} , \mathbf{V}_{REC} , and \mathbf{W} are diagonal matrices containing bootstrapped standard errors for the related moments and Γ denotes the feasible domain of γ . The moments in the New Keynesian model are denoted by $\psi_{EXP}(\gamma)$, $\psi_{REC}(\gamma)$, and $\mathbf{m}(\gamma)$, which we compute using the third-order pruned approximation around the risky steady state. The impulse responses to an uncertainty shock are here obtained using a procedure similar to the one applied in the IVAR. That is, for each γ , we simulate 10,000 observations for output in the New Keynesian model to find the set of states where output is below its 10% percentile (denoted \mathbf{X}^{REC}) and above its 90% percentile (denoted \mathbf{X}^{EXP}). The impulse response functions are then computed as the average of the GIRFs across these selected states, i.e., $\psi_m(\gamma, h) = \frac{1}{250} \sum_{i=1}^{250} GIRF_{\mathbf{Y}}(h, \delta_{unc}, \mathbf{x}^{(i)})$ for $\mathbf{x}^{(i)} \in \mathbf{X}^m$, where $\psi_m(\gamma) \equiv \{\psi_m(\gamma, h)\}_{h=1}^{20}$ and $m = \{EXP, REC\}$ using 250 selected states. The expression for $GIRF_{\mathbf{Y}}(h, \delta_{unc}, \mathbf{x}^{(i)})$ is here evaluated in closed form using the observation in Section 4.3, which greatly reduces the computational costs in relation to the estimation.¹⁷ Finally, we set Λ to ensure that the model implies a reasonable fit to the unconditional moments, and hence replicates both the impulse responses from the IVAR and the selected unconditional macro moments.

¹⁷Given that a simulated sample is needed to find the two sets \mathbf{X}^{rec} and \mathbf{X}^{exp} , we settle by only computing unconditional means in $\mathbf{m}(\gamma)$ in closed form, while all unconditional second moments in $\mathbf{m}(\gamma)$ are obtained from the simulated sample to avoid the more computational evolved expression for these moments provided in Andreasen et al. (2018).

While most of the structural parameters in the model are estimated, we calibrate a few parameters that would be hard to pin down by our estimation procedure. Following Basu and Bundick (2017), we calibrate $\nu = 0.9$ for firm leverage, $\alpha_p = 1/3$ in the production function, $\delta = 0.025$ for steady state capital depreciations, $\delta_2 = 0.0003$ in the function for depreciation costs (with $\delta_1 = 1/\beta - 1 + \delta$), and the fixed cost Φ to remove pure profit for intermediate firms using the procedure in Basu and Bundick (2017). For households, the values of N_{ss} and η are set to match a steady state Frisch labour supply of two.

5.2 Estimated Structural Parameters

The estimation results for our preferred version of the model are reported in the first column of Table 4, where RRA is constrained to a plausible level of ten. We find a standard value for the subjective discount factor ($\beta = 0.994$), and evidence in favor of habit formation in consumption ($b = 0.26$). The preference parameter σ is somewhat high at 39.06, but this reflects the low calibrated value of $\eta = 0.017$, and we therefore find a fairly standard exponent for consumption of $\eta(1 - \sigma) = -0.64$ in (4). These estimates imply that $V_t < 0$, meaning that negative values of α reflect preferences for early resolution of risk. We find $\alpha = -138$, which is very similar to the estimate reported in Andreasen and Jørgensen (2020) when RRA = 10. Our estimate of α is also extremely precise, with a bootstrapped standard error of 3.89. To aid the interpretation of the estimated price adjustment parameter $\phi_P = 163$, Table 4 reports the corresponding Calvo parameter ξ_{Calvo} that implies the same slope of the aggregate supply relation as ϕ_P . We find $\xi_{Calvo} = 0.84$, which corresponds to an average price duration of about 6 quarters. The substitution elasticity θ_μ between intermediate goods is 6.45, which gives an average price markup of about 18%. Finally, the central bank assigns more weight to stabilizing inflation than output growth with $\zeta_\Pi = 1.04$ and $\zeta_{\Delta Y} = 0.39$.

Table 4: Estimated Structural Parameters

This table reports the estimated structural parameters in the New Keynesian model using (16) with $\Lambda = 10^5$, where bootstrapped standard errors are shown in parenthesis. These standard errors are obtained by simulated 196 samples of the same length as in the data from the IVAR model by drawing with replacement from the estimated residuals $\hat{\eta}_t$. From these samples, the required sample moments for the estimator in (16) are generated, where the median target impulse responses, i.e. \mathbf{B}_{MT} , are used to identify uncertainty shocks. The results in column (1) are for the benchmark model where RRA = 10, which implies $u_0 = -1.01$. The results in column (2) are for the standard formulation of recursive preferences with $u_0 = 0$, where the estimates imply an RRA of 124. The estimates of ϕ_P are reported as the corresponding Calvo parameter ξ_{Calvo} , i.e. the probability of not adjusting prices, that gives the same slope of the aggregate supply relation.

		(1)	(2)
	Description	Benchmark model	Standard specification of recursive preferences ($u_0 = 0$)
β	Subjective discount factor	0.994 (0.002)	0.994 (0.002)
b	Habit formation	0.26 (0.04)	0.27 (0.04)
σ	Preference parameter	39.06 (0.30)	38.93 (0.29)
α	Timing attitude	-137.75 (3.08)	-144.37 (3.58)
ϕ_K	Investment adjustment costs	5.50 (0.90)	5.46 (0.90)
ξ_{Calvo}	Price stickiness	0.84 (0.06)	0.84 (0.05)
θ_μ	Substitution elasticity of goods	6.45 (1.59)	6.27 (1.63)
ζ_Π	Weight on inflation gap	1.04 (0.02)	1.04 (0.02)
$\zeta_{\Delta Y}$	Weight on output growth	0.39 (0.05)	0.39 (0.05)
Π_{ss}	Steady state inflation rate	1.015 (0.001)	1.015 (0.001)
Stochastic processes			
ρ_σ	Persistence of uncertainty shock	0.69 (0.08)	0.69 (0.08)
σ_σ	Volatility of uncertainty shock	1.04 (0.03)	1.05 (0.006)
ρ_a	Persistence of demand shock	0.96 (0.01)	0.96 (0.01)
σ_a	Volatility of demand shock $\times 10^3$	0.20 (0.04)	0.22 (0.04)
ρ_z	Persistence of technology shock	0.63 (0.06)	0.62 (0.08)
σ_z	Volatility of technology shock	0.005 (0.0006)	0.006 (0.0009)
ρ_{θ_μ}	Persistent of markup shock	0.68 (0.06)	0.66 (0.06)
σ_{θ_μ}	Volatility of markup shock	0.20 (0.007)	0.20 (0.006)

The second column in Table 4 shows the corresponding estimates when applying the standard formulation of recursive preferences with $u_0 = 0$. We find that the estimates are very similar (but not identical) to those reported for our preferred specification.

The key difference relates to RRA, which is 124 when $u_0 = 0$ and hence comparable to other estimates in the macro literature as in Binsbergen et al. (2012) and Rudebusch and Swanson (2012) but much larger than implied by micro evidence (see, for instance, Barsky et al. (1997)).

5.3 Model Fit

Figure 4 shows the ability of the New Keynesian model to reproduce the median target responses in the IVAR following an uncertainty shock of the same size in recessions and expansions. We find that the model successfully matches the drop in output, consumption, and the substantially larger reduction in investment, which is more severe in recessions than in expansions. This ability of the model to generate state-dependent effects of an uncertainty shock is seen clearly from Figure 5, which compares the responses in the New Keynesian model across expansions and recessions. The model produces also a larger contraction of hours in recessions than in expansions, though it does not quantitatively replicate the contraction estimated with the IVAR.¹⁸ The effects on the price level are well matched in recessions, whereas the responses in expansions are at the lower end of the 90% confidence band. The negative response in the policy rate on impact is perfectly captured by the model, but it generally predicts a less accommodating path for the policy rate following uncertainty shocks than implied by the IVAR.

¹⁸It is well known that without modeling labor market frictions, the response of hours in this type of model tends to be weaker than in the data. See Basu and Bundick (2017) and Fernández-Villaverde and Guerron-Quintana (2020) for discussions on this point.

Figure 4: New Keynesian Model: IRFs to an Uncertainty Shock

This figure shows the impulse response functions following a positive one-standard deviation shock to uncertainty in the IVAR at the median target responses and their 90 percentage confidence bands. The corresponding responses in the the New Keynesian model are computed for $\epsilon_{\sigma,t} = 1$ using the estimates in column (1) of Table 4. The responses are shown for strong expansions (charts to the left) and deep recessions (charts to the right). All responses are shown in percentage deviations, except for the policy rate where changes in percentage points are reported.

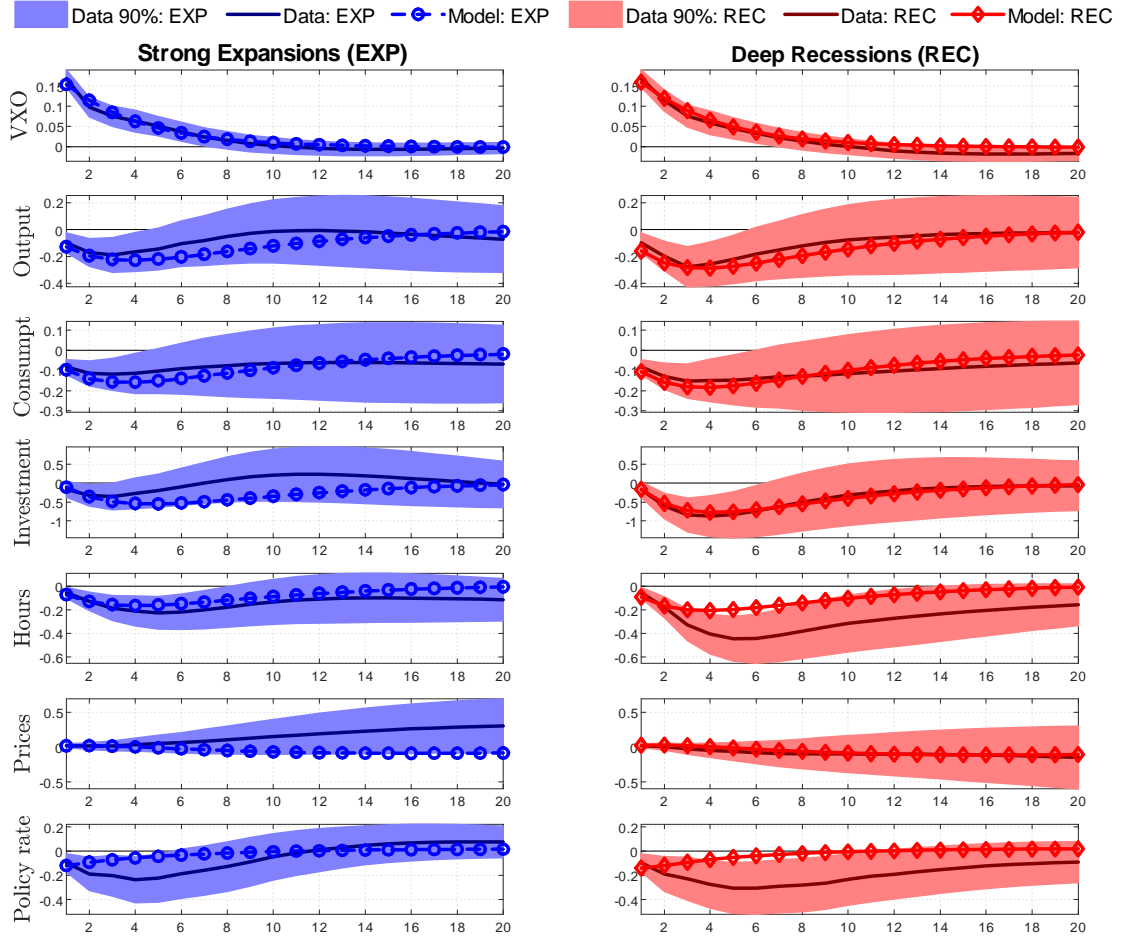
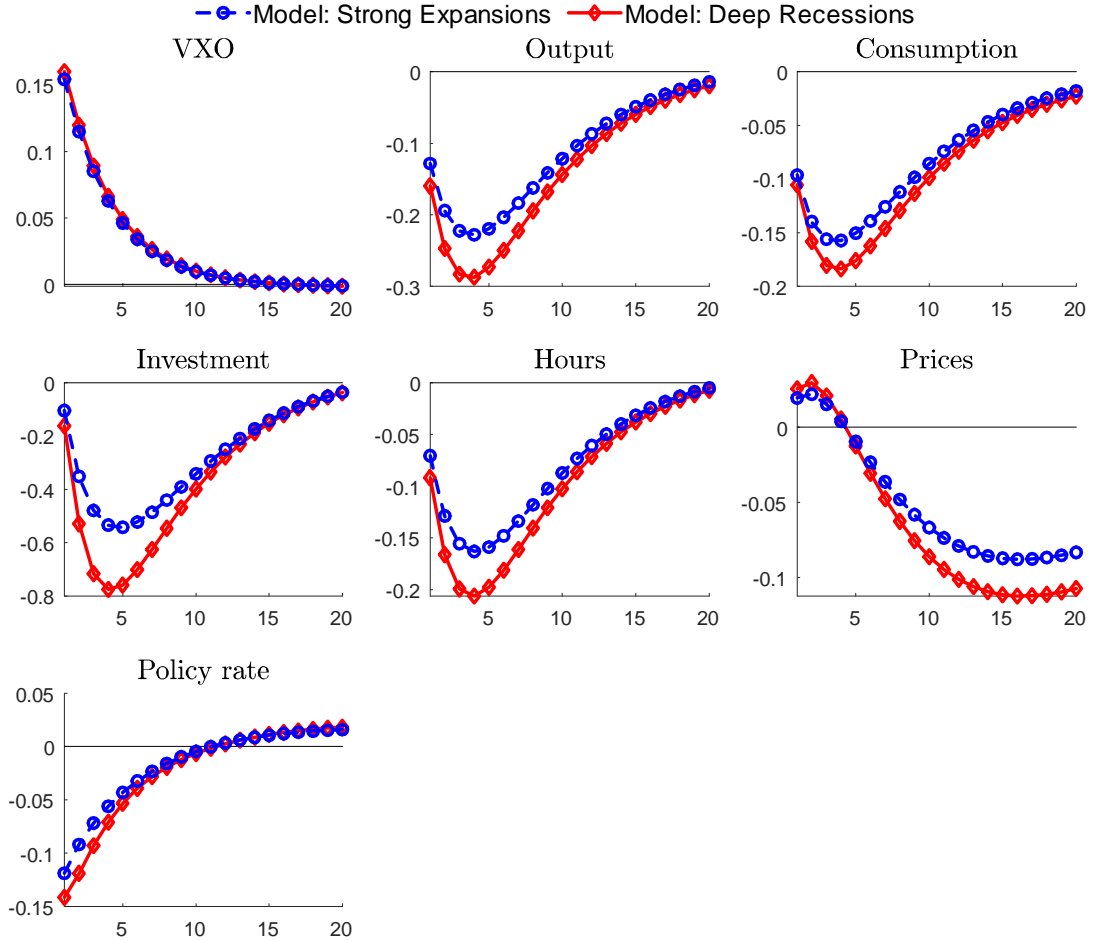


Table 5 reports the means and a scaled version of the second moments that also enter in the estimation. We find that the model closely matches the average level of inflation and the policy rate, while the mean of detrended output, consumption, investment and hours are (by construction) zero and therefore not included. The model is also successful in matching all standard deviations and autocorrelations, and it also captures the cross-correlations of consumption, investment, hours, inflation, and the policy rate with respect to detrended output.

Accordingly, this model goes a long way in reproducing the different impulse responses

Figure 5: New Keynesian Model: A State-Dependent Uncertainty Shock

This figure shows the impulse response functions following a positive one-standard deviation uncertainty shock (i.e. $\epsilon_{\sigma,t} = 1$) in the New Keynesian model using the estimates in column (1) of Table 4. The responses are shown for strong expansions and deep recessions. All responses are shown in percentage deviations, except for the policy rate where changes in percentage points are reported.



of real activity to an uncertainty shock in expansions and recessions, while providing a fairly accurate description of a variety of other macroeconomic moments. Crucially, the differences in these impulse responses between the two states of the business cycle are not explained by changes in the structural parameters or by larger uncertainty shocks in recessions than in expansions. Instead, these asymmetric responses are due to different initial conditions, as captured by the states \mathbf{x}_t , which through the model's endogenous propagation mechanisms make an uncertainty shock more severe in recessions than in expansions.

Table 5: New Keynesian Model: Fit to Unconditional Moments

This table reports the means along with the standard deviations and correlations that are related to the covariances and auto-covariances included in the estimator in (16). The data moments are computed using quarterly US data from 1962Q3 to 2017Q4, while the corresponding model-implied moments are computed in closed form for the means and using a simulated sample of 10,000 observations for the second moments. Moments for output, consumption, investment, and hours are in deviation from steady state, as indicated by the "hat" notation, while the moments for inflation and the policy rate are annualized. The detrending of the moments in US data are done using the procedure in Hamilton (2018).

Moments	(1) Data	(2) Benchmark Model	(3) Standard specification of recursive preferences ($u_0 = 0$)
Means			
$\log \Pi_t$	0.034	0.034	0.033
$\log R_t$	0.051	0.055	0.056
Standard deviations			
\hat{Y}_t	0.034	0.036	0.036
\hat{C}_t	0.022	0.022	0.022
\hat{I}_t	0.101	0.098	0.099
\hat{N}_t	0.032	0.030	0.030
$\log \Pi_t$	0.022	0.025	0.026
$\log R_t$	0.041	0.025	0.026
Cross-correlations			
$corr(\hat{Y}_t, \hat{C}_t)$	0.86	0.68	0.65
$corr(\hat{Y}_t, \hat{I}_t)$	0.86	0.93	0.93
$corr(\hat{Y}_t, \hat{N}_t)$	0.90	0.96	0.96
$corr(\hat{Y}_t, \log \Pi_t)$	-0.38	-0.04	-0.05
$corr(\hat{Y}_t, \log R_t)$	-0.04	0.03	0.02
Auto-correlations			
$corr(\hat{Y}_t, \hat{Y}_{t-1})$	0.92	0.97	0.97
$corr(\hat{C}_t, \hat{C}_{t-1})$	0.90	0.97	0.96
$corr(\hat{I}_t, \hat{I}_{t-1})$	0.91	0.97	0.97
$corr(\hat{N}_t, \hat{N}_{t-1})$	0.91	0.96	0.96
$corr(\log \Pi_t, \log \Pi_{t-1})$	0.99	0.92	0.92
$corr(\log R_t, \log R_{t-1})$	0.97	0.96	0.96

6 Inspecting the Mechanisms

This section identifies the mechanisms in the New Keynesian model that generate larger effects of an uncertainty shock in recessions than in expansions. We first show in Section 6.1 that the state-dependent effects of an uncertainty shock are primarily generated by the upward nominal pricing-bias channel. The economic interpretation of this channel is

presented in Section 6.2, while Section 6.3 provides some external validation that supports the importance of this channel.

6.1 Channels for an Uncertainty Shock

As emphasized by Bianchi et al. (2019), each of the intertemporal Euler-equations in the model reflects expectations to uncertain realizations of state and control variables in the future and hence introduce different channels for an uncertainty shock to affect the economy. This implies that our model has the following channels for uncertainty shocks: i) the precautionary savings channel as captured by the consumption Euler-equation; ii) the nominal upward pricing bias channel as captured by the New Keynesian Phillips curve (NKPC) related to firms' optimality condition for the nominal price; iii) the inflation risk premium channel related to the Fisherian equation; and iv) the investment adjustment channel, that arises due to investment adjustment costs.¹⁹

We evaluate the relative importance of each channel by solving the model as described in Section 4, except that each Euler-equation is linearized one at the time to eliminate its implied channel for uncertainty shocks. For each of these modified solutions, we calculate the differences in the impulse responses between recessions and expansions, and compare them to the baseline case where all channels are active. Our findings are summarized in Figure 6. The results show that omitting the nominal pricing bias channel (the green line with stars) removes nearly all of the asymmetry in the responses between recessions and expansions, whereas none of the other channels have similar profound effects. This shows that the upward nominal pricing bias channel is the crucial channel to generate larger responses of output, consumption, investment, and hours to uncertainty shocks in recessions than in expansions.²⁰

¹⁹The Euler-equation for stock returns may also imply an equity risk premium channel for uncertainty shocks. However, this channel is not present in our New Keynesian model because it omits feedback effects from the stock market to the real economy.

²⁰In the Online Appendix we draw the same conclusion by considering the reverse exercise, where only the upward nominal pricing bias channel is active in the model. The Online Appendix also shows that the upward nominal pricing bias channel does not affect the overall magnitude of the impulse responses to an uncertainty shock but only the state-dependence of these responses.

6.2 A State-Dependent Upward Nominal Pricing Bias Channel

This upward nominal pricing bias channel arises because firms' profit function is asymmetric around the optimum in absence of uncertainty.²¹ Hence, in the presence of uncertainty and sticky prices, it is beneficial for firms to set a relatively high nominal price. That is, firms respond to higher uncertainty by biasing their prices upwards. Our results show that firms bias their prices upward relatively more in recessions than in expansions and hence display a *state-dependent upward nominal pricing bias*. This effect is also evident from Figure 5, as prices in the baseline responses increase by more in recessions than in expansions following the first quarters after the uncertainty shock, whereas this difference disappears in Figure 6 when omitting the upward nominal pricing bias channel. To understand the state-dependent nature of this pricing bias, we first study the firm's pricing problem in a stylized two-period partial equilibrium setting, where the various effects are very transparent. The following subsection then shows that these insights carry over to the full general equilibrium model studied above.

6.2.1 A Two-Period Setting

Consider the following setting for the i th firm, which generalizes the static example in Fernández-Villaverde et al. (2015) and Born and Pfeifer (2020) to two periods and with quadratic price adjustment costs. The firm lives for two periods, and is initially at the deterministic steady state where $\Pi_{ss} = 1$ and $P_{ss} = 1$. No shocks affect real quantities, meaning that marginal costs $MC_t(i)$ and aggregate output Y_t are constant at $(\theta_\mu - 1)/\theta_\mu$ and 1, respectively. The objective of the firm is to set the current price $P_t(i)$ and the future price $P_{t+1}(i)$ when accounting for uncertainty about the aggregate price level in the next period, i.e., P_{t+1} , whereas the current price level is known at $P_t = 1$. The expression for real profit is otherwise identical to the one provided in the full model, except that future profits are discounted by β . Hence, the firm solves the problem

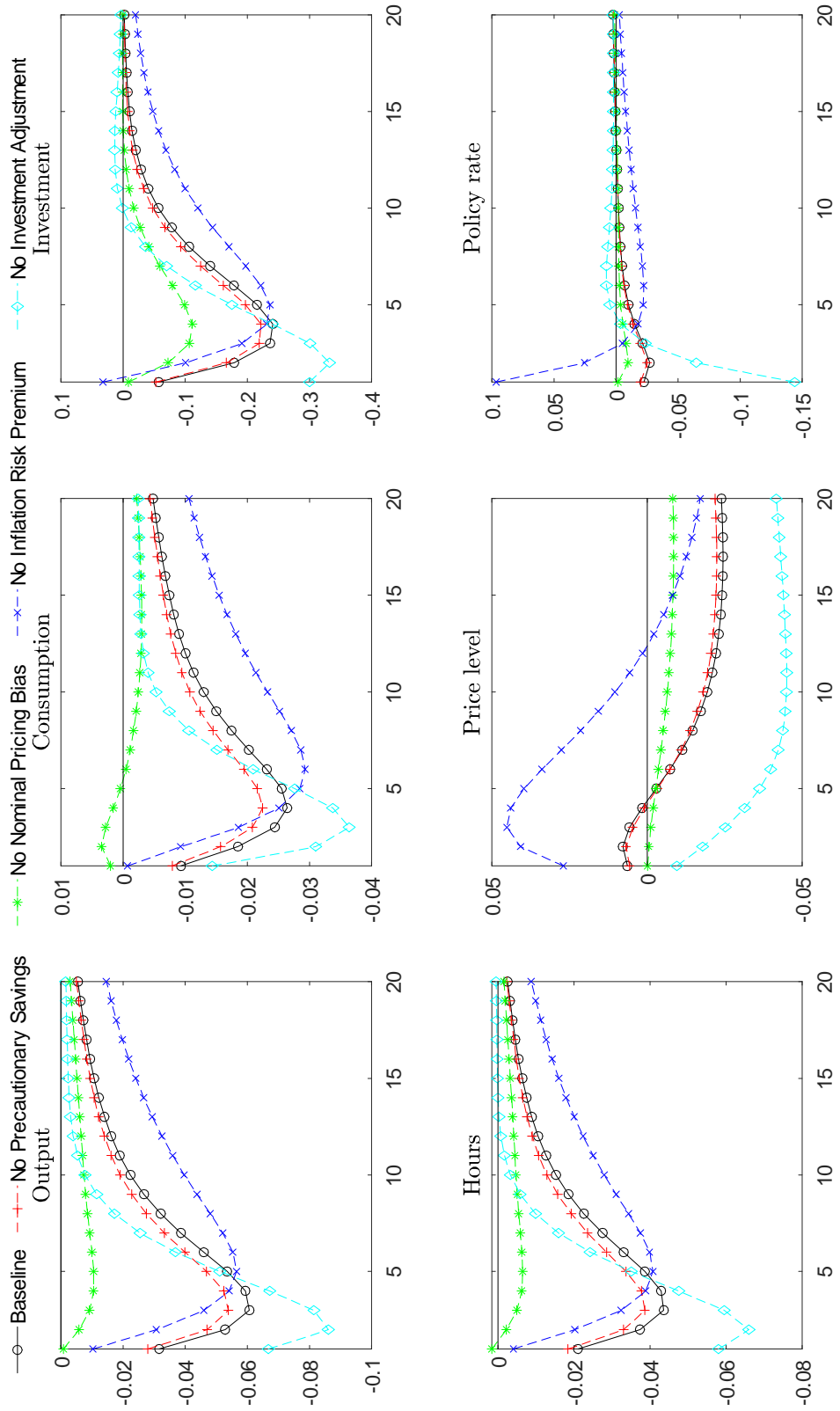
$$\underset{P_t(i), P_{t+1}(i)}{\text{Max}} \quad \sum_{j=\{0,1\}} \mathbb{E}_t \beta^j \left[\left(\frac{P_{t+j}(i)}{P_{t+j}} - \frac{\theta_\mu - 1}{\theta_\mu} \right) \left(\frac{P_{t+j}(i)}{P_{t+j}} \right)^{-\theta_\mu} - \frac{\phi_P}{2} \left(\frac{P_{t+j}(i)}{P_{t-1+j}(i)} - 1 \right)^2 \right]. \quad (17)$$

Suppose that the firm expects an aggregate price level in period $t + 1$ of either $P_{t+1} = P_t + \sigma$ or $P_{t+1} = P_t - \sigma$ with equal probability. Without price adjustment costs ($\phi_P = 0$), it is easy to see that (17) reduces to two static optimization problems, where the current optimal price is $P_t(i) = 1$ (because P_t is known), and the optimal price in the next period $P_{t+1}(i)$ displays the familiar upward pricing bias due to uncertainty about P_{t+1} (see Fernández-Villaverde et al. (2015) and Born and Pfeifer (2020)). To illustrate the

²¹As clarified by Fernández-Villaverde et al. (2015) and Born and Pfeifer (2020), the asymmetry of the profit function is due to the combination of the isoelastic Dixit-Stiglitz demand function and the assumption that demand always has to be satisfied.

Figure 6: New Keynesian Model: Transmission Channels for an Uncertainty Shock

For a positive one-standard deviation uncertainty shock, this figure shows the difference in the responses between recessions and expansions. The baseline case is when all channels for uncertainty shocks are present in the model. A given channel is removed from this baseline by solving the model using a third-order approximation at the risky steady state with the modification that the Euler-equation for a particular channel is only linearized. All responses are computed using the estimates in column (1) of Table 4 for the New Keynesian model.



effects of accounting for price stickiness, we let $\theta_\mu = 6$, $\phi_P = 163$, and $\beta = 0.994$ as implied by our estimates in Table 4. The first chart in Figure 7 shows the profit function for different values of the current price $P_t(i)$ around the optimum of $P_{t+1}(i)$. The novel observation is that this profit function is asymmetric around one as $\phi_P > 0$, despite the aggregate price level P_t is known. In contrast, without price stickiness $\phi_P = 0$, the profit function is perfectly symmetric around one with a known price level, as shown in the Online Appendix. The second chart in Figure 7 plots the entire profit function and reveals that both $P_t(i)$ and $P_{t+1}(i)$ display upwards pricing biases. Thus, although there is no uncertainty about the current price level P_t , the presence of price stickiness makes it optimal for the firm to bias its current price upwards to smooth out its price adjustment costs. In other words, uncertainty about the aggregate price level in the next period is sufficient to generate an upward pricing bias in the current price $P_t(i)$. This is an important observation because it corresponds to the situation in the full general equilibrium model, as firms realize that uncertainty will be higher in the next period but already in the current period decide to bias their prices upwards.

Figure 7: The Firm's Profit Function

This figure plots the firm's profit function as stated in (17), where $P_t = 1$ and the aggregate price level in the next period is uncertain and given by either $P_{t+1} = P_t + \sigma$ or $P_{t+1} = P_t - \sigma$ with equal probability. The applied values are $\theta_\mu = 6$, $\phi_P = 163$, and $\beta = 0.994$.

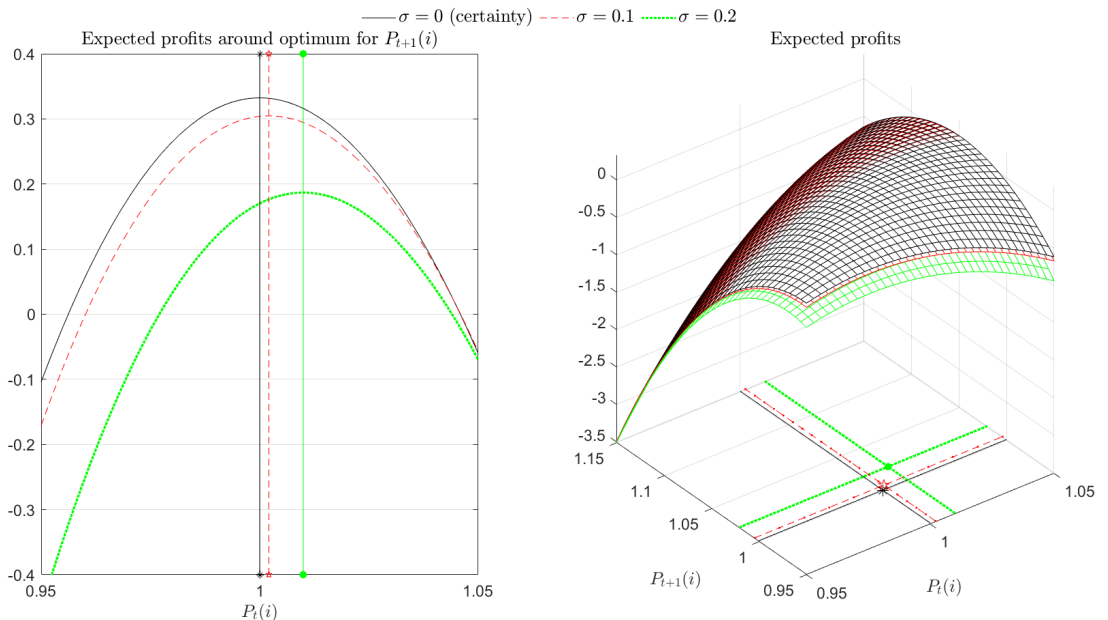


Figure 7 also shows that these pricing biases are increasing in the amount of uncertainty about P_{t+1} - and hence future inflation $\Pi_{t+1} \equiv P_{t+1}/P_t$ - as captured by higher values of σ . This finding is closely related to the result in Born and Pfeifer (2020), who show that higher uncertainty about the aggregate price level generates a higher upward

pricing bias within their static setting. Unreported results also reveal that the pricing biases in $P_t(i)$ and $P_{t+1}(i)$ are increasing for higher values of β , because it increases the importance of the price adjustment costs. Hence, in a more elaborated setting where firms discount profits by a stochastic discount factor, higher values of this discount factor in recessions (due to low consumption and high marginal utility) will increase the pricing bias in $P_t(i)$, and vice versa for expansions with a low discount factor (due to high consumption and low marginal utility).

6.2.2 The Full Model

To understand the determinants behind this state-dependent pricing bias in the full model, let us look at the NKPC which reads

$$\phi_P \left(\frac{\Pi_t}{\Pi_{ss}} - 1 \right) \frac{\Pi_t}{\Pi_{ss}} = (1 - \theta_{\mu,t}) + \frac{\theta_{\mu,t}}{\mu_t} + \mathbb{E}_t \left[M_{t+1} \phi_P \frac{Y_{t+1}}{Y_t} \left(\frac{\Pi_{t+1}}{\Pi_{ss}} - 1 \right) \frac{\Pi_{t+1}}{\Pi_{ss}} \right]. \quad (18)$$

An uncertainty shock enters in this equation through the term with the conditional expectation, i.e., $\mathbb{E}_t \left[M_{t+1} \phi_P \frac{Y_{t+1}}{Y_t} \left(\frac{\Pi_{t+1}}{\Pi_{ss}} - 1 \right) \frac{\Pi_{t+1}}{\Pi_{ss}} \right]$, which captures the nominal pricing bias. To simplify the interpretation of this term, we show in the Online Appendix that the presence of Y_{t+1}/Y_t does not affect the impulse responses for an uncertainty shock, implying that it is sufficient to study the term $P_t^\Pi \equiv \mathbb{E}_t \left[M_{t+1} \phi_P \left(\left(\frac{\Pi_{t+1}}{\Pi_{ss}} \right)^2 - \frac{\Pi_{t+1}}{\Pi_{ss}} \right) \right]$. One way to analyze this term is to note that P_t^Π is equivalent to the price of a hypothetical asset with pay-off $\phi_P \left(\left(\frac{\Pi_{t+1}}{\Pi_{ss}} \right)^2 - \frac{\Pi_{t+1}}{\Pi_{ss}} \right)$. This pay-off increases monotonically for higher values of Π_{t+1} (with slope coefficient $\phi_P (2\Pi_{t+1}/\Pi_{ss}^2 - 1/\Pi_{ss})$), implying that P_t^Π represents the price for the firm of buying protection against high inflation in the future. The value of this asset can be decomposed as

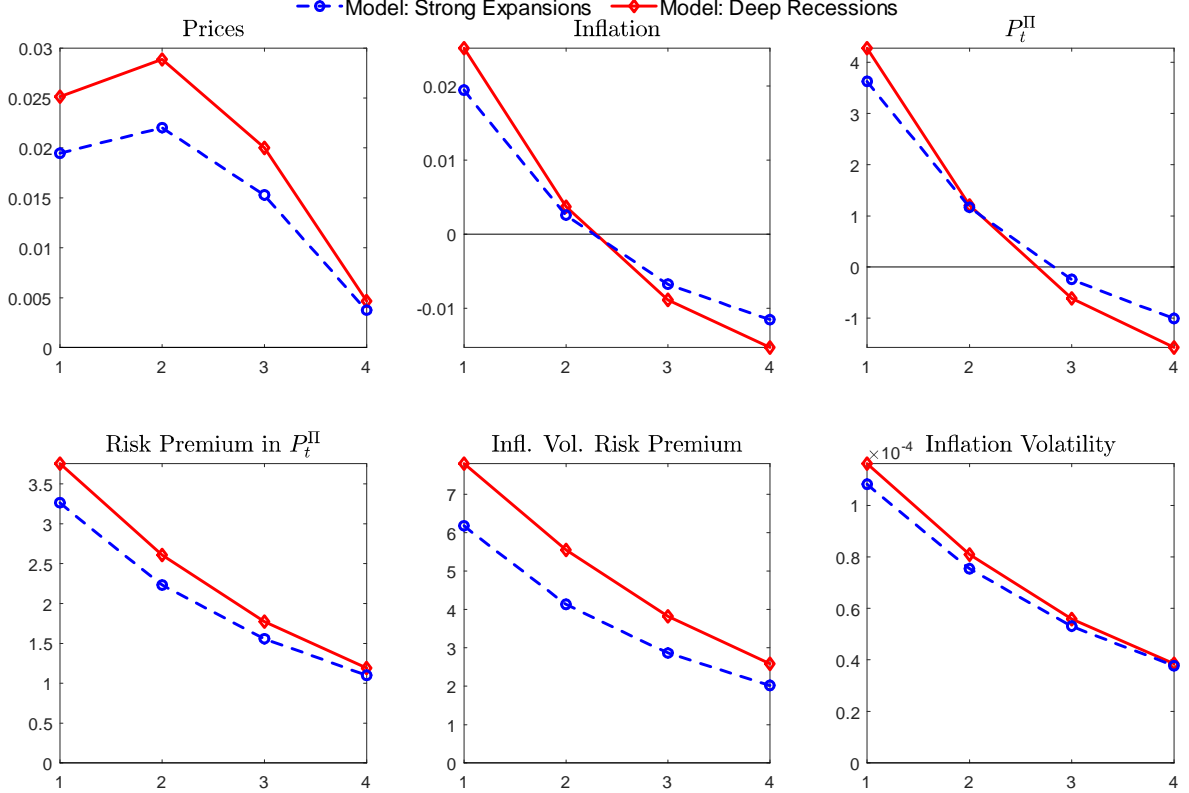
$$P_t^\Pi = \underbrace{\frac{1}{R_t^R} \mathbb{E}_t \left[\phi_P \left(\left(\frac{\Pi_{t+1}}{\Pi_{ss}} \right)^2 - \frac{\Pi_{t+1}}{\Pi_{ss}} \right) \right]}_{\text{Risk-neutral price}} + \underbrace{\text{Cov}_t \left[M_{t+1}, \phi_P \left(\left(\frac{\Pi_{t+1}}{\Pi_{ss}} \right)^2 - \frac{\Pi_{t+1}}{\Pi_{ss}} \right) \right]}_{\text{Risk premium}}, \quad (19)$$

where $R_t^R = 1/\mathbb{E}_t [M_{t+1}]$ denotes the gross real interest rate. The first term on the right hand side in (19) is the risk-neutral price of this hypothetical asset with its expected pay-off discounted by the real rate. The second term is the additional price that a risk-averse investor is willing to pay for inflation protection and constitutes a risk premium. The unconditional mean of this risk premium is 1.9% in the model, but it displays considerable counter-cyclical variation with a low mean of 0.9% in expansions and a high mean of 3.7% in recessions.

The top row of Figure 8 shows that the asymmetric responses of prices and inflation to an uncertainty shock go hand in hand with the asymmetric response of the price of this hypothetical asset P_t^Π . In the bottom row of this figure, we further show that

Figure 8: New Keynesian Model: Determinants of the Upward Pricing Bias

This figure shows the impulse response functions following a positive one-standard deviation uncertainty shock (i.e. $\epsilon_{\sigma,t} = 1$) in the New Keynesian model using the estimates in column (1) of Table 4. The responses are shown for strong expansions and deep recessions. The risk premium in P_t^Π is given by $\text{Cov}_t \left[M_{t+1}, \phi_P \left(\left(\frac{\Pi_{t+1}}{\Pi_{ss}} \right)^2 - \frac{\Pi_{t+1}}{\Pi_{ss}} \right) \right]$, the inflation volatility risk premium is defined as $\text{Cov}_t \left[M_{t+1}, \phi_P \left(\frac{\Pi_{t+1}}{\Pi_{ss}} \right)^2 \right]$, and inflation volatility is measured by $\mathbb{V}_t [\Pi_{t+1}]$. The responses of prices and inflation are shown in percentage deviations, whereas the other response are scaled by 100 and shown in absolute deviations.



these asymmetric responses in P_t^Π are generated by the risk premium. The dominating term in this risk premium is the squared term for inflation, i.e., $\text{Cov}_t \left[M_{t+1}, \phi_P \left(\frac{\Pi_{t+1}}{\Pi_{ss}} \right)^2 \right]$, which can be interpreted as an inflation volatility risk premium. To understand why this conditional covariance displays larger responses in recessions than in expansions, we exploit two insights from the simplified two-period setting discussed above.

First, the inflation volatility risk premium is closely related to the amount of inflation volatility, which increases the pricing bias as shown in Section 6.2.1. One way to measure the degree of inflation volatility is to compute the conditional variance of inflation $\mathbb{V}_t [\Pi_{t+1}]$. We find that the mean of $\mathbb{V}_t [\Pi_{t+1}]$ in recessions is 19% higher than the mean in expansions, showing that recessions in the New Keynesian model are characterized by much more inflation volatility than expansions.²² The process for stochastic volatility

²²This is consistent with empirical evidence, both when measuring inflation volatility by the interquar-

$\sigma_{a,t}$ contributes in two important ways to generate this asymmetry. First, recessions have a higher value of $\sigma_{a,t}$ than expansions, implying that an equal-size preference shock $\epsilon_{a,t+1}$ is expected to have a larger impact on inflation in recessions than in expansions. Second, the bottom right chart in Figure 8 shows that an uncertainty shock increases inflation volatility by more in recessions than in expansions.

Second, another key driver of the inflation volatility risk premium is the dynamics of the stochastic discount factor M_{t+1} . In the New Keynesian model, we find that the realized values of M_{t+1} have a higher level in recessions than in expansions due to lower consumption and higher marginal utility than in expansions. As shown in Section 6.2.1, a higher value of the discount factor increases the weight in the profit function to the intertemporal smoothing of the pricing bias, and as a result helps to generate a larger upward pricing bias in recessions than in expansions.

Thus, the economic intuition behind the state-contingent upward nominal pricing bias is as follows. With price stickiness as in Rotemberg (1982), firms can reset their prices in every period but face costs when doing so. In this multiperiod setting, inflation volatility affects the current price, because it is optimal for firms to set higher prices after an uncertainty shock to avoid large expensive future increases in prices. Two effects help to make this pricing bias stronger in recessions than expansions. First, inflation volatility is higher in recessions than in expansions. Second, firms discount future profits by the stochastic discount factor, which has a higher level in recessions than in expansions. This implies that firms assign more weight to future profits, which also helps to increase their pricing bias by more in recessions than in expansions.

6.3 External Validation of the Key Mechanism

The reduction in real activity following uncertainty shocks implies that wages and the rental rate of capital also fall in the New Keynesian model (not shown). With higher prices, we therefore see a higher price markup, which Fernández-Villaverde et al. (2015) and Basu and Bundick (2017) show is the key driver behind the real effects of uncertainty shocks in the model, although Born and Pfeifer (2020) challenge this effect. Our finding that the upward nominal pricing bias is state-contingent helps to clarify how this channel works across the business cycle. This is illustrated in Figure 9, which shows that the price markup increases by more in recessions than in expansions (top chart to the left), and that this difference disappears when we omit the state-contingent nominal pricing bias (top chart to the right).

Thus, a simple way to validate the key mechanism in the New Keynesian model for generating asymmetric responses to an uncertainty shock is to explore if the price markup

the range of the one quarter ahead forecast of inflation in the Survey of Professional Forecasts or by a GARCH(1,1) model applied to the residuals of an autoregression with four lags for CPI inflation.

in the US displays asymmetric effects across the business cycle. We implement this external validation of the model by extending the IVAR with the price markup, which we measure by the inverse of the labor share in the business sector as in Fernández-Villaverde et al. (2015). Similar to our baseline analysis in Section 2, we allow the responses of the price markup and the other variables in the IVAR to change across the business cycle. The middle row in Figure 9 reports the median target responses for the price markup in expansions and recessions along with their 90 percent confidence bands. The responses in recessions are much larger than in expansions, in particular after the first four quarters. This is seen clearly from the bottom left chart in Figure 9, which shows that the median target response in recessions is substantially above the response in expansions. The bottom right chart shows that the differences in these median target responses are significant at the 90% level. Thus, the dynamic responses of the price markup in the US appear to be consistent with the predictions from the New Keynesian model, which leaves further support for the presence of a state-contingent upward nominal pricing bias.²³

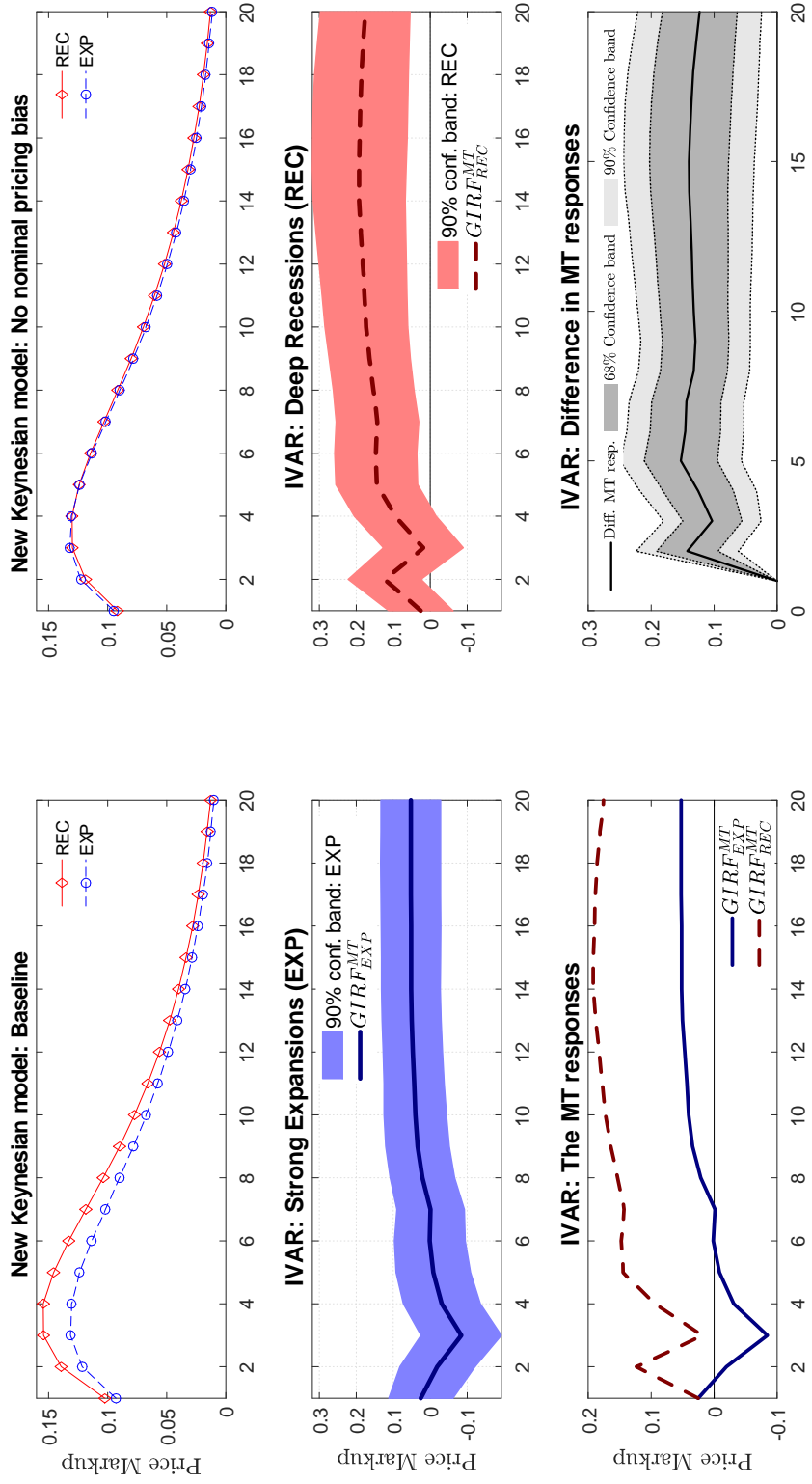
7 Conclusion

This paper employs a nonlinear VAR and a non-recursive identification strategy using a combination of narrative, correlation, and sign restrictions to show that the real effects of an uncertainty shock are stronger when growth is low (as in recessions) than when growth is high (as in expansions). An estimated medium-scale New Keynesian model approximated to third order around the risky steady state goes a long way in reproducing these state-dependent impulse responses to an uncertainty shock. The key mechanism is that firms display a stronger nominal upward pricing bias in recessions than in expansions, as firms face more inflation uncertainty and have a higher value of the discount factor in these states of the business cycle. This leads firms to post higher prices through higher markups in recessions when compared to expansions, which then worsens the real effects of an uncertainty shock in recessions. This prediction is supported by a nonlinear VAR that produces a larger response in an empirical measure of the price markup in recessions than in expansions following an uncertainty shock.

²³In the Online Appendix, we further show that the only channel that eliminates the state-dependent responses of the price markup to an uncertainty shock is the nominal upward pricing bias channel.

Figure 9: Price Markup

This figure shows the generalized impulse response functions for the price markup in percent to a one-standard deviation uncertainty shock. The top row shows the responses in the baseline New Keynesian model (to the left) and when omitting the nominal pricing bias (to the right) using the estimates in column (1) of Table 4. The charts in the middle row show the median target (MT) responses in the extended IVAR during strong expansions (to the left) and deep recessions (to the right) along with the 90% confidence bands. At the bottom row, the differences in the median target responses in the IVAR are reported (to the left), while the difference in these responses between deep recessions and strong expansions are shown to the right along with the bootstrapped 68% and 90% confidence bands.



References

- Alessandri, P. and Mumtaz, H. (2019), ‘Financial regimes and uncertainty shocks’, *Journal of Monetary Economics* **101**, 31–46.
- Andreasen, M. M. (2012), ‘On the effects of rare disasters and uncertainty shocks for risk premia in non-linear dsge models’, *Review of Economic Dynamics* **15(3)**, 295–316.
- Andreasen, M. M., Fernández-Villaverde, J. and Rubio-Ramírez, J. F. (2018), ‘The pruned state-space system for non-linear dsge models: Theory and empirical applications’, *Review of Economic Studies* **85(1)**, 1–49.
- Andreasen, M. M. and Jørgensen, K. (2020), ‘The importance of timing attitudes in consumption-based asset pricing models’, *Journal of Monetary Economics* **111**, 95–117.
- Antolín-Díaz, J. and Rubio-Ramírez, J. F. (2018), ‘Narrative sign restrictions’, *American Economic Review* **108(10)**, 2802–2829.
- Aruoba, S., Bocola, L. and Schorfheide, F. (2017), ‘Assessing DSGE Model Nonlinearities’, *Journal of Economic Dynamics & Control* **83**, 34–54.
- Barrero, J. M. and Bloom, N. (2020), ‘Economic uncertainty and recovery’, **Jackson Hole Economic Policy Symposium Paper, August**.
- Barsky, R., Juster, F., Kimball, M. and Shapiro, M. (1997), ‘Preference parameters and behavioral heterogeneity: An experimental approach in the health and retirement study’, *Quarterly Journal of Economics* **112(2)((2))**, 537–579.
- Basu, S. and Bundick, B. (2017), ‘Uncertainty shocks in a model of effective demand’, *Econometrica* **85(3)**, 937–958.
- Basu, S. and Bundick, B. (2018), ‘Uncertainty shocks in a model of effective demand: Reply’, *Econometrica* **86(4)**, 1527–1531.
- Bianchi, F., Kung, H. and Tirsikh, M. (2019), ‘The origins and effects of macroeconomic uncertainty’, **Duke University and London Business School, available at <https://sites.google.com/view/francescobianchi/home>**.
- Binning, A. (2013), ‘Solving second and third-order approximations to dsge models: A recursive sylvester equation solution’, **Norges Bank Working Paper No. 18**.
- Binsbergen, J. H. V., Fernández-Villaverde, J., Koijen, R. S. and Rubio-Ramírez, J. (2012), ‘The term structure of interest rates in a dsge model with recursive preferences’, *Journal of Monetary Economics* **59(7)**, 634–648.

- Bloom, N. (2009), ‘The impact of uncertainty shocks’, *Econometrica* **77(3)**, 623–685.
- Bloom, N. (2014), ‘Fluctuations in uncertainty’, *Journal of Economic Perspectives* **28(2)**, 153–176.
- Born, B. and Pfeifer, J. (2014), ‘Risk matters: The real effects of volatility shocks: Comment’, *American Economic Review* **104(12)**, 4231–4239.
- Born, B. and Pfeifer, J. (2020), ‘Uncertainty-driven business cycles: assessing the markup channel’, *Quantitative Economics* **forthcoming**.
- Cacciatore, M. and Ravenna, F. (2020), ‘Uncertainty, wages, and the business cycle’, *Economic Journal* **forthcoming**.
- Caggiano, G., Castelnuovo, E. and Groshenny, N. (2014), ‘Uncertainty shocks and unemployment dynamics: An analysis of post-wwii u.s. recessions’, *Journal of Monetary Economics* **67**, 78–92.
- Coeurdacier, N., Rey, H. and Winant, P. (2011), ‘The Risky Steady State’, *American Economic Review: Papers & Proceedings* **101(3)**, 398–401.
- Collard, F. and Juillard, M. (2001*a*), ‘Accuracy of stochastic perturbation methods: The case of asset pricing models’, *Journal of Economic Dynamics and Control* **25(6-7)**, 979–999.
- Collard, F. and Juillard, M. (2001*b*), ‘A higher-order taylor expansion approach to simulation of stochastic forward-looking models with an application to a nonlinear phillips curve model’, *Computational Economics* **17(2-3)**, 125–139.
- de Groot, O. (2013), ‘Computing The Risky Steady State of DSGE Models’, *Economic Letter* **120(3)**, 566–569.
- de Groot, O. (2016), ‘What order? perturbation methods for stochastic volatility asset pricing and business cycle models’, **Centre for Dynamic Macroeconomic Analysis Working Paper No. 201606**.
- de Groot, O., Richter, A. W. and Throckmorton, N. A. (2018), ‘Uncertainty shocks in a model of effective demand: Comment’, *Econometrica* **86(4)**, 1513–1526.
- Diercks, A. M., Hsu, A. and Tamoni, A. (2020), ‘When it rains it pours: Cascading uncertainty shocks’, **available at <https://andreatamoni.meltinbit.com/>**.
- Epstein, L. and Zin, S. (1989), ‘Substitution, risk aversion, and the temporal behavior of consumption and asset returns: A theoretical framework’, *Econometrica* **57(4)**, 937–969.

- Fernández-Villaverde, J. and Guerron-Quintana, P. (2020), ‘Uncertainty shocks and business cycle research’, *Review of Economic Dynamics* **forthcoming**.
- Fernández-Villaverde, J., Guerrón-Quintana, P., Kuester, K. and Rubio-Ramírez, J. F. (2015), ‘Fiscal volatility shocks and economic activity’, *American Economic Review* **105(11)**, 3352–3384.
- Fernández-Villaverde, J., Guerrón-Quintana, P., Rubio-Ramírez, J. F. and Uribe, M. (2011), ‘Risk matters: The real effects of volatility shocks’, *American Economic Review* **101**, 2530–2561.
- Fry, R. and Pagan, A. (2011), ‘Sign restrictions in structural vector autoregressions: A critical review’, *Journal of Economic Literature* **49(4)**, 938–960.
- Guerron-Quintana, P. A., Khazanov, A. and Zhong, M. (2021), ‘Nonlinear Dynamic Factor Models’, *Working Paper* pp. 1–34.
- Hamilton, J. D. (2018), ‘Why you should never use the hodrick-prescott filter’, *Review of Economics and Statistics* **100**, 831–843.
- King, R. G., Plosser, C. I. and Rebelo, S. T. (2002), ‘Production, growth and business cycles: Technical appendix’, *Computational Economics* **20**, 87–116.
- Koop, G., Pesaran, M. and Potter, S. (1996), ‘Impulse response analysis in nonlinear multivariate models’, *Journal of Econometrics* **74(1)**, 119–147.
- Levintal, O. (2017), ‘Fifth-order perturbation solution to dsge models’, *Journal of Economic Dynamics and Control* **80**, 1–16.
- Ludvigson, S. C., Ma, S. and Ng, S. (2019), ‘Uncertainty and business cycles: Exogenous impulse or endogenous response?’, *American Economic Journal: Macroeconomics* **forthcoming**.
- Rotemberg, J. J. (1982), ‘Monopolistic price adjustment and aggregate output’, *Review of Economic Studies* **49**, 517–531.
- Rubio-Ramírez, J. F., Waggoner, D. F. and Zha, T. (2010), ‘Structural vector autoregressions: Theory of identification and algorithms for inference’, *Review of Economic Studies* **77**, 665–696.
- Rudebusch, G. D. and Swanson, E. T. (2012), ‘The bond premium in a dsge model with long-run real and nominal risks’, *American Economic Journal: Macroeconomics* **4(1)**, 105–143.

- Salgado, S., Guvenen, F. and Bloom, N. (2019), ‘Skewed Business Cycles’, *NBER Working Paper* (No. 26565).
- Schmitt-Grohe, S. and Uribe, M. (2004), ‘Solving dynamic general equilibrium models using a second-order approximation to the policy function’, *Journal of Economic Dynamics and Control* **28**, 755–775.
- Swanson, E. T. (2018), ‘Risk aversion, risk premia, and the labor margin with generalized recursive preferences’, *Review of Economic Dynamics* **28**, 290–321.
- Weil, P. (1990), ‘Nonexpected utility in macroeconomics’, *Quarterly Journal of Economics* **105(1)**, 29–42.
- Wu, J. C. and Xia, F. D. (2016), ‘Measuring the macroeconomic impact of monetary policy at the zero lower bound’, *Journal of Money, Credit, and Banking* **48(2-3)**, 253–291.

Online Appendix (not for publication): Why Does Risk Matter More in Recessions than in Expansions?

Martin M. Andreasen* Giovanni Caggiano[†]

Efrem Castelnuovo[‡] Giovanni Pellegrino[§]

1 The Interacted VAR

1.1 Computing the Generalized Impulse Response Functions

The algorithm for computing the generalized impulse response functions (GIRFs) follows the steps suggested by Koop, Pesaran & Potter (1996), and it is designed to simulate the effects of an orthogonal structural shock as in Kilian and Vigfusson (2011). The idea is to compute the empirical counterpart of the theoretical $GIRF_{\mathbf{Y}}(h, \delta, \boldsymbol{\omega}_{t-1})$ of the vector of endogenous variables \mathbf{Y}_t , h periods ahead, for a given initial condition $\boldsymbol{\omega}_{t-1} = \{\mathbf{Y}_{t-1}, \dots, \mathbf{Y}_{t-L}\}$. Below, we use the notation that L is the number of lags in the IVAR, and δ_{unc} is size of the structural shock hitting at time t . Following Koop et al. (1996), such GIRF can be expressed as

$$GIRF_{\mathbf{Y}}(h, \delta_{unc}, \boldsymbol{\omega}_{t-1}) = \mathbb{E}[\mathbf{Y}_{t+h} | \delta_{unc}, \boldsymbol{\omega}_{t-1}] - \mathbb{E}[\mathbf{Y}_{t+h} | \boldsymbol{\omega}_{t-1}], \quad (1)$$

where $\mathbb{E}[\cdot]$ is the expectation operator, and $h = 0, 1, \dots, H$ indicates the horizons at which the GIRF are computed. We compute the GIRFs as follows:

1. We pick a matrix $\hat{\mathbf{B}}$ among the set of retained matrices that satisfy our identifying restrictions, as stated in the main paper;
2. Conditioning on a $\boldsymbol{\omega}_{t-1}$ and the IVAR, we randomly extract (with repetition) residuals $\left\{ \left\{ \tilde{\boldsymbol{\eta}}_{t+h}^s \right\}_{s=1}^{500} \right\}_{h=0}^{19}$ from $d(0, \hat{\boldsymbol{\Omega}})$, where $\hat{\boldsymbol{\Omega}}$ is the estimated covariance matrix and $d(\cdot)$ is the empirical distribution of the residuals. We use these residuals to simulate 500 realizations of $\left\{ \mathbf{Y}_{t+h}^s | \boldsymbol{\omega}_{t-1} \right\}_{s=1}^{500}$ for $h = \{0, 1, \dots, 19\}$;
3. Given the residuals $\left\{ \left\{ \tilde{\boldsymbol{\eta}}_{t+h}^s \right\}_{s=1}^{500} \right\}_{h=0}^{19}$ from step 2, we transform them to the structural shocks by using the relation $\mathbf{e}_t^s = \hat{\mathbf{B}}^{-1} \tilde{\boldsymbol{\eta}}_t^s$. At the position in \mathbf{e}_t^s which corresponds to the uncertainty shock, denoted $e_{unc,t}^s$, we add the quantity δ_{unc} . Then we transform the structural shocks back to the IVAR residuals using $\hat{\mathbf{B}} \mathbf{e}_t^s = \tilde{\boldsymbol{\eta}}_t^s$, which we use to compute $\left\{ \mathbf{Y}_{t+h}^s | \delta, \boldsymbol{\omega}_{t-1} \right\}_{s=1}^{500}$;
4. We then estimate the GIRFs conditional on $\boldsymbol{\omega}_{t-1}$ as $\widehat{GIRF}^{\mathbf{B}}_{\mathbf{Y}}(h, \delta_{unc}, \boldsymbol{\omega}_{t-1}) = \frac{1}{500} \sum_{s=1}^{500} (\mathbf{Y}_{t+h}^s | \delta_{unc}, \boldsymbol{\omega}_{t-1} - \mathbf{Y}_{t+h}^s | \boldsymbol{\omega}_{t-1})$ for $h = \{0, 1, \dots, 19\}$;

*Aarhus University, CREATES, and the Danish Finance Institute. Email: mandreasen@econ.au.dk.

[†]Monash University and the University of Padova. Email: giovanni.caggiano@monash.edu.

[‡]The University of Melbourne and the University of Padova. Email: efrem.castelnuovo@gmail.com.

[§]Aarhus University. Email: gpellegrino@econ.au.dk.

5. We repeat steps 2-4 for all the initial conditions ω_{t-1} that belong to two subsets. An initial condition $\omega_{t-1} = \{\mathbf{Y}_{t-1}, \dots, \mathbf{Y}_{t-L}\}$ is classified to belong to "deep contractions" if $\Delta \ln GDP_{t-1}$ is in the bottom decile of the quarter-on-quarter GDP growth rate for the empirical distribution and to "strong expansions" if $\Delta \ln GDP_{t-1}$ is in the top decile of the quarter-on-quarter GDP growth for the rate empirical distribution;
6. We take the average of the GIRFs obtained in step 5 over the initial states that belong to either deep contractions or strong expansions, i.e., $\widehat{GIRF}^{\mathbf{B}_Y}(h, \delta_{unc}, \Omega_{t-1}^{contr.})$ and $\widehat{GIRF}^{\mathbf{B}_Y}(h, \delta_{unc}, \Omega_{t-1}^{exp.})$, respectively;
7. We repeat steps 2-6 for each matrix $\hat{\mathbf{B}}$ that satisfies our identifying restrictions to obtain the identified set.

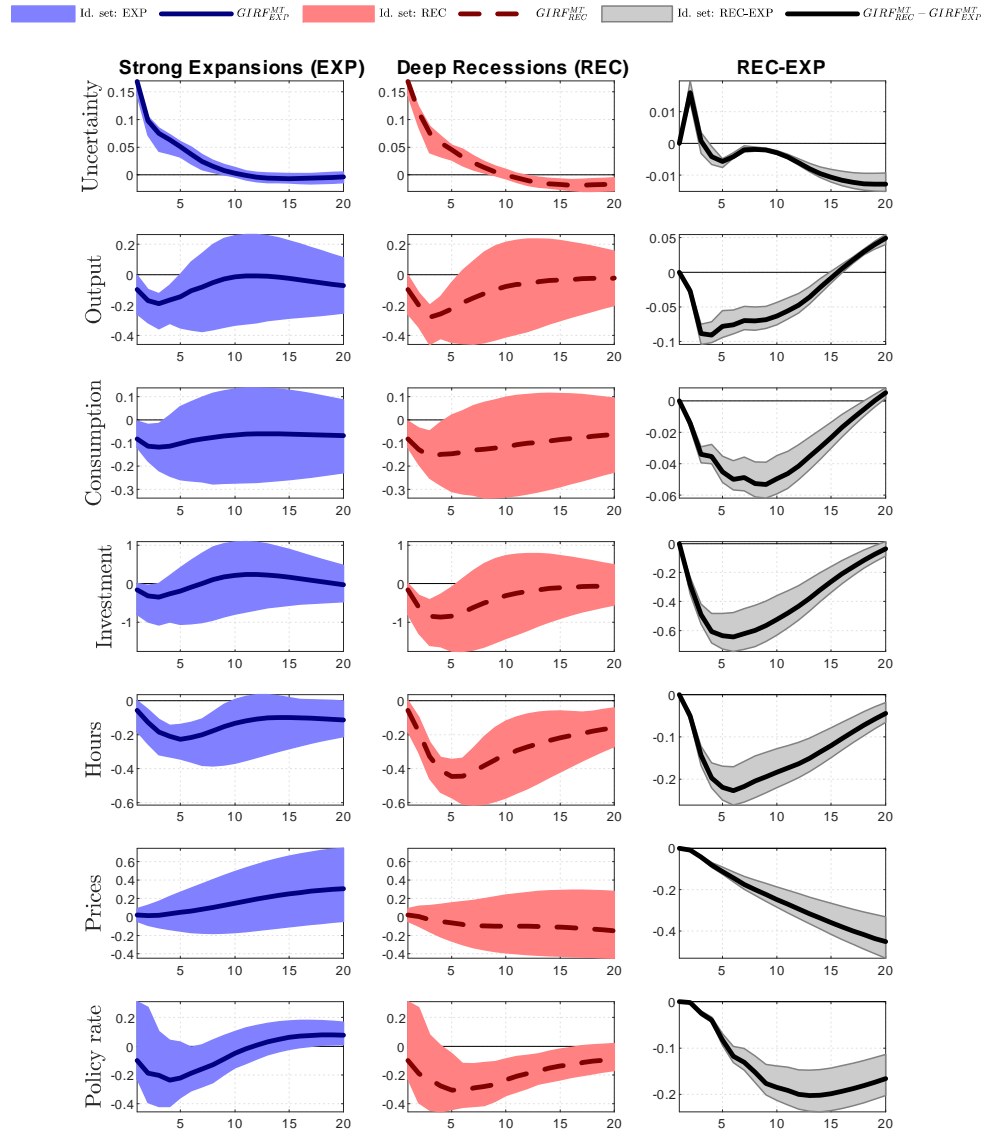
To plot a summary state-dependent GIRF out of the identified set, we use the Median Target (MT) response proposed by Fry & Pagan (2011) on our IVAR. That is, we select GIRFs that correspond to the single $\hat{\mathbf{B}}$ which minimizes the distance to the responses implied by the median of the identified set in recessions and expansions. This matrix is denoted $\hat{\mathbf{B}}^{MT}$. As mentioned in our paper, we compute confidence bands for the MT GIRFs by running a residual-based bootstrap. That is, we use a residual-based bootstrap of the IVAR to simulate $R = 1,000$ samples of the same length as in our empirical sample.¹ Then, for each simulated sample, we estimate the IVAR and compute the GIRFs for an uncertainty shock as outlined above. When implementing this procedure, the initial conditions and the covariance matrix for the IVAR residuals now depend on the particular dataset r , i.e., ω_{t-1}^r and Ω_t^r . This means that in the procedure rather than using the $\hat{\mathbf{B}}^{MT}$, we use the rotation \mathbf{Q}^{MT} which corresponds to the MT response, i.e., we use $\hat{\mathbf{B}}^{r,MT} = \mathbf{P}^s \mathbf{Q}^{MT}$ with \mathbf{P}^s being the unique lower-triangular Cholesky factor associated to Ω_t^r , i.e., $\Omega_t^r = \mathbf{P}^r \mathbf{P}^{r'}$.

In the main paper we only show median target responses and a test for their difference that (only) accounts for estimation (or sampling) uncertainty by using this residual-based bootstrap. Figure 1 instead shows our identified set for the state-dependent responses and their difference for the whole identified set, which (only) accounts for model uncertainty, i.e., the uncertainty related to all the responses in the identified set. As the results show, *all* models belonging to the identified set suggest a stronger response of real activity to an uncertainty shock in recessions. This means that model uncertainty is not an important source of uncertainty as regards the difference of our state-dependent median target responses.

¹The bootstrap used is similar to the one used by Christiano, Eichenbaum, and Evans (1999) (see their footnote 23). The code discards the explosive artificial draws to be sure that exactly 1,000 draws are used. In our simulations, this happens a negligible fraction of times.

Figure 1: Excess Effects of Uncertainty Shock in Recessions: Model Uncertainty

This figure in the first two columns shows the identified set for the generalized impulse response functions (GIRFs) to a positive one-standard deviation shock to uncertainty in strong expansions (first column) and deep recessions (second column) as estimated by the IVAR on historical US data from 1962Q3 to 2017Q4. The set for strong expansions are constructed as follows: i) for an accepted draw of \mathbf{B} , the dates are located where the economy is in a strong expansion, ii) at these dates, the GIRFs are computed using (1) and the average GIRF across these dates are reported. A similar procedure is used for deep recessions. Each GIRF is computed using Monte Carlo integration with 500 draws. The solid (dashed) lines report the median target impulse responses in strong expansions (deep recessions) when computed as suggested by Fry & Pagan (2011). The number of retained draws for identifying uncertainty shocks is 187 out a total of 500,000 draws. The third column shows the differences between the median target (MT) responses between deep recessions and strong expansions when only accounting for model uncertainty. Grey bands represent the identified set for the difference of responses. All responses are shown in percentage deviations, except for the policy rate where changes in percentage points are reported.



1.2 Validation of the Empirical Identification Under the DGP of the Model

We have adopted a mix of Narrative Sign Restrictions (NSR) and standard Sign Restrictions (SR) to identify uncertainty shocks from our estimated IVAR. This section checks whether this approach can be validated under the DGP of the DSGE model we adopt.

The DSGE model we use features an endogenous measure of financial uncertainty, a model-consistent VXO, which responds to four shocks, i.e., a first-moment technology shock, a first-moment cost-push shock, a first-moment preference shock, and a second-moment preference shock, which is the uncertainty shock.

We conduct a Monte Carlo exercise with artificial data simulated using our DSGE model to assess our empirical identification strategy. The model is solved with our proposed third-order approximation around the risky steady state, which allows all shocks, including the uncertainty shock, to have state-dependent effects. We conduct a population analysis and simulate a sample of 3,000 observations with the model using the benchmark estimate of the structural parameters as provided in the paper.² We then estimate an IVAR and produce impulse responses to uncertainty shocks by adopting our identification strategies, i.e., the baseline mix of NSR and SR. Consistently with what is done to identify the dates in our baseline analysis, we select the dates with the biggest spikes in the VXO and combine them with the biggest spikes in the volatility process.^{3,4} Similarly to our baseline analysis, we require the realizations of our identified uncertainty shocks to be larger than the median value of the empirical density of the uncertainty shocks in the selected dates.⁵ As in the baseline, we also require a negative on-impact response of real GDP, investment, consumption, and hours to an uncertainty shock. In the paper, we verify the ability of these restrictions in the IVAR to replicate the impulse responses in the DSGE model by the IVAR MT responses. Figures 2 and 3 below supplement this analysis by showing the identified set for the responses in the IVAR and the state-dependent MT responses from the IVAR.

²Note that our DSGE model with four shocks does not imply stochastic singularity in the IVAR with seven variables because the DSGE model is solved with nonlinear terms.

³Although the word "Narrative" loses its meaning for an exercise based on data simulated from a model, the proposed exercise wants to resemble the identification strategy we used in our baseline analysis where uncertainty shocks are identified using information from the VXO biggest spikes coupled with an estimate of the economy-wide stochastic volatility process (given by the LMN financial volatility indicator). The assumption at the basis of this exercise is that the econometrician perfectly knows the economy-wide stochastic volatility process at the basis of financial volatility, rather than knowing its estimate.

⁴We select the dates that at the same time correspond to the biggest 1.5% among the VXO spikes and the biggest 1.5% among the stochastic volatility process spikes. This threshold seems appropriate as it guarantees that enough responses are retained and that selected dates are informative enough to identify the uncertainty shocks. We retained 46 draws out of 500,000 rotations.

⁵Similarly to our baseline analysis, we impose that the correlation between the series of identified uncertainty shocks and (model-implied) stock market returns be smaller than the median value of the empirical density of the correlation coefficients for all draws.

Figure 2: Simulation Exercise for the IVAR: IRFs to Uncertainty Shocks

This figure shows the identified set for the generalized impulse response functions (GIRFs) in the IVAR to a positive one-standard deviation shock to uncertainty in strong expansions (to the left) and deep recessions (to the right) on a simulated sample of 3,000 draws from the New Keynesian DSGE model using the estimates in column (1) of Table 3 as given in the paper. The set for strong expansions is constructed as follows: i) for an accepted draw of \mathbf{B} , the dates are located where the economy is in a strong expansion, ii) at these dates, the GIRFs are computed using (1) and the average GIRF across these dates are reported. A similar procedure is used for deep recessions. Each GIRF is computed using Monte Carlo integration with 500 draws. The solid (dashed) lines report the median target impulse responses in strong expansions (deep recessions) when computed as suggested by Fry & Pagan (2011). The marked solid lines denote the true responses in the DSGE model. All responses are shown in percentage deviations, except for the policy rate where changes in percentage points are reported.

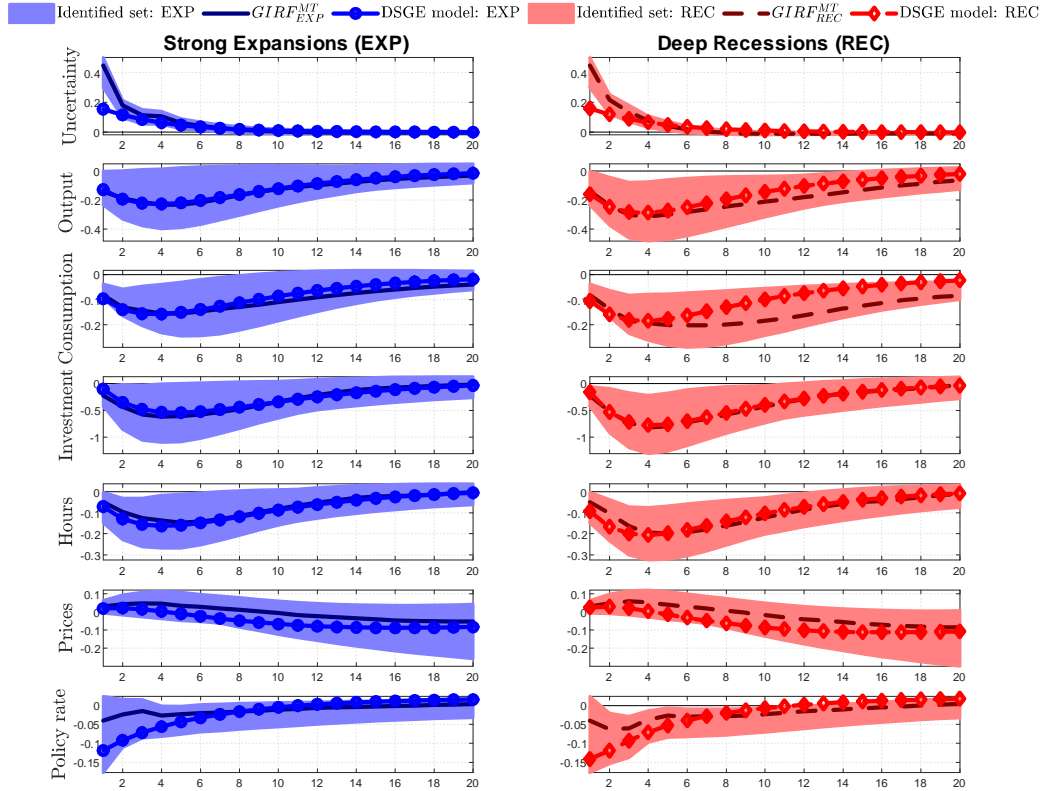
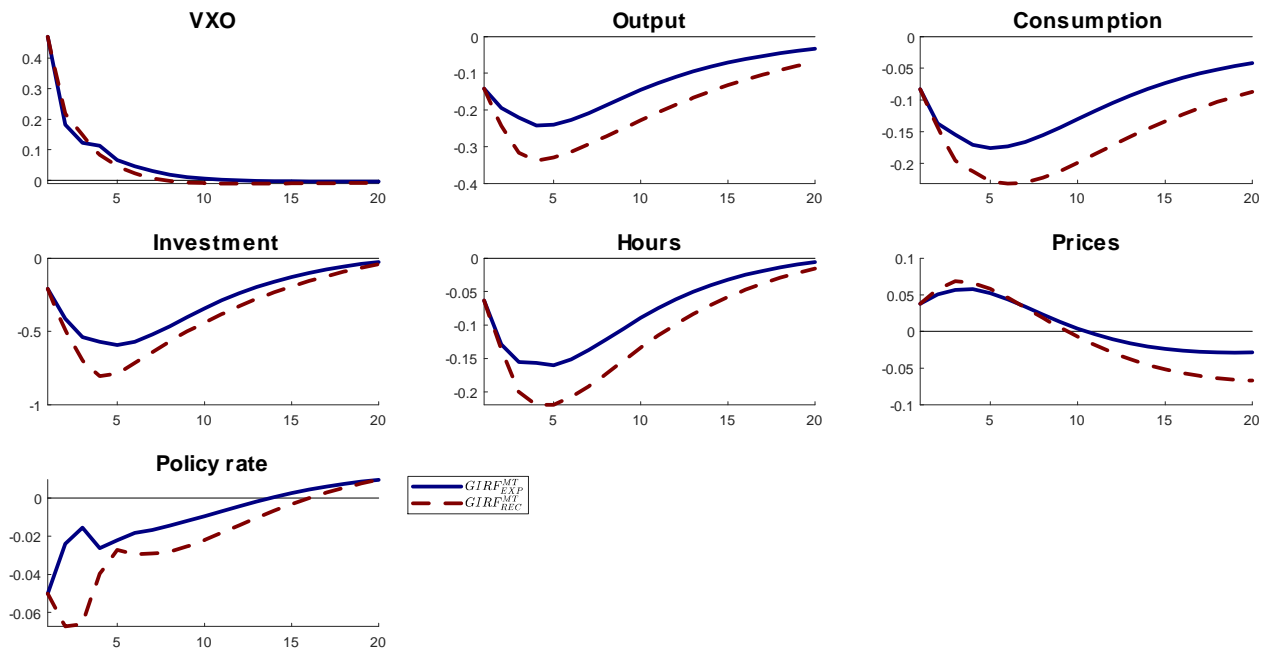


Figure 3: Simulation Exercise for the IVAR: MT responses

This figure shows the identified set for the generalized impulse response functions (GIRFs) in the IVAR to a positive one-standard deviation shock to uncertainty in strong expansions and deep recessions on a simulated sample of 3,000 draws from the New Keynesian DSGE model using the estimates in column (1) of Table 3 of the paper. The set for strong expansions are constructed as follows: i) for an accepted draw of \mathbf{B} , the dates are located where the economy is in a strong expansion, ii) at these dates, the GIRFs are computed using (1) and the average GIRF across these dates are reported. A similar procedure is used for deep recessions. Each GIRF is computed using Monte Carlo integration with 500 draws. The solid (dashed) lines report the median target impulse responses in strong expansions (deep recessions) when computed as suggested by Fry & Pagan (2011). All responses are shown in percentage deviations, except for the policy rate where changes in percentage points are reported.



1.3 Robustness checks for the nonlinear SVAR model

No sign restrictions. Among the baseline set of restrictions for our IVAR we also include traditional sign restrictions, and specifically we impose a non-positive impact response of GDP, investment, consumption, and hours to a (positive) uncertainty shock. These sign restrictions, which we impose to sharpen the identification of the set of admissible rotations, are supported by a large number of theoretical and empirical analyses on the business cycle effects of uncertainty shocks (for a survey, see Bloom (2014)). Figure 4 shows the IVAR results when omitting the additional sign restrictions (SR). Figure 1 reveals that these sign restrictions help to narrow the identified set, but hardly affect the estimated median target model, which is the focus of our paper.

Control for skewness shocks. Several recent studies investigate the role of skewness shocks as a driver of business cycle fluctuations (see, e.g., Salgado, Guvenen & Bloom (2019)). In particular, skewness shocks may be behind the findings of the emerging growth-at-risk literature (see, e.g., Adrian, Boyarchenko & Giannone (2019)). These considerations raise the concern that our baseline identification strategy may confound second and third-moment shocks. As follows we perform an exercise that aims to control for financial skewness shocks when identifying financial uncertainty shocks.

We first construct a measure of realized financial skewness as the monthly skewness of daily SP500 returns.⁶ We transform our monthly measure of skewness to make it comparable to the CBOE SKEW index. Let S_t be the month- t skewness, then we define a new index $Skew_t = 100 - 10 \cdot S_t$. Hence if $Skew < (>)100$ the distribution of stock market returns is right (left) skewed.⁷ We take the quarterly average of such financial skewness index, which we log-transform. This variable is then added to the endogenous variables of our IVAR (a similar approach is applied in Salgado et al. (2019)). To ensure that skewness shocks do not disrupt the identified uncertainty shocks, we adopt the following identification strategy. First, we do not impose any timing restrictions on the skewness-uncertainty contemporaneous relationship, as it is not needed when using narrative sign restrictions. Second, in addition to our baseline set of restrictions, we follow Furlanetto, Ravazzolo & Sarferaz (2019) and impose that a financial uncertainty (skewness) shock generates an on-impact response of the financial uncertainty-skewness ratio that is bigger (smaller) than one.⁸ Third, we also impose that the skewness shock and the uncertainty shock have a positive on-impact effect on the uncertainty and skewness proxies, respectively, to ensure that the ratios that we constrain are positive. The results for this robustness check are provided in Figure 5, which shows that our baseline results are robust to controlling for skewness shocks. One way to clearly see this is from the second column in Figure 5, where the difference in the MT-responses are well within the confidence bands for the difference in the MT-responses in the baseline IVAR that does *not* control for skewness shocks.

Control for first-moment financial shocks. Our baseline IVAR model does not feature any measure of financial stress such as credit spreads. This choice is consistent with the Basu & Bundick (2017) model, where first-moment financial shocks do not have any role due to the frictionless financial markets hypothesis. However, controlling for credit spreads and first-moment financial shocks is important for at least three reasons. First, credit spreads have large predictive power for the United States' real activity (see Gilchrist & Zakrajsek (2012)), so they may represent a relevant omitted variable. Second, as advocated by recent studies, financial frictions and credit spreads are important for the transmission of uncertainty shocks (Gilchrist, Sim & Zakrajsek (2014); Alfaro, Bloom & Lin (2019); Arellano, Bai & Kehoe (2019)). Third, as financial stress and financial uncertainty go hand-in-hand, the use of a credit spread indicator may help to improve the identification of financial uncertainty shocks, avoiding confounding second-moment financial shocks with first-moment financial shocks. Our narrative sign restrictions approach has the advantage of not imposing any timing restrictions on the credit spread-uncertainty contemporaneous relationship.

To disentangle uncertainty shocks from first-moment financial shocks, first, we augment our baseline IVAR vector of endogenous variables with a measure of credit spread meant to capture stress in financial markets, i.e., the difference between the BAA yield and the AAA one. Second, as with the previous check for skewness shocks, we add some ratio constraints to our baseline set of restrictions following the approach proposed by Furlanetto et al. (2019). They identify financial and uncertainty shocks using a sign restrictions approach which features, among others, restrictions on ratios of the impulse responses of proxies for first and second-moment financial indicators. Following their approach, we impose that a financial uncertainty (credit spread) shock generates an on-impact response of the financial uncertainty-credit spread ratio

⁶We use the series SP500 Composite price index, daily data, downloaded from Datastream (Code S&PCOMP(PI)). The series starts in 1964.

⁷The CBOE implied skewness (SKEW) index starts only in 1990. We do not splice our monthly series with the SKEW index because, differently than with realized volatility and the VXO index of implied volatility, their behavior in the common sample is quite different (their correlation coefficient is only 0.05).

⁸To implement this identification strategy, we standardized the financial skewness index to impose the same standard deviation of our uncertainty proxy.

that is bigger (smaller) than one.⁹ As earlier, we also impose that the credit spread shock and the uncertainty shock have a positive on-impact effect on the uncertainty and the credit spread proxies, respectively, to ensure that the ratios that we constrain are positive. Figure 6 reports the findings from this robustness check. The impulse responses are state-dependent and their difference is very similar to the baseline difference. Hence, the figure suggests that our baseline results are robust to controlling for first-moment financial shocks.

Sample from 1987. In our baseline analysis we follow Bloom (2009) and Ludvigson, Ma & Ng (2019) and use a long sample that starts in the '60s, in particular in 1962Q3 like in Bloom (2009). For the IVAR, a long sample featuring several recessions is advisable because it sharpens our inference for the state-dependent responses. As a robustness check for our main finding, in Figure 7 we report that the results from an IVAR estimated on a sample starting in 1987Q1, i.e. when the VXO implied-volatility index is available. In performing this exercise we lose 8 out of our 18 event restrictions in Table 1 of the paper. This notwithstanding, Figure 7 shows that we still find large differences in the impulse response functions across expansions and recessions. From the second column in this figure, we actually find that these differences for several variables are outside the confidence bands for the corresponding responses in the baseline IVAR on the long sample and hence *larger* than the responses reported in the main paper.¹⁰

Alternative control for unconventional monetary policy. In the baseline analysis, we account for unconventional monetary policy during the zero lower bound period from 2008Q4 to 2015Q4 by using the Wu and Xia's (2016) shadow rate instead of the federal funds rate in this period. But the estimate in Wu and Xia is admittedly only one estimate of the shadow rate (see, e.g., Bauer & Rudebusch (2016) and Krippner (2020), who find that estimated shadow rates are quite sensitive to several modeling assumptions). Hence, we conduct an alternative exercise where we use the federal funds rate along with the 10-year treasury zero-coupon yield in our IVAR as another way to account for unconventional monetary policy. The rationale for including the 10-year interest rate is that it may capture effects of quantitative easing and forward guidance even when the short rate is at the lower bound. Figure 8 shows that the impulse responses for this alternative version of our IVAR are virtually identical to our baseline estimate, showing that the specific way we account for unconventional monetary policy is not essential for our main finding.

PMI as an alternative conditioning variable. Our baseline IVAR features an interaction term of uncertainty – i.e., the variable we shock – with the quarterly GDP growth rate – i.e., the conditioning variable we use to define the states of deep recessions and strong expansions. To document the robustness of our main findings along the definition of our two states, we now consider the PMI (Purchasing Managers Index) as an alternative conditioning variable, which we also add to our vector of endogenous variables. Consistently with our baseline analysis, we define expansions as episodes when the PMI is above its 90% percentile, whereas deep recessions are defined as episodes when the PMI is less than or equal to 44.5, consistent with the findings in Berge & Jordà (2011). The results in Figure 9 document that we still find large differences in the responses to uncertainty shocks when we use this alternative conditioning variable to identify recessions and expansions.

Wider expansions state. In our baseline analysis, we use the initial conditions corresponding to the bottom and top deciles of the GDP growth rate distribution to define the states of deep contractions and strong expansions, respectively. Defining two extreme states allow us to not confound them and hence miss relevant nonlinearities (see, e.g., Caggiano, Castelnuovo, Colombo & Nodari (2015)). However, arguably strong expansions do not include the typical expansionary (or non-contractionary) phases of the business cycle of the US economy. To document whether our results are robust along this dimension, here we contrast our baseline findings for strong expansions to an alternative expansionary state, defined as not being a deep recession. The results in the right panels of Figure 10 show that the differences in state-dependent responses get only slightly smaller than the baseline case but are still statistically indistinguishable from them (as the difference is within the baseline difference band).

⁹We standardized the credit spread index to impose the same standard deviation of our uncertainty proxy.

¹⁰For this shorter sample, it is sufficient to only use 2 lags in the IVAR as oppose to the 4 lags we use in the long sample.

Figure 4: IVAR impulse responses to uncertainty shocks: No sign restrictions

This figure shows the identified set for the generalized impulse response functions (GIRFs) to a positive one-standard deviation shock to uncertainty in strong expansions (to the left) and deep recessions (to the right) as estimated by the IVAR on historical US data from 1962Q3 to 2017Q4 when omitting the traditional sign restrictions. The set for strong expansions are constructed as follows: i) for an accepted draw of \mathbf{B} , the dates are located where the economy is in a strong expansion, ii) at these dates, the GIRFs are computed using (1) and the average GIRF across these dates are reported. A similar procedure is used for deep recessions. Each GIRF is computed using Monte Carlo integration with 500 draws. The solid (dashed) lines report the median target impulse responses in strong expansions (deep recessions) when computed as suggested by Fry & Pagan (2011). All responses are shown in percentage deviations, except for the policy rate where changes in percentage points are reported.

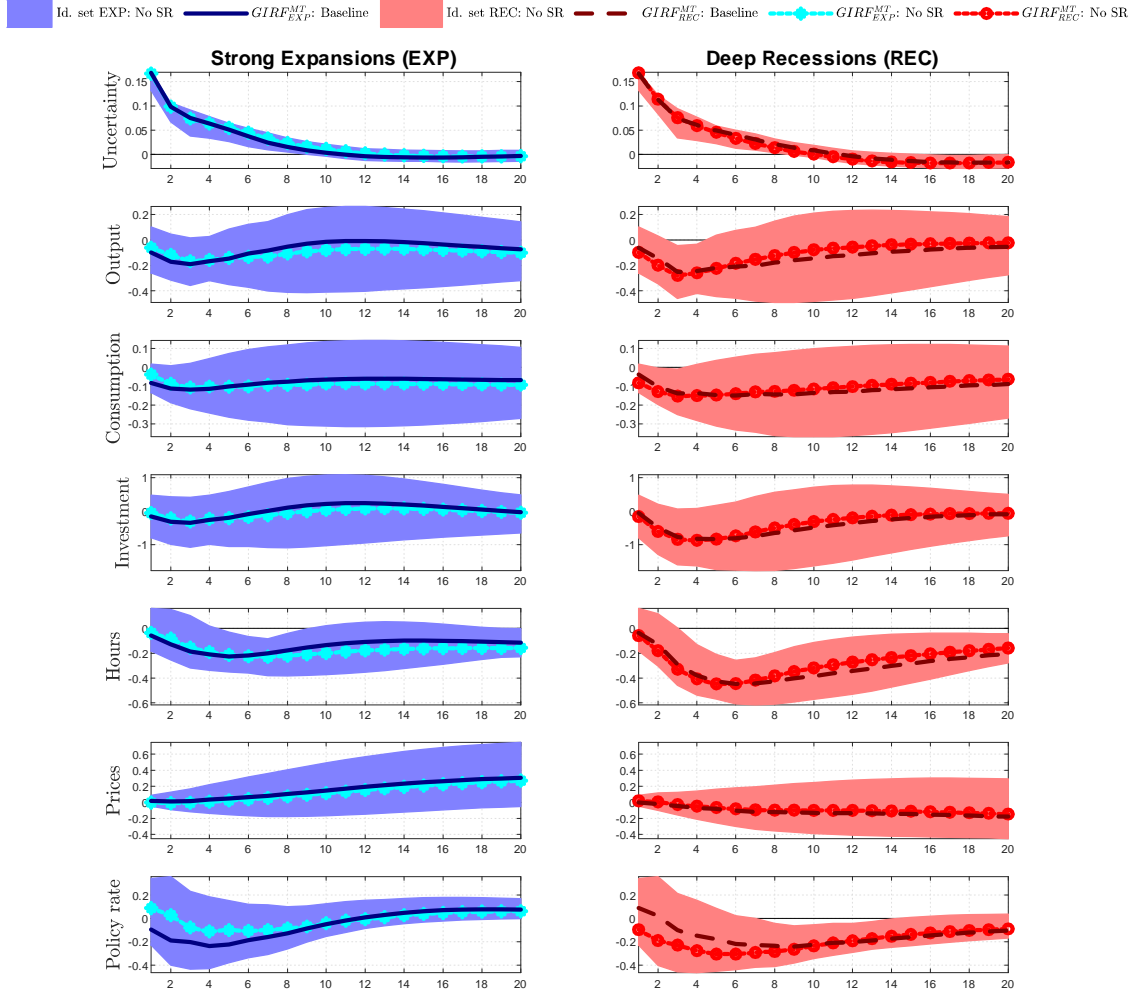


Figure 5: IVAR impulse responses to uncertainty shocks: Control for skewness shocks

This figure shows the identified set for the generalized impulse response functions (GIRFs) to a positive one-standard deviation shock to uncertainty in strong expansions (to the left) and deep recessions (to the right) as estimated by the IVAR on historical US data from 1964Q1 to 2017Q4 for the case we control for skewness shocks. The set for strong expansions are constructed as follows: i) for an accepted draw of \mathbf{B} , the dates are located where the economy is in a strong expansion, ii) at these dates, the GIRFs are computed using (1) and the average GIRF across these dates are reported. A similar procedure is used for deep recessions. Each GIRF is computed using Monte Carlo integration with 500 draws. The solid (dashed) lines report the median target impulse responses in strong expansions (deep recessions) when computed as suggested by Fry & Pagan (2011). All responses are shown in percentage deviations, except for the policy rate where changes in percentage points are reported.

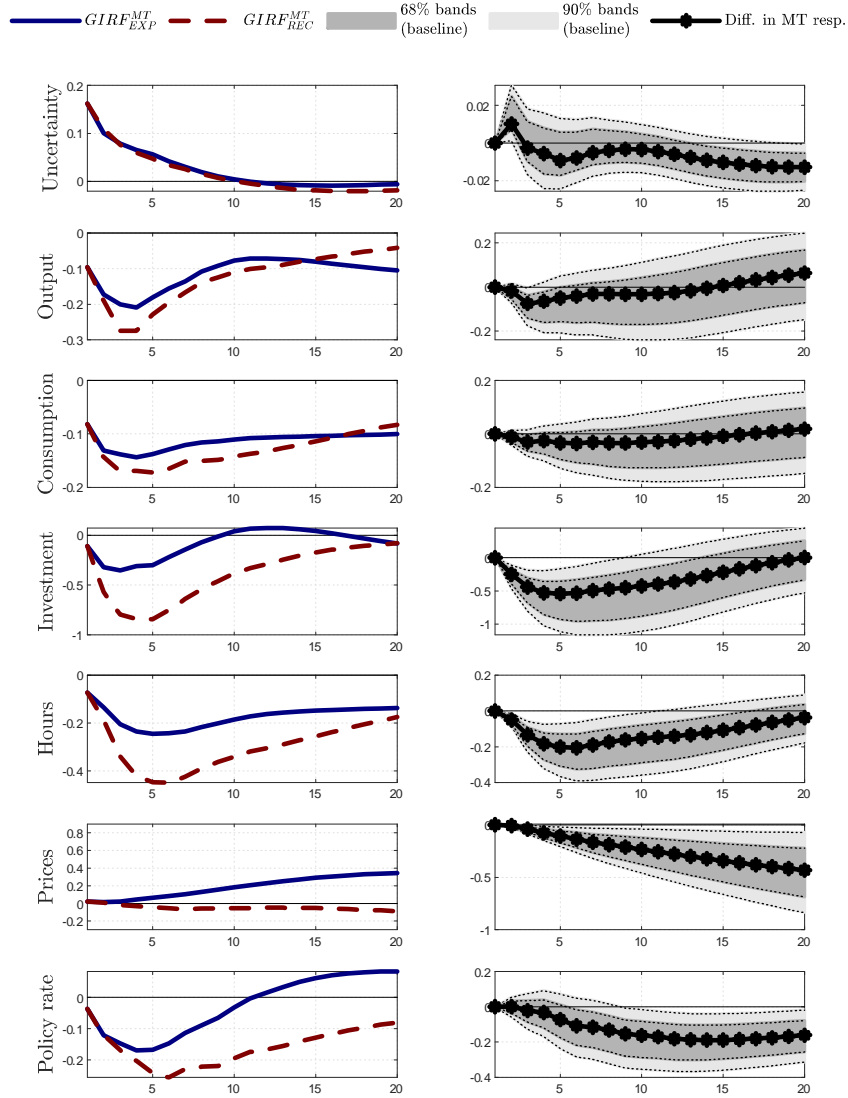


Figure 6: IVAR impulse responses to uncertainty shocks: Control for credit spread shocks

This figure shows the identified set for the generalized impulse response functions (GIRFs) to a positive one-standard deviation shock to uncertainty in strong expansions (to the left) and deep recessions (to the right) as estimated by the IVAR on historical US data from 1964Q1 to 2017Q4 for the case we control for credit spread shocks. The set for strong expansions are constructed as follows: i) for an accepted draw of \mathbf{B} , the dates are located where the economy is in a strong expansion, ii) at these dates, the GIRFs are computed using (1) and the average GIRF across these dates are reported. A similar procedure is used for deep recessions. Each GIRF is computed using Monte Carlo integration with 500 draws. The solid (dashed) lines report the median target impulse responses in strong expansions (deep recessions) when computed as suggested by Fry & Pagan (2011). All responses are shown in percentage deviations, except for the policy rate where changes in percentage points are reported.

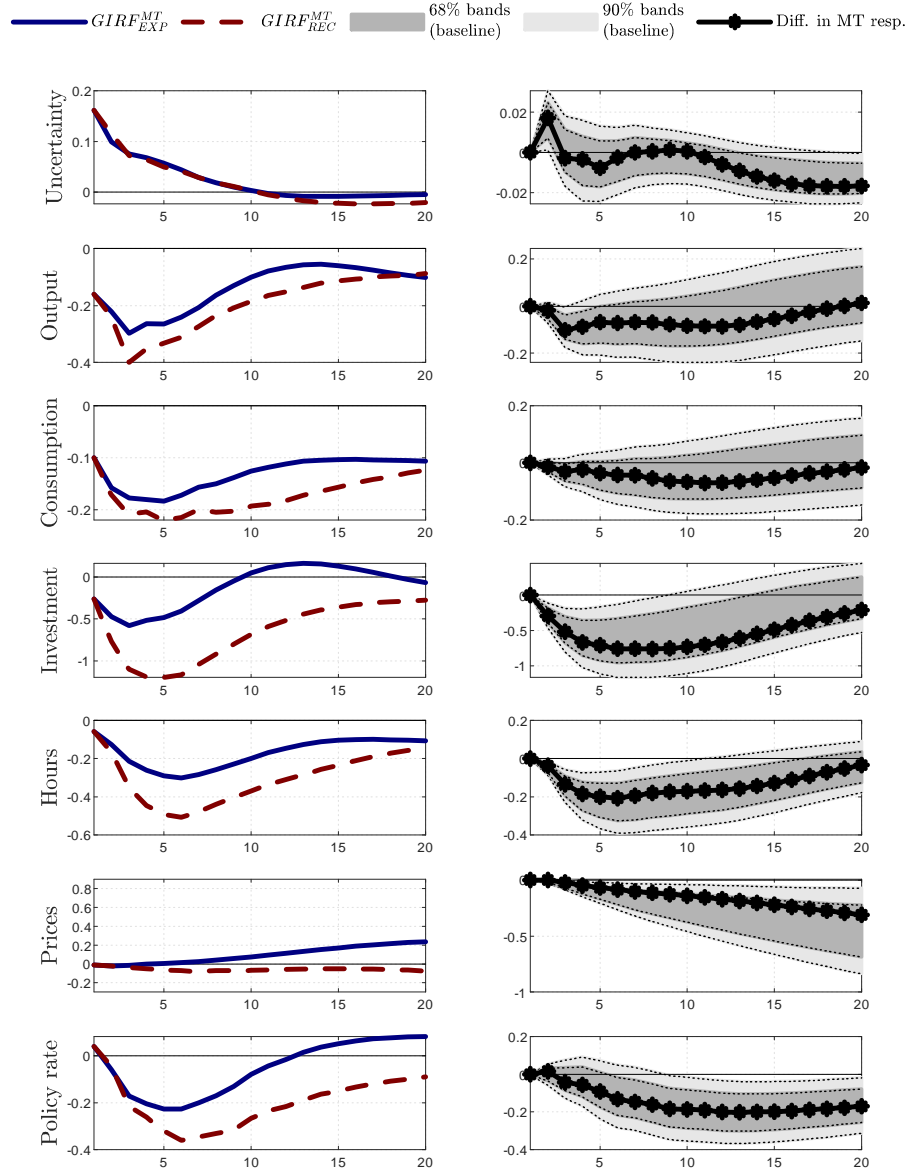


Figure 7: IVAR impulse responses to uncertainty shocks: Sample from 1987

This figure shows the identified set for the generalized impulse response functions (GIRFs) to a positive one-standard deviation shock to uncertainty in strong expansions (to the left) and deep recessions (to the right) as estimated by the IVAR on historical US data from 1987Q1 to 2017Q4. The set for strong expansions are constructed as follows: i) for an accepted draw of \mathbf{B} , the dates are located where the economy is in a strong expansion, ii) at these dates, the GIRFs are computed using (1) and the average GIRF across these dates are reported. A similar procedure is used for deep recessions. Each GIRF is computed using Monte Carlo integration with 500 draws. The solid (dashed) lines report the median target impulse responses in strong expansions (deep recessions) when computed as suggested by Fry & Pagan (2011). All responses are shown in percentage deviations, except for the policy rate where changes in percentage points are reported.

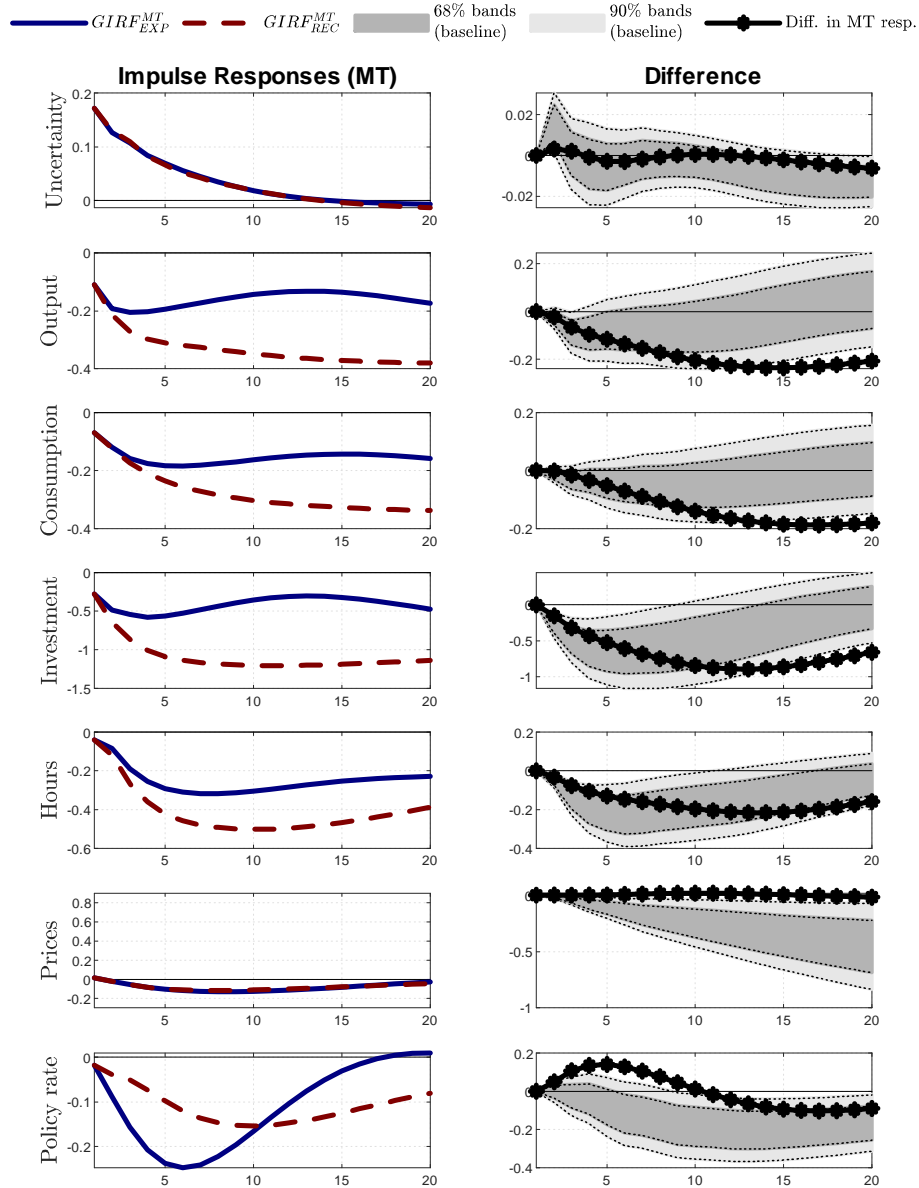


Figure 8: IVAR impulse responses to uncertainty shocks: Alternative control for unconventional monetary policy

This figure shows the identified set for the generalized impulse response functions (GIRFs) to a positive one-standard deviation shock to uncertainty in strong expansions (to the left) and deep recessions (to the right) as estimated by the IVAR on historical US data from 1962Q3 to 2017Q4 for the case we control for unconventional monetary policy via the 10-year treasury bill rate. The set for strong expansions are constructed as follows: i) for an accepted draw of \mathbf{B} , the dates are located where the economy is in a strong expansion, ii) at these dates, the GIRFs are computed using (1) and the average GIRF across these dates are reported. A similar procedure is used for deep recessions. Each GIRF is computed using Monte Carlo integration with 500 draws. The solid (dashed) lines report the median target impulse responses in strong expansions (deep recessions) when computed as suggested by Fry & Pagan (2011). All responses are shown in percentage deviations, except for the policy rate where changes in percentage points are reported.

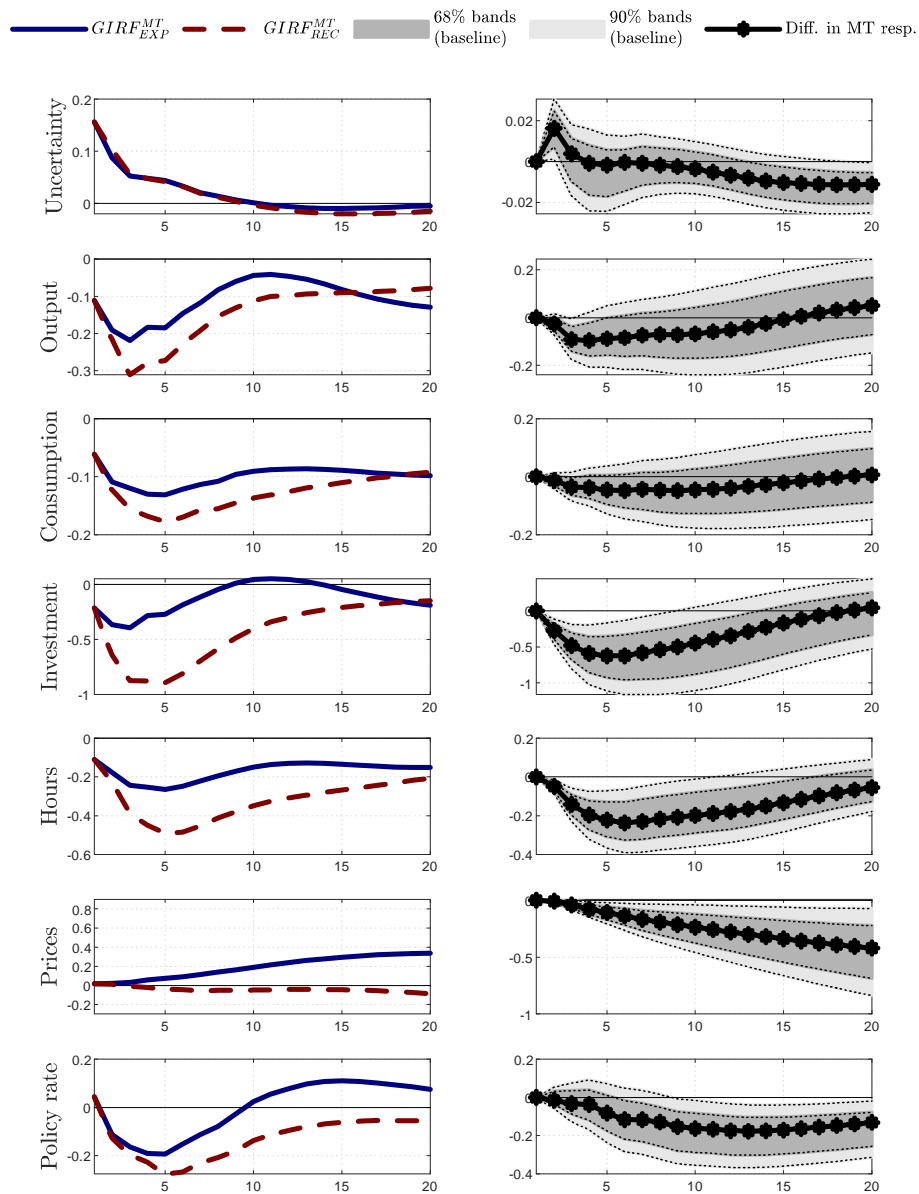


Figure 9: IVAR impulse responses to uncertainty shock: PMI as an alternative conditioning variable

This figure shows the identified set for the generalized impulse response functions (GIRFs) to a positive one-standard deviation shock to uncertainty in strong expansions (to the left) and deep recessions (to the right) as estimated by the IVAR on historical US data from 1962Q3 to 2016Q4 for the case we use the PMI index as an alternative conditioning variable. The set for strong expansions are constructed as follows: i) for an accepted draw of \mathbf{B} , the dates are located where the economy is in a strong expansion, ii) at these dates, the GIRFs are computed using (1) and the average GIRF across these dates are reported. A similar procedure is used for deep recessions. Each GIRF is computed using Monte Carlo integration with 500 draws. The solid (dashed) lines report the median target impulse responses in strong expansions (deep recessions) when computed as suggested by Fry & Pagan (2011). All responses are shown in percentage deviations, except for the policy rate where changes in percentage points are reported.

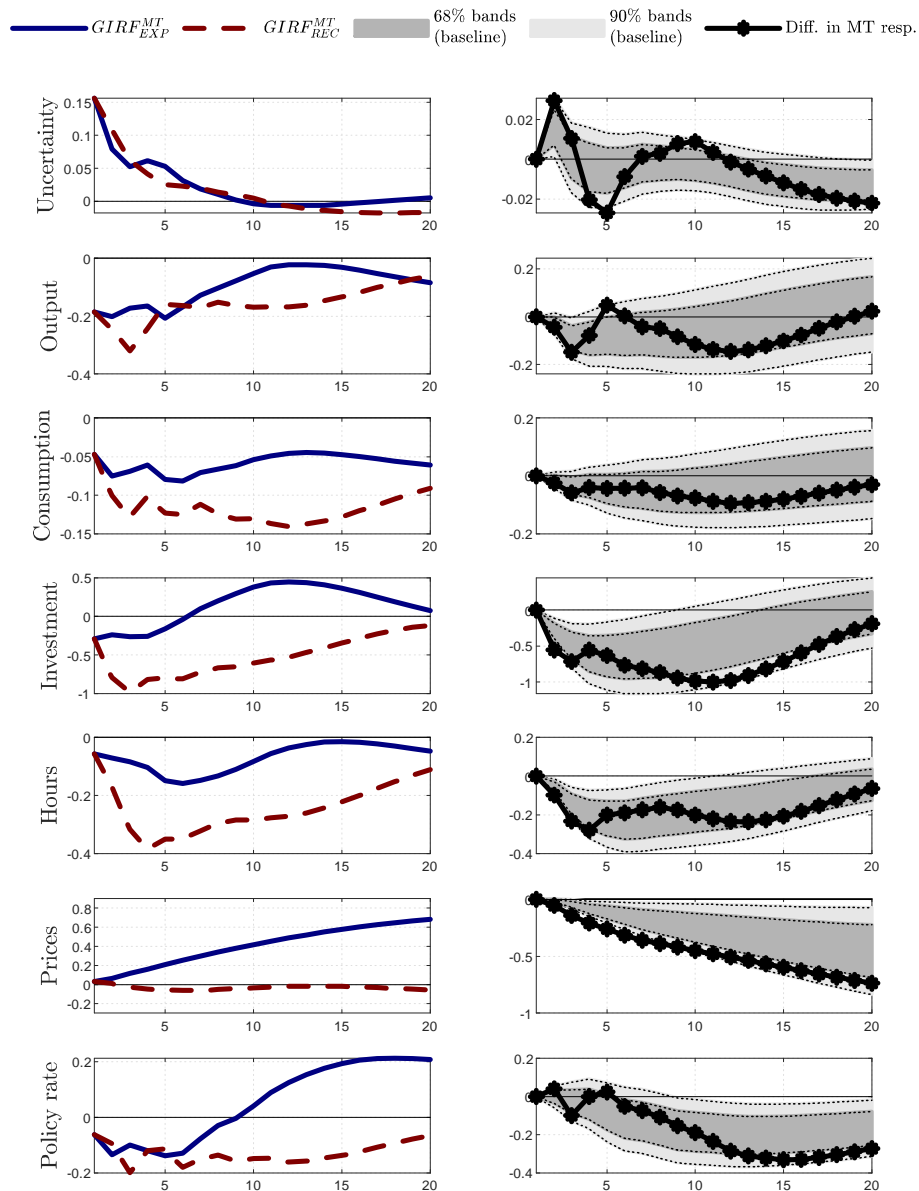
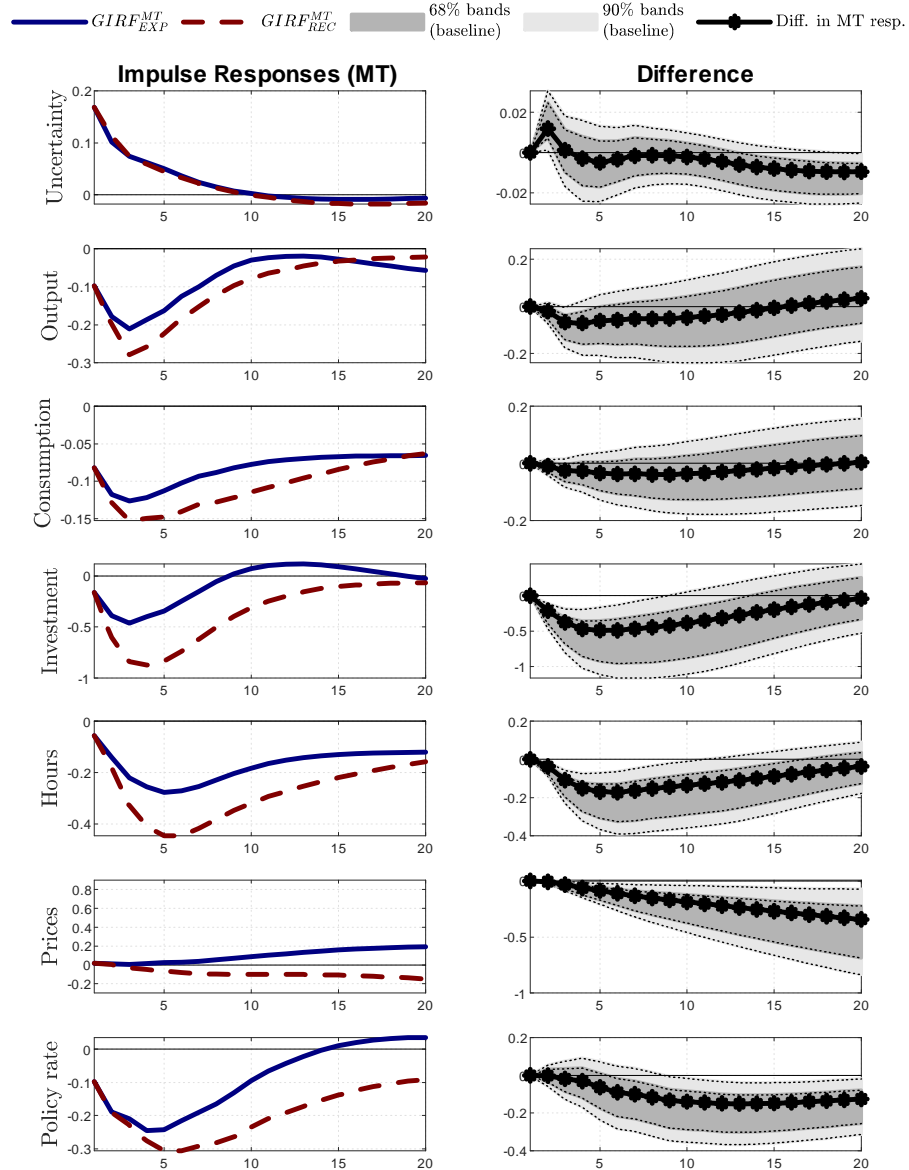


Figure 10: IVAR impulse responses to uncertainty shock: Wider expansions state

This figure shows the identified set for the generalized impulse response functions (GIRFs) to a positive one-standard deviation shock to uncertainty in strong expansions (to the left) and deep recessions (to the right) as estimated by the IVAR on historical US data from 1962Q3 to 2017Q4 for the case we use an alternative definition for the expansions state that collects all initial conditions not in the deep contractions state. The set of responses for the expansions state is constructed as follows: i) for an accepted draw of \mathbf{B} , the dates are located where the economy is in an expansion, ii) at these dates, the GIRFs are computed using (1) and the average GIRF across these dates are reported. A similar procedure is used for deep recessions. Each GIRF is computed using Monte Carlo integration with 500 draws. The solid (dashed) lines report the median target impulse responses in strong expansions (deep recessions) when computed as suggested by Fry & Pagan (2011). All responses are shown in percentage deviations, except for the policy rate where changes in percentage points are reported.



2 The DSGE model

The DSGE model we adopt is based on Basu & Bundick (2017) and its modification in Basu & Bundick (2018). The model is summarized below.

2.1 Households

A representative household maximizes lifetime utility given by recursive preferences over consumption C_t and leisure $1 - N_t$. The utility of consumption and leisure are subject to preference shocks, denoted a_t . The household receives labor income W_t for each unit of labor N_t supplied to the intermediate goods producing firms. The household owns these firms and hold equity shares S_t in these firms. Each equity shares have a real price of P_t^E and pay dividends D_t^E per share S_t . The household also holds one-period real and nominal bonds issued by the government, giving a gross return of and R_t^R and R_t , respectively.

The household maximizes lifetime utility by choosing C_{t+s} , N_{t+s} , B_{t+s+1} , and S_{t+s+1} for all $s = 0, 1, 2, \dots$ by solving the problem

$$V_t = \max \left[a_t^{1-\sigma} \left(\frac{1}{1-\sigma} \left((C_t - bC_{t-1})^\eta (1 - N_t)^{1-\eta} \right)^{1-\sigma} + u_0^{(1)} \right) + u_0^{(2)} + \beta (\mathbb{E}_t [V_{t+1}^{1-\alpha^{Swan}}])^{\frac{1}{1-\alpha^{Swan}}} \right],$$

subject to its real intertemporal budget constraint each period

$$C_t + P_t^E S_{t+1} + \frac{1}{R_t^R} B_{t+1} \leq W_t N_t + (D_t^E + P_t^E) S_t + \frac{B_t}{\Pi_t}$$

where Π_t is gross inflation. Note that we in this Online Appendix accommodate two constants, i.e. $u_0^{(1)}$ and $u_0^{(2)}$, with the implicit understanding that only one of these constants are "active" in the model. The reason for introducing two constants is to see the effects of having preference shocks hitting the constant (with $u_0^{(1)}$) and not hitting the constant (with $u_0^{(2)}$).

Standard derivations imply

$$\begin{aligned} \frac{\partial V_t}{\partial C_t} &= \eta a_t^{1-\sigma} \frac{((C_t - bC_{t-1})^\eta (1 - N_t)^{1-\eta})^{1-\sigma}}{C_t - bC_{t-1}} \\ \frac{\partial V_{t+1}}{\partial C_{t+1}} &= \eta a_{t+1}^{1-\sigma} \frac{((C_{t+1} - bC_t)^\eta (1 - N_{t+1})^{1-\eta})^{1-\sigma}}{C_{t+1} - bC_t} \\ \frac{\partial V_t}{\partial C_{t+1}} &= \beta (\mathbb{E}_t V_{t+1}^{1-\alpha})^{\frac{1}{1-\alpha}-1} \mathbb{E}_t \left[V_{t+1}^{-\alpha} \frac{\partial V_{t+1}}{\partial C_{t+1}} \right] \end{aligned}$$

where λ_t denotes the Lagrange multiplier on the household budget constraint. Thus, the household's stochastic discount factor M_{t+1} between periods t and $t+1$ is

$$\begin{aligned} M_{t+1} &= \frac{\partial V_t / \partial C_{t+1}}{\partial V_t / \partial C_t} \\ &= \beta \left(\frac{a_{t+1}}{a_t} \right)^{1-\sigma} \frac{(C_t - bC_{t-1})}{(C_{t+1} - bC_t)} \left(\frac{(C_{t+1} - bC_t)^\eta (1 - N_{t+1})^{1-\eta}}{(C_t - bC_{t-1})^\eta (1 - N_t)^{1-\eta}} \right)^{1-\sigma} \left(\frac{V_{t+1}}{\mathbb{E}_t [V_{t+1}^{1-\alpha^{Swan}}]^{\frac{1}{1-\alpha^{Swan}}}} \right)^{-\alpha^{Swan}} \end{aligned}$$

The first-order conditions for the household are then easily shown to be

$$\begin{aligned} \frac{(1-\eta)}{\eta} \frac{C_t - bC_{t-1}}{1 - N_t} &= W_t, \\ P_t^E &= \mathbb{E}_t [M_{t+1} (D_{t+1}^E + P_{t+1}^E)], \\ 1 &= R_t^R \mathbb{E}_t \left[\frac{\lambda_{t+1}}{\lambda_t} \right], \\ 1 &= R_t \mathbb{E}_t \left[\frac{\lambda_{t+1}}{\lambda_t} \frac{1}{\Pi_{t+1}} \right], \end{aligned}$$

which represent the household intratemporal optimality condition with respect to consumption and leisure, the Euler equations for equity shares, and one-period risk-less firm bonds, respectively.

2.2 Intermediate Goods Producing Firms

The i th intermediate goods producing firm rents labor $N_t(i)$ from the household to produce the intermediate good $Y_t(i)$, where $i \in [0, 1]$. Each intermediate good is produced in a monopolistically competitive market, where the producer faces quadratic costs à la Rotemberg (1982) (determined by ϕ_P) of changing the nominal price $P_t(i)$ each period. The intermediate firm owns its capital stock $K_t(i)$ and faces convex adjustment costs (controlled by ϕ_K) when changing the quantity of installed capital. The firm also chooses its investment $I_t(i)$ and the rate of utilization $U_t(i)$ of its capital stock. Each firm issues equity shares $S_t(i)$ and one-period risk-less bonds $B_t(i)$. Firm i chooses $N_t(i)$, $I_t(i)$, $U_t(i)$, and $P_t(i)$ to maximize firm cash flows $D_t(i)/P_t(i)$ given aggregate demand Y_t , the elasticity of substitution among intermediate goods $\theta_{\mu,t}$, and the price P_t of the finished good. Note that we deviate from Basu & Bundick (2017) by allowing the elasticity of substitution among intermediate goods to be time-varying to capture the present of cost-push shocks. All intermediate firms have the same constant-returns-to-scale Cobb–Douglas production function, subject to a fixed cost of production Φ and the level of productivity Z_t .

Each intermediate firm maximizes the discounted cash flow using the household's real stochastic discount factor $M_{t,t+s}$, i.e.

$$\max \mathbb{E}_t \sum_{s=0}^{\infty} M_{t,t+s} D_{t+s}(i),$$

subject to the production function

$$\left[\frac{P_t(i)}{P_t} \right]^{-\theta_{\mu,t}} Y_t = [K_{t-1}(i)U_t(i)]^\alpha [Z_t N_t(i)]^{1-\alpha} - \Phi,$$

and the capital accumulation equation

$$K_t(i) = \left(1 - \delta(U_t(i)) - \frac{\phi_K}{2} \left(\frac{I_t(i)}{K_{t-1}(i)} - \delta_0 \right)^2 \right) K_{t-1}(i) + I_t(i).$$

The expression for dividends is given by

$$D_t(i) = \left[\frac{P_t(i)}{P_t} \right]^{1-\theta_{\mu,t}} Y_t - W_t N_t(i) - I_t(i) - \frac{\phi_P}{2} \left(\frac{P_t(i)}{\Pi_{ss} P_{t-1}(i)} - 1 \right)^2 Y_t,$$

where Π_{ss} denotes gross inflation in the steady state. The depreciations depend on utilization in the following way

$$\delta(U_t(i)) = \delta_0 + \delta_1(U_t(i) - U) + \frac{\delta_2}{2}(U_t(i) - U)^2,$$

where U is the utilization rate in the steady state.

Each intermediate firm finances a percentage ν of its capital stock each period with one-period risk-less bonds. Thus, the quantity of issued bonds equals $B_t(i) = \nu K_{t-1}(i)$. The total real cash flow of the firm is divided between payments to bond holders and equity holders as follows

$$D_t^E = D_t - \nu \left(K_{t-1} - \frac{1}{R_t^R} K_t \right).$$

The optimization problem for the firm reads

$$\begin{aligned} & \text{Max}_{N_t(i), U_t(i), K_t(i), P_t(i), I_t(i)} \forall t > 0 \\ \mathcal{L} = & \mathbb{E}_t \sum_{s=0}^{\infty} M_{t,t+s} \left[\left[\frac{P_{t+s}(i)}{P_{t+s}} \right]^{1-\theta_{\mu,t+s}} Y_{t+s} - W_{t+s} N_{t+s}(i) - I_{t+s}(i) - \frac{\phi_P}{2} \left(\frac{P_{t+s}(i)}{\Pi_{ss} P_{t-1+s}(i)} - 1 \right)^2 Y_{t+s} \right] \\ & + \mathbb{E}_t \sum_{s=0}^{\infty} M_{t,t+s} \Xi_{t+s} \left([K_{t-1+s}(i)U_{t+s}(i)]^\alpha [Z_{t+s} N_{t+s}(i)]^{1-\alpha} - \Phi - \left[\frac{P_{t+s}(i)}{P_{t+s}} \right]^{-\theta_{\mu,t+s}} Y_{t+s} \right) \end{aligned}$$

$$+\mathbb{E}_t \sum_{s=0}^{\infty} M_{t+s} q_{t+s} \left[\left(1 - \delta(U_{t+s}(i)) - \frac{\phi_K}{2} \left(\frac{I_{t+s}(i)}{K_{t-1+s}(i)} - \delta \right)^2 \right) K_{t+s}(i) + I_{t+s}(i) - K_{t+s}(i) \right]$$

where the lagrange multipliers Ξ_t and q_t denote, respectively, the marginal cost of producing one additional unit of intermediate good i and the price of a marginal unit of installed capital.

We get the following first order conditions

1) For $N_t(i)$

$$\frac{\partial \mathcal{L}}{\partial N_t(i)} = -W_t + \Xi_t (1 - \alpha) [K_{t-1}(i)U_t(i)]^\alpha [Z_t N_t(i)]^{-\alpha} Z_t = 0$$

⇕

$$W_t = \Xi_t (1 - \alpha) [K_{t-1}(i)U_t(i)]^\alpha \frac{[Z_t N_t(i)]^{1-\alpha}}{N_t(i)}$$

⇕

$$W_t N_t(i) = \Xi_t (1 - \alpha) [K_{t-1}(i)U_t(i)]^\alpha [Z_t N_t(i)]^{1-\alpha}$$

Alternatively, we also note that this equation can be expressed as

$$W_t N_t(i) = \Xi_t (1 - \alpha) Output_t$$

where $[K_{t-1}(i)U_t(i)]^\alpha [Z_t N_t(i)]^{1-\alpha} = Output_t$, implying that

$$1 = \Xi_t (1 - \alpha) \frac{Output_t}{W_t N_t(i)}$$

⇕

$$\frac{1}{\Xi_t} = (1 - \alpha) \frac{1}{\underbrace{\frac{Output_t}{W_t N_t(i)}}_{s_{output,t}}}$$

where $s_{output,t}$ is the labor share of output (See 1059 in Rotemberg and Woodford, 1999).

2) For $U_t(i)$:

$$\frac{\partial \mathcal{L}}{\partial U_t(i)} = \Xi_t \alpha [K_{t-1}(i)U_t(i)]^{\alpha-1} K_{t-1}(i) [Z_t N_t(i)]^{1-\alpha} - q_t \delta'(U_t(i)) K_{t-1}(i) = 0$$

⇕

$$q_t \delta'(U_t(i)) K_{t-1}(i) U_t(i) = \Xi_t \alpha [K_{t-1}(i)U_t(i)]^\alpha [Z_t N_t(i)]^{1-\alpha}$$

3) For $P_t(i)$:

$$\begin{aligned} \frac{\partial \mathcal{L}}{\partial P_t(i)} &= (1 - \theta_{\mu,t}) \left[\frac{P_t(i)}{P_t} \right]^{-\theta_{\mu,t}} \frac{Y_t}{P_t} - \phi_P \left(\frac{P_t(i)}{\Pi_{ss} P_{t-1}(i)} - 1 \right) \frac{1}{\Pi_{ss} P_{t-1}(i)} Y_t + \Xi_t \theta_{\mu,t} \left[\frac{P_t(i)}{P_t} \right]^{-\theta_{\mu,t}-1} \frac{1}{P_t} Y_t \\ &\quad - \phi_P \mathbb{E}_t \left\{ M_{t+1} \left(\frac{P_{t+1}(i)}{\Pi_{ss} P_t(i)} - 1 \right) \frac{-\Pi_{ss} P_{t+1}(i)}{(\Pi_{ss} P_t(i))^2} Y_{t+1} \right\} \\ &= 0 \end{aligned}$$

⇕

$$\begin{aligned} \phi_P \left(\frac{P_t(i)}{\Pi_{ss} P_{t-1}(i)} - 1 \right) \frac{1}{\Pi_{ss} P_{t-1}(i)} Y_t &= (1 - \theta_{\mu,t}) \left[\frac{P_t(i)}{P_t} \right]^{-\theta_{\mu,t}} \frac{Y_t}{P_t} + \Xi_t \theta_{\mu,t} \left[\frac{P_t(i)}{P_t} \right]^{-\theta_{\mu,t}-1} \frac{1}{P_t} Y_t \\ &\quad + \phi_P \mathbb{E}_t \left[M_{t+1} \left(\frac{P_{t+1}(i)}{\Pi_{ss} P_t(i)} - 1 \right) \frac{P_{t+1}(i)}{\Pi_{ss} (P_t(i))^2} Y_{t+1} \right] \end{aligned}$$

⇕

$$\begin{aligned} \phi_P \left(\frac{P_t(i)}{\Pi_{ss} P_{t-1}(i)} - 1 \right) \frac{P_t}{\Pi_{ss} P_{t-1}(i)} &= (1 - \theta_{\mu,t}) \left[\frac{P_t(i)}{P_t} \right]^{-\theta_{\mu,t}} + \theta_{\mu,t} \Xi_t \left[\frac{P_t(i)}{P_t} \right]^{-\theta_{\mu,t}-1} \\ &+ \phi_P \mathbb{E}_t \left[M_{t+1} \frac{Y_{t+1}}{Y_t} \left(\frac{P_{t+1}(i)}{\Pi_{ss} P_t(i)} - 1 \right) \frac{P_{t+1}(i)}{\Pi_{ss} P_t(i)} \frac{P_t}{P_t(i)} \right] \end{aligned}$$

4) For $K_{t+1}(i)$:

Before we derive this expression, it is convenient to define R_t^K as the marginal product per unit of capital services $K_{t-1}(i)U_t(i)$, which is paid to the owners of the capital stock, i.e.:

$$R_t^K \equiv \Xi_t \frac{\partial F(K_{t-1}(i)U_t(i), Z_t N_t(i))}{\partial (K_{t-1}(i)U_t(i))} = \Xi_t \alpha [K_{t-1}(i)U_t(i)]^{\alpha-1} [Z_t N_t(i)]^{1-\alpha}$$

⇕

$$R_t^K K_{t-1}(i)U_t(i) = \Xi_t \alpha [K_{t-1}(i)U_t(i)]^\alpha [Z_t N_t(i)]^{1-\alpha}$$

This will allow us to simplify the expression below. Now let us consider the first-order condition for capital:

$$\begin{aligned} \frac{\partial \mathcal{L}}{\partial K_t(i)} &= -q_t + \mathbb{E}_t \left[M_{t+1} \Xi_{t+1} \alpha [K_t(i)U_{t+1}(i)]^{\alpha-1} U_{t+1}(i) [Z_{t+1} N_{t+1}(i)]^{1-\alpha} \right] \\ &+ \mathbb{E}_t \left[M_{t+1} q_{t+1} \left\{ \left(1 - \delta(U_{t+1}(i)) - \frac{\phi_K}{2} \left(\frac{I_{t+1}(i)}{K_t(i)} - \delta_0 \right)^2 \right) - \phi_K \left(\frac{I_{t+1}(i)}{K_t(i)} - \delta_0 \right) \frac{-I_{t+1}(i)}{[K_t(i)]^2} K_t(i) \right\} \right] \\ &= 0 \end{aligned}$$

⇕

$$\begin{aligned} q_t &= \mathbb{E}_t \left[M_{t+1} \underbrace{\Xi_{t+1} \alpha [K_t(i)U_{t+1}(i)]^{\alpha-1} [Z_{t+1} N_{t+1}(i)]^{1-\alpha}}_{R_{t+1}^K} U_{t+1}(i) \right] \\ &+ \mathbb{E}_t \left[M_{t+1} q_{t+1} \left\{ \left(1 - \delta(U_{t+1}(i)) - \frac{\phi_K}{2} \left(\frac{I_{t+1}(i)}{K_t(i)} - \delta_0 \right)^2 \right) - \phi_K \left(\frac{I_{t+1}(i)}{K_t(i)} - \delta \right) \frac{-I_{t+1}(i)}{[K_t(i)]^2} K_t(i) \right\} \right] \end{aligned}$$

⇕

$$q_t = \mathbb{E}_t M_{t+1} \left[R_t^K U_{t+1}(i) + q_{t+1} \left\{ \left(1 - \delta(U_{t+1}(i)) - \frac{\phi_K}{2} \left(\frac{I_{t+1}(i)}{K_t(i)} - \delta_0 \right)^2 \right) + \phi_K \left(\frac{I_{t+1}(i)}{K_t(i)} - \delta \right) \frac{I_{t+1}(i)}{K_t(i)} \right\} \right]$$

5) For $I_t(i)$

$$\frac{\partial \mathcal{L}}{\partial I_t(i)} = -1 + q_t \left(1 - \phi_K \left(\frac{I_t(i)}{K_{t-1}(i)} - \delta_0 \right) \frac{1}{K_{t-1}(i)} K_{t-1}(i) \right) = 0$$

⇓

$$1 = q_t \left(1 - \phi_K \left(\frac{I_t(i)}{K_{t-1}(i)} - \delta_0 \right) \right)$$

2.3 The Final Good Producing Firm

A representative final good producer combines the intermediate goods to construct the final output good Y_t . The profit maximizing problem for the final good producing firm results in the following first-order condition, which is the demand schedule for intermediate firms (which has been already used above):

$$Y_t(i) = \left[\frac{P_t(i)}{P_t} \right]^{-\theta_{\mu,t}} Y_t.$$

The market for the final good is perfectly competitive, and thus, the final good producing firm earns zero profits in equilibrium.

2.4 Equilibrium

In the symmetric equilibrium, all intermediate goods firms choose the same price $P_t(i) = P_t$, employ the same amount of labor $N_t(i) = N_t$, and choose the same level of capital and utilization rate $K_t(i) = K_t$ and $U_t(i) = U_t$. Thus, all firms have the same cash flows and are financed with the mix of bonds and equity. The markup of price over marginal cost is $\mu_t = 1/\Xi_t$, and gross inflation is $\Pi_t = P_t/P_{t-1}$.

Note that the households budget constraint implies to (as stocks are $S_t = S_{t+1} = 1$)

$$C_t + P_t^E S_{t+1} + \frac{1}{R_t^R} B_{t+1} = W_t N_t + (D_t^E + P_t^E) S_t + B_t$$

↓

$$C_t + \frac{1}{R_t^R} B_{t+1} = \frac{W_t}{P_t} N_t + D_t^E + B_t$$

⇕

$$C_t + \frac{1}{R_t^R} \nu K_t = W_t N_t + D_t^E + \nu K_{t-1}.$$

2.5 Monetary Policy

The central bank adjusts the nominal gross one-period interest rate R_t in accordance with the following rule:

$$\begin{aligned} \log(R_t/R) &= \rho_r \log(R_{t-1}/R) + (1 - \rho_r) (\rho_\pi \log(\Pi_t/\Pi) + \rho_y \log(Y_t/Y_{t-1})) \\ &\quad + (1 - \rho_r) \zeta_{VR_t^{eq}} (VR_t^{eq} - aux_t). \end{aligned}$$

where $VR_t^{eq} = \mathbb{V}_t [R_{t+1}^E]$ is the quarterly conditional variance of the return on equity and

$$\begin{aligned} aux_t &= (1 - \gamma) \sum_{i=0}^{\infty} \gamma^i VR_{t-i}^{eq} \\ &= (1 - \gamma) VR_t^{eq} + \gamma \mathbb{E}_t [aux_{t+1}] \end{aligned}$$

where $\gamma = 0.9999$ to let aux_t approximate the unconditional mean of VR_t^{eq} . Note that we let $\rho_r = \zeta_{VR_t^{eq}} = 0$ in the paper.

2.6 Shock processes

We assume the following processes for the exogenous shocks:

$$\begin{aligned} \ln a_{t+1} &= \rho_a \ln a_t + \sigma_{a,t} \epsilon_{a,t+1} \\ \sigma_{a,t+1} &= (1 - \rho_\sigma) \sigma_a + \rho_\sigma \sigma_{a,t} + \sigma_\sigma \epsilon_{\sigma,t+1} \\ \ln Z_t &= \rho_Z \ln Z_{t-1} + \sigma_Z \epsilon_{Z,t+1} \\ \ln(\theta_{\mu,t+1}/\theta_\mu) &= \rho_{\theta_\mu} \log(\theta_{\mu,t}/\theta_\mu) + \sigma_{\theta_\mu} \epsilon_{\theta,t+1}, \end{aligned}$$

where $\epsilon_{a,t+1}$, $\epsilon_{\sigma,t+1}$, $\epsilon_{Z,t+1}$, and $\epsilon_{\theta,t+1}$ are standard Gaussian, independent across time, and mutually independent.

2.7 The VXO index

The VXO index in the U.S. is a market estimate of the expected volatility in the Standard and Poor's 100 index obtained from option prices. A model-implied VXO index can be computed as the expected conditional volatility of the return on firm equity, i.e. as

$$\begin{aligned} R_{t+1}^E &= \frac{D_{t+1}^E + P_{t+1}^E}{P_t^E} \\ VXO_t &= 100 \sqrt{4 \times \mathbb{V}_t [R_{t+1}^E]}, \end{aligned}$$

where $\mathbb{V}_t [R_{t+1}^E]$ is the quarterly conditional variance of the return on equity R_{t+1}^E . We annualize the quarterly conditional variance and then transform this variance into a standard deviation in percentage points.

2.8 Risk Aversion at the Steady State

We follow Swanson (2012) and Swanson (2018) and compute two measures of relative risk aversion in our model. With recursive Epstein-Zin preferences controlled by α , there are two measures of relative risk aversion. The first measure RRA^c applies when there is no upper bound for labor and therefore total household wealth A_t equals the present discounted value of consumption. The other measure RRA^{cl} applies when the upper bound for the household's time endowment is well-specified, meaning that total household wealth \bar{A}_t equals the present discounted value of leisure plus consumption.

Throughout this section we use the notational convention in Swanson (2012) where a variable in the steady state is denoted without a subscript. For instance c is the steady state value of c_t . Moreover, $u = u(c, n)$.

The general formulas with external habit formation are (see Swanson (2012), page 24, eq 53 and eq 54)

$$RRA^{cl} = \frac{-u_{11} + \lambda u_{12}}{u_1} \frac{c + w(1-n)}{1+w\lambda} + \alpha^{Swan} \frac{(c + w(1-n))u_1}{u}$$

$$RRA^c = c \left(\frac{-u_{11} + \lambda u_{12}}{u_1} \frac{1}{1+w\lambda} + \alpha^{Swan} \frac{u_1}{u} \right)$$

where

$$w = -\frac{u_2}{u_1}$$

$$\lambda = \frac{wu_{11} + u_{12}}{u_{22} + wu_{12}}$$

Note that

$$RRA^{cl} = \frac{-u_{11} + \lambda u_{12}}{u_1} \frac{c + w(1-n)}{1+w\lambda} + \alpha^{Swan} \frac{(c + w(1-n))u_1}{u}$$

$$= \frac{c + w(1-n)}{c} c \left[\frac{-u_{11} + \lambda u_{12}}{u_1} \frac{1}{1+w\lambda} + \alpha^{Swan} \frac{u_1}{u} \right]$$

\Downarrow

$$RRA^{cl} = \left(1 + \frac{w}{c} (1-n) \right) RRA^c$$

Here, we use the notation that

- u = the utility function
- u_1 = the partial derivative of u with respect to consumption
- u_2 = the partial derivative of u with respect to hours worked
- w = the steady state wage level
- c = the steady state consumption level
- n = hours worked

Note that the way Swanson (2012) defines λ is different from the way we define λ_t in our model (i.e. the lagrange multiplier on households' budget restriction). Recall that our utility function reads (ignoring preference shocks)

$$u = \frac{\theta_V}{1-\sigma} \left((c_t - bc_{t-1})^\eta (1-n_t)^{1-\eta} \right)^{\frac{1-\sigma}{\theta_V}} + u_0$$

$$= \frac{\theta_V}{1-\sigma} (c_t - bc_{t-1})^{\eta \frac{1-\sigma}{\theta_V}} (1-n_t)^{(1-\eta) \frac{1-\sigma}{\theta_V}} + u_0$$

Hence, in the steady state we have

$$\begin{aligned}
u_1 &= \eta (c_t - bc_{t-1})^{\eta \frac{1-\sigma}{\theta_V} - 1} (1 - n_t)^{(1-\eta) \frac{1-\sigma}{\theta_V}} \\
u_{11} &= \eta \left(\eta \frac{1-\sigma}{\theta_V} - 1 \right) (c_t - bc_{t-1})^{\eta \frac{1-\sigma}{\theta_V} - 2} (1 - n_t)^{(1-\eta) \frac{1-\sigma}{\theta_V}} \\
u_2 &= - (1 - \eta) (c_t - bc_{t-1})^{\eta \frac{1-\sigma}{\theta_V}} (1 - n_t)^{(1-\eta) \frac{1-\sigma}{\theta_V} - 1} \\
u_{22} &= (1 - \eta) \left((1 - \eta) \frac{1-\sigma}{\theta_V} - 1 \right) (c_t - bc_{t-1})^{\eta \frac{1-\sigma}{\theta_V}} (1 - n_t)^{(1-\eta) \frac{1-\sigma}{\theta_V} - 2} \\
u_{12} &= -\eta (1 - \eta) \frac{1-\sigma}{\theta_V} (c_t - bc_{t-1})^{\eta \frac{1-\sigma}{\theta_V} - 1} (1 - n_t)^{(1-\eta) \frac{1-\sigma}{\theta_V} - 1}
\end{aligned}$$

Thus

$$\begin{aligned}
w_t &= -\frac{u_2}{u_1} = -\frac{-(1-\eta)(c_t - bc_{t-1})^{\eta \frac{1-\sigma}{\theta_V}} (1 - n_t)^{(1-\eta) \frac{1-\sigma}{\theta_V} - 1}}{\eta (c_t - bc_{t-1})^{\eta \frac{1-\sigma}{\theta_V} - 1} (1 - n_t)^{(1-\eta) \frac{1-\sigma}{\theta_V}}} \\
&= \frac{(1-\eta)(1 - n_t)^{-1}}{\eta (c_t - bc_{t-1})^{-1}} \\
&= \frac{1-\eta}{\eta} \frac{c_t - bc_{t-1}}{1 - n_t}
\end{aligned}$$

And

$$\lambda_t = \frac{wu_{11} + u_{12}}{u_{22} + wu_{12}}$$

$$\begin{aligned}
&= \frac{\frac{1-\eta}{\eta} \frac{c_t - bc_{t-1}}{1 - n_t} \eta \left(\eta \frac{1-\sigma}{\theta_V} - 1 \right) (c_t - bc_{t-1})^{\eta \frac{1-\sigma}{\theta_V} - 2} (1 - n_t)^{(1-\eta) \frac{1-\sigma}{\theta_V}} - \eta (1-\eta) \frac{1-\sigma}{\theta_V} (c_t - bc_{t-1})^{\eta \frac{1-\sigma}{\theta_V} - 1} (1 - n_t)^{(1-\eta) \frac{1-\sigma}{\theta_V} - 1}}{(1-\eta) \left((1-\eta) \frac{1-\sigma}{\theta_V} - 1 \right) (c_t - bc_{t-1})^{\eta \frac{1-\sigma}{\theta_V}} (1 - n_t)^{(1-\eta) \frac{1-\sigma}{\theta_V} - 2} - \frac{1-\eta}{\eta} \frac{c_t - bc_{t-1}}{1 - n_t} \eta (1-\eta) \frac{1-\sigma}{\theta_V} (c_t - bc_{t-1})^{\eta \frac{1-\sigma}{\theta_V} - 1} (1 - n_t)^{(1-\eta) \frac{1-\sigma}{\theta_V} - 1}} \\
&= \frac{\frac{1-\eta}{\eta} \eta \left(\eta \frac{1-\sigma}{\theta_V} - 1 \right) (c_t - bc_{t-1})^{\eta \frac{1-\sigma}{\theta_V} - 1} (1 - n_t)^{(1-\eta) \frac{1-\sigma}{\theta_V} - 1} - \eta (1-\eta) \frac{1-\sigma}{\theta_V} (c_t - bc_{t-1})^{\eta \frac{1-\sigma}{\theta_V} - 1} (1 - n_t)^{(1-\eta) \frac{1-\sigma}{\theta_V} - 1}}{(1-\eta) \left((1-\eta) \frac{1-\sigma}{\theta_V} - 1 \right) (c_t - bc_{t-1})^{\eta \frac{1-\sigma}{\theta_V}} (1 - n_t)^{(1-\eta) \frac{1-\sigma}{\theta_V} - 2} - \frac{1-\eta}{\eta} \eta (1-\eta) \frac{1-\sigma}{\theta_V} (c_t - bc_{t-1})^{\eta \frac{1-\sigma}{\theta_V} - 1} (1 - n_t)^{(1-\eta) \frac{1-\sigma}{\theta_V} - 2}} \\
&= \frac{\left[(c_t - bc_{t-1})^{\eta \frac{1-\sigma}{\theta_V} - 1} (1 - n_t)^{(1-\eta) \frac{1-\sigma}{\theta_V} - 1} \right] \left((1-\eta) \left(\eta \frac{1-\sigma}{\theta_V} - 1 \right) - \eta (1-\eta) \frac{1-\sigma}{\theta_V} \right)}{\left[(c_t - bc_{t-1})^{\eta \frac{1-\sigma}{\theta_V}} (1 - n_t)^{(1-\eta) \frac{1-\sigma}{\theta_V} - 2} \right] \left((1-\eta) \left((1-\eta) \frac{1-\sigma}{\theta_V} - 1 \right) - \frac{1-\eta}{\eta} \eta (1-\eta) \frac{1-\sigma}{\theta_V} \right)} \\
&= \frac{\left[(c_t - bc_{t-1})^{\eta \frac{1-\sigma}{\theta_V} - 1} (1 - n_t)^{(1-\eta) \frac{1-\sigma}{\theta_V} - 1} \right] \left((1-\eta) \eta \frac{1-\sigma}{\theta_V} - (1-\eta) - \eta (1-\eta) \frac{1-\sigma}{\theta_V} \right)}{\left[(c_t - bc_{t-1})^{\eta \frac{1-\sigma}{\theta_V}} (1 - n_t)^{(1-\eta) \frac{1-\sigma}{\theta_V} - 2} \right] \left((1-\eta)^2 \frac{1-\sigma}{\theta_V} - (1-\eta) - (1-\eta)^2 \frac{1-\sigma}{\theta_V} \right)} \\
&= \frac{\left[(c_t - bc_{t-1})^{\eta \frac{1-\sigma}{\theta_V} - 1} (1 - n_t)^{(1-\eta) \frac{1-\sigma}{\theta_V} - 1} \right] (- (1-\eta))}{\left[(c_t - bc_{t-1})^{\eta \frac{1-\sigma}{\theta_V}} (1 - n_t)^{(1-\eta) \frac{1-\sigma}{\theta_V} - 2} \right] (- (1-\eta))} \\
&= \frac{(c_t - bc_{t-1})^{-1}}{(1 - n_t)^{-1}} \\
&= \frac{1 - n_t}{c_t - bc_{t-1}}
\end{aligned}$$

Thus

$$w_t \lambda_t = \frac{1-\eta}{\eta} \frac{c_t - bc_{t-1}}{1 - n_t} \frac{1 - n_t}{c_t - bc_{t-1}} = \frac{1-\eta}{\eta}$$

Hence, the first measure of relative risk-aversion is:

$$RRA^c = c \left(\frac{-u_{11} + \lambda u_{12}}{u_1} \frac{1}{1 + w\lambda} + \alpha^{Swan} \frac{u_1}{u} \right)$$

$$\begin{aligned}
&= c \left(\frac{-\eta \left(\eta^{\frac{1-\sigma}{\theta_V}} - 1 \right) (c-bc)^{\eta \frac{1-\sigma}{\theta_V} - 2} (1-n)^{(1-\eta) \frac{1-\sigma}{\theta_V}} - \frac{1-n}{c-bc} \eta (1-\eta)^{\frac{1-\sigma}{\theta_V}} (c-bc)^{\eta \frac{1-\sigma}{\theta_V} - 1} (1-n)^{(1-\eta) \frac{1-\sigma}{\theta_V} - 1}}{\eta (c-bc)^{\eta \frac{1-\sigma}{\theta_V} - 1} (1-n)^{(1-\eta) \frac{1-\sigma}{\theta_V}}} \frac{1}{1 + \frac{1}{\eta}} \right. \\
&+ \left. \alpha^{Swan} \frac{\eta (c-bc)^{\eta \frac{1-\sigma}{\theta_V} - 1} (1-n)^{(1-\eta) \frac{1-\sigma}{\theta_V}}}{\frac{\theta_V}{1-\sigma} ((c-bc)^\eta (1-n)^{1-\eta})^{\frac{1-\sigma}{\theta_V}} + u_0^{(1)} + u_0^{(2)}} \right) \\
&= c \left(\frac{-\left(\eta^{\frac{1-\sigma}{\theta_V}} - 1 \right) (c-bc)^{-1} - \frac{1-n}{c-bc} (1-\eta)^{\frac{1-\sigma}{\theta_V}} (1-n)^{-1}}{1} \frac{1}{1 + \frac{1}{\eta}} + \alpha^{Swan} \frac{\eta (c-bc)^{\eta \frac{1-\sigma}{\theta_V} - 1} (1-n)^{(1-\eta) \frac{1-\sigma}{\theta_V}}}{\frac{\theta_V}{1-\sigma} ((c-bc)^\eta (1-n)^{1-\eta})^{\frac{1-\sigma}{\theta_V}} + u_0^{(1)} + u_0^{(2)}} \right) \\
&= c \left(\frac{-\left(\eta^{\frac{1-\sigma}{\theta_V}} - 1 \right) (c-bc)^{-1} - \frac{1}{c-bc} (1-\eta)^{\frac{1-\sigma}{\theta_V}}}{1} \frac{1}{1 + \frac{1}{\eta}} + \alpha^{Swan} \frac{\eta (c-bc)^{\eta \frac{1-\sigma}{\theta_V} - 1} (1-n)^{(1-\eta) \frac{1-\sigma}{\theta_V}}}{\frac{\theta_V}{1-\sigma} ((c-bc)^\eta (1-n)^{1-\eta})^{\frac{1-\sigma}{\theta_V}} + u_0^{(1)} + u_0^{(2)}} \right) \\
&= \frac{\frac{1}{1-b} \left\{ \left(1 - \eta^{\frac{1-\sigma}{\theta_V}} \right) - (1-\eta)^{\frac{1-\sigma}{\theta_V}} \right\}}{1 + \frac{1}{\eta}} + \alpha^{Swan} \frac{c \eta (c-bc)^{\eta \frac{1-\sigma}{\theta_V} - 1} (1-n)^{(1-\eta) \frac{1-\sigma}{\theta_V}}}{\frac{\theta_V}{1-\sigma} ((c-bc)^\eta (1-n)^{1-\eta})^{\frac{1-\sigma}{\theta_V}} + u_0^{(1)} + u_0^{(2)}} \\
&= \frac{1}{1-b} \frac{\eta \left(1 - \eta^{\frac{1-\sigma}{\theta_V}} - \frac{1-\sigma}{\theta_V} + \eta^{\frac{1-\sigma}{\theta_V}} \right)}{\eta + 1 - \eta} + \alpha^{Swan} \frac{c \eta (c-bc)^{\eta \frac{1-\sigma}{\theta_V} - 1} (1-n)^{(1-\eta) \frac{1-\sigma}{\theta_V}}}{\frac{\theta_V}{1-\sigma} ((c-bc)^\eta (1-n)^{1-\eta})^{\frac{1-\sigma}{\theta_V}} + u_0^{(1)} + u_0^{(2)}} \\
&= \frac{\eta \left(1 - \frac{1-\sigma}{\theta_V} \right)}{1-b} + \alpha^{Swan} \frac{c \eta (c-bc)^{\eta \frac{1-\sigma}{\theta_V} - 1} (1-n)^{(1-\eta) \frac{1-\sigma}{\theta_V}}}{\frac{\theta_V}{1-\sigma} ((c-bc)^\eta (1-n)^{1-\eta})^{\frac{1-\sigma}{\theta_V}} + u_0^{(1)} + u_0^{(2)}} \\
&= \frac{\eta \left(1 - \frac{1-\sigma}{\theta_V} \right)}{1-b} + \alpha^{Swan} \frac{\frac{c}{c-bc} \eta (c-bc)^{\eta \frac{1-\sigma}{\theta_V}} (1-n)^{(1-\eta) \frac{1-\sigma}{\theta_V}}}{\frac{\theta_V}{1-\sigma} ((c-bc)^\eta (1-n)^{1-\eta})^{\frac{1-\sigma}{\theta_V}} + u_0^{(1)} + u_0^{(2)}} \\
&= \frac{\eta \left(1 - \frac{1-\sigma}{\theta_V} \right)}{1-b} + \frac{\alpha^{Swan} \eta}{1-b} \frac{(c-bc)^{\eta \frac{1-\sigma}{\theta_V}} (1-n)^{(1-\eta) \frac{1-\sigma}{\theta_V}}}{\frac{\theta_V}{1-\sigma} ((c-bc)^\eta (1-n)^{1-\eta})^{\frac{1-\sigma}{\theta_V}} + u_0^{(1)} + u_0^{(2)}}
\end{aligned}$$

Thus, for a given value of RRA^c we can back out the constant, i.e.

$$\begin{aligned}
RRA^c - \frac{\eta \left(1 - \frac{1-\sigma}{\theta_V} \right)}{1-b} &= \frac{\alpha^{Swan} \eta}{1-b} \frac{(c-bc)^{\eta \frac{1-\sigma}{\theta_V}} (1-n)^{(1-\eta) \frac{1-\sigma}{\theta_V}}}{\frac{\theta_V}{1-\sigma} ((c-bc)^\eta (1-n)^{1-\eta})^{\frac{1-\sigma}{\theta_V}} + u_0^{(1)} + u_0^{(2)}} \\
\Downarrow \\
\frac{RRA^c - \frac{\eta \left(1 - \frac{1-\sigma}{\theta_V} \right)}{1-b}}{\frac{\alpha^{Swan} \eta}{1-b} \frac{(c-bc)^{\eta \frac{1-\sigma}{\theta_V}} (1-n)^{(1-\eta) \frac{1-\sigma}{\theta_V}}}{\frac{\theta_V}{1-\sigma} ((c-bc)^\eta (1-n)^{1-\eta})^{\frac{1-\sigma}{\theta_V}} + u_0^{(1)} + u_0^{(2)}}} &= \frac{1}{\frac{\theta_V}{1-\sigma} ((c-bc)^\eta (1-n)^{1-\eta})^{\frac{1-\sigma}{\theta_V}} + u_0^{(1)} + u_0^{(2)}} \\
\Downarrow \\
\frac{\frac{\theta_V}{1-\sigma} ((c-bc)^\eta (1-n)^{1-\eta})^{\frac{1-\sigma}{\theta_V}} + u_0^{(1)} + u_0^{(2)}}{\frac{\alpha^{Swan} \eta}{1-b} \frac{(c-bc)^{\eta \frac{1-\sigma}{\theta_V}} (1-n)^{(1-\eta) \frac{1-\sigma}{\theta_V}}}{\frac{\theta_V}{1-\sigma} ((c-bc)^\eta (1-n)^{1-\eta})^{\frac{1-\sigma}{\theta_V}} + u_0^{(1)} + u_0^{(2)}}} &= \frac{\frac{\alpha^{Swan} \eta}{1-b} \frac{(c-bc)^{\eta \frac{1-\sigma}{\theta_V}} (1-n)^{(1-\eta) \frac{1-\sigma}{\theta_V}}}{\frac{\theta_V}{1-\sigma} ((c-bc)^\eta (1-n)^{1-\eta})^{\frac{1-\sigma}{\theta_V}} + u_0^{(1)} + u_0^{(2)}}}{RRA^c - \frac{\eta \left(1 - \frac{1-\sigma}{\theta_V} \right)}{1-b}} \\
\Downarrow \\
u_0^{(1)} + u_0^{(2)} &= \frac{\frac{\alpha^{Swan} \eta}{1-b} \frac{(c-bc)^{\eta \frac{1-\sigma}{\theta_V}} (1-n)^{(1-\eta) \frac{1-\sigma}{\theta_V}}}{\frac{\theta_V}{1-\sigma} ((c-bc)^\eta (1-n)^{1-\eta})^{\frac{1-\sigma}{\theta_V}} + u_0^{(1)} + u_0^{(2)}}}{RRA^c - \frac{\eta \left(1 - \frac{1-\sigma}{\theta_V} \right)}{1-b}} - \frac{\theta_V}{1-\sigma} ((c-bc)^\eta (1-n)^{1-\eta})^{\frac{1-\sigma}{\theta_V}}
\end{aligned}$$

2.9 Solution for the deterministic steady state

To facilitate the derivations, we follow introduce the two constants $const1$ and $const2$ scaling the production function and the value function, respectively. Below we let $\mu_t = \frac{1}{\Xi_t}$. Hence, the model reads (without stating the exogenous processes)

1	$Y_t + \Phi = \text{const1}([K_{t-1}U_t]^\alpha [Z_t N_t]^{1-\alpha})$
2	$C_t + \frac{1}{R_t^E} \nu K_t = W_t N_t + D_t^E + \nu K_{t-1}$
3	$\frac{(1-\eta)}{\eta} \frac{C_t - bC_{t-1}}{1-N_t} = W_t$
4	$V_t = \text{const2} \cdot \left\{ a_t^{\frac{1-\sigma}{\theta_V}} \left[\frac{\theta_V}{1-\sigma} \left((C_t - bC_{t-1})^\eta (1-N_t)^{1-\eta} \right)^{\frac{1-\sigma}{\theta_V}} + u_0^{(1)} \right] + u_0^{(2)} \right\} + \beta (EV_t)^{\frac{1}{1-\alpha^{Swan}}}$
5	$EV_t = \mathbb{E}_t \left[V_{t+1}^{1-\alpha^{Swan}} \right]$
6	$W_t N_t = (1-\alpha) (Y_t + \Phi) \frac{1}{\mu_t}$
7	$R_t^K K_{t-1} U_t = \alpha (Y_t + \Phi) \frac{1}{\mu_t}$
8	$q_t (\delta_1 + \delta_2 (U_t - 1)) K_{t-1} U_t = \alpha (Y_t + \Phi) \frac{1}{\mu_t}$
9	$K_t = \left(1 - (\delta_0 + \delta_1 (U_t - 1) + \frac{\delta_2}{2} (U_t - 1)^2) - \frac{\phi_K}{2} \left(\frac{I_t}{K_{t-1}} - \delta_0 \right)^2 \right) K_{t-1} + I_t$
10	$1 = R_t^R \mathbb{E}_t [M_{t+1}]$
11	$1 = R_t \mathbb{E}_t \left[M_{t+1} \frac{1}{\Pi_{t+1}} \right]$
12	$P_t^E = \mathbb{E}_t [M_{t+1} (D_{t+1}^E + P_{t+1}^E)]$
13	$\log(R_t) = \rho_r \log(R_{t-1}) + (1-\rho_r) (\log(R_{ss}) + \zeta_\pi \log(\frac{\Pi_t}{\Pi_{ss}}) + \zeta_{\Delta y} \log(\frac{Y_t}{Y_{t-1}}) + \zeta_y \log(\frac{Y_t}{Y_{ss}}))$ $+ (1-\rho_r) \zeta_V R_t^{eq} (VR_t^{eq} - aux_t)$
14	$D_t^E = Y_t - W_t N_t - I_t - \frac{\phi_P}{2} \left(\frac{\Pi_t}{\Pi_{ss}} - 1 \right)^2 Y_t - \nu (K_{t-1} - \frac{1}{R_t^E} K_t)$
15	$q_t = \mathbb{E}_t [M_{t+1} [R_{t+1}^K U_{t+1}$ $+ q_{t+1} \left(1 - (\delta_0 + \delta_1 (U_{t+1} - 1) + \frac{\delta_2}{2} (U_{t+1} - 1)^2) - \frac{\phi_K}{2} \left(\frac{I_{t+1}}{K_t} - \delta_0 \right)^2 \right) + \phi_K \left(\frac{I_{t+1}}{K_t} - \delta_0 \right) \frac{I_{t+1}}{K_t}]]$
16	$\frac{1}{q_t} = 1 - \phi_K \left(\frac{I_t}{K_{t-1}} - \delta_0 \right)$
17	$\phi_P \left(\frac{\Pi_t}{\Pi_{ss}} - 1 \right) \frac{\Pi_t}{\Pi_{ss}} = (1 - \theta_{\mu,t}) + \frac{\theta_{\mu,t}}{\mu_t} + \phi_P \mathbb{E}_t \left[M_{t+1} \frac{Y_{t+1}}{Y_t} \left(\frac{\Pi_{t+1}}{\Pi_{ss}} - 1 \right) \frac{\Pi_{t+1}}{\Pi_{ss}} \right]$
18	$ER_t^{eq} = \mathbb{E}_t \left[\frac{D_{t+1}^E + P_{t+1}^E}{P_t^E} \right]$
19	$ER_t^{eq2} = \mathbb{E}_t \left[\left(\frac{D_{t+1}^E + P_{t+1}^E}{P_t^E} \right)^2 \right]$
20	$VR_t^{eq} = ER_t^{eq2} - (ER_t^{eq})^2$
21	$aux_t = (1-\gamma) VR_t^{eq} + \gamma \mathbb{E}_t [aux_{t+1}]$

Recall that

$$M_{t+1} = \beta \left(\frac{a_{t+1}}{a_t} \right)^{1-\sigma} \frac{(C_t - bC_{t-1})}{(C_{t+1} - bC_t)} \left(\frac{(C_{t+1} - bC_t)^\eta (1 - N_{t+1})^{1-\eta}}{(C_t - bC_{t-1})^\eta (1 - N_t)^{1-\eta}} \right)^{1-\sigma} \left(\frac{V_{t+1}}{\mathbb{E}_t [V_{t+1}^{1-\alpha^{Swan}}]^{1-\alpha^{Swan}}} \right)^{-\alpha^{Swan}}$$

and therefore $M_{ss} = \beta$. We use *const1* and *const2* to ensure that $Y_{ss} = 1$ and $V_{ss} = 1$. We also have that $U_{ss} = 1$, and clearly $a_{ss} = Z_{ss} = 1$.

From EQ 10:

$$1 = R_t^R \mathbb{E}_t [M_{t+1}]$$

↓

$$R_{ss}^R = \frac{1}{\beta}.$$

From EQ 11:

$$1 = R_t \mathbb{E}_t \left[M_{t+1} \frac{1}{\Pi_{t+1}} \right]$$

↓

$$R_t = \frac{\Pi_{ss}}{\beta}.$$

From EQ 17:

$$\phi_P \left(\frac{\Pi_t}{\Pi_{ss}} - 1 \right) \frac{\Pi_t}{\Pi_{ss}} = (1 - \theta_{\mu,t}) + \frac{\theta_{\mu,t}}{\mu_t} + \phi_P \mathbb{E}_t \left[M_{t+1} \frac{Y_{t+1}}{Y_t} \left(\frac{\Pi_{t+1}}{\Pi_{ss}} - 1 \right) \frac{\Pi_{t+1}}{\Pi_{ss}} \right]$$

↓

$$\theta_{\mu} - 1 = \frac{\theta_{\mu}}{\mu_{ss}}$$

⇕

$$\mu_{ss} = \frac{\theta_{\mu}}{\theta_{\mu} - 1}.$$

EQ 9:

$$K_t = \left(1 - \left(\delta_0 + \delta_1(U_t - 1) + \frac{\delta_2}{2}(U_t - 1)^2 \right) - \frac{\phi_K}{2} \left(\frac{I_t}{K_{t-1}} - \delta_0 \right)^2 \right) K_{t-1} + I_t$$

↓

$$K_{ss} = \left(1 - \delta_0 - \frac{\phi_K}{2} \left(\frac{I_t}{K_{t-1}} - \delta_0 \right)^2 \right) K_{ss} + I_{ss}$$

⇕

$$1 = 1 - \delta_0 - \frac{\phi_K}{2} \left(\frac{I_{ss}}{K_{ss}} - \delta_0 \right)^2 + \frac{I_{ss}}{K_{ss}}$$

⇕

$$0 = -\frac{\phi_K}{2} \left(\frac{I_{ss}}{K_{ss}} - \delta_0 \right)^2 + \left(\frac{I_{ss}}{K_{ss}} - \delta_0 \right)$$

⇕

$$0 = \left[1 - \frac{\phi_K}{2} \left(\frac{I_{ss}}{K_{ss}} - \delta_0 \right) \right] \left(\frac{I_{ss}}{K_{ss}} - \delta_0 \right)$$

We consider the solution

$$\frac{I_{ss}}{K_{ss}} = \delta_0,$$

while the other solution is as $\frac{2}{\phi_K} + \delta_0 = \frac{I_{ss}}{K_{ss}}$.

From EQ 16

$$\frac{1}{q_t} = 1 - \phi_K \left(\frac{I_t}{K_{t-1}} - \delta_0 \right)$$

↓

$$q_{ss} = 1.$$

From EQ 15:

$$\begin{aligned} q_t &= \mathbb{E}_t [M_{t+1} [R_{t+1}^K U_{t+1} \\ &\quad + q_{t+1} \left(1 - \left(\delta_0 + \delta_1(U_{t+1} - 1) + \frac{\delta_2}{2}(U_{t+1} - 1)^2 \right) - \frac{\phi_K}{2} \left(\frac{I_{t+1}}{K_t} - \delta_0 \right)^2 \right) + \phi_K \left(\frac{I_{t+1}}{K_t} - \delta_0 \right) \frac{I_{t+1}}{K_t}]] \end{aligned}$$

↓

$$1 = \beta [R_{ss}^K + (1 - \delta_0)]$$

$$R_{ss}^K = \frac{1}{\beta} - (1 - \delta_0)$$

To determine Φ , we first need an expression for pure profits in firms. Here, we note that

$$D_t(i) = \left[\frac{P_t(i)}{P_t} \right]^{1-\theta_{\mu,t}} Y_t - W_t N_t(i) - I_t(i) - \frac{\phi_P}{2} \left(\frac{P_t(i)}{\Pi_{ss} P_{t-1}(i)} - 1 \right)^2 Y_t$$

which in the symmetric equilibrium reduces to

$$D_t = Y_t - W_t N_t - I_t - \frac{\phi_P}{2} \left(\frac{\Pi_t}{\Pi_{ss}} - 1 \right)^2 Y_t.$$

Hence, in the steady state we get

$$D_{ss} = Y_{ss} - W_{ss} N_{ss} - I_{ss}$$

Now from EQ 6, $W_{ss} N_{ss} = (1 - \alpha) (Y_{ss} + \Phi) \frac{1}{\mu_{ss}}$. Insertin gives

$$\begin{aligned} D_{ss} &= Y_{ss} - (1 - \alpha) (Y_{ss} + \Phi) \frac{1}{\mu_{ss}} - I_{ss} \\ &= Y_{ss} - (1 - \alpha) (Y_{ss} + \Phi) \frac{1}{\mu_{ss}} - \delta_0 K_{ss} \end{aligned}$$

as $\frac{I_{ss}}{K_{ss}} = \delta_0$, so $I_{ss} = \delta_0 K_{ss}$. Now note that because β is close to one, we have $R_{ss}^K = \frac{1}{\beta} - (1 - \delta_0) \approx \delta_0$. Importantly, this approximation does not affect the perturbation approximation because the expression for pure profits does not enter on its own as an equilibrium condition. Thus, we get

$$D_{ss} \approx Y_{ss} - (1 - \alpha) (Y_{ss} + \Phi) \frac{1}{\mu_{ss}} - R^K K_{ss}$$

From EQ 7

$$\begin{aligned} R_t^K K_{t-1} U_t &= \alpha (Y_t + \Phi) \frac{1}{\mu_t} \\ \Downarrow \\ R_{ss}^K K_{ss} &= \alpha (Y_{ss} + \Phi) \frac{1}{\mu_{ss}} \end{aligned}$$

Thus we get

$$\begin{aligned} D_{ss} &\approx Y_{ss} - (1 - \alpha) (Y_{ss} + \Phi) \frac{1}{\mu_{ss}} - \alpha (Y_{ss} + \Phi) \frac{1}{\mu_{ss}} \\ &= Y_{ss} - (Y_{ss} + \Phi) \frac{1}{\mu_{ss}} \end{aligned}$$

$$\Downarrow \\ D_{ss} \mu_{ss} = Y_{ss} \mu_{ss} - Y_{ss} - \Phi$$

$$\Downarrow \\ D_{ss} \mu_{ss} = Y_{ss} (\mu_{ss} - 1) - \Phi$$

Thus, given $\mu_{ss} > 0$, for $D_{ss} = 0$ we require that

$$\Phi = Y_{ss} (\mu_{ss} - 1).$$

From EQ 7:

$$R_t^K K_{t-1} U_t = \alpha (Y_t + \Phi) \frac{1}{\mu_t}$$

\Downarrow

$$K_{ss} = \frac{\alpha (Y_{ss} + \Phi) \frac{1}{\mu_{ss}}}{R_{ss}^K}.$$

Then

$$I_{ss} = \delta_0 K_{ss}$$

From EQ 2:

$$C_t + \frac{1}{R_t^R} \nu K_t = W_t N_t + D_t^E + \nu K_{t-1}$$

↓

$$\begin{aligned} C_{ss} &= W_{ss} N_{ss} + D_{ss}^E + \nu K_{ss} - \frac{1}{R_{ss}^R} \nu K_{ss} \\ &= W_{ss} N_{ss} + \left[Y_{ss} - W_{ss} N_{ss} - I_{ss} - \frac{\phi_P}{2} \left(\frac{\Pi_{ss}}{\Pi_{ss}} - 1 \right)^2 Y_{ss} - \nu \left(K_{ss} - \frac{1}{R_{ss}^R} K_{ss} \right) \right] + \nu K_{ss} - \frac{1}{R_{ss}^R} \nu K_{ss} \\ &= Y_{ss} - I_{ss} \end{aligned}$$

where we use EQ 14 to get an expression for D_{ss}^E .

From EQ 8:

$$q_{ss} (\delta_1 + \delta_2 (U_{ss} - 1)) K_{ss} U_{ss} = \alpha (Y_{ss} + \Phi) \frac{1}{\mu_{ss}}$$

↓

$$\delta_1 K_{ss} = \alpha (Y_{ss} + \Phi) \frac{1}{\mu_{ss}}$$

↕

$$\delta_1 = \frac{\alpha (Y_{ss} + \Phi) \frac{1}{\mu_{ss}}}{K_{ss}}$$

↕

$$\begin{aligned} \delta_1 &= \frac{\alpha (Y_{ss} + \Phi) \frac{1}{\mu_{ss}}}{\frac{R_{ss}^K}{\mu_{ss}}} \\ &= R_{ss}^K \\ &= \frac{1}{\beta} - (1 - \delta_0) \end{aligned}$$

The next subsection explains how we set N_{ss} and η . Given these values, we get from EQ 6

$$W_{ss} = (1 - \alpha) (Y_{ss} + \Phi) \frac{1}{\mu_{ss} N_{ss}}$$

The constant scaling the production function is then given by (see EQ 1)

$$const1 = \frac{Y_{ss} + \Phi}{K_{ss}^\alpha [Z_{ss} N_{ss}]^{1-\alpha}}$$

Also the constant scaling the utility function can be found (see EQ 4)

$$V_{ss} = const2 \cdot \left\{ \left[\frac{\theta_V}{1-\sigma} \left((C_{ss} - bC_{ss})^\eta (1 - N_{ss})^{1-\eta} \right)^{\frac{1-\sigma}{\theta_V}} + u_0^{(1)} \right] + u_0^{(2)} \right\} + \beta V_{ss}$$

↕

$$V_{ss} = const2 \cdot \frac{\left\{ \left[\frac{\theta_V}{1-\sigma} \left((C_{ss} - bC_{ss})^\eta (1 - N_{ss})^{1-\eta} \right)^{\frac{1-\sigma}{\theta_V}} + u_0^{(1)} \right] + u_0^{(2)} \right\}}{1 - \beta}$$

↕

$$const2 = \frac{V_{ss}(1-\beta)}{\left[\frac{\theta_V}{1-\sigma} ((C_{ss} - bC_{ss})^\eta (1 - N_{ss})^{1-\eta})^{\frac{1-\sigma}{\theta_V}} + u_0^{(1)} \right] + u_0^{(2)}}$$

From EQ 2 we get

$$C_{ss} + \frac{1}{R_{ss}^R} \nu K_{ss} = W_{ss} N_{ss} + D_{ss}^E + \nu K_{ss}$$

↕

$$D_{ss}^E = C_{ss} + \frac{1}{R_{ss}^R} \nu K_{ss} - W_{ss} N_{ss} - \nu K_{ss}$$

and from EQ 12

$$P_{ss}^E = M_{ss}(D_{ss}^E + P_{ss}^E)$$

↕

$$P_{ss}^E = \frac{\beta D_{ss}^E}{1-\beta}$$

Finally, from EQ 18

$$\begin{aligned} ER_{ss}^{eq} &= \frac{D_{ss}^E + P_{ss}^E}{P_{ss}^E} \\ &= \frac{D_{ss}^E}{P_{ss}^E} + 1 \\ &= \frac{1-\beta}{\beta} + 1 \\ &= \frac{1}{\beta}, \end{aligned}$$

and from EQ 19

$$ER_t^{eq2} = \frac{1}{\beta^2}.$$

2.9.1 Determining N_{ss} and η

The value of N_{ss} and η are determined jointly based on a desired to set the Frisch labor supply elasticity to 2. In general, we have that the Frisch elasticity of labor supply is defined as

$$Frisch_t \equiv \left. \frac{\partial N_t}{\partial W_t} \frac{W_t}{N_t} \right|_{\lambda_t},$$

where λ_t is the lagrange multiplier associated to the household's budget constraint. We start by using the first-order conditions for consumption and labour, which imply

$$\eta a_t^{1-\sigma} \frac{((C_t - bC_{t-1})^\eta (1 - N_t)^{1-\eta})^{1-\sigma}}{C_t - bC_{t-1}} = \lambda_t$$

$$a_t^{1-\sigma} (\eta - 1) \frac{((C_t - bC_{t-1})^\eta (1 - N_t)^{1-\eta})^{1-\sigma}}{1 - N_t} = \lambda_t W_t$$

From the first-order condition for consumption we have

$$\eta a_t^{1-\sigma} (C_t - bC_{t-1})^{\eta(1-\sigma)-1} (1 - N_t)^{(1-\eta)(1-\sigma)} = \lambda_t$$

↕

$$(C_t - bC_{t-1})^{\eta(1-\sigma)-1} = \frac{\lambda_t}{\eta a_t^{1-\sigma}} (1 - N_t)^{-(1-\eta)(1-\sigma)}$$

↕

$$\begin{aligned} C_t &= bC_{t-1} + \left[\frac{\lambda_t}{\eta a_t^{1-\sigma}} (1 - N_t)^{-(1-\eta)(1-\sigma)} \right]^{\frac{1}{\eta(1-\sigma)-1}} \\ &= bC_{t-1} + \left[\frac{\lambda_t}{\eta a_t^{1-\sigma}} (1 - N_t)^{(\eta-1)(1-\sigma)} \right]^{\frac{1}{\eta(1-\sigma)-1}} \end{aligned}$$

Inserting this expression for consumption in the first-order condition for labour we have

$$a_t^{1-\sigma} (\eta - 1) \frac{\left(\left[\frac{\lambda_t}{\eta a_t^{1-\sigma}} (1 - N_t)^{(\eta-1)(1-\sigma)} \right]^{\frac{\eta}{\eta(1-\sigma)-1}} (1 - N_t)^{1-\eta} \right)^{1-\sigma}}{1 - N_t} = \lambda_t W_t$$

↕

$$a_t^{1-\sigma} (\eta - 1) \left(\left[\frac{\lambda_t}{\eta a_t^{1-\sigma}} \right]^{\frac{\eta}{\eta(1-\sigma)-1}} (1 - N_t)^{(\eta-1)(1-\sigma) \frac{\eta}{\eta(1-\sigma)-1} + 1 - \eta} \right)^{(1-\sigma)} = \lambda_t W_t (1 - N_t)$$

↕

$$a_t^{1-\sigma} (\eta - 1) \left[\frac{\lambda_t}{\eta a_t^{1-\sigma}} \right]^{\frac{\eta(1-\sigma)}{\eta(1-\sigma)-1}} (1 - N_t)^{((\eta-1)(1-\sigma) \frac{\eta}{\eta(1-\sigma)-1} + 1 - \eta)(1-\sigma) - 1} = \lambda_t W_t$$

But note that the long exponent reduces to:

$$\begin{aligned} & \left((\eta - 1)(1 - \sigma) \frac{\eta}{\eta(1-\sigma)-1} + 1 - \eta \right) (1 - \sigma) - 1 \\ &= \left(\frac{\eta(\eta-1)(1-\sigma)}{\eta(1-\sigma)-1} + 1 - \eta \right) (1 - \sigma) - 1 \\ &= \left(\frac{\eta(\eta-1)(1-\sigma)}{\eta(1-\sigma)-1} + \frac{(1-\eta)(\eta(1-\sigma)-1)}{\eta(1-\sigma)-1} \right) (1 - \sigma) - \frac{\eta(1-\sigma)-1}{\eta(1-\sigma)-1} \\ &= \left(\frac{\eta(\eta-1)(1-\sigma)^2}{\eta(1-\sigma)-1} + \frac{(1-\eta)(\eta(1-\sigma)^2 - (1-\sigma))}{\eta(1-\sigma)-1} \right) - \frac{\eta(1-\sigma)-1}{\eta(1-\sigma)-1} \\ &= \frac{-(1-\eta)(1-\sigma)}{\eta(1-\sigma)-1} - \frac{\eta(1-\sigma)-1}{\eta(1-\sigma)-1} \\ &= \frac{-((1-\sigma)-\eta(1-\sigma))}{\eta(1-\sigma)-1} - \frac{\eta(1-\sigma)-1}{\eta(1-\sigma)-1} \\ &= \frac{-(1-\sigma)+\eta(1-\sigma)}{\eta(1-\sigma)-1} - \frac{\eta(1-\sigma)-1}{\eta(1-\sigma)-1} \\ &= \frac{-1+\sigma}{\eta(1-\sigma)-1} - \frac{-1}{\eta(1-\sigma)-1} \\ &= \frac{\sigma}{\eta(1-\sigma)-1} \end{aligned}$$

Thus, we have

$$a_t^{1-\sigma} (\eta - 1) \left[\frac{\lambda_t}{\eta a_t^{1-\sigma}} \right]^{\frac{\eta(1-\sigma)}{\eta(1-\sigma)-1}} (1 - N_t)^{\frac{\sigma}{\eta(1-\sigma)-1}} = \lambda_t W_t$$

From this equation, we can isolate for N_t to get

$$(1 - N_t)^{\frac{\sigma}{\eta(1-\sigma)-1}} = \frac{\lambda_t W_t}{a_t^{1-\sigma} (\eta - 1)} \left[\frac{\lambda_t}{\eta a_t^{1-\sigma}} \right]^{\frac{-\eta(1-\sigma)}{\eta(1-\sigma)-1}}$$

⇕

$$1 - N_t = \left[\frac{\lambda_t W_t}{a_t^{1-\sigma} (\eta - 1)} \left[\frac{\lambda_t}{\eta a_t^{1-\sigma}} \right]^{\frac{-\eta(1-\sigma)}{\eta(1-\sigma)-1}} \right]^{\frac{\eta(1-\sigma)-1}{\sigma}}$$

⇕

$$N_t = 1 - \left[\frac{\lambda_t W_t}{a_t^{1-\sigma} (\eta - 1)} \left[\frac{\lambda_t}{\eta a_t^{1-\sigma}} \right]^{\frac{-\eta(1-\sigma)}{\eta(1-\sigma)-1}} \right]^{\frac{\eta(1-\sigma)-1}{\sigma}}.$$

Now for a given value of λ_t we obtain the partial derivative

$$\frac{\partial N_t}{\partial W_t} = -\frac{\eta(1-\sigma)-1}{\sigma} \left[\frac{\lambda_t W_t}{a_t^{1-\sigma} (\eta - 1)} \left[\frac{\lambda_t}{\eta a_t^{1-\sigma}} \right]^{\frac{-\eta(1-\sigma)}{\eta(1-\sigma)-1}} \right]^{\frac{\eta(1-\sigma)-1}{\sigma}-1} \frac{\lambda_t}{a_t^{1-\sigma} (\eta - 1)} \left[\frac{\lambda_t}{\eta a_t^{1-\sigma}} \right]^{\frac{-\eta(1-\sigma)}{\eta(1-\sigma)-1}}.$$

Now, notice that the definition of the Frisch elasticity can be re-written as

$$Frisch_t = \frac{\partial N_t}{\partial W_t} \Big|_{\lambda_t} \frac{W_t}{1 - N_t} \frac{1 - N_t}{N_t}$$

so that:

$$\begin{aligned} Frisch_t &= -\frac{\eta(1-\sigma)-1}{\sigma} \left[\frac{\lambda_t W_t}{a_t^{1-\sigma} (\eta - 1)} \left[\frac{\lambda_t}{\eta a_t^{1-\sigma}} \right]^{\frac{-\eta(1-\sigma)}{\eta(1-\sigma)-1}} \right]^{\frac{\eta(1-\sigma)-1}{\sigma}-1} \\ &\quad \times \frac{\lambda_t}{a_t^{1-\sigma} (\eta - 1)} \left[\frac{\lambda_t}{\eta a_t^{1-\sigma}} \right]^{\frac{-\eta(1-\sigma)}{\eta(1-\sigma)-1}} \frac{W_t}{\left[\frac{\lambda_t W_t}{a_t^{1-\sigma} (\eta - 1)} \left[\frac{\lambda_t}{\eta a_t^{1-\sigma}} \right]^{\frac{-\eta(1-\sigma)}{\eta(1-\sigma)-1}} \right]^{\frac{\eta(1-\sigma)-1}{\sigma}-1}} \frac{1 - N_t}{N_t} \\ &= -\frac{\eta(1-\sigma)-1}{\sigma} \left[\frac{\lambda_t W_t}{a_t^{1-\sigma} (\eta - 1)} \left[\frac{\lambda_t}{\eta a_t^{1-\sigma}} \right]^{\frac{-\eta(1-\sigma)}{\eta(1-\sigma)-1}} \right]^{-1} \frac{W_t \lambda_t}{a_t^{1-\sigma} (\eta - 1)} \left[\frac{\lambda_t}{\eta a_t^{1-\sigma}} \right]^{\frac{-\eta(1-\sigma)}{\eta(1-\sigma)-1}} \frac{1}{1} \frac{1 - N_t}{N_t} \\ &= -\frac{\eta(1-\sigma)-1}{\sigma} \frac{1 - N_t}{N_t} \\ &= (1 - \eta(1 - \sigma)) \frac{1}{\sigma} \frac{1 - N_t}{N_t} \end{aligned}$$

Thus, at the steady state, we get

$$Frisch_{ss} = (1 - \eta(1 - \sigma)) \frac{1}{\sigma} \frac{1 - N_{ss}}{N_{ss}}$$

From EQ 3 we have in steady state

$$\frac{(1 - \eta) C_{ss} (1 - b)}{\eta} \frac{1}{1 - N_{ss}} = W_{ss}$$

⇕

$$(1 - \eta) C_{ss} (1 - b) = W_{ss} (1 - N_{ss}) \eta$$

⇕

$$C_{ss} (1 - b) = (W_{ss} (1 - N_{ss}) + C_{ss} (1 - b)) \eta$$

↕

$$\begin{aligned}\eta &= \frac{C_{ss}(1-b)}{W_{ss}(1-N_{ss}) + C_{ss}(1-b)} \\ &= \left[\frac{W_{ss}(1-N_{ss})}{C_{ss}(1-b)} + 1 \right]^{-1}\end{aligned}$$

Also from EQ 6 we have

$$W_{ss} = (1-\alpha)(Y_{ss} + \Phi) \frac{1}{\mu_{ss}N_{ss}}$$

which when inserted gives

$$\eta = \left[\frac{(1-\alpha)(Y_{ss} + \Phi)(1-N_{ss})}{C_{ss}(1-b)\mu_{ss}N_{ss}} + 1 \right]^{-1}$$

Finally, substituting this expression in to the one for the Frisch elasticity gives

$$Frisch_{ss} = (1-\eta(1-\sigma)) \frac{1}{\sigma} \frac{1-N_{ss}}{N_{ss}}$$

↕

$$\frac{\sigma N_{ss}}{1-N_{ss}} Frisch_{ss} = \left(1 - \left[\frac{(1-\alpha)(Y_{ss} + \Phi)(1-N_{ss})}{C_{ss}(1-b)\mu_{ss}N_{ss}} + 1 \right]^{-1} (1-\sigma) \right).$$

For at given value of $Frisch_{ss}$, this expressions allow us to solve nonlinearly for N_{ss} . Given this value, we then find the value of η that is consistent with $Frisch_{ss}$ and N_{ss} , i.e.

$$\eta = \frac{C_{ss}(1-b)}{W_{ss}(1-N_{ss}) + C_{ss}(1-b)}$$

3 Approximation around the Risky Steady State

This section derives the first-, second-, and third-order approximated solutions to a general class of DSGE models. Our notation follows the one in Schmitt-Grohé & Uribe (2004) but our procedure is different as we aim to do the approximation around an estimate of the risk steady state and not around the deterministic steady state as in Schmitt-Grohé & Uribe (2004). The risky steady state is defined as the point where agents respond to uncertainty, but at this particular point no uncertainty is present. The adopted procedure follows the one suggested in Collard & Juillard (2001a) for models solved up to second order.¹¹

3.1 The Class of DSGE Models

We consider the class of DSGE models where the set of equilibrium conditions can be written as

$$E_t [\mathbf{f}(\mathbf{y}_{t+1}, \mathbf{y}_t, \mathbf{x}_{t+1}, \mathbf{x}_t)] = \mathbf{0}. \quad (2)$$

Here, E_t is the conditional expectation given information available at time t . The vector \mathbf{x}_t is the set of state variables (pre-determined variables) and has dimension $n_x \times 1$. The vector \mathbf{y}_t contains the set of control variables (non pre-determined variables) and has dimension $n_y \times 1$. We also let $n \equiv n_x + n_y$.

The state vector is partitioned as $\mathbf{x}_t \equiv [\mathbf{x}'_{1,t} \quad \mathbf{x}'_{2,t}]'$, where $\mathbf{x}_{1,t}$ with dimension $n_{x_1} \times 1$ contains the set of endogenous state variables and $\mathbf{x}_{2,t}$ with dimension $n_{x_2} \times 1$ contains the set of exogenous state variables. Note also that $n_{x_1} + n_{x_2} = n_x$. For the exogenous state variables we assume that

$$\mathbf{x}_{2,t+1} = \mathbf{h}(\mathbf{x}_{2,t}) + \tilde{\boldsymbol{\eta}}\boldsymbol{\epsilon}_{t+1}, \quad (3)$$

¹¹See also Collard & Juillard (2001b) for an application of this method beyond second order in a small endowment model.

where $\boldsymbol{\epsilon}_{t+1}$ has dimension $n_e \times 1$, and thus, $\tilde{\boldsymbol{\eta}}$ has dimension $n_{x_2} \times n_e$.

The general solution to this class of DSGE model is given by

$$\mathbf{y}_t = \mathbf{g}(\mathbf{x}_t) \quad (4)$$

$$\mathbf{x}_{t+1} = \mathbf{h}(\mathbf{x}_t) + \boldsymbol{\eta}\boldsymbol{\epsilon}_{t+1} \quad (5)$$

$$\boldsymbol{\eta} = \begin{bmatrix} \mathbf{0} \\ \tilde{\boldsymbol{\eta}} \end{bmatrix} \quad (6)$$

where the functions $\mathbf{g}(\cdot)$ and $\mathbf{h}(\cdot)$ are unknown. We will approximate these functions up to third order. This is done around an estimate of the risky steady state, which we denote by $\bar{\mathbf{x}}$ for the states and by $\bar{\mathbf{y}}$ for the controls. For this purpose, let us express (2) as

$$E_t [\mathbf{F}(\mathbf{x}_t, \boldsymbol{\epsilon}_{t+1})] \equiv E_t [\mathbf{f}(\mathbf{y}_{t+1}, \mathbf{y}_t, \mathbf{x}_{t+1}, \mathbf{x}_t)] = \mathbf{0}$$

$$\Downarrow \quad E_t [\mathbf{F}(\mathbf{x}_t, \boldsymbol{\epsilon}_{t+1})] \equiv E_t [\mathbf{f}(\mathbf{g}(\mathbf{h}(\mathbf{x}_t) + \boldsymbol{\eta}\boldsymbol{\epsilon}_{t+1}), \mathbf{g}(\mathbf{x}_t), \mathbf{h}(\mathbf{x}_t) + \boldsymbol{\eta}\boldsymbol{\epsilon}_{t+1}, \mathbf{x}_t)] = \mathbf{0}. \quad (7)$$

Note that we generally do not have

$$\bar{\mathbf{f}} \equiv \mathbf{f}(\bar{\mathbf{y}}, \bar{\mathbf{y}}, \bar{\mathbf{x}}, \bar{\mathbf{x}}) = \mathbf{0} \quad (8)$$

due to the presence of uncertainty. Importantly, we need to ensure that $\bar{\mathbf{x}}$ is a fixed-point in (5).

The approach is to consider a Taylor-series expansion of $\mathbf{F}(\mathbf{x}_t, \boldsymbol{\epsilon}_{t+1})$, and take conditional expectations to this expansion. Then the method of undetermined coefficients is used to find the required loadings of $\mathbf{g}(\cdot)$ and $\mathbf{h}(\cdot)$, as well as the point at which any derivatives are taken. For the indices we adopt the convention that the subscript is related to the order of differentiation. I.e. a "1" is for the first time we take derivatives and so on. Thus,

$$\alpha_1, \alpha_2, \alpha_3 = 1, 2, \dots, n_x$$

$$\gamma_1, \gamma_2, \gamma_3 = 1, 2, \dots, n_x$$

$$\beta_1, \beta_2, \beta_3 = 1, 2, \dots, n_y$$

$$\phi_1, \phi_2, \phi_3 = 1, 2, \dots, n_\epsilon$$

while $i = 1, 2, \dots, n$ will be used to index the n equations in the model. We will also use the condense notation:

$$\mathbf{g}^{t+1} \equiv \mathbf{g}(\mathbf{x}_{t+1})$$

$$\mathbf{g}^t \equiv \mathbf{g}(\mathbf{x}_t)$$

$$\mathbf{h}^t \equiv \mathbf{h}(\mathbf{x}_t)$$

where the superscript denotes the time index for the state variable at which the functions $\mathbf{g}(\cdot)$ and $\mathbf{h}(\cdot)$ are to be evaluated. Thus, we can write (7) condensely as

$$E_t [\mathbf{F}(\mathbf{x}_t, \boldsymbol{\epsilon}_{t+1})] \equiv E_t [\mathbf{f}(\mathbf{g}^{t+1}, \mathbf{g}^t, \mathbf{h}^t + \boldsymbol{\eta}\boldsymbol{\epsilon}_{t+1}, \mathbf{x}_t)] = \mathbf{0}, \quad (9)$$

where both \mathbf{x}_t and $\boldsymbol{\epsilon}_{t+1}$ are variables in the function $\mathbf{F}(\mathbf{x}_t, \boldsymbol{\epsilon}_{t+1})$.

3.2 The First-Order Approximation

We consider a solution of the form

$$\mathbf{g}(\mathbf{x}_t) = \mathbf{g}(\bar{\mathbf{x}}) + \mathbf{g}_x(\bar{\mathbf{x}})(\mathbf{x}_t - \bar{\mathbf{x}})$$

⇕

$$\mathbf{g}(\mathbf{x}_t) = \bar{\mathbf{y}} + \mathbf{g}_x(\bar{\mathbf{x}})(\mathbf{x}_t - \bar{\mathbf{x}})$$

⇕

$$\mathbf{y}_t - \bar{\mathbf{y}} = \mathbf{g}_x(\bar{\mathbf{x}})(\mathbf{x}_t - \bar{\mathbf{x}}). \quad (10)$$

and

$$\mathbf{h}(\mathbf{x}_t) = \mathbf{h}(\bar{\mathbf{x}}) + \mathbf{h}_x(\bar{\mathbf{x}})(\mathbf{x}_t - \bar{\mathbf{x}}) + \boldsymbol{\eta}\boldsymbol{\epsilon}_{t+1}$$

⇕

$$\mathbf{x}_{t+1} - \bar{\mathbf{x}} = \mathbf{h}_x(\bar{\mathbf{x}})(\mathbf{x}_t - \bar{\mathbf{x}}) + \boldsymbol{\eta}\boldsymbol{\epsilon}_{t+1}. \quad (11)$$

Note that $\bar{\mathbf{x}}$ clearly is a fixed-point for (11) because $E[\boldsymbol{\epsilon}_{t+1}] = \mathbf{0}$, i.e. $\mathbf{x}_{t+1} = \mathbf{x}_t = \bar{\mathbf{x}}$, and therefore $\mathbf{y}_{t+1} = \mathbf{y}_t = \bar{\mathbf{y}}$.

3.2.1 The Solution

We start by a general first-order approximation to (9):

$$[\mathbf{F}(\bar{\mathbf{x}}, \mathbf{0})]^i + E_t \left[[\mathbf{F}_x(\bar{\mathbf{x}}, \mathbf{0})]_{\alpha_1}^i [\mathbf{x}_t - \bar{\mathbf{x}}]^{\alpha_1} + [\mathbf{F}_\epsilon(\bar{\mathbf{x}}, \mathbf{0})]_{\phi_1}^i [\boldsymbol{\epsilon}_{t+1}]^{\phi_1} \right] = 0$$

⇕

$$[\mathbf{F}(\bar{\mathbf{x}}, \mathbf{0})]^i + [\mathbf{F}_x(\bar{\mathbf{x}}, \mathbf{0})]_{\alpha_1}^i [\mathbf{x}_t - \bar{\mathbf{x}}]^{\alpha_1} = 0 \quad (12)$$

because $E_t[\boldsymbol{\epsilon}_{t+1}] = \mathbf{0}$. We then compute $[\mathbf{F}_{x_t}(\bar{\mathbf{x}}, \mathbf{0})]_{\alpha_1}^i$ and $[\mathbf{F}_\epsilon(\bar{\mathbf{x}}, \mathbf{0})]_{\phi_1}^i$ in turn, i.e.

$$[\mathbf{F}_{x_t}(\bar{\mathbf{x}}, \mathbf{0})]_{\alpha_1}^i = [\mathbf{f}_{y_{t+1}}]_{\beta_1}^i [\mathbf{g}_x^{t+1}]_{\gamma_1}^{\beta_1} [\mathbf{h}_x^t]_{\alpha_1}^{\gamma_1} + [\mathbf{f}_{y_t}]_{\beta_1}^i [\mathbf{g}_x^t]_{\alpha_1}^{\beta_1} + [\mathbf{f}_{x_{t+1}}]_{\gamma_1}^i [\mathbf{h}_x^t]_{\alpha_1}^{\gamma_1} + [\mathbf{f}_{x_t}]_{\alpha_1}^i$$

and

$$[\mathbf{F}_\epsilon(\bar{\mathbf{x}}, \mathbf{0})]_{\phi_1}^i = [\mathbf{f}_{y_{t+1}}]_{\beta_1}^i [\mathbf{g}_x^{t+1}]_{\gamma_1}^{\beta_1} [\boldsymbol{\eta}]_{\phi_1}^{\gamma_1} + [\mathbf{f}_{x_{t+1}}]_{\gamma_1}^i [\boldsymbol{\eta}]_{\phi_1}^{\gamma_1},$$

where all derivatives of \mathbf{f} , $\mathbf{g}(\cdot)$, and $\mathbf{h}(\cdot)$ are evaluated at $\mathbf{x}_t = \bar{\mathbf{x}}$ and $\boldsymbol{\epsilon}_{t+1} = \mathbf{0}$. Note that (12) must hold for all values of \mathbf{x}_t . Hence, we must require that

$$\mathbf{F}(\bar{\mathbf{x}}, \mathbf{0}) = \mathbf{0},$$

meaning that $\bar{\mathbf{x}} = \mathbf{x}_{ss}$ and $\bar{\mathbf{y}} = \mathbf{y}_{ss}$ as in the standard perturbation approximation. We must also require that $[\mathbf{F}_{x_t}(\bar{\mathbf{x}}, \mathbf{0})]_{\alpha_1}^i = \mathbf{0}$, implying that we obtain \mathbf{g}_x and \mathbf{h}_x by solving the standard quadratic problem

$$[\mathbf{f}_{y_{t+1}}]_{\beta_1}^i [\mathbf{g}_x]_{\gamma_1}^{\beta_1} [\mathbf{h}_x]_{\alpha_1}^{\gamma_1} + [\mathbf{f}_{y_t}]_{\beta_1}^i [\mathbf{g}_x]_{\alpha_1}^{\beta_1} + [\mathbf{f}_{x_{t+1}}]_{\gamma_1}^i [\mathbf{h}_x]_{\alpha_1}^{\gamma_1} + [\mathbf{f}_{x_t}]_{\alpha_1}^i = 0,$$

where all derivatives of \mathbf{f} , $\mathbf{g}(\cdot)$, and $\mathbf{h}(\cdot)$ are evaluated at $\mathbf{x}_t = \bar{\mathbf{x}}$ and $\boldsymbol{\epsilon}_{t+1} = \mathbf{0}$. Hence, we get the same expression for \mathbf{g}_x and \mathbf{h}_x as in the standard perturbation approximation. Thus, at first order, this alternative approximation is identical to the standard perturbation approximation.

3.3 The Second-Order Approximation

We consider a solution of the form

$$[\mathbf{g}(\mathbf{x}_t)]^{\beta_1} = \mathbf{g}(\bar{\mathbf{x}}) + [\mathbf{g}_x(\bar{\mathbf{x}})]_{\alpha_1}^{\beta_1} [(\mathbf{x}_t - \bar{\mathbf{x}})]^{\alpha_1} + \frac{1}{2} [\mathbf{g}_{xx}(\bar{\mathbf{x}})]_{\alpha_1 \alpha_2}^{\beta_1} [(\mathbf{x}_t - \bar{\mathbf{x}})]^{\alpha_1} [(\mathbf{x}_t - \bar{\mathbf{x}})]^{\alpha_2}$$

⇕

$$[\mathbf{y}_t - \bar{\mathbf{y}}]^{\beta_1} = [\mathbf{g}_x(\bar{\mathbf{x}})]_{\alpha_1}^{\beta_1} [(\mathbf{x}_t - \bar{\mathbf{x}})]^{\alpha_1} + \frac{1}{2} [\mathbf{g}_{xx}(\bar{\mathbf{x}})]_{\alpha_1 \alpha_2}^{\beta_1} [(\mathbf{x}_t - \bar{\mathbf{x}})]^{\alpha_1} [(\mathbf{x}_t - \bar{\mathbf{x}})]^{\alpha_2} \quad (13)$$

where $\bar{\mathbf{y}} = \mathbf{g}(\bar{\mathbf{x}})$ and

$$[\mathbf{h}(\mathbf{x}_t)]^{\gamma_1} = \mathbf{h}(\bar{\mathbf{x}}) + [\mathbf{h}_{\mathbf{x}}(\bar{\mathbf{x}})]_{\alpha_1}^{\gamma_1} [(\mathbf{x}_t - \bar{\mathbf{x}})]^{\alpha_1} + \frac{1}{2} [\mathbf{h}_{\mathbf{xx}}(\bar{\mathbf{x}})]_{\alpha_1 \alpha_2}^{\gamma_1} [(\mathbf{x}_t - \bar{\mathbf{x}})]^{\alpha_1} [(\mathbf{x}_t - \bar{\mathbf{x}})]^{\alpha_2} + \boldsymbol{\eta} \boldsymbol{\epsilon}_{t+1}$$

⇕

$$[\mathbf{x}_{t+1} - \bar{\mathbf{x}}]^{\gamma_1} = [\mathbf{h}_{\mathbf{x}}(\bar{\mathbf{x}})]_{\alpha_1}^{\gamma_1} [(\mathbf{x}_t - \bar{\mathbf{x}})]^{\alpha_1} + \frac{1}{2} [\mathbf{h}_{\mathbf{xx}}(\bar{\mathbf{x}})]_{\alpha_1 \alpha_2}^{\gamma_1} [(\mathbf{x}_t - \bar{\mathbf{x}})]^{\alpha_1} [(\mathbf{x}_t - \bar{\mathbf{x}})]^{\alpha_2} + \boldsymbol{\eta} \boldsymbol{\epsilon}_{t+1} \quad (14)$$

where $\bar{\mathbf{x}} = \mathbf{h}(\bar{\mathbf{x}})$. Note that $\bar{\mathbf{x}}$ clearly is a fixed-point for (14) because $E[\boldsymbol{\epsilon}_{t+1}] = \mathbf{0}$, i.e. $\mathbf{x}_{t+1} = \mathbf{x}_t = \bar{\mathbf{x}}$, and therefore $\mathbf{y}_{t+1} = \mathbf{y}_t = \bar{\mathbf{y}}$.

3.3.1 The Solution

We start by a general second-order approximation to (9)

$$\begin{aligned} & [\mathbf{F}(\bar{\mathbf{x}}, \mathbf{0})]^i + E_t \left[[\mathbf{F}_{\mathbf{x}}(\bar{\mathbf{x}}, \mathbf{0})]_{\alpha_1}^i [\mathbf{x}_t - \bar{\mathbf{x}}]^{\alpha_1} + [\mathbf{F}_{\boldsymbol{\epsilon}}(\bar{\mathbf{x}}, \mathbf{0})]_{\phi_1}^i [\boldsymbol{\epsilon}_{t+1}]^{\phi_1} \right] \\ & + E_t \left[\frac{1}{2} [\mathbf{F}_{\mathbf{xx}}(\bar{\mathbf{x}}, \mathbf{0})]_{\alpha_1 \alpha_2}^i [\mathbf{x}_t - \bar{\mathbf{x}}]^{\alpha_1} [\mathbf{x}_t - \bar{\mathbf{x}}]^{\alpha_2} + \frac{1}{2} [\mathbf{F}_{\boldsymbol{\epsilon}\boldsymbol{\epsilon}}(\bar{\mathbf{x}}, \mathbf{0})]_{\phi_1 \phi_2}^i [\boldsymbol{\epsilon}_{t+1}]^{\phi_1} [\boldsymbol{\epsilon}_{t+1}]^{\phi_2} + [\mathbf{F}_{\mathbf{x}\boldsymbol{\epsilon}}(\bar{\mathbf{x}}, \mathbf{0})]_{\alpha_1 \phi_2}^i [\mathbf{x}_t - \bar{\mathbf{x}}]^{\alpha_1} [\boldsymbol{\epsilon}_{t+1}]^{\phi_2} \right] = \\ & \mathbf{0} \end{aligned}$$

⇕

$$\begin{aligned} & \left[\mathbf{F}(\bar{\mathbf{x}}, \mathbf{0}) \right]^i + [\mathbf{F}_{\mathbf{x}}(\bar{\mathbf{x}}, \mathbf{0})]_{\alpha_1}^i [\mathbf{x}_t - \bar{\mathbf{x}}]^{\alpha_1} + \frac{1}{2} [\mathbf{F}_{\mathbf{xx}}(\bar{\mathbf{x}}, \mathbf{0})]_{\alpha_1 \alpha_2}^i [\mathbf{x}_t - \bar{\mathbf{x}}]^{\alpha_1} [\mathbf{x}_t - \bar{\mathbf{x}}]^{\alpha_2} + \frac{1}{2} [\mathbf{F}_{\boldsymbol{\epsilon}\boldsymbol{\epsilon}}(\bar{\mathbf{x}}, \mathbf{0})]_{\phi_1 \phi_2}^i E_t \left[[\boldsymbol{\epsilon}_{t+1}]^{\phi_1} [\boldsymbol{\epsilon}_{t+1}]^{\phi_2} \right] = \mathbf{0} \\ & \text{because } E_t[\boldsymbol{\epsilon}_{t+1}] = \mathbf{0}. \end{aligned}$$

⇕

$$\begin{aligned} & \left[\mathbf{F}(\bar{\mathbf{x}}, \mathbf{0}) \right]^i + [\mathbf{F}_{\mathbf{x}}(\bar{\mathbf{x}}, \mathbf{0})]_{\alpha_1}^i [\mathbf{x}_t - \bar{\mathbf{x}}]^{\alpha_1} + \frac{1}{2} [\mathbf{F}_{\mathbf{xx}}(\bar{\mathbf{x}}, \mathbf{0})]_{\alpha_1 \alpha_2}^i [\mathbf{x}_t - \bar{\mathbf{x}}]^{\alpha_1} [\mathbf{x}_t - \bar{\mathbf{x}}]^{\alpha_2} + \frac{1}{2} [\mathbf{F}_{\boldsymbol{\epsilon}\boldsymbol{\epsilon}}(\bar{\mathbf{x}}, \mathbf{0})]_{\phi_1 \phi_2}^i [\mathbf{I}]_{\phi_2}^{\phi_1} = \mathbf{0} \\ & \text{because } \text{Var}_t[\boldsymbol{\epsilon}_{t+1}] = \mathbf{I}. \text{ This equation must hold for all values of } \mathbf{x}_t. \text{ So we must require that} \end{aligned}$$

$$[\mathbf{F}(\bar{\mathbf{x}}, \mathbf{0})]^i + \frac{1}{2} [\mathbf{F}_{\boldsymbol{\epsilon}\boldsymbol{\epsilon}}(\bar{\mathbf{x}}, \mathbf{0})]_{\phi_1 \phi_2}^i [\mathbf{I}]_{\phi_2}^{\phi_1} = \mathbf{0} \quad (15)$$

$$[\mathbf{F}_{\mathbf{x}}(\bar{\mathbf{x}}, \mathbf{0})]_{\alpha_1}^i = \mathbf{0} \quad (16)$$

$$[\mathbf{F}_{\mathbf{xx}}(\bar{\mathbf{x}}, \mathbf{0})]_{\alpha_1 \alpha_2}^i = \mathbf{0} \quad (17)$$

where the two last conditions are well-known from the standard perturbation approximation. In relation to the first condition, recall that

$$[\mathbf{F}_{\boldsymbol{\epsilon}}]_{\phi_1}^i = [\mathbf{f}_{\mathbf{y}_{t+1}}]_{\beta_1}^i [\mathbf{g}_{\mathbf{x}^{t+1}}]_{\gamma_1}^{\beta_1} [\boldsymbol{\eta}]_{\phi_1}^{\gamma_1} + [\mathbf{f}_{\mathbf{x}_{t+1}}]_{\gamma_1}^i [\boldsymbol{\eta}]_{\phi_1}^{\gamma_1}.$$

Therefore

$$\begin{aligned} [\mathbf{F}_{\boldsymbol{\epsilon}\boldsymbol{\epsilon}}]_{\phi_1 \phi_2}^i &= \left([\mathbf{f}_{\mathbf{y}_{t+1}\mathbf{y}_{t+1}}]_{\beta_1 \beta_2}^i [\mathbf{g}_{\mathbf{x}^{t+1}}]_{\gamma_2}^{\beta_2} [\boldsymbol{\eta}]_{\phi_2}^{\gamma_2} + [\mathbf{f}_{\mathbf{y}_{t+1}\mathbf{x}_{t+1}}]_{\beta_1 \gamma_2}^i [\boldsymbol{\eta}]_{\phi_2}^{\gamma_2} \right) [\mathbf{g}_{\mathbf{x}^{t+1}}]_{\gamma_1}^{\beta_1} [\boldsymbol{\eta}]_{\phi_1}^{\gamma_1} \\ &+ [\mathbf{f}_{\mathbf{y}_{t+1}}]_{\beta_1}^i [\mathbf{g}_{\mathbf{xx}^{t+1}}]_{\gamma_1 \gamma_2}^{\beta_1} [\boldsymbol{\eta}]_{\phi_1}^{\gamma_1} [\boldsymbol{\eta}]_{\phi_2}^{\gamma_2} \\ &+ \left([\mathbf{f}_{\mathbf{x}_{t+1}\mathbf{y}_{t+1}}]_{\gamma_1 \beta_2}^i [\mathbf{g}_{\mathbf{x}^{t+1}}]_{\gamma_2}^{\beta_2} [\boldsymbol{\eta}]_{\phi_2}^{\gamma_2} + [\mathbf{f}_{\mathbf{x}_{t+1}\mathbf{x}_{t+1}}]_{\gamma_1 \gamma_2}^i [\boldsymbol{\eta}]_{\phi_2}^{\gamma_2} \right) [\boldsymbol{\eta}]_{\phi_1}^{\gamma_1} \end{aligned}$$

⇕

$$\begin{aligned} [\mathbf{F}_{\boldsymbol{\epsilon}\boldsymbol{\epsilon}}]_{\phi_1 \phi_2}^i &= [\mathbf{f}_{\mathbf{y}_{t+1}\mathbf{y}_{t+1}}]_{\beta_1 \beta_2}^i [\mathbf{g}_{\mathbf{x}^{t+1}}]_{\gamma_2}^{\beta_2} [\boldsymbol{\eta}]_{\phi_2}^{\gamma_2} [\mathbf{g}_{\mathbf{x}^{t+1}}]_{\gamma_1}^{\beta_1} [\boldsymbol{\eta}]_{\phi_1}^{\gamma_1} \\ &+ [\mathbf{f}_{\mathbf{y}_{t+1}\mathbf{x}_{t+1}}]_{\beta_1 \gamma_2}^i [\boldsymbol{\eta}]_{\phi_2}^{\gamma_2} [\mathbf{g}_{\mathbf{x}^{t+1}}]_{\gamma_1}^{\beta_1} [\boldsymbol{\eta}]_{\phi_1}^{\gamma_1} \\ &+ [\mathbf{f}_{\mathbf{y}_{t+1}}]_{\beta_1}^i [\mathbf{g}_{\mathbf{xx}^{t+1}}]_{\gamma_1 \gamma_2}^{\beta_1} [\boldsymbol{\eta}]_{\phi_1}^{\gamma_1} [\boldsymbol{\eta}]_{\phi_2}^{\gamma_2} \\ &+ [\mathbf{f}_{\mathbf{x}_{t+1}\mathbf{y}_{t+1}}]_{\gamma_1 \beta_2}^i [\mathbf{g}_{\mathbf{x}^{t+1}}]_{\gamma_2}^{\beta_2} [\boldsymbol{\eta}]_{\phi_2}^{\gamma_2} [\boldsymbol{\eta}]_{\phi_1}^{\gamma_1} \\ &+ [\mathbf{f}_{\mathbf{x}_{t+1}\mathbf{x}_{t+1}}]_{\gamma_1 \gamma_2}^i [\boldsymbol{\eta}]_{\phi_2}^{\gamma_2} [\boldsymbol{\eta}]_{\phi_1}^{\gamma_1}, \end{aligned}$$

⇕

$$\begin{aligned}
[\mathbf{F}\epsilon\epsilon]_{\phi_1\phi_2}^i &= [\mathbf{f}_{\mathbf{y}_{t+1}\mathbf{y}_{t+1}}]_{\beta_1\beta_2}^i [\mathbf{g}_{\mathbf{x}}^{t+1}]_{\gamma_2}^{\beta_2} [\boldsymbol{\eta}]_{\phi_2}^{\gamma_2} [\mathbf{g}_{\mathbf{x}}^{t+1}]_{\gamma_1}^{\beta_1} [\boldsymbol{\eta}]_{\phi_1}^{\gamma_1} \\
&+ [\mathbf{f}_{\mathbf{y}_{t+1}}]_{\beta_1}^i [\mathbf{g}_{\mathbf{xx}}^{t+1}]_{\gamma_1\gamma_2}^{\beta_1} [\boldsymbol{\eta}]_{\phi_1}^{\gamma_1} [\boldsymbol{\eta}]_{\phi_2}^{\gamma_2} \\
&+ 2 [\mathbf{f}_{\mathbf{x}_{t+1}\mathbf{y}_{t+1}}]_{\gamma_1\beta_2}^i [\mathbf{g}_{\mathbf{x}}^{t+1}]_{\gamma_2}^{\beta_2} [\boldsymbol{\eta}]_{\phi_2}^{\gamma_2} [\boldsymbol{\eta}]_{\phi_1}^{\gamma_1} \\
&+ [\mathbf{f}_{\mathbf{x}_{t+1}\mathbf{x}_{t+1}}]_{\gamma_1\gamma_2}^i [\boldsymbol{\eta}]_{\phi_2}^{\gamma_2} [\boldsymbol{\eta}]_{\phi_1}^{\gamma_1},
\end{aligned}$$

which is identical to the expression obtained in Andreasen (2012) for $\mathbf{F}_{\sigma\sigma}(\mathbf{x}_{ss}, \sigma)$ when setting all derivatives with respect to the perturbation parameter σ equal to zero.

The suggestive procedure for solving the equations in (15) to (17) is as follows

1. Compute $(\mathbf{g}_{\mathbf{x}}(\mathbf{x}_{ss}), \mathbf{g}_{\mathbf{xx}}(\mathbf{x}_{ss}))$ and $(\mathbf{h}_{\mathbf{x}}(\mathbf{x}_{ss}, 0), \mathbf{h}_{\mathbf{xx}}(\mathbf{x}_{ss}))$ by standard perturbation at the deterministic steady state \mathbf{x}_{ss} . Let $\bar{\mathbf{x}}^{(0)} = \mathbf{x}_{ss}$ and $\bar{\mathbf{y}}^{(0)} = \mathbf{y}_{ss}$, and let $i = 1$.
2. Given $(\mathbf{g}_{\mathbf{x}}(\bar{\mathbf{x}}^{(i-1)}), \mathbf{g}_{\mathbf{xx}}(\bar{\mathbf{x}}^{(i-1)}))$ and $(\mathbf{h}_{\mathbf{x}}(\bar{\mathbf{x}}^{(i-1)}), \mathbf{h}_{\mathbf{xx}}(\bar{\mathbf{x}}^{(i-1)}))$, solve (15) to get $\bar{\mathbf{x}}^{(i)}$ and $\bar{\mathbf{y}}^{(i)}$.
3. Given $\bar{\mathbf{x}}^{(i)}$ and $\bar{\mathbf{y}}^{(i)}$, compute $\mathbf{g}_{\mathbf{x}}(\bar{\mathbf{x}}^{(i)})$, $\mathbf{h}_{\mathbf{x}}(\bar{\mathbf{x}}^{(i)})$ from (16) and $(\mathbf{g}_{\mathbf{xx}}(\bar{\mathbf{x}}^{(i)}), \mathbf{h}_{\mathbf{xx}}(\bar{\mathbf{x}}^{(i)}))$ from (17).
4. If $\bar{\mathbf{x}}^{(i)} \approx \bar{\mathbf{x}}^{(i-1)}$ then stop, otherwise let $i = i + 1$ and go to step 2.

Hence, we use the $n \times 1$ equations in (15) to determine $(\bar{\mathbf{x}}, \bar{\mathbf{y}})$ by solving a nonlinear fixed-point problem, conditioning on the derivatives of $\mathbf{g}(\cdot)$ and $\mathbf{h}(\cdot)$. Given a value of $(\bar{\mathbf{x}}, \bar{\mathbf{y}})$, we then solve for $\mathbf{g}_{\mathbf{x}}(\bar{\mathbf{x}})$ and $\mathbf{h}_{\mathbf{x}}(\bar{\mathbf{x}})$ using the $n \times n_x$ equations in (16), which is a standard quadratic problem known from solving in a standard linearized approximation around the deterministic steady state. The $n \times n_x^2$ equations in (17) are identical to those derived for the second order derivatives solely with respect to state vector in Schmitt-Grohé & Uribe (2004), except that all derivatives are evaluated at $(\bar{\mathbf{x}}, \bar{\mathbf{y}})$ and not at the steady state. Hence, (22) allow us to obtain $\mathbf{g}_{\mathbf{xx}}(\bar{\mathbf{x}})$ and $\mathbf{h}_{\mathbf{xx}}(\bar{\mathbf{x}})$ by solving a linear system.

3.4 The Third-Order Approximation

We consider a solution of the form

$$\begin{aligned}
[\mathbf{g}(\mathbf{x}_t)]^{\beta_1} &= \mathbf{g}(\bar{\mathbf{x}}) + [\mathbf{g}_{\mathbf{x}}(\bar{\mathbf{x}})]_{\alpha_1}^{\beta_1} [(\mathbf{x}_t - \bar{\mathbf{x}})]^{\alpha_1} + \frac{1}{2} [\mathbf{g}_{\mathbf{xx}}(\bar{\mathbf{x}})]_{\alpha_1\alpha_2}^{\beta_1} [(\mathbf{x}_t - \bar{\mathbf{x}})]^{\alpha_1} [(\mathbf{x}_t - \bar{\mathbf{x}})]^{\alpha_2} \\
&+ \frac{1}{6} [\mathbf{g}_{\mathbf{xxx}}(\bar{\mathbf{x}})]_{\alpha_1\alpha_2\alpha_3}^{\beta_1} [(\mathbf{x}_t - \bar{\mathbf{x}})]^{\alpha_1} [(\mathbf{x}_t - \bar{\mathbf{x}})]^{\alpha_2} [(\mathbf{x}_t - \bar{\mathbf{x}})]^{\alpha_3}
\end{aligned}$$

⇕

$$\begin{aligned}
[\mathbf{y}_t - \bar{\mathbf{y}}]^{\beta_1} &= [\mathbf{g}_{\mathbf{x}}(\bar{\mathbf{x}})]_{\alpha_1}^{\beta_1} [(\mathbf{x}_t - \bar{\mathbf{x}})]^{\alpha_1} + \frac{1}{2} [\mathbf{g}_{\mathbf{xx}}(\bar{\mathbf{x}})]_{\alpha_1\alpha_2}^{\beta_1} [(\mathbf{x}_t - \bar{\mathbf{x}})]^{\alpha_1} [(\mathbf{x}_t - \bar{\mathbf{x}})]^{\alpha_2} \\
&+ \frac{1}{6} [\mathbf{g}_{\mathbf{xxx}}(\bar{\mathbf{x}})]_{\alpha_1\alpha_2\alpha_3}^{\beta_1} [(\mathbf{x}_t - \bar{\mathbf{x}})]^{\alpha_1} [(\mathbf{x}_t - \bar{\mathbf{x}})]^{\alpha_2} [(\mathbf{x}_t - \bar{\mathbf{x}})]^{\alpha_3}
\end{aligned} \tag{18}$$

where $\bar{\mathbf{y}} = \mathbf{g}(\bar{\mathbf{x}})$ and

$$\begin{aligned}
[\mathbf{x}_{t+1}]^{\gamma_1} &= \mathbf{h}(\bar{\mathbf{x}}) + [\mathbf{h}_{\mathbf{x}}(\bar{\mathbf{x}})]_{\alpha_1}^{\gamma_1} [(\mathbf{x}_t - \bar{\mathbf{x}})]^{\alpha_1} + \frac{1}{2} [\mathbf{h}_{\mathbf{xx}}(\bar{\mathbf{x}})]_{\alpha_1\alpha_2}^{\gamma_1} [(\mathbf{x}_t - \bar{\mathbf{x}})]^{\alpha_1} [(\mathbf{x}_t - \bar{\mathbf{x}})]^{\alpha_2} \\
&+ \frac{1}{6} [\mathbf{h}_{\mathbf{xxx}}(\bar{\mathbf{x}})]_{\alpha_1\alpha_2\alpha_3}^{\gamma_1} [(\mathbf{x}_t - \bar{\mathbf{x}})]^{\alpha_1} [(\mathbf{x}_t - \bar{\mathbf{x}})]^{\alpha_2} [(\mathbf{x}_t - \bar{\mathbf{x}})]^{\alpha_3} + \boldsymbol{\eta}\epsilon_{t+1}
\end{aligned}$$

⇕

$$\begin{aligned}
[\mathbf{x}_{t+1} - \bar{\mathbf{x}}]^{\gamma_1} &= [\mathbf{h}_{\mathbf{x}}(\bar{\mathbf{x}})]_{\alpha_1}^{\gamma_1} [(\mathbf{x}_t - \bar{\mathbf{x}})]^{\alpha_1} + \frac{1}{2} [\mathbf{h}_{\mathbf{xx}}(\bar{\mathbf{x}})]_{\alpha_1\alpha_2}^{\gamma_1} [(\mathbf{x}_t - \bar{\mathbf{x}})]^{\alpha_1} [(\mathbf{x}_t - \bar{\mathbf{x}})]^{\alpha_2} \\
&+ \frac{1}{6} [\mathbf{h}_{\mathbf{xxx}}(\bar{\mathbf{x}})]_{\alpha_1\alpha_2\alpha_3}^{\gamma_1} [(\mathbf{x}_t - \bar{\mathbf{x}})]^{\alpha_1} [(\mathbf{x}_t - \bar{\mathbf{x}})]^{\alpha_2} [(\mathbf{x}_t - \bar{\mathbf{x}})]^{\alpha_3} + \boldsymbol{\eta}\epsilon_{t+1}
\end{aligned} \tag{19}$$

where $\bar{\mathbf{x}} = \mathbf{h}(\bar{\mathbf{x}})$. Note that $\bar{\mathbf{x}}$ clearly is a fixed-point for (19) because $E[\boldsymbol{\epsilon}_{t+1}] = \mathbf{0}$, i.e. $\mathbf{x}_{t+1} = \mathbf{x}_t = \bar{\mathbf{x}}$, and therefore $\mathbf{y}_{t+1} = \mathbf{y}_t = \bar{\mathbf{y}}$.

3.4.1 The Solution

We start by a general third-order approximation to (9)

$$\begin{aligned} & [\mathbf{F}(\bar{\mathbf{x}}, \mathbf{0})]^i + E_t \left[[\mathbf{F}_{\mathbf{x}}(\bar{\mathbf{x}}, \mathbf{0})]_{\alpha_1}^i [\mathbf{x}_t - \bar{\mathbf{x}}]^{\alpha_1} + [\mathbf{F}_{\boldsymbol{\epsilon}}(\bar{\mathbf{x}}, \mathbf{0})]_{\phi_1}^i [\boldsymbol{\epsilon}_{t+1}]^{\phi_1} \right] \\ & + E_t \left[\frac{1}{2} [\mathbf{F}_{\mathbf{xx}}(\bar{\mathbf{x}}, \mathbf{0})]_{\alpha_1 \alpha_2}^i [\mathbf{x}_t - \bar{\mathbf{x}}]^{\alpha_1} [\mathbf{x}_t - \bar{\mathbf{x}}]^{\alpha_2} + \frac{1}{2} [\mathbf{F}_{\boldsymbol{\epsilon}\boldsymbol{\epsilon}}(\bar{\mathbf{x}}, \mathbf{0})]_{\phi_1 \phi_2}^i [\boldsymbol{\epsilon}_{t+1}]^{\phi_1} [\boldsymbol{\epsilon}_{t+1}]^{\phi_2} + [\mathbf{F}_{\mathbf{x}\boldsymbol{\epsilon}}(\bar{\mathbf{x}}, \mathbf{0})]_{\alpha_1 \phi_2}^i [\mathbf{x}_t - \bar{\mathbf{x}}]^{\alpha_1} [\boldsymbol{\epsilon}_{t+1}]^{\phi_2} \right] \\ & + E_t \left[\frac{1}{6} [\mathbf{F}_{\mathbf{xxx}}(\bar{\mathbf{x}}, \mathbf{0})]_{\alpha_1 \alpha_2 \alpha_3}^i [\mathbf{x}_t - \bar{\mathbf{x}}]^{\alpha_1} [\mathbf{x}_t - \bar{\mathbf{x}}]^{\alpha_2} [\mathbf{x}_t - \bar{\mathbf{x}}]^{\alpha_3} + \frac{3}{6} [\mathbf{F}_{\boldsymbol{\epsilon}\boldsymbol{\epsilon}\boldsymbol{\epsilon}}(\bar{\mathbf{x}}, \mathbf{0})]_{\phi_1 \phi_2 \phi_3}^i [\boldsymbol{\epsilon}_{t+1}]^{\phi_1} [\boldsymbol{\epsilon}_{t+1}]^{\phi_2} [\boldsymbol{\epsilon}_{t+1}]^{\phi_3} \right] \\ & + E_t \left[\frac{3}{6} [\mathbf{F}_{\mathbf{x}\boldsymbol{\epsilon}\boldsymbol{\epsilon}}(\bar{\mathbf{x}}, \mathbf{0})]_{\alpha_1 \phi_2 \phi_3}^i [\mathbf{x}_t - \bar{\mathbf{x}}]^{\alpha_1} [\boldsymbol{\epsilon}_{t+1}]^{\phi_2} [\boldsymbol{\epsilon}_{t+1}]^{\phi_3} + \frac{1}{6} [\mathbf{F}_{\boldsymbol{\epsilon}\boldsymbol{\epsilon}\boldsymbol{\epsilon}}(\bar{\mathbf{x}}, \mathbf{0})]_{\phi_1 \phi_2 \phi_3}^i [\boldsymbol{\epsilon}_{t+1}]^{\phi_1} [\boldsymbol{\epsilon}_{t+1}]^{\phi_2} [\boldsymbol{\epsilon}_{t+1}]^{\phi_3} \right] = \mathbf{0} \\ & \Downarrow \end{aligned}$$

$$\begin{aligned} & [\mathbf{F}(\bar{\mathbf{x}}, \mathbf{0})]^i + [\mathbf{F}_{\mathbf{x}}(\bar{\mathbf{x}}, \mathbf{0})]_{\alpha_1}^i [\mathbf{x}_t - \bar{\mathbf{x}}]^{\alpha_1} \\ & + \frac{1}{2} [\mathbf{F}_{\mathbf{xx}}(\bar{\mathbf{x}}, \mathbf{0})]_{\alpha_1 \alpha_2}^i [\mathbf{x}_t - \bar{\mathbf{x}}]^{\alpha_1} [\mathbf{x}_t - \bar{\mathbf{x}}]^{\alpha_2} + \frac{1}{2} [\mathbf{F}_{\boldsymbol{\epsilon}\boldsymbol{\epsilon}}(\bar{\mathbf{x}}, \mathbf{0})]_{\phi_1 \phi_2}^i [\mathbf{I}]_{\phi_2}^{\phi_1} \\ & + \frac{1}{6} [\mathbf{F}_{\mathbf{xxx}}(\bar{\mathbf{x}}, \mathbf{0})]_{\alpha_1 \alpha_2 \alpha_3}^i [\mathbf{x}_t - \bar{\mathbf{x}}]^{\alpha_1} [\mathbf{x}_t - \bar{\mathbf{x}}]^{\alpha_2} [\mathbf{x}_t - \bar{\mathbf{x}}]^{\alpha_3} + \frac{3}{6} [\mathbf{F}_{\boldsymbol{\epsilon}\boldsymbol{\epsilon}\boldsymbol{\epsilon}}(\bar{\mathbf{x}}, \mathbf{0})]_{\phi_1 \phi_2 \phi_3}^i [\mathbf{I}]_{\phi_2}^{\phi_1} [\mathbf{x}_t - \bar{\mathbf{x}}]^{\alpha_3} \\ & + \frac{1}{6} [\mathbf{F}_{\boldsymbol{\epsilon}\boldsymbol{\epsilon}\boldsymbol{\epsilon}}(\bar{\mathbf{x}}, \mathbf{0})]_{\phi_1 \phi_2 \phi_3}^i [\mathbf{m}^3]_{\phi_2 \phi_3}^{\phi_1} = \mathbf{0} \end{aligned}$$

because $E_t[\boldsymbol{\epsilon}_{t+1}] = \mathbf{0}$ and $Var_t[\boldsymbol{\epsilon}_{t+1}] = \mathbf{I}$. Here, we have introduced the notation

$$[\mathbf{m}^3]_{\phi_2 \phi_3}^{\phi_1} = \begin{cases} m^3(\boldsymbol{\epsilon}_{t+1}(\phi_1, 1)) & \text{if } \phi_1 = \phi_2 = \phi_3 \\ 0 & \text{else} \end{cases},$$

where $m^3(\boldsymbol{\epsilon}_{t+1}(\phi_1, 1))$ denotes the third moment of $\boldsymbol{\epsilon}_{t+1}(\phi_1, 1)$ for $\phi_1 = 1, 2, \dots, n_{\boldsymbol{\epsilon}}$. Notice that \mathbf{m}^3 has dimensions $n_{\boldsymbol{\epsilon}} \times n_{\boldsymbol{\epsilon}} \times n_{\boldsymbol{\epsilon}}$ and that we do not accommodate co-skewness. This equation must hold for all values of \mathbf{x}_t . So we must require that

$$[\mathbf{F}(\bar{\mathbf{x}}, \mathbf{0})]^i + \frac{1}{2} [\mathbf{F}_{\boldsymbol{\epsilon}\boldsymbol{\epsilon}}(\bar{\mathbf{x}}, \mathbf{0})]_{\phi_1 \phi_2}^i [\mathbf{I}]_{\phi_2}^{\phi_1} + \frac{1}{6} [\mathbf{F}_{\boldsymbol{\epsilon}\boldsymbol{\epsilon}\boldsymbol{\epsilon}}(\bar{\mathbf{x}}, \mathbf{0})]_{\phi_1 \phi_2 \phi_3}^i [\mathbf{m}^3]_{\phi_2 \phi_3}^{\phi_1} = 0 \quad (20)$$

$$[\mathbf{F}_{\mathbf{x}}(\bar{\mathbf{x}}, \mathbf{0})]_{\alpha_1}^i + \frac{3}{6} [\mathbf{F}_{\boldsymbol{\epsilon}\boldsymbol{\epsilon}\boldsymbol{\epsilon}}(\bar{\mathbf{x}}, \mathbf{0})]_{\phi_1 \phi_2 \phi_3}^i [\mathbf{I}]_{\phi_2}^{\phi_1} = 0 \quad (21)$$

$$[\mathbf{F}_{\mathbf{xx}}(\bar{\mathbf{x}}, \mathbf{0})]_{\alpha_1 \alpha_2}^i = 0 \quad (22)$$

$$[\mathbf{F}_{\mathbf{xxx}}(\bar{\mathbf{x}}, \mathbf{0})]_{\alpha_1 \alpha_2 \alpha_3}^i = 0 \quad (23)$$

where $i = \{1, 2, \dots, n\}$, $\phi_1, \phi_2, \phi_3 = \{1, 2, \dots, n_{\boldsymbol{\epsilon}}\}$, and $\alpha_1, \alpha_2, \alpha_3 = \{1, 2, \dots, n_x\}$. The suggestive procedure for solving the equations in (20) to (23) is as follows

1. Compute $(\mathbf{g}_{\mathbf{x}}(\mathbf{x}_{ss}), \mathbf{g}_{\mathbf{xx}}(\mathbf{x}_{ss}), \mathbf{g}_{\mathbf{xxx}}(\mathbf{x}_{ss}))$ and $(\mathbf{h}_{\mathbf{x}}(\mathbf{x}_{ss}), \mathbf{h}_{\mathbf{xx}}(\mathbf{x}_{ss}), \mathbf{h}_{\mathbf{xxx}}(\mathbf{x}_{ss}))$ by standard perturbation at the deterministic steady state \mathbf{x}_{ss} . Let $\bar{\mathbf{x}}^{(0)} = \mathbf{x}_{ss}$ and $\bar{\mathbf{y}}^{(0)} = \mathbf{y}_{ss}$, and let $i = 1$.
2. Given $(\mathbf{g}_{\mathbf{x}}(\bar{\mathbf{x}}^{(i-1)}), \mathbf{g}_{\mathbf{xx}}(\bar{\mathbf{x}}^{(i-1)}), \mathbf{g}_{\mathbf{xxx}}(\bar{\mathbf{x}}^{(i-1)}))$ and $(\mathbf{h}_{\mathbf{x}}(\bar{\mathbf{x}}^{(i-1)}), \mathbf{h}_{\mathbf{xx}}(\bar{\mathbf{x}}^{(i-1)}), \mathbf{h}_{\mathbf{xxx}}(\bar{\mathbf{x}}^{(i-1)}))$, solve (20) to get $\bar{\mathbf{x}}^{(i)}$ and $\bar{\mathbf{y}}^{(i)}$.
3. Given $\bar{\mathbf{x}}^{(i)}$ and $\bar{\mathbf{y}}^{(i)}$, compute $(\mathbf{g}_{\mathbf{x}}(\bar{\mathbf{x}}^{(i)}), \mathbf{h}_{\mathbf{x}}(\bar{\mathbf{x}}^{(i)}))$ from (21), then $(\mathbf{g}_{\mathbf{xx}}(\bar{\mathbf{x}}^{(i)}), \mathbf{h}_{\mathbf{xx}}(\bar{\mathbf{x}}^{(i)}))$ from (22), and finally $(\mathbf{g}_{\mathbf{xxx}}(\bar{\mathbf{x}}^{(i)}), \mathbf{h}_{\mathbf{xxx}}(\bar{\mathbf{x}}^{(i)}))$ from (23).
4. If $\bar{\mathbf{x}}^{(i)} \approx \bar{\mathbf{x}}^{(i-1)}$ then stop, otherwise let $i = i + 1$ and go to step 2.

Hence, we use the $n \times 1$ equations in (20) to determine $(\bar{\mathbf{x}}, \bar{\mathbf{y}})$ by solving a nonlinear fixed-point problem, conditioning on the derivatives of $\mathbf{g}(\cdot)$ and $\mathbf{h}(\cdot)$. Given a value of $(\bar{\mathbf{x}}, \bar{\mathbf{y}})$, we then solve for $\mathbf{g}_{\mathbf{x}}(\bar{\mathbf{x}})$ and $\mathbf{h}_{\mathbf{x}}(\bar{\mathbf{x}})$ using the $n \times n_x$ equations in (21). As we show below, this is done by solving a quadratic problem that is very similar to the quadratic problem solving in a standard linearized approximation around the deterministic steady state except that (21) includes the adjustment

$\frac{3}{6} [\mathbf{F}_{\epsilon\epsilon\mathbf{x}}(\bar{\mathbf{x}}, \mathbf{0})]_{\phi_1\phi_2\alpha_3}^i [\mathbf{I}]_{\phi_2}^{\phi_1}$ for variance risk. The $n \times n_x^2$ equations in (22) are identical to those derived for the second order derivatives solely with respect to state vector in Schmitt-Grohé & Uribe (2004), except that all derivatives are evaluated at $(\bar{\mathbf{x}}, \bar{\mathbf{y}})$ and not at the steady state. Hence, (22) allow us to obtain $\mathbf{g}_{\mathbf{x}\mathbf{x}}(\bar{\mathbf{x}})$ and $\mathbf{h}_{\mathbf{x}\mathbf{x}}(\bar{\mathbf{x}})$ by solving a linear system. Finally, the $n \times n_x^3$ equations in (23) are identical to those derived for the third order derivatives solely with respect to state vector in Andreasen (2012) and enable us to obtain $\mathbf{g}_{\mathbf{x}\mathbf{x}\mathbf{x}}(\bar{\mathbf{x}})$ and $\mathbf{h}_{\mathbf{x}\mathbf{x}\mathbf{x}}(\bar{\mathbf{x}})$ by solving a linear system.

Next, we derive $[\mathbf{F}_{\epsilon\epsilon\mathbf{x}}]_{\phi_1\phi_2\alpha_3}^i$ in Section 3.4.2 and $[\mathbf{F}_{\epsilon\epsilon\epsilon}]_{\phi_1\phi_2\phi_3}^i$ in Section 3.4.3, before outlining how to solve the system in (21) in Section 3.4.4.

3.4.2 Computing $[\mathbf{F}_{\epsilon\epsilon\mathbf{x}}]_{\phi_1\phi_2\alpha_3}^i$

Recall that

$$\begin{aligned} [\mathbf{F}_{\epsilon\epsilon}]_{\phi_1\phi_2}^i &= [\mathbf{f}_{\mathbf{y}_{t+1}\mathbf{y}_{t+1}}]_{\beta_1\beta_2}^i [\mathbf{g}_{\mathbf{x}}^{t+1}]_{\gamma_2}^{\beta_2} [\boldsymbol{\eta}]_{\phi_2}^{\gamma_2} [\mathbf{g}_{\mathbf{x}}^{t+1}]_{\gamma_1}^{\beta_1} [\boldsymbol{\eta}]_{\phi_1}^{\gamma_1} \\ &+ [\mathbf{f}_{\mathbf{y}_{t+1}\mathbf{x}_{t+1}}]_{\beta_1\gamma_2}^i [\boldsymbol{\eta}]_{\phi_2}^{\gamma_2} [\mathbf{g}_{\mathbf{x}}^{t+1}]_{\gamma_1}^{\beta_1} [\boldsymbol{\eta}]_{\phi_1}^{\gamma_1} \\ &+ [\mathbf{f}_{\mathbf{y}_{t+1}}]_{\beta_1}^i [\mathbf{g}_{\mathbf{x}\mathbf{x}}^{t+1}]_{\gamma_1\gamma_2}^{\beta_1} [\boldsymbol{\eta}]_{\phi_1}^{\gamma_1} [\boldsymbol{\eta}]_{\phi_2}^{\gamma_2} \\ &+ [\mathbf{f}_{\mathbf{x}_{t+1}\mathbf{y}_{t+1}}]_{\gamma_1\beta_2}^i [\mathbf{g}_{\mathbf{x}}^{t+1}]_{\gamma_2}^{\beta_2} [\boldsymbol{\eta}]_{\phi_2}^{\gamma_2} [\boldsymbol{\eta}]_{\phi_1}^{\gamma_1} \\ &+ [\mathbf{f}_{\mathbf{x}_{t+1}\mathbf{x}_{t+1}}]_{\gamma_1\gamma_2}^i [\boldsymbol{\eta}]_{\phi_2}^{\gamma_2} [\boldsymbol{\eta}]_{\phi_1}^{\gamma_1} \\ &= \sum_{j=1}^5 Q_j^i \end{aligned}$$

where

$$\begin{aligned} Q_1^i &\equiv [\mathbf{f}_{\mathbf{y}_{t+1}\mathbf{y}_{t+1}}]_{\beta_1\beta_2}^i [\mathbf{g}_{\mathbf{x}}^{t+1}]_{\gamma_2}^{\beta_2} [\boldsymbol{\eta}]_{\phi_2}^{\gamma_2} [\mathbf{g}_{\mathbf{x}}^{t+1}]_{\gamma_1}^{\beta_1} [\boldsymbol{\eta}]_{\phi_1}^{\gamma_1} \\ Q_2^i &\equiv [\mathbf{f}_{\mathbf{y}_{t+1}\mathbf{x}_{t+1}}]_{\beta_1\gamma_2}^i [\boldsymbol{\eta}]_{\phi_2}^{\gamma_2} [\mathbf{g}_{\mathbf{x}}^{t+1}]_{\gamma_1}^{\beta_1} [\boldsymbol{\eta}]_{\phi_1}^{\gamma_1} \\ Q_3^i &\equiv [\mathbf{f}_{\mathbf{y}_{t+1}}]_{\beta_1}^i [\mathbf{g}_{\mathbf{x}\mathbf{x}}^{t+1}]_{\gamma_1\gamma_2}^{\beta_1} [\boldsymbol{\eta}]_{\phi_1}^{\gamma_1} [\boldsymbol{\eta}]_{\phi_2}^{\gamma_2} \\ Q_4^i &\equiv [\mathbf{f}_{\mathbf{x}_{t+1}\mathbf{y}_{t+1}}]_{\gamma_1\beta_2}^i [\mathbf{g}_{\mathbf{x}}^{t+1}]_{\gamma_2}^{\beta_2} [\boldsymbol{\eta}]_{\phi_2}^{\gamma_2} [\boldsymbol{\eta}]_{\phi_1}^{\gamma_1} \\ Q_5^i &\equiv [\mathbf{f}_{\mathbf{x}_{t+1}\mathbf{x}_{t+1}}]_{\gamma_1\gamma_2}^i [\boldsymbol{\eta}]_{\phi_2}^{\gamma_2} [\boldsymbol{\eta}]_{\phi_1}^{\gamma_1} \end{aligned}$$

Thus, we have

$$\begin{aligned} [Q_{1,\mathbf{x}}]_{\alpha_3}^i &= ([\mathbf{f}_{\mathbf{y}_{t+1}\mathbf{y}_{t+1}\mathbf{y}_{t+1}}]_{\beta_1\beta_2\beta_3}^i [\mathbf{g}_{\mathbf{x}}^{t+1}]_{\gamma_3}^{\beta_3} [\mathbf{h}_{\mathbf{x}}^t]_{\alpha_3}^{\gamma_3} + [\mathbf{f}_{\mathbf{y}_{t+1}\mathbf{y}_{t+1}\mathbf{y}_t}]_{\beta_1\beta_2\beta_3}^i [\mathbf{g}_{\mathbf{x}}^t]_{\alpha_3}^{\beta_3} \\ &+ [\mathbf{f}_{\mathbf{y}_{t+1}\mathbf{y}_{t+1}\mathbf{x}_{t+1}}]_{\beta_1\beta_2\gamma_3}^i [\mathbf{h}_{\mathbf{x}}^t]_{\alpha_3}^{\gamma_3} + [\mathbf{f}_{\mathbf{y}_{t+1}\mathbf{y}_{t+1}\mathbf{x}_t}]_{\beta_1\beta_2\alpha_3}^i) \\ &\times [\mathbf{g}_{\mathbf{x}}^{t+1}]_{\gamma_2}^{\beta_2} [\boldsymbol{\eta}]_{\phi_2}^{\gamma_2} [\mathbf{g}_{\mathbf{x}}^{t+1}]_{\gamma_1}^{\beta_1} [\boldsymbol{\eta}]_{\phi_1}^{\gamma_1} \\ &+ [\mathbf{f}_{\mathbf{y}_{t+1}\mathbf{y}_{t+1}}]_{\beta_1\beta_2}^i [\mathbf{g}_{\mathbf{x}\mathbf{x}}^{t+1}]_{\gamma_2\gamma_3}^{\beta_2} [\mathbf{h}_{\mathbf{x}}^t]_{\alpha_3}^{\gamma_3} [\boldsymbol{\eta}]_{\phi_2}^{\gamma_2} [\mathbf{g}_{\mathbf{x}}^{t+1}]_{\gamma_1}^{\beta_1} [\boldsymbol{\eta}]_{\phi_1}^{\gamma_1} \\ &+ [\mathbf{f}_{\mathbf{y}_{t+1}\mathbf{y}_{t+1}}]_{\beta_1\beta_2}^i [\mathbf{g}_{\mathbf{x}}^{t+1}]_{\gamma_2}^{\beta_2} [\boldsymbol{\eta}]_{\phi_2}^{\gamma_2} [\mathbf{g}_{\mathbf{x}\mathbf{x}}^{t+1}]_{\gamma_1\gamma_3}^{\beta_1} [\mathbf{h}_{\mathbf{x}}^t]_{\alpha_3}^{\gamma_3} [\boldsymbol{\eta}]_{\phi_1}^{\gamma_1} \end{aligned}$$

$$\begin{aligned} [Q_{2,\mathbf{x}}]_{\alpha_3}^i &= ([\mathbf{f}_{\mathbf{y}_{t+1}\mathbf{x}_{t+1}\mathbf{y}_{t+1}}]_{\beta_1\gamma_2\beta_3}^i [\mathbf{g}_{\mathbf{x}}^{t+1}]_{\gamma_3}^{\beta_3} [\mathbf{h}_{\mathbf{x}}^t]_{\alpha_3}^{\gamma_3} + [\mathbf{f}_{\mathbf{y}_{t+1}\mathbf{x}_{t+1}\mathbf{y}_t}]_{\beta_1\gamma_2\beta_3}^i [\mathbf{g}_{\mathbf{x}}^t]_{\alpha_3}^{\beta_3} \\ &+ [\mathbf{f}_{\mathbf{y}_{t+1}\mathbf{x}_{t+1}\mathbf{x}_{t+1}}]_{\beta_1\gamma_2\gamma_3}^i [\mathbf{h}_{\mathbf{x}}^t]_{\alpha_3}^{\gamma_3} + [\mathbf{f}_{\mathbf{y}_{t+1}\mathbf{x}_{t+1}\mathbf{x}_t}]_{\beta_1\gamma_2\alpha_3}^i) \\ &\times [\boldsymbol{\eta}]_{\phi_2}^{\gamma_2} [\mathbf{g}_{\mathbf{x}}^{t+1}]_{\gamma_1}^{\beta_1} [\boldsymbol{\eta}]_{\phi_1}^{\gamma_1} \\ &+ [\mathbf{f}_{\mathbf{y}_{t+1}\mathbf{x}_{t+1}}]_{\beta_1\gamma_2}^i [\boldsymbol{\eta}]_{\phi_2}^{\gamma_2} [\mathbf{g}_{\mathbf{x}\mathbf{x}}^{t+1}]_{\gamma_1\gamma_3}^{\beta_1} [\mathbf{h}_{\mathbf{x}}^t]_{\alpha_3}^{\gamma_3} [\boldsymbol{\eta}]_{\phi_1}^{\gamma_1} \end{aligned}$$

$$\begin{aligned} [Q_{3,\mathbf{x}}]_{\alpha_3}^i &= ([\mathbf{f}_{\mathbf{y}_{t+1}\mathbf{y}_{t+1}}]_{\beta_1\beta_3}^i [\mathbf{g}_{\mathbf{x}}^{t+1}]_{\gamma_3}^{\beta_3} [\mathbf{h}_{\mathbf{x}}^t]_{\alpha_3}^{\gamma_3} + [\mathbf{f}_{\mathbf{y}_{t+1}\mathbf{y}_t}]_{\beta_1\beta_3}^i [\mathbf{g}_{\mathbf{x}}^t]_{\alpha_3}^{\beta_3} + [\mathbf{f}_{\mathbf{y}_{t+1}\mathbf{x}_{t+1}}]_{\beta_1\gamma_3}^i [\mathbf{h}_{\mathbf{x}}^t]_{\alpha_3}^{\gamma_3} + [\mathbf{f}_{\mathbf{y}_{t+1}\mathbf{x}_t}]_{\beta_1\alpha_3}^i) \\ &\times [\mathbf{g}_{\mathbf{x}\mathbf{x}}^{t+1}]_{\gamma_1\gamma_2}^{\beta_1} [\boldsymbol{\eta}]_{\phi_1}^{\gamma_1} [\boldsymbol{\eta}]_{\phi_2}^{\gamma_2} \\ &+ [\mathbf{f}_{\mathbf{y}_{t+1}}]_{\beta_1}^i [\mathbf{g}_{\mathbf{x}\mathbf{x}\mathbf{x}}^{t+1}]_{\gamma_1\gamma_2\gamma_3}^{\beta_1} [\mathbf{h}_{\mathbf{x}}^t]_{\alpha_3}^{\gamma_3} [\boldsymbol{\eta}]_{\phi_2}^{\gamma_2} [\boldsymbol{\eta}]_{\phi_1}^{\gamma_1} \end{aligned}$$

$$\begin{aligned}
& +3 [\mathbf{f}_{\mathbf{y}_{t+1}\mathbf{x}_{t+1}\mathbf{x}_{t+1}}]_{\beta_1\gamma_2\gamma_3}^i [\boldsymbol{\eta}]_{\phi_3}^{\gamma_3} [\boldsymbol{\eta}]_{\phi_2}^{\gamma_2} [\mathbf{g}_{\mathbf{x}}^{t+1}]_{\gamma_1}^{\beta_1} [\boldsymbol{\eta}]_{\phi_1}^{\gamma_1} \\
& +3 [\mathbf{f}_{\mathbf{y}_{t+1}\mathbf{x}_{t+1}}]_{\beta_1\gamma_2}^i [\boldsymbol{\eta}]_{\phi_2}^{\gamma_2} [\mathbf{g}_{\mathbf{xx}}^{t+1}]_{\gamma_1\gamma_3}^{\beta_1} [\boldsymbol{\eta}]_{\phi_3}^{\gamma_3} [\boldsymbol{\eta}]_{\phi_1}^{\gamma_1} \\
& +0 \\
& +0 \\
& + [\mathbf{f}_{\mathbf{y}_{t+1}}]_{\beta_1}^i [\mathbf{g}_{\mathbf{xxx}}^{t+1}]_{\gamma_1\gamma_2\gamma_3}^{\beta_1} [\boldsymbol{\eta}]_{\phi_1}^{\gamma_1} [\boldsymbol{\eta}]_{\phi_2}^{\gamma_2} [\boldsymbol{\eta}]_{\phi_3}^{\gamma_3} \\
& +0 \\
& +0 \\
& +0 \\
& +0 \\
& + [\mathbf{f}_{\mathbf{x}_{t+1}\mathbf{x}_{t+1}\mathbf{x}_{t+1}}]_{\gamma_1\gamma_2\gamma_3}^i [\boldsymbol{\eta}]_{\phi_3}^{\gamma_3} [\boldsymbol{\eta}]_{\phi_2}^{\gamma_2} [\boldsymbol{\eta}]_{\phi_1}^{\gamma_1} \\
& \Downarrow
\end{aligned}$$

$$\begin{aligned}
[\mathbf{F}_{\boldsymbol{\epsilon}\boldsymbol{\epsilon}\boldsymbol{\epsilon}}]_{\phi_1\phi_2\phi_3}^i &= [\mathbf{f}_{\mathbf{y}_{t+1}\mathbf{y}_{t+1}\mathbf{y}_{t+1}}]_{\beta_1\beta_2\beta_3}^i [\mathbf{g}_{\mathbf{x}}^{t+1}]_{\gamma_3}^{\beta_3} [\boldsymbol{\eta}]_{\phi_3}^{\gamma_3} [\mathbf{g}_{\mathbf{x}}^{t+1}]_{\gamma_2}^{\beta_2} [\boldsymbol{\eta}]_{\phi_2}^{\gamma_2} [\mathbf{g}_{\mathbf{x}}^{t+1}]_{\gamma_1}^{\beta_1} [\boldsymbol{\eta}]_{\phi_1}^{\gamma_1} \\
& +3 [\mathbf{f}_{\mathbf{y}_{t+1}\mathbf{y}_{t+1}\mathbf{x}_{t+1}}]_{\beta_1\beta_2\gamma_3}^i [\boldsymbol{\eta}]_{\phi_3}^{\gamma_3} [\mathbf{g}_{\mathbf{x}}^{t+1}]_{\gamma_2}^{\beta_2} [\boldsymbol{\eta}]_{\phi_2}^{\gamma_2} [\mathbf{g}_{\mathbf{x}}^{t+1}]_{\gamma_1}^{\beta_1} [\boldsymbol{\eta}]_{\phi_1}^{\gamma_1} \\
& +3 [\mathbf{f}_{\mathbf{y}_{t+1}\mathbf{y}_{t+1}}]_{\beta_1\beta_2}^i [\mathbf{g}_{\mathbf{xx}}^{t+1}]_{\gamma_2\gamma_3}^{\beta_2} [\boldsymbol{\eta}]_{\phi_3}^{\gamma_3} [\boldsymbol{\eta}]_{\phi_2}^{\gamma_2} [\mathbf{g}_{\mathbf{x}}^{t+1}]_{\gamma_1}^{\beta_1} [\boldsymbol{\eta}]_{\phi_1}^{\gamma_1} \\
& +3 [\mathbf{f}_{\mathbf{y}_{t+1}\mathbf{x}_{t+1}\mathbf{x}_{t+1}}]_{\beta_1\gamma_2\gamma_3}^i [\boldsymbol{\eta}]_{\phi_3}^{\gamma_3} [\boldsymbol{\eta}]_{\phi_2}^{\gamma_2} [\mathbf{g}_{\mathbf{x}}^{t+1}]_{\gamma_1}^{\beta_1} [\boldsymbol{\eta}]_{\phi_1}^{\gamma_1} \\
& +3 [\mathbf{f}_{\mathbf{y}_{t+1}\mathbf{x}_{t+1}}]_{\beta_1\gamma_2}^i [\boldsymbol{\eta}]_{\phi_2}^{\gamma_2} [\mathbf{g}_{\mathbf{xx}}^{t+1}]_{\gamma_1\gamma_3}^{\beta_1} [\boldsymbol{\eta}]_{\phi_3}^{\gamma_3} [\boldsymbol{\eta}]_{\phi_1}^{\gamma_1} \\
& + [\mathbf{f}_{\mathbf{y}_{t+1}}]_{\beta_1}^i [\mathbf{g}_{\mathbf{xxx}}^{t+1}]_{\gamma_1\gamma_2\gamma_3}^{\beta_1} [\boldsymbol{\eta}]_{\phi_1}^{\gamma_1} [\boldsymbol{\eta}]_{\phi_2}^{\gamma_2} [\boldsymbol{\eta}]_{\phi_3}^{\gamma_3} \\
& + [\mathbf{f}_{\mathbf{x}_{t+1}\mathbf{x}_{t+1}\mathbf{x}_{t+1}}]_{\gamma_1\gamma_2\gamma_3}^i [\boldsymbol{\eta}]_{\phi_3}^{\gamma_3} [\boldsymbol{\eta}]_{\phi_2}^{\gamma_2} [\boldsymbol{\eta}]_{\phi_1}^{\gamma_1}
\end{aligned}$$

which is identical to the expression obtained in Andreasen (2012) for $\mathbf{F}_{\sigma\sigma\sigma}(\mathbf{x}_{ss}, \sigma)$ by setting all derivatives with respect to the perturbation parameter σ equal to zero.

3.4.4 Solving the System in (21)

The only new issue to address when going from second to third order is how to solve (21). Now recall that

$$[\mathbf{F}_{\mathbf{x}_t}(\bar{\mathbf{x}}, \mathbf{0})]_{\alpha_1}^i = [\mathbf{f}_{\mathbf{y}_{t+1}}]_{\beta_1}^i [\mathbf{g}_{\mathbf{x}}^{t+1}]_{\gamma_1}^{\beta_1} [\mathbf{h}_{\mathbf{x}}^t]_{\alpha_1}^{\gamma_1} + [\mathbf{f}_{\mathbf{y}_t}]_{\beta_1}^i [\mathbf{g}_{\mathbf{x}}^t]_{\alpha_1}^{\beta_1} + [\mathbf{f}_{\mathbf{x}_{t+1}}]_{\gamma_1}^i [\mathbf{h}_{\mathbf{x}}^t]_{\alpha_1}^{\gamma_1} + [\mathbf{f}_{\mathbf{x}_t}]_{\alpha_1}^i,$$

where all derivatives of \mathbf{f} , $\mathbf{g}(\cdot)$, and $\mathbf{h}(\cdot)$ are evaluated at $\mathbf{x}_t = \bar{\mathbf{x}}$ and $\boldsymbol{\epsilon}_{t+1} = \mathbf{0}$. Hence, we have

$$[\mathbf{F}_{\mathbf{x}}(\bar{\mathbf{x}}, \mathbf{0})]_{\alpha_1}^i + \frac{3}{6} [\mathbf{F}_{\boldsymbol{\epsilon}\boldsymbol{\epsilon}\mathbf{x}}(\bar{\mathbf{x}}, \mathbf{0})]_{\phi_1\phi_2\alpha_3}^i [\mathbf{I}]_{\phi_2}^{\phi_1} = 0$$

\Downarrow

$$[\mathbf{f}_{\mathbf{y}_{t+1}}]_{\beta_1}^i [\mathbf{g}_{\mathbf{x}}]_{\gamma_1}^{\beta_1} [\mathbf{h}_{\mathbf{x}}]_{\alpha_1}^{\gamma_1} + [\mathbf{f}_{\mathbf{y}_t}]_{\beta_1}^i [\mathbf{g}_{\mathbf{x}}]_{\alpha_1}^{\beta_1} + [\mathbf{f}_{\mathbf{x}_{t+1}}]_{\gamma_1}^i [\mathbf{h}_{\mathbf{x}}^t]_{\alpha_1}^{\gamma_1} + [\mathbf{f}_{\mathbf{x}_t}]_{\alpha_1}^i + \frac{3}{6} [\mathbf{F}_{\boldsymbol{\epsilon}\boldsymbol{\epsilon}\mathbf{x}}(\bar{\mathbf{x}}, \mathbf{0})]_{\phi_1\phi_2\alpha_3}^i [\mathbf{I}]_{\phi_2}^{\phi_1} = \mathbf{0}.$$

Note that $[\mathbf{F}_{\mathbf{x}}]_{\alpha_1}^i + \frac{3}{6} [\mathbf{F}_{\boldsymbol{\epsilon}\boldsymbol{\epsilon}\mathbf{x}}]_{\phi_1\phi_2\alpha_3}^i [\mathbf{I}]_{\phi_2}^{\phi_1} = \mathbf{0}$ implies

$$\left([\mathbf{F}_{\mathbf{x}}(\bar{\mathbf{x}}, \mathbf{0})]_{\alpha_1} + \frac{3}{6} [\mathbf{I}]_{\phi_2}^{\phi_1} [\mathbf{F}_{\boldsymbol{\epsilon}\boldsymbol{\epsilon}\mathbf{x}}(\bar{\mathbf{x}}, \mathbf{0})]_{\phi_1\phi_2\alpha_3} \right) [\mathbf{x}_t - \bar{\mathbf{x}}]^{\alpha_1} = \mathbf{0}$$

\Downarrow

$$\left(\mathbf{f}_{\mathbf{y}_{t+1}} \mathbf{g}_{\mathbf{x}} \mathbf{h}_{\mathbf{x}} + \mathbf{f}_{\mathbf{y}_t} \mathbf{g}_{\mathbf{x}} + \mathbf{f}_{\mathbf{x}_{t+1}} \mathbf{h}_{\mathbf{x}} + \mathbf{f}_{\mathbf{x}_t} + \frac{3}{6} [\mathbf{F}_{\boldsymbol{\epsilon}\boldsymbol{\epsilon}\mathbf{x}}(\bar{\mathbf{x}}, \mathbf{0})]_{\phi_1\phi_2} [\mathbf{I}]_{\phi_2}^{\phi_1} \right) (\mathbf{x}_t - \bar{\mathbf{x}}) = \mathbf{0}$$

⇕

$$(-\mathbf{f}_{\mathbf{y}_{t+1}} \mathbf{g}_{\mathbf{x}} \mathbf{h}_{\mathbf{x}} - \mathbf{f}_{\mathbf{x}_{t+1}} \mathbf{h}_{\mathbf{x}}) (\mathbf{x}_t - \bar{\mathbf{x}}) = \left(\mathbf{f}_{\mathbf{y}_t} \mathbf{g}_{\mathbf{x}} + \mathbf{f}_{\mathbf{x}_t} + \frac{3}{6} [\mathbf{I}]_{\phi_2}^{\phi_1} [\mathbf{F}_{\epsilon\epsilon\mathbf{x}}(\bar{\mathbf{x}}, \mathbf{0})]_{\phi_1\phi_2} \right) (\mathbf{x}_t - \bar{\mathbf{x}})$$

⇕

$$\begin{aligned} & \begin{bmatrix} -\mathbf{f}_{\mathbf{x}_{t+1}} & -\mathbf{f}_{\mathbf{y}_{t+1}} \end{bmatrix} \begin{bmatrix} \mathbf{h}_{\mathbf{x}}(\mathbf{x}_t - \bar{\mathbf{x}}) \\ \mathbf{g}_{\mathbf{x}} \mathbf{h}_{\mathbf{x}}(\mathbf{x}_t - \bar{\mathbf{x}}) \end{bmatrix} \\ &= \begin{bmatrix} \mathbf{f}_{\mathbf{x}_t} + \frac{3}{6} [\mathbf{I}]_{\phi_2}^{\phi_1} [\mathbf{F}_{\epsilon\epsilon\mathbf{x}}]_{\phi_1\phi_2} & \mathbf{f}_{\mathbf{y}_t} \end{bmatrix} \begin{bmatrix} (\mathbf{x}_t - \bar{\mathbf{x}}) \\ \mathbf{g}_{\mathbf{x}}(\mathbf{x}_t - \bar{\mathbf{x}}) \end{bmatrix}. \end{aligned}$$

Hence, for a linearized system we get

$$\begin{aligned} & \begin{bmatrix} -\mathbf{f}_{\mathbf{x}_{t+1}} & -\mathbf{f}_{\mathbf{y}_{t+1}} \end{bmatrix} \begin{bmatrix} E_t[\mathbf{x}_{t+1} - \bar{\mathbf{x}}] \\ E_t[\mathbf{y}_{t+1} - \bar{\mathbf{y}}] \end{bmatrix} \\ &= \begin{bmatrix} \mathbf{f}_{\mathbf{x}_t} + \frac{3}{6} [\mathbf{I}]_{\phi_2}^{\phi_1} [\mathbf{F}_{\epsilon\epsilon\mathbf{x}}(\bar{\mathbf{x}}, \mathbf{0})]_{\phi_1\phi_2} & \mathbf{f}_{\mathbf{y}_t} \end{bmatrix} \begin{bmatrix} \mathbf{x}_t - \bar{\mathbf{x}} \\ \mathbf{y}_t - \bar{\mathbf{y}} \end{bmatrix}, \end{aligned}$$

where all derivatives of \mathbf{f} are evaluated at $\mathbf{x}_t = \bar{\mathbf{x}}$. Accordingly, this risk-adjusted quadratic system of equations can be solved as in Klein (2000) using the Matlab code `gx_hx.m`.

3.5 Summary of the Algorithm at Third order

To present the algorithm let $\mathcal{D}_{\mathbf{g}}(\mathbf{x}_t) \equiv (\mathbf{g}(\mathbf{x}_t), \mathbf{g}_{\mathbf{xx}}(\mathbf{x}_t), \mathbf{g}_{\mathbf{xxx}}(\mathbf{x}_t))$ and $\mathcal{D}_{\mathbf{h}}(\mathbf{x}_t) \equiv (\mathbf{h}(\mathbf{x}_t), \mathbf{h}_{\mathbf{xx}}(\mathbf{x}_t), \mathbf{h}_{\mathbf{xxx}}(\mathbf{x}_t))$. The suggestive procedure for solving (20) to (23) is:

1. Compute $\mathcal{D}_{\mathbf{g}}(\mathbf{x}_{ss})$ and $\mathcal{D}_{\mathbf{h}}(\mathbf{x}_{ss})$ by the standard perturbation method. Let $\bar{\mathbf{x}}^{(0)} = \mathbf{x}_{ss}$ and $\bar{\mathbf{y}}^{(0)} = \mathbf{y}_{ss}$, and let $i = 1$.
2. Compute $\mathbf{F}_{\epsilon\epsilon}(\bar{\mathbf{x}}^{(i-1)}, \mathbf{0})$, $\mathbf{F}_{\epsilon\epsilon\mathbf{x}}(\bar{\mathbf{x}}^{(i-1)}, \mathbf{0})$, and $\mathbf{F}_{\epsilon\epsilon\epsilon}(\bar{\mathbf{x}}^{(i-1)}, \mathbf{0})$ using $\mathcal{D}_{\mathbf{g}}(\bar{\mathbf{x}}^{(i-1)})$ and $\mathcal{D}_{\mathbf{h}}(\bar{\mathbf{x}}^{(i-1)})$. Then solve for (20) to get $\bar{\mathbf{x}}^{(i)}$ and $\bar{\mathbf{y}}^{(i)}$.
3. Use $\bar{\mathbf{x}}^{(i)}$, $\bar{\mathbf{y}}^{(i)}$, $\mathcal{D}_{\mathbf{g}}(\bar{\mathbf{x}}^{(i-1)})$, and $\mathcal{D}_{\mathbf{h}}(\bar{\mathbf{x}}^{(i-1)})$ to compute $\mathbf{F}_{\epsilon\epsilon\mathbf{x}}(\bar{\mathbf{x}}^{(i)}, \mathbf{0})$.
4. Given $\bar{\mathbf{x}}^{(i)}$, $\bar{\mathbf{y}}^{(i)}$, and $\mathbf{F}_{\epsilon\epsilon\mathbf{x}}(\bar{\mathbf{x}}^{(i)}, \mathbf{0})$, compute $(\mathbf{g}_{\mathbf{x}}(\bar{\mathbf{x}}^{(i)}), \mathbf{h}_{\mathbf{x}}(\bar{\mathbf{x}}^{(i)}))$ from (21), $(\mathbf{g}_{\mathbf{xx}}(\bar{\mathbf{x}}^{(i)}), \mathbf{h}_{\mathbf{xx}}(\bar{\mathbf{x}}^{(i)}))$ from (22), and $(\mathbf{g}_{\mathbf{xxx}}(\bar{\mathbf{x}}^{(i)}), \mathbf{h}_{\mathbf{xxx}}(\bar{\mathbf{x}}^{(i)}))$ from (23).
5. If $\bar{\mathbf{x}}^{(i)} \approx \bar{\mathbf{x}}^{(i-1)}$ then stop, otherwise let $i = i + 1$ and go to step 2.

In terms of the expressions for all derivatives of \mathbf{F} , we directly have that $\mathbf{F}_{\mathbf{x}}$, $\mathbf{F}_{\mathbf{xx}}$, and $\mathbf{F}_{\mathbf{xxx}}$ correspond to those stated in Schmitt-Grohé & Uribe (2004) and Andreasen (2012) for the standard perturbation method. We have also shown that the expressions for $\mathbf{F}_{\epsilon\epsilon}(\bar{\mathbf{x}}, \mathbf{0})$, $\mathbf{F}_{\epsilon\epsilon\mathbf{x}}(\bar{\mathbf{x}}, \mathbf{0})$, and $\mathbf{F}_{\epsilon\epsilon\epsilon}(\bar{\mathbf{x}}, \mathbf{0})$ are identical to those provided for $\mathbf{F}_{\sigma\sigma}$, $\mathbf{F}_{\sigma\sigma\mathbf{x}}$, and $\mathbf{F}_{\sigma\sigma\sigma}$, respectively, in Schmitt-Grohé & Uribe (2004) and Andreasen (2012), when setting all derivatives of $\mathbf{g}(\cdot)$ and $\mathbf{h}(\cdot)$ with respect to the perturbation parameter σ equal to zero. Thus, this algorithm for solving (20) to (23) is easy to implement from existing results and computer packages on the standard perturbation method. In our case, we modify the highly efficient Matlab codes of Binning (2013). The only new issue to address is how to solve (21), which reads

$$[\mathbf{f}_{\mathbf{y}_{t+1}}]_{\beta_1}^i [\mathbf{g}_{\mathbf{x}}]_{\gamma_1}^{\beta_1} [\mathbf{h}_{\mathbf{x}}]_{\alpha_1}^{\gamma_1} + [\mathbf{f}_{\mathbf{y}_t}]_{\beta_1}^i [\mathbf{g}_{\mathbf{x}}]_{\alpha_1}^{\beta_1} + [\mathbf{f}_{\mathbf{x}_{t+1}}]_{\gamma_1}^i [\mathbf{h}_{\mathbf{x}}]_{\alpha_1}^{\gamma_1} + [\mathbf{f}_{\mathbf{x}_t}^{adj}]_{\alpha_1}^i = \mathbf{0}.$$

where $[\mathbf{f}_{\mathbf{x}_t}^{adj}]_{\alpha_1}^i \equiv [\mathbf{f}_{\mathbf{x}_t}]_{\alpha_1}^i + \frac{3}{6} [\mathbf{F}_{\epsilon\epsilon\mathbf{x}}(\bar{\mathbf{x}}, \mathbf{0})]_{\phi_1\phi_2\alpha_3}^i [\mathbf{I}]_{\phi_2}^{\phi_1}$ all derivatives of \mathbf{f} , $\mathbf{g}(\cdot)$, and $\mathbf{h}(\cdot)$ are evaluated at $\mathbf{x}_t = \bar{\mathbf{x}}$ and $\epsilon_{t+1} = \mathbf{0}$. Thus, when conditioning on a given value of $\mathbf{F}_{\epsilon\epsilon\mathbf{x}}(\bar{\mathbf{x}}, \mathbf{0})$, this system can be solved using existing routines for a linear rational expectation model (see for instance Klein (2000)).

3.6 An Efficient Solution of (20)

This subsection shows how to derive an efficient solution of (20) for the considered New Keynesian model. Recall that the model reads (without stating the exogenous processes):

1	$Y_t + \Phi = \text{const1}([K_{t-1}U_t]^\alpha [Z_t N_t]^{1-\alpha})$
2	$C_t + \frac{1}{R_t^R} \nu K_t = W_t N_t + D_t^E + \nu K_{t-1}$
3	$\frac{(1-\eta)}{\eta} \frac{C_t - bC_{t-1}}{1-N_t} = W_t$
4	$V_t = \text{const2} \cdot \left\{ a_t^{\frac{1-\sigma}{\theta_V}} \left[\frac{\theta_V}{1-\sigma} \left((C_t - bC_{t-1})^\eta (1-N_t)^{1-\eta} \right)^{\frac{1-\sigma}{\theta_V}} + u_0^{(1)} \right] + u_0^{(2)} \right\} + \beta (EV_t)^{\frac{1}{1-\alpha^{Swan}}}$
5	$EV_t = \mathbb{E}_t \left[V_{t+1}^{1-\alpha^{Swan}} \right]$
6	$W_t N_t = (1-\alpha) (Y_t + \Phi) \frac{1}{\mu_t}$
7	$R_t^K K_{t-1} U_t = \alpha (Y_t + \Phi) \frac{1}{\mu_t}$
8	$q_t (\delta_1 + \delta_2 (U_t - 1)) K_{t-1} U_t = \alpha (Y_t + \Phi) \frac{1}{\mu_t}$
9	$K_t = \left(1 - (\delta_0 + \delta_1 (U_t - 1) + \frac{\delta_2}{2} (U_t - 1)^2) - \frac{\phi_K}{2} \left(\frac{I_t}{K_{t-1}} - \delta \right)^2 \right) K_{t-1} + I_t$
10	$1 = R_t^R \mathbb{E}_t [M_{t+1}]$
11	$1 = R_t \mathbb{E}_t \left[M_{t+1} \frac{1}{\Pi_{t+1}} \right]$
12	$P_t^E = \mathbb{E}_t [M_{t+1} (D_{t+1}^E + P_{t+1}^E)]$
13	$\log(R_t) = \rho_r \log(R_{t-1}) + (1-\rho_r) (\log(R_{ss}) + \zeta_\pi \log(\frac{\Pi_t}{\Pi_{ss}}) + \zeta_{\Delta y} \log(\frac{Y_t}{Y_{t-1}}) + \zeta_y \log(\frac{Y_t}{Y_{ss}}))$ $+ (1-\rho_r) \zeta_{VR} \zeta_V (VR_t^{eq} - aux_t)$
14	$D_t^E = Y_t - W_t N_t - I_t - \frac{\phi_P}{2} \left(\frac{\Pi_t}{\Pi_{ss}} - 1 \right)^2 Y_t - \nu (K_{t-1} - \frac{1}{R_t^R} K_t)$
15	$q_t = \mathbb{E}_t [M_{t+1} [R_{t+1}^K U_{t+1}$ $+ q_{t+1} \left(1 - (\delta_0 + \delta_1 (U_{t+1} - 1) + \frac{\delta_2}{2} (U_{t+1} - 1)^2) - \frac{\phi_K}{2} \left(\frac{I_{t+1}}{K_t} - \delta \right)^2 \right) + \phi_K \left(\frac{I_{t+1}}{K_t} - \delta \right) \frac{I_{t+1}}{K_t}]]$
16	$\frac{1}{q_t} = 1 - \phi_K \left(\frac{I_t}{K_{t-1}} - \delta \right)$
17	$\phi_P \left(\frac{\Pi_t}{\Pi_{ss}} - 1 \right) \frac{\Pi_t}{\Pi_{ss}} = (1 - \theta_{\mu,t}) + \frac{\theta_{\mu,t}}{\mu_t} + \phi_P \mathbb{E}_t \left[M_{t+1} \frac{Y_{t+1}}{Y_t} \left(\frac{\Pi_{t+1}}{\Pi_{ss}} - 1 \right) \frac{\Pi_{t+1}}{\Pi_{ss}} \right]$
18	$ER_t^{eq} = \mathbb{E}_t \left[\frac{D_{t+1}^E + P_{t+1}^E}{P_t^E} \right]$
19	$ER_t^{eq2} = \mathbb{E}_t \left[\left(\frac{D_{t+1}^E + P_{t+1}^E}{P_t^E} \right)^2 \right]$
20	$VR_t^{eq} = ER_t^{eq2} - (ER_t^{eq})^2$
21	$aux_t = (1-\gamma) VR_t^{eq} + \gamma \mathbb{E}_t [aux_{t+1}]$

Note also that

$$M_{t+1} = \beta \left(\frac{a_{t+1}}{a_t} \right)^{\frac{1-\sigma}{\theta_V}} \frac{(C_{t+1} - bC_t)^{\eta \frac{1-\sigma}{\theta_V} - 1} (1 - N_{t+1})^{(1-\eta) \frac{1-\sigma}{\theta_V}}}{(C_t - bC_{t-1})^{\eta \frac{1-\sigma}{\theta_V} - 1} (1 - N_t)^{(1-\eta) \frac{1-\sigma}{\theta_V}}} \left(\frac{V_{t+1}}{\left(\mathbb{E}_t \left[V_{t+1}^{1-\alpha^{Swan}} \right] \right)^{\frac{1}{1-\alpha^{Swan}}}} \right)^{-\alpha^{Swan}}$$

In all equations with forward looking variables, we allow for an expectation error E , or risk adjustment, which is given by $\frac{1}{2} [\mathbf{F}_{\epsilon\epsilon}(\bar{\mathbf{x}}, \mathbf{0})]_{\phi_1 \phi_2}^i [\mathbf{I}]_{\phi_2}^{\phi_1} + \frac{1}{6} [\mathbf{F}_{\epsilon\epsilon\epsilon}(\bar{\mathbf{x}}, \mathbf{0})]_{\phi_1 \phi_2 \phi_3}^i [\mathbf{m}^3]_{\phi_2 \phi_3}^{\phi_1}$. Note also that we summarize the equations exactly as stated in our unit-free implementation of the model in Matlab. That is:

f1	$-1 - \frac{\Phi}{Y_t} + const1([K_{t-1}U_t]^\alpha [Z_tN_t]^{1-\alpha}/Y_t = 0$
f2	$-1 + \left(-\frac{1}{R_t^k} \nu K_t + W_t N_t + D_t^E + \nu K_{t-1}\right) / C_t = 0$
f3	$-1 + \frac{1}{W_t} \frac{(1-\eta)}{\eta} \frac{C_t - bC_{t-1}}{1 - N_t} = 0$
f4	$-1 + \left[const2 \cdot \left\{ a_t^{\frac{1-\sigma}{\theta_V}} \left[\frac{\theta_V}{1-\sigma} \left((C_t - bC_{t-1})^\eta (1 - N_t)^{1-\eta} \right)^{\frac{1-\sigma}{\theta_V}} + u_0^{(1)} \right] + u_0^{(2)} \right\} + \beta(EV_t)^{\frac{1}{1-\alpha^{Swan}}}\right] / V_t = 0$
f5	$-1 + \mathbb{E}_t \left[V_{t+1}^{1-\alpha^{Swan}} \right] / EV_t + E_5 = 0$
f6	$-1 + \frac{(1-\alpha)(Y_t + \Phi) \frac{1}{\mu_t}}{W_t N_t} = 0$
f7	$-1 + \frac{\alpha(Y_t + \Phi) \frac{1}{\mu_t}}{R_t^k K_{t-1} U_t} = 0$
f8	$-1 + \frac{\alpha(Y_t + \Phi) \frac{1}{\mu_t}}{q_t (\delta_1 + \delta_2 (U_t - 1)) K_{t-1} U_t} = 0$
f9	$-\frac{K_t}{I_t} + \frac{\left(1 - (\delta_0 + \delta_1 (U_t - 1) + \frac{\delta_2}{2} (U_t - 1)^2) - \frac{\phi_K}{2} \left(\frac{I_t}{K_{t-1}} - \delta\right)^2\right) K_{t-1}}{I_t} + 1 = 0$
f10	$-1 + R_t^R \mathbb{E}_t [M_{t+1}] + E_{10} = 0$
f11	$-1 + R_t \mathbb{E}_t \left[M_{t+1} \frac{1}{\Pi_{t+1}} \right] + E_{11} = 0$
f12	$-1 + \frac{\mathbb{E}_t [M_{t+1} (D_{t+1}^E + P_{t+1}^E)]}{P_t^E} + E_{12} = 0$
f13	$\log(R_t) = \rho_r \log(R_{t-1}) + (1 - \rho_r)(\log(R_{ss}) + \zeta_\pi \log(\frac{\Pi_t}{\Pi_{ss}}) + \zeta_{\Delta y} \log(\frac{Y_t}{Y_{t-1}}) + \zeta_y \log(\frac{Y_t}{Y_{ss}}))$ $+ (1 - \rho_r) \zeta_V R_t^{eq} (V R_t^{eq} - aux_t)$
f14	$-1 + \frac{Y_t - W_t N_t - I_t - \frac{\phi_P}{2} \left(\frac{\Pi_t}{\Pi_{ss}} - 1\right)^2 Y_t - \nu (K_{t-1} - \frac{1}{R_t^R} K_t)}{D_t^E} = 0$
f15	$-1 + \mathbb{E}_t \left[\frac{M_{t+1}}{q_t} [R_{t+1}^K U_{t+1} + q_{t+1} \left(1 - (\delta_0 + \delta_1 (U_{t+1} - 1) + \frac{\delta_2}{2} (U_{t+1} - 1)^2) - \frac{\phi_K}{2} \left(\frac{I_{t+1}}{K_t} - \delta_0\right)^2\right) \right. \right.$ $\left. + \phi_K \left(\frac{I_{t+1}}{K_t} - \delta_0\right) \frac{I_{t+1}}{K_t} \right] + E_{15} = 0$
f16	$-\frac{1}{q_t} + 1 - \phi_K \left(\frac{I_t}{K_{t-1}} - \delta_0\right) = 0$
f17	$-\phi_P \left(\frac{\Pi_t}{\Pi_{ss}} - 1\right) \frac{\Pi_t}{\Pi_{ss}} + (1 - \theta_{\mu,t}) + \frac{\theta_{\mu,t}}{\mu_t} + \phi_P \mathbb{E}_t \left[M_{t+1} \frac{Y_{t+1}}{Y_t} \left(\frac{\Pi_{t+1}}{\Pi_{ss}} - 1\right) \frac{\Pi_{t+1}}{\Pi_{ss}} \right] + E_{17} = 0$
f18	$-1 + \mathbb{E}_t \left[\frac{D_{t+1}^E + P_{t+1}^E}{E R_t^{eq} P_t^E} \right] + E_{18} = 0$
f19	$-1 + \mathbb{E}_t \left[\left(\frac{D_{t+1}^E + P_{t+1}^E}{P_t^E}\right)^2 \frac{1}{E R_t^{eq2}} \right] + E_{19} = 0$
f20	$-V R_t^{eq} + E R_t^{eq2} - (E R_t^{eq})^2 = 0$
f21	$-aux_t + (1 - \gamma) V R_t^{eq} + \gamma aux_{t+1} + E_{21} = 0$
f22	$a_t = (1 - \rho_a) a_{ss} + \rho_a a_{t-1} + \sigma_{t-1}^a \varepsilon_t^a$
f23	$z_t = (1 - \rho_z) z_{ss} + \rho_z z_{t-1} + \sigma_{t-1}^{\omega z} \varepsilon_{z,t}$
f24	$\sigma_t = (1 - \rho_\sigma) \sigma_{ss} + \rho_\sigma \sigma_{t-1} + \sigma_\sigma \varepsilon_{\sigma,t}$

We want to derive a procedure to easily find the solution for the risky steady state - denoted by a bar. We assume that $\zeta_y = 0$. We obtain this solution by solving the system in closed form up to a guess of C_{bar} , N_{bar} , U_{bar} , EV_{bar} , and VR_{bar}^{eq} . Thus for a given value of C_{bar} , N_{bar} , U_{bar} , EV_{bar} , and VR_{bar}^{eq} , we can solve the system. From equations 22 to 24 we clearly have

$$\begin{aligned}
a_{bar} &= a_{ss} \\
z_{bar} &= z_{ss} \\
\sigma_{bar} &= \sigma_{ss}
\end{aligned}$$

Equation 4 gives

$$V_{bar} = const2 \cdot \left\{ a_{bar}^{\frac{1-\sigma}{\theta_V}} \left[\frac{\theta_V}{1-\sigma} \left((C_{bar} - bC_{bar})^\eta (1 - N_{bar})^{1-\eta} \right)^{\frac{1-\sigma}{\theta_V}} + u_0^{(1)} \right] + u_0^{(2)} \right\} + \beta(EV_{bar})^{\frac{1}{1-\alpha^{Swan}}}$$

Thus, we have

$$\begin{aligned} M_{t+1} &= \beta \frac{(C_{bar} - bC_{bar})^{\eta \frac{1-\sigma}{\theta_V} - 1} (1 - N_{bar})^{(1-\eta) \frac{1-\sigma}{\theta_V}} \left(\frac{V_{bar}}{(EV_{bar})^{\frac{1}{1-\alpha}}} \right)^{-\alpha^{Swan}}}{(C_{bar} - bC_{bar})^{\eta \frac{1-\sigma}{\theta_V} - 1} (1 - N_{bar})^{(1-\eta) \frac{1-\sigma}{\theta_V}}} \\ &= \beta \left(\frac{V_{bar}}{(EV_{bar})^{\frac{1}{1-\alpha}}} \right)^{-\alpha^{Swan}} \end{aligned}$$

Equation 10 implies

$$-1 + R_t^R \mathbb{E}_t [M_{t+1}] + E_{10} = 0$$

⇓

$$R_{bar}^R = \frac{1 - E_{10}}{M_{bar}}$$

From Equation 21 we have

$$-aux_{bar} + (1 - \gamma) VR_{bar}^{eq} + \gamma aux_{bar} + E_{21} = 0$$

⇕

$$(1 - \gamma) VR_{bar}^{eq} + E_{21} = aux_{bar} (1 - \gamma)$$

⇕

$$aux_{bar} = VR_{bar}^{eq} + \frac{E_{21}}{1 - \gamma}$$

Also, Equation 11 implies

$$R_t \mathbb{E}_t \left[M_{t+1} \frac{1}{\Pi_{t+1}} \right] = 1 - E_{11}$$

⇓

$$\Pi_{bar} = \frac{R_{bar} M_{bar}}{1 - E_{11}}$$

and inserting into Equation 13 (recall $\zeta_y = 0$)

$$\begin{aligned} \log(R_{bar}) &= \rho_r \log(R_{bar}) + (1 - \rho_r) (\log R_{ss} + \zeta_\pi \log\left(\frac{\Pi_{bar}}{\Pi_{ss}}\right)) \\ &\quad + (1 - \rho_r) \zeta_{VR_t^{eq}} (VR_{bar}^{eq} - aux_{bar}) \end{aligned}$$

⇕

$$\log(R_{bar}) = \log R_{ss} + \zeta_\pi \log\left(\frac{\Pi_{bar}}{\Pi_{ss}}\right) + \zeta_{VR_t^{eq}} (VR_{bar}^{eq} - aux_{bar})$$

⇕

$$\log(R_{bar}) = \log R_{ss} + \zeta_\pi \log\left(\frac{1}{\Pi_{ss}} \frac{R_{bar} M_{bar}}{1 - E_{11}}\right) + \zeta_{VR_t^{eq}} (VR_{bar}^{eq} - aux_{bar})$$

⇕

$$\log R_{bar} = \log R_{ss} + \zeta_\pi \log\left(\frac{1}{\Pi_{ss}} \frac{M_{bar}}{1 - E_{11}}\right) + \zeta_\pi \log R_{bar} + \zeta_{VR_t^{eq}} (VR_{bar}^{eq} - aux_{bar})$$

⇕

$$R_{bar} = \exp \left\{ \frac{1}{1 - \zeta_\pi} \left[\log R_{ss} + \zeta_\pi \log\left(\frac{1}{\Pi_{ss}} \frac{M_{bar}}{1 - E_{11}}\right) \right] + \zeta_{VR_t^{eq}} (VR_{bar}^{eq} - aux_{bar}) \right\}$$

Thus

$$\Pi_{bar} = \frac{R_{bar} M_{bar}}{1 - E_{11}}$$

Equation 17 gives

$$-\phi_P \left(\frac{\Pi_t}{\Pi_{ss}} - 1 \right) \frac{\Pi_t}{\Pi_{ss}} + (1 - \theta_{\mu,t}) + \frac{\theta_{\mu,t}}{\mu_t} + \phi_P \mathbb{E}_t \left[M_{t+1} \frac{Y_{t+1}}{Y_t} \left(\frac{\Pi_{t+1}}{\Pi_{ss}} - 1 \right) \frac{\Pi_{t+1}}{\Pi_{ss}} \right] + E_{17} = 0$$

↓

$$\frac{\theta_\mu}{\mu_{bar}} = \phi_P \left(\frac{\Pi_{bar}}{\Pi_{ss}} - 1 \right) \frac{\Pi_{bar}}{\Pi_{ss}} - (1 - \theta_\mu) - \phi_P \left[M_{bar} \left(\frac{\Pi_{bar}}{\Pi_{ss}} - 1 \right) \frac{\Pi_{bar}}{\Pi_{ss}} \right] - E_{17}$$

⇕

$$\mu_{bar} = \frac{\theta_\mu}{\phi_P \left(\frac{\Pi_{bar}}{\Pi_{ss}} - 1 \right) \frac{\Pi_{bar}}{\Pi_{ss}} - (1 - \theta_\mu) - \phi_P \left[M_{bar} \left(\frac{\Pi_{bar}}{\Pi_{ss}} - 1 \right) \frac{\Pi_{bar}}{\Pi_{ss}} \right] - E_{17}}$$

From Equation 3, we get

$$W_{bar} = \frac{(1 - \eta) C_{bar} - b C_{bar}}{\eta (1 - N_{bar})}.$$

Equation 6 implies

$$1 = \frac{(1 - \alpha) (Y_t + \Phi) \frac{1}{\mu_t}}{W_t N_t}.$$

↓

$$Y_{bar} = \frac{W_{bar} N_{bar} \mu_{bar}}{(1 - \alpha)} - \Phi$$

Also, Equation 1 gives

$$-1 - \frac{\Phi}{Y_t} + const1 ([K_{t-1} U_t]^\alpha [Z_t N_t]^{1-\alpha} / Y_t) = 0$$

↓

$$Y_{bar} + \Phi = const1 ([K_{bar} U_{bar}]^\alpha [Z_{bar} N_{bar}]^{1-\alpha})$$

⇕

$$[K_{bar} U_{bar}]^\alpha = \frac{Y_{bar} + \Phi}{const1 \times [Z_{bar} N_{bar}]^{1-\alpha}}$$

⇕

$$K_{bar} = \left[\frac{Y_{bar} + \Phi}{const1 \times [Z_{bar} N_{bar}]^{1-\alpha}} \right]^{\frac{1}{\alpha}} \frac{1}{U_{bar}}.$$

For Equation 7, we have

$$R_{bar}^K = \frac{\alpha (Y_{bar} + \Phi) \frac{1}{\mu_{bar}}}{K_{bar} U_{bar}}.$$

Using Equation 14, we get

$$D_t^E = Y_t - W_t N_t - I_t - \frac{\phi_P}{2} \left(\frac{\Pi_t}{\Pi_{ss}} - 1 \right)^2 Y_t - \nu (K_{t-1} - \frac{1}{R_t^R} K_t)$$

↓

$$D_{bar}^E = Y_{bar} - W_{bar} N_{bar} - I_{bar} - \frac{\phi_P}{2} \left(\frac{\Pi_{bar}}{\Pi_{ss}} - 1 \right)^2 Y_{bar} - \nu (K_{bar} - \frac{1}{R_{bar}^R} K_{bar}),$$

and Equation 2 gives

$$C_t = W_t N_t + D_t^E + \nu K_{t-1} - \frac{1}{R_t^R} \nu K_t$$

↓

$$\begin{aligned}
C_{bar} &= W_{bar}N_{bar} + D_{bar}^E + \nu K_{bar} - \frac{1}{R_{bar}^R} \nu K_{bar} \\
&= W_{bar}N_{bar} + Y_{bar} - W_{bar}N_{bar} - I_{bar} - \frac{\phi_P}{2} \left(\frac{\Pi_{bar}}{\Pi_{ss}} - 1 \right)^2 Y_{bar} - \nu \left(K_{bar} - \frac{1}{R_{bar}^R} K_{bar} \right) \\
&\quad + \nu K_{bar} - \frac{1}{R_{bar}^R} \nu K_{bar} \\
&= Y_{bar} - I_{bar} - \frac{\phi_P}{2} \left(\frac{\Pi_{bar}}{\Pi_{ss}} - 1 \right)^2 Y_{bar}
\end{aligned}$$

↕

$$I_{bar} = Y_{bar} - C_{bar} - \frac{\phi_P}{2} \left(\frac{\Pi_{bar}}{\Pi_{ss}} - 1 \right)^2 Y_{bar}.$$

Therefore we also have

$$D_{bar}^E = Y_{bar} - W_{bar}N_{bar} - I_{bar} - \frac{\phi_P}{2} \left(\frac{\Pi_{bar}}{\Pi_{ss}} - 1 \right)^2 Y_{bar} - \nu \left(K_{bar} - \frac{1}{R_{bar}^R} K_{bar} \right).$$

From Equation 12 we get

$$-1 + \frac{\mathbb{E}_t [M_{t+1}(D_{t+1}^E + P_{t+1}^E)]}{P_t^E} + E_{12} = 0$$

↓

$$M_{bar}(D_{bar}^E + P_{bar}^E) = (1 - E_{12}) P_{bar}^E$$

↕

$$M_{bar}D_{bar}^E = (1 - E_{12} - M_{bar}) P_{bar}^E$$

↕

$$P_{bar}^E = \frac{M_{bar}D_{bar}^E}{1 - E_{12} - M_{bar}}.$$

Equation 16 implies

$$\frac{1}{q_t} = 1 - \phi_K \left(\frac{I_t}{K_{t-1}} - \delta_0 \right)$$

↓

$$q_{bar} = \frac{1}{1 - \phi_K \left(\frac{I_{bar}}{K_{bar}} - \delta_0 \right)}.$$

From Equation 18, we get

$$-1 + \mathbb{E}_t \left[\frac{D_{t+1}^E + P_{t+1}^E}{ER_t^{eq} P_t^E} \right] + E_{18} = 0$$

↓

$$\frac{D_{bar}^E + P_{bar}^E}{ER_{bar}^{eq} P_{bar}^E} = 1 - E_{18}$$

↕

$$ER_{bar}^{eq} = \frac{D_{bar}^E + P_{bar}^E}{(1 - E_{18}) P_{bar}^E}.$$

Finally, Equation 19 implies

$$-1 + \mathbb{E}_t \left[\left(\frac{D_{t+1}^E + P_{t+1}^E}{P_t^E} \right)^2 \frac{1}{ER_t^{eq2}} \right] + E_{19} = 0$$

↓

$$ER_{bar}^{eq2} = \left(\frac{D_{bar}^E + P_{bar}^E}{P_{bar}^E} \right)^2 \frac{1}{1 - E_{19}}.$$

Thus, this leaves us with f5, f8, f9, f15, and f20 to determine C_{bar} , N_{bar} , U_{bar} , EV_{bar} , and VR_{bar}^{eq} . Note that if $\rho_y \neq 0$, then we can add R_{bar} and f13 to this last step, meaning that six variables would have to be determined by a nonlinear root solver.

4 Extra results for the Section "Inspecting the Mechanism"

4.1 Counterfactual exercises on the uncertainty channels

In the paper, we evaluate the relative importance of each uncertainty channel of our DSGE model in generating state-dependent effects to an uncertainty shock. Each of the intertemporal Euler-equations in the model reflects expectations over future uncertain realizations of state and control variables in the model, and hence introduce different channels for uncertainty to affect the economy. This implies that our model presented in Section 2 has the following five channels for uncertainty shocks, which we associate with the respective intertemporal Euler-equations:

1. the *precautionary savings channel* as captured by the households' optimality condition for one-period risk-less firm bonds and reflecting the consumption Euler-equation:

$$1 = R_t^R \mathbb{E}_t [M_{t+1}] ,$$

where M_{t+1} denotes the household's stochastic discount factor as defined above;¹²

2. the *equity risk premium channel*, which emerges from the Euler-equation for stock returns (i.e., households' optimality condition for equity shares):

$$P_t^E = \mathbb{E}_t [M_{t+1}(D_{t+1}^E + P_{t+1}^E)] ;$$

3. the *nominal upward pricing bias channel* as captured by firms' optimality condition for the nominal price (i.e. the nonlinear aggregate supply relation):

$$\phi_P \left(\frac{\Pi_t}{\Pi} - 1 \right) \frac{\Pi_t}{\Pi} = (1 - \theta_{\mu,t}) + \frac{\theta_{\mu,t}}{\mu_t} + \phi_P \mathbb{E}_t \left[M_{t+1} \frac{Y_{t+1}}{Y_t} \left(\frac{\Pi_{t+1}}{\Pi_{ss}} - 1 \right) \frac{\Pi_{t+1}}{\Pi_{ss}} \right] ;$$

4. the *inflation risk premium channel* related to the Fisherian equation:

$$1 = R_t \mathbb{E}_t \left[M_{t+1} \left(\frac{1}{\Pi_{t+1}} \right) \right] ;$$

5. the *investment adjustment channel*, which arises due to investment adjustment costs, connected to the firms' optimality condition for physical capital:

$$q_t = \mathbb{E}_t \left[M_{t+1} \left[R_{t+1}^K U_{t+1} + q_{t+1} \left[\left(1 - \delta(U_{t+1}) - \frac{\phi_K}{2} \left(\frac{I_{t+1}}{K_t} - \delta \right)^2 \right) + \phi_K \left(\frac{I_{t+1}}{K_t} - \delta \right) \frac{I_{t+1}}{K_t} \right] \right] \right] .$$

We conduct counterfactual exercises that solve the model with our proposed solution method, except that we linearize each Euler equation one at the time so to sterilize the effects of uncertainty shocks propagated through that specific channel. The results, presented in the paper, suggest that the nominal pricing bias channel is the crucial channel to generate larger responses of output, consumption, investment, and hours to an uncertainty shock in recessions than in expansions.

¹²For the definition of the variables the reader is referred to Section 2 of this Online Appendix.

Here we support our conclusion with a "reverse" counterfactual exercise, where only the nominal pricing bias channel is active in the model. Specifically, we linearize every model equation, including the intertemporal Euler equations above, but the equation connected to the nominal pricing bias channel, i.e., the nonlinear aggregate supply relation, and the nonlinear equation where the stochastic volatility shock hits, i.e., $a_{t+1} = \rho_a a_t + \sigma_{a,t} \epsilon_{a,t+1}$.¹³ For the modified solution, we calculate the differences in the impulse responses between recessions and expansions, and compare them with the baseline scenario where all channels are active. Results are shown in Figure 11. Most of the state-dependence in response to uncertainty shocks arises because of the nonlinear terms connected to the New Keynesian Phillips curve. Further, the bigger on-impact increase in prices during recessions than expansions is virtually all explained by these nonlinear terms. Hence, we draw the same conclusion as in the paper: the nominal pricing bias channel is the crucial channel to generate larger responses of real variables to an uncertainty shock in recessions than in expansions.

Finally, is the nominal pricing bias channel also important unconditionally, i.e., in affecting the overall magnitude of the impulse responses to uncertainty shocks, on top of being important for generating state-dependent dynamics? Figure 12 compares the baseline state-dependent impulse responses to the counterfactual state-dependent responses for the case where all uncertainty channels are active except for the nominal pricing bias channel. The results show that the upward pricing bias channel does not affect the overall magnitude of the impulse responses to uncertainty shocks but only its state-dependency.

¹³The last equation must be nonlinear to properly capture the real effects of uncertainty shocks. But the nonlinear terms connected to this equation do not generate any state-dependent dynamics to an uncertainty shock. Hence, by construction, any state-dependence found in this exercise is only generated by the nominal pricing bias channel.

Figure 11: New Keynesian Model: State-dependent role of the nominal pricing bias channel

For a positive one-standard deviation uncertainty shock, this figure shows the difference in the responses between recessions and expansions. The baseline case is when all channels for uncertainty shocks are present in the model. The counterfactual case is obtained by solving the model using a third-order approximation at the risky steady state with the modification that all the model equations are linearized but the nonlinear aggregate supply relation and the nonlinear equation where the stochastic volatility shock hits, i.e., $a_{t+1} = \rho_a a_t + \sigma_{a,t} \epsilon_{a,t+1}$. All responses are computed using the estimates for the New Keynesian model in column (1) of Table 3 of the paper.

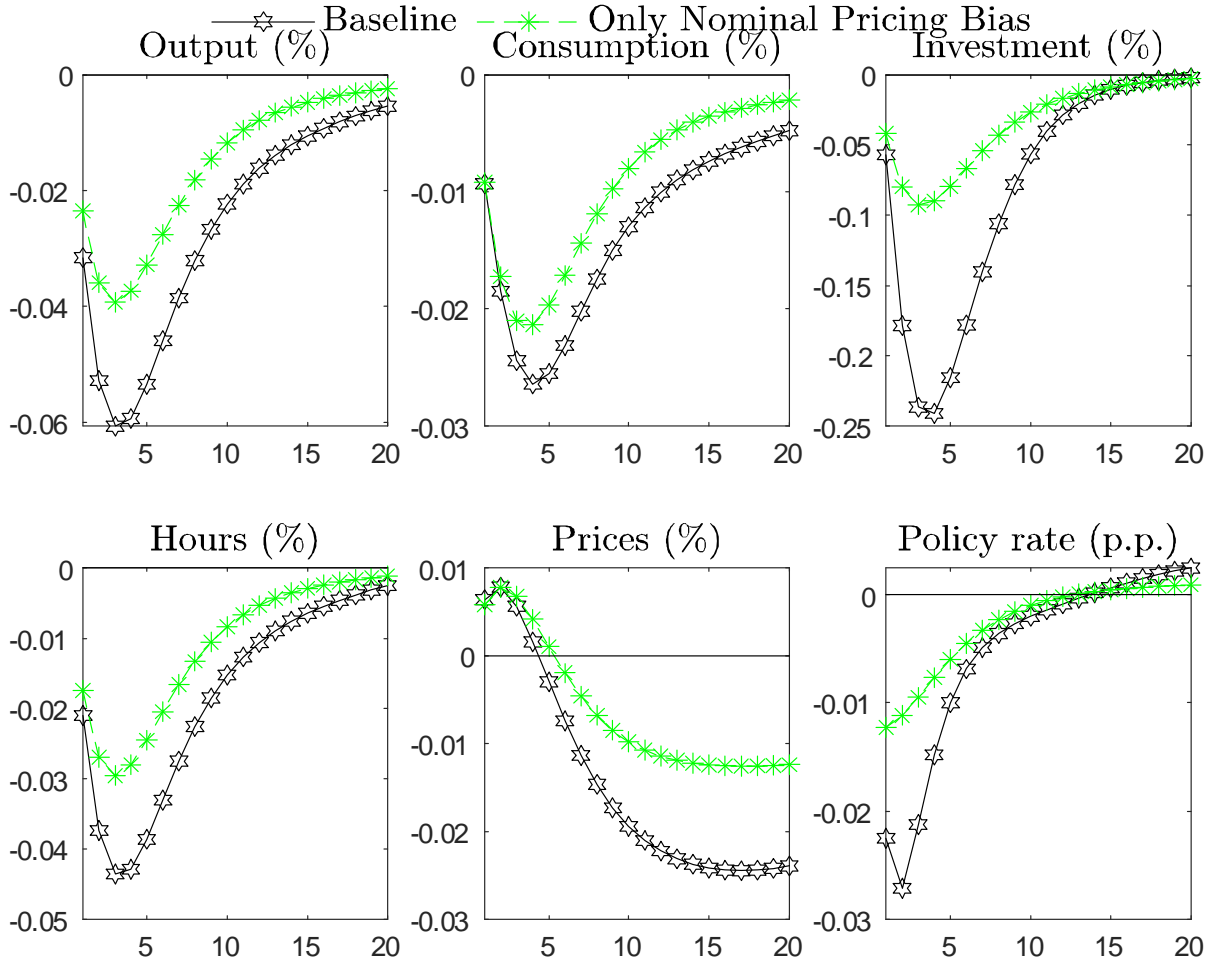
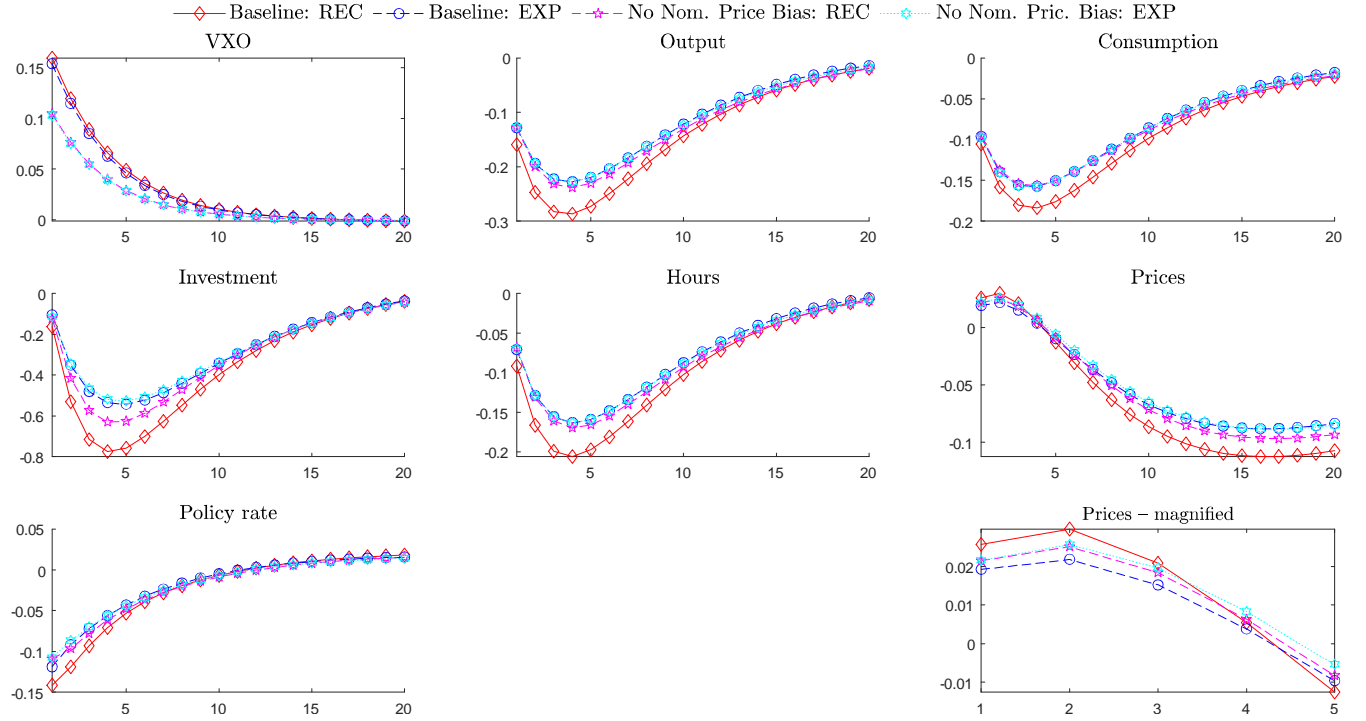


Figure 12: New Keynesian Model: Unconditional role of the nominal pricing bias channel

This figure shows the impulse response functions following a positive one-standard deviation uncertainty shock (i.e. $\epsilon_{\sigma,t} = 1$) in the New Keynesian model using the estimates in column (1) of Table 3 of the paper. The baseline case is when all channels for uncertainty shocks are present in the model. The nominal pricing bias channel is removed from this baseline by solving the model using a third-order approximation at the risky steady state with the modification that the nonlinear aggregate supply relation is only linearized. All responses are shown in percentage deviations, except for the policy rate where changes in percentage points are reported.



4.2 Exercise on the nonlinear expectation term of the Phillips curve

The nonlinear aggregate supply relation connected to the nominal pricing bias in our model is given by:

$$\phi_P \left(\frac{\Pi_t}{\Pi} - 1 \right) \frac{\Pi_t}{\Pi} = (1 - \theta_{\mu,t}) + \frac{\theta_{\mu,t}}{\mu_t} + \phi_P \mathbb{E}_t \left\{ M_{t+1} \frac{Y_{t+1}}{Y_t} \left(\frac{\Pi_{t+1}}{\Pi} - 1 \right) \frac{\Pi_{t+1}}{\Pi} \right\}, \quad (24)$$

where $\Pi_{t+1} = P_{t+1}/P_t$. Focusing on the expectation term, i.e.,:

$$TermE_t \equiv \mathbb{E}_t \left\{ M_{t+1} \frac{Y_{t+1}}{Y_t} \left(\frac{\Pi_{t+1}}{\Pi} - 1 \right) \frac{\Pi_{t+1}}{\Pi} \right\},$$

we have that, everything else equal, the more this expectation term will react to an uncertainty shock, the more firms will prudently bias their price decision upward after the shock.

We now assess which of the (nonlinear) terms of the expectation term is important for generating the state-dependent firms' upward price bias decision. Specifically, we perform an exercise where we replace the expectation term in the Phillips curve of the model with the following one:

$$\begin{aligned} TermE_t = & \gamma_2 \cdot \mathbb{E}_t \left\{ M_{t+1} \left(\frac{Y_{t+1}}{Y_t} \right)^{\gamma_1} \left(\frac{\Pi_{t+1}}{\Pi} - 1 \right) \frac{\Pi_{t+1}}{\Pi} \right\} + \\ & + (1 - \gamma_2) \cdot \mathbb{E}_t \left\{ M_{t+1} \left(\frac{Y_{t+1}}{Y_t} \right)^{\gamma_1} \left(\frac{\Pi_{t+1}}{\Pi} - 1 \right) \right\}, \end{aligned}$$

which, when $\gamma_1 = 1$ and $\gamma_2 = 1$, reduces to the baseline Phillips curve. Instead, when $\gamma_1 = 0$ we exclude the growth rate of output ($\frac{Y_{t+1}}{Y_t}$) from the expectation term, and when $\gamma_2 = 0$ we do not consider the quadratic term in expected inflation, i.e., we only consider $\left(\frac{\Pi_{t+1}}{\Pi} - 1 \right)$.

Figure 13 shows the results for the difference between state-conditional responses for four cases: baseline model (i.e., $\gamma_1 = 1$ and $\gamma_2 = 1$), no nonlinear terms in the Phillips curve (same case as in Figure 6 in the paper), no output growth term (i.e., $\gamma_1 = 0$ and $\gamma_2 = 1$), and no quadratic terms in expected inflation (i.e., $\gamma_1 = 1$ and $\gamma_2 = 0$). Two results can be drawn from the figure. First, the growth rate of output in the expectation term of the Phillips curve is not a determinant of the state-dependent responses, i.e., if we deviate from the baseline model by adopting $\gamma_1 = 0$ the results do not change with respect to baseline case. Second, the quadratic terms in expected inflation are the important driver behind the bigger increase in prices and larger contraction in economic activity that we observe in recessions compared to expansions following uncertainty shocks. Indeed, if we instead deviate from the baseline by adopting $\gamma_2 = 0$, then the bigger upward price bias in recession vanishes. In particular, the difference between state-dependent responses (and the same responses, not shown here) become very similar to the one obtained for the case when the Phillips curve is linearized, i.e., for the case when the nominal price bias is not active. Hence, the quadratic terms of expected inflation Π_{t+1} are the key terms in the Phillips curve to generate the state-dependent upward price bias.¹⁴

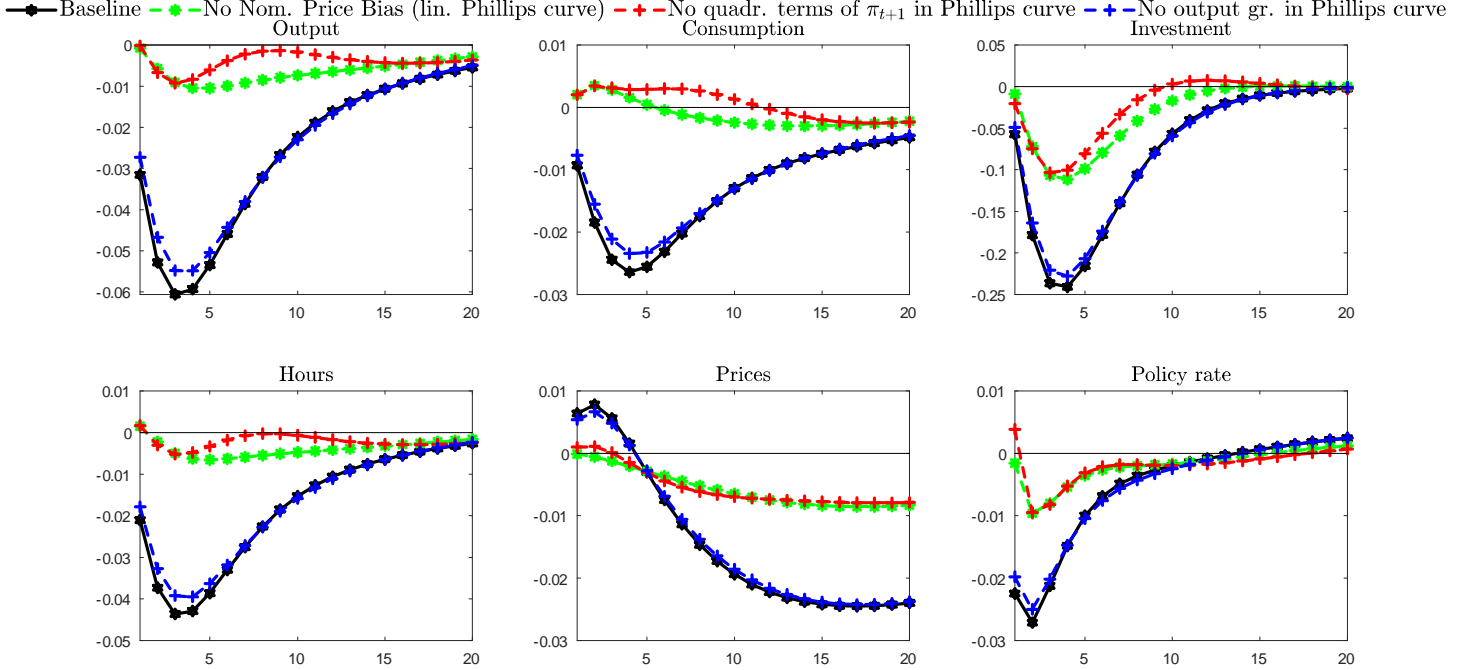
4.3 Upward pricing bias under Rotemberg price setting

In the paper we conclude that the higher the level of inflation volatility, the higher the upward price bias in today's price due to precautionary pricing behavior. But, why is inflation volatility $\mathbb{V}ar_t(\Pi_{t+1})$ important for determining today's price even under the Rotemberg price setting, i.e., in a setting in which firms can reset their prices in every period? In this subsection we show that it is because of the influence of today's price on future adjustment costs. Intuitively, higher inflation volatility translates into a higher future price level due to the asymmetry in the firm's profit function as explained by Fernández-Villaverde, Guerrón-Quintana, Kuester & Rubio-Ramírez (2015) and Born & Pfeifer (2020). But, the convex adjustment costs for changing prices imply that the firm, rather than just upward bias tomorrow's price, prefers to upward bias today's price to to upward bias tomorrow's price by less (and hence pay overall less discounted adjustment costs).

¹⁴We also performed an exercise to assess the role of the nonlinear terms of current inflation, at the left-hand side of the Phillips curve, but their neglectation does not reduce the state-dependent response of prices. This confirms that the nonlinear terms connected with expected inflation are the important ones for generating the state-dependent upward price bias.

Figure 13: New Keynesian Model: Role of the nonlinear terms of the Phillips curve

For a positive one-standard deviation uncertainty shock, this figure shows the difference in the responses between recessions and expansions. The baseline case is when all channels for uncertainty shocks are present in the model. The nominal pricing bias channel is removed from this baseline by solving the model using a third-order approximation at the risky steady state with the modification that the nonlinear aggregate supply relation is only linearized. The other cases considered in the figure are explained in the detail in the main text. All responses are computed using the estimates in column (1) of Table 3 of the paper for the New Keynesian model.



This intuition is confirmed by a simple inspection of the derivation of the aggregate Phillips curve under Rotemberg pricing (equation 24). The aggregate Phillips curve is the firm’s optimality condition for today’s price evaluated in equilibrium (its derivation is available in Section 2.2 of this Appendix). The only reason why tomorrow’s price appears in the firm’s optimality condition for today’s price is because of the influence of today’s price on tomorrow’s adjustment costs.¹⁵ By contrast, in the absence of Rotemberg adjustment costs, the Phillips curve will not contain tomorrow’s price in the optimality condition (and it would make sense, as the firm – differently than Calvo pricing – can reset its price in every period). We next illustrate this point in a stylized example.¹⁶

¹⁵Recall that the dynamic optimization problem of firm indexed by i is the following:

$$\begin{aligned}
 & \underset{N_t(i), U_t(i), K_{t+1}(i), P_t(i) \forall t > 0}{Max} \mathbb{E}_t \sum_{s=0}^{\infty} M_{t+s} \left[\left[\frac{P_{t+s}(i)}{P_{t+s}} \right]^{1-\theta} \mu_{t+s} Y_{t+s} - W_{t+s} N_{t+s}(i) - I_{t+s}(i) - \frac{\phi_P}{2} \left(\frac{P_{t+s}(i)}{\Pi P_{t-1+s}(i)} - 1 \right)^2 Y_{t+s} \right] \\
 \text{s.t. } & \left[\frac{P_t(i)}{P_t} \right]^{-\theta} Y_t = [K_t(i) U_t(i)]^\alpha [Z_t N_t(i)]^{1-\alpha} - \Phi \\
 & \& K_{t+1}(i) = \left(1 - \delta(U_t(i)) - \frac{\phi_K}{2} \left(\frac{I_t(i)}{K_t(i)} - \delta \right)^2 \right) K_t(i) + I_t(i),
 \end{aligned}$$

The first-order condition for $P_t(i)$ is at the basis of the Phillips curve. It can be seen that Rotemberg adjustment costs also make yesterday’s price important for determining today’s price. This introduces state-dependence in the price decision.

¹⁶Oh (2020) provides simulations for Rotemberg vs. Calvo pricing that show that the upward pricing bias is more potent under Calvo pricing. On the basis of steady state aggregate considerations, he also finds that under Rotemberg pricing (of the form we are using) there is no upward pricing bias. We show that outside of steady state (when adjustment costs are present) also Rotemberg pricing implies an aggregate upward

Consider the following problem of the representative firm, which generalizes the problem considered in Fernández-Villaverde et al. (2015) and Born & Pfeifer (2020) to the case of two periods and to the presence of adjustment costs. Consider a firm living for two periods, today (t) and tomorrow ($t + 1$), subject to Rotemberg adjustment costs. Suppose also, without loss of generality, that the firm is initially in steady state with inflation $\Pi = 1$ when an *ex-ante* mean-preserving spread (uncertainty) shock regarding tomorrow aggregate price level realizes (today's aggregate price level is assumed certain, i.e. $P_t = 1$). Suppose that the firm sets prices at the beginning of each period, i.e., the firm will have to set tomorrow's price before tomorrow's uncertainty is resolved. For simplicity, assume two equally-likely states of the world in $t + 1$, so that the firm expects an aggregate price of either $P_{t+1} = P_t + \sigma$ or $P_{t+1} = P_t - \sigma$ with 50% probability each, where σ denotes the standard deviation of the realizations of tomorrow's price level, or $\sigma = \sqrt{\text{Var}_t(P_{t+1})}$. We have that $\mathbb{E}_t(P_{t+1}) = P_t$. Real firm's profits of period t are given by $\pi_t = \left(\frac{P_t(i)}{P_t} - MC(i)\right) \left(\frac{P_t(i)}{P_t}\right)^{-\theta_\mu} Y - \frac{\phi_P}{2} \left(\frac{P_t(i)}{P_{t-1}(i)} - 1\right)^2 Y$, where $MC(i)$ denotes the firm's real marginal costs and Y denotes real aggregate output. We further assume that there is neither growth nor other shocks affecting real quantities, meaning that $MC_t(i) = MC_{t+1}(i) = MC(i)$ and $Y_t = Y_{t+1} = Y$. Hence, we only focus on uncertainty over the price level because it is the only variable with respect to which the profit function is asymmetric, and hence it is the only variable for which future uncertainty matters. For simplicity, we also assume that the firm discounts future profits with the discount rate β . Hence, to determine today's price $P_t(i)$ and tomorrow's price $P_{t+1}(i)$, the firm solves the following intertemporal problem:

$$\begin{aligned} & \text{Max}_{P_t(i), P_{t+1}(i)} \left(\frac{P_t(i)}{P_t} \right)^{1-\theta_\mu} Y - MC(i) \left(\frac{P_t(i)}{P_t} \right)^{-\theta_\mu} Y - \frac{\phi_P}{2} \left(\frac{P_t(i)}{P_{t-1}(i)} - 1 \right)^2 Y + \\ & + \beta \left\{ \begin{array}{l} 0.5 \left[\left(\frac{P_{t+1}(i)}{P_t + \sigma} \right)^{1-\theta_\mu} Y - MC(i) \left(\frac{P_{t+1}(i)}{P_t + \sigma} \right)^{-\theta_\mu} Y \right] + \\ 0.5 \left[\left(\frac{P_{t+1}(i)}{P_t - \sigma} \right)^{1-\theta_\mu} Y - MC(i) \left(\frac{P_{t+1}(i)}{P_t - \sigma} \right)^{-\theta_\mu} Y \right] + \\ - \frac{\phi_P}{2} \left(\frac{P_{t+1}(i)}{P_t(i)} - 1 \right)^2 Y \end{array} \right\}, \end{aligned}$$

where the variables follows the same notation of Section 2 above.

The firm's optimality condition for $P_t(i)$ can be shown to be the following:

$$\begin{aligned} \phi_P \left(\frac{P_t(i)}{P_{t-1}(i)} - 1 \right) \frac{P_t}{P_{t-1}(i)} &= (1 - \theta_\mu) \left[\frac{P_t(i)}{P_t} \right]^{-\theta_\mu} + MC(i) \cdot \theta_\mu \left[\frac{P_t(i)}{P_t} \right]^{-\theta_\mu - 1} \\ &+ \beta \phi_P \left\{ \left(\frac{P_{t+1}(i)}{P_t(i)} - 1 \right) \frac{P_{t+1}(i)}{P_t(i)} \frac{P_t}{P_t(i)} \right\}, \end{aligned} \quad (25)$$

which evaluated in equilibrium is just a simplified version of our Phillips curve (recall, indeed, that we have $1/\mu_t = MC_t$):

$$\phi_P \left(\frac{P_t}{P_{t-1}} - 1 \right) \frac{P_t}{P_{t-1}} = (1 - \theta_\mu) + MC \cdot \theta_\mu + \beta \phi_P \left\{ \left(\frac{P_{t+1}}{P_t} - 1 \right) \frac{P_{t+1}}{P_t} \right\}.$$

The firm's optimality condition for $P_{t+1}(i)$ is

$$\begin{aligned} & \beta 0.5 \left[(1 - \theta_\mu) \left(\frac{P_{t+1}(i)}{P_t + \sigma} \right)^{-\theta_\mu} \frac{Y}{P_t + \sigma} + MC(i) \theta_\mu \left(\frac{P_{t+1}(i)}{P_t + \sigma} \right)^{-\theta_\mu - 1} \frac{Y}{P_t + \sigma} \right] \\ & + \beta 0.5 \left[(1 - \theta_\mu) \left(\frac{P_{t+1}(i)}{P_t - \sigma} \right)^{-\theta_\mu} \frac{Y}{P_t - \sigma} + MC(i) \theta_\mu \left(\frac{P_{t+1}(i)}{P_t - \sigma} \right)^{-\theta_\mu - 1} \frac{Y}{P_t - \sigma} \right] \\ & - \phi_P \left(\frac{P_{t+1}(i)}{P_t(i)} - 1 \right) \frac{Y}{P_t(i)} \\ & = 0 \end{aligned}$$

pricing bias in presence of higher inflation volatility. A simple second-order approximation of the NKPC (available upon request) is enough to show that this is indeed one of the implications of the model we are adopting.

↕

$$\begin{aligned}
& \phi_P (P_{t+1}(i) - P_t(i)) \\
= & \beta 0.5 \left[(1 - \theta_\mu) \left(\frac{P_{t+1}(i)}{P_t + \sigma} \right)^{-\theta_\mu} \frac{1}{P_t + \sigma} + MC(i) \theta_\mu \left(\frac{P_{t+1}(i)}{P_t + \sigma} \right)^{-\theta_\mu - 1} \frac{1}{P_t + \sigma} \right] \\
& + \beta 0.5 \left[(1 - \theta_\mu) \left(\frac{P_{t+1}(i)}{P_t - \sigma} \right)^{-\theta_\mu} \frac{1}{P_t - \sigma} + MC(i) \theta_\mu \left(\frac{P_{t+1}(i)}{P_t - \sigma} \right)^{-\theta_\mu - 1} \frac{1}{P_t - \sigma} \right]
\end{aligned}$$

↕

$$P_{t+1}(i) = P_t(i) + \frac{\beta}{\phi_P} 0.5 \left[(1 - \theta_\mu) \left(\frac{P_{t+1}(i)}{P_t + \sigma} \right)^{-\theta_\mu} \frac{1}{P_t + \sigma} + MC(i) \theta_\mu \left(\frac{P_{t+1}(i)}{P_t + \sigma} \right)^{-\theta_\mu - 1} \frac{1}{P_t + \sigma} \right]$$

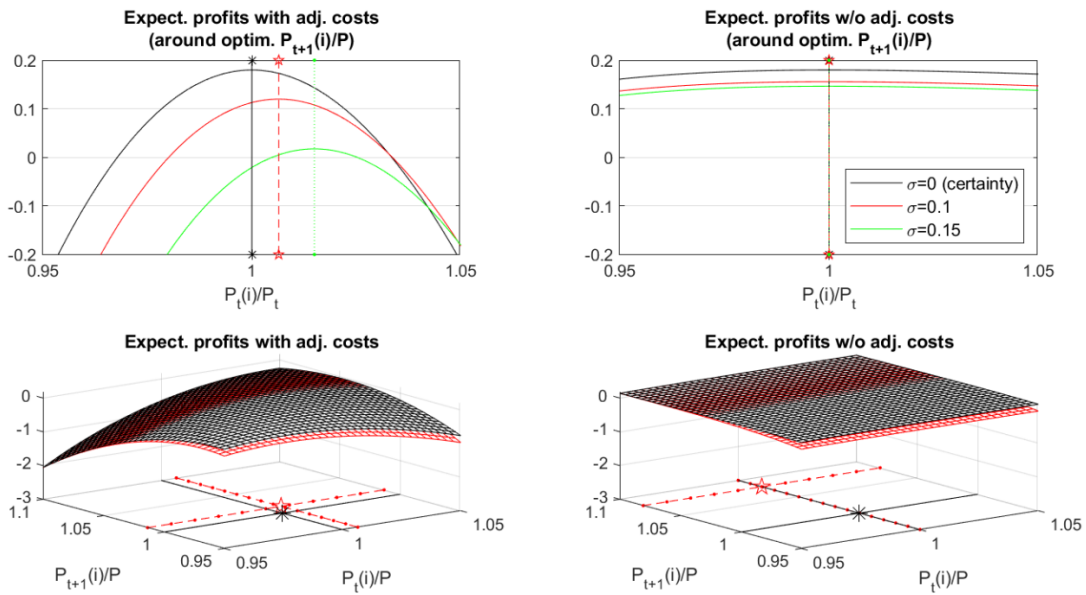
The previous equation confirms that this stylized two-period firm's problem has aggregate implications very similar to the firm's price-setting problem in our DSGE model. It also confirms that tomorrow's optimal price matters when deciding today's price. In solving the previous firm's problem we use the following parameters: $\beta = 0.98$, $\theta_\mu = 11$ (implying a 10% markup), $\phi_P = 163.3$ (our estimate), $\mathbb{E}_t(P_{t+1}) = P_t = P = 1$, and, for simplicity, $Y = 1$.¹⁷

Figure 14 upper panels plot firm's expected profit function and optimal today's price – i.e., the function maximum – given optimal tomorrow's price for both the cases of certainty ($\sigma = 0$) and uncertainty ($\sigma = 0.1$ or $\sigma = 0.15$) over tomorrow's aggregate price, and for the cases of Rotemberg adjustment costs ($\phi_P = 163.3$, left panels) or no adjustment costs ($\phi_P = 0$, right panels). Several conclusions can be drawn. First, the lifetime profit function is asymmetric in $\frac{P_t(i)}{P}$ only when Rotemberg adjustment costs are present. Second, this asymmetry implies an upward price bias in today's price only when Rotemberg adjustment costs are present. Third, the lifetime profit function is asymmetric in $\frac{P_{t+1}(i)}{P}$ with or without adjustment costs. This can be seen from the lower panels of Figure 14, which represent the lifetime expected profit function over today's and tomorrow's prices. Tomorrow's price is upward biased as the price is set before uncertainty is resolved and because the generic period profit function, $\left(\frac{P(i)}{P}\right)^{1-\theta_\mu} Y - MC(i) \left(\frac{P(i)}{P}\right)^{-\theta_\mu} Y$, is asymmetric in $\frac{P(i)}{P}$ (Fernández-Villaverde et al. (2015) and Born & Pfeifer (2020)). Fourth, Rotemberg adjustment costs introduce a trade-off in the price-setting firm's decision. Indeed, as it is evident from the lower panels of Figure 14, under Rotemberg pricing the firm prefers to upward bias today's price so that to upward bias by less tomorrow's price with respect to a situation without the convex adjustment costs. In other words, in a multiperiod context, after an (ex-ante) uncertainty shock firms find it optimal to set higher prices today (than in absence of uncertainty) not to be forced to raise their prices too much in the future, i.e., they smooth their upward price bias over time. Fifth, as the upper panels document, the bigger the variance over future prices, σ^2 , the bigger the upward price bias in today's price. This confirms that expected inflation variance is important for today's price setting. Provided that expected inflation variance is higher in recessions than in expansions in our model, this explains why our model predicts a bigger upward price bias in response to an uncertainty shock during recessions.

¹⁷Since the firm is initially in steady state with inflation $\Pi = 1$, we also have that period $t-1$ firm's price is equal to the steady state aggregate price, i.e., $P_{t-1}(i) = P_{t-1} = P_t = 1$.

Figure 14: Asymmetric profit function: Upward pricing bias under ex-ante uncertainty and Rotemberg price setting

This figure shows the solution of the firm’s problem outlined in the Section 4.3 for the parameters values indicated in the same Section. The upper panels plot firm’s expected profit function and optimal today’s price – i.e., the function maximum – given optimal tomorrow’s price for both the cases of certainty ($\sigma = 0$) and uncertainty ($\sigma = 0.1$ or $\sigma = 0.15$), and for the cases of Rotemberg adjustment costs ($\phi_P = 163.3$, left panels) or no adjustment costs ($\phi_P = 0$, right panels). Vertical lines represent optimal prices. The lower panels represent the lifetime expected profit function over today’s and tomorrow’s prices. Optimal today’s and tomorrow’s prices by the intersection of straight lines and are indicated with stars/asterisks.

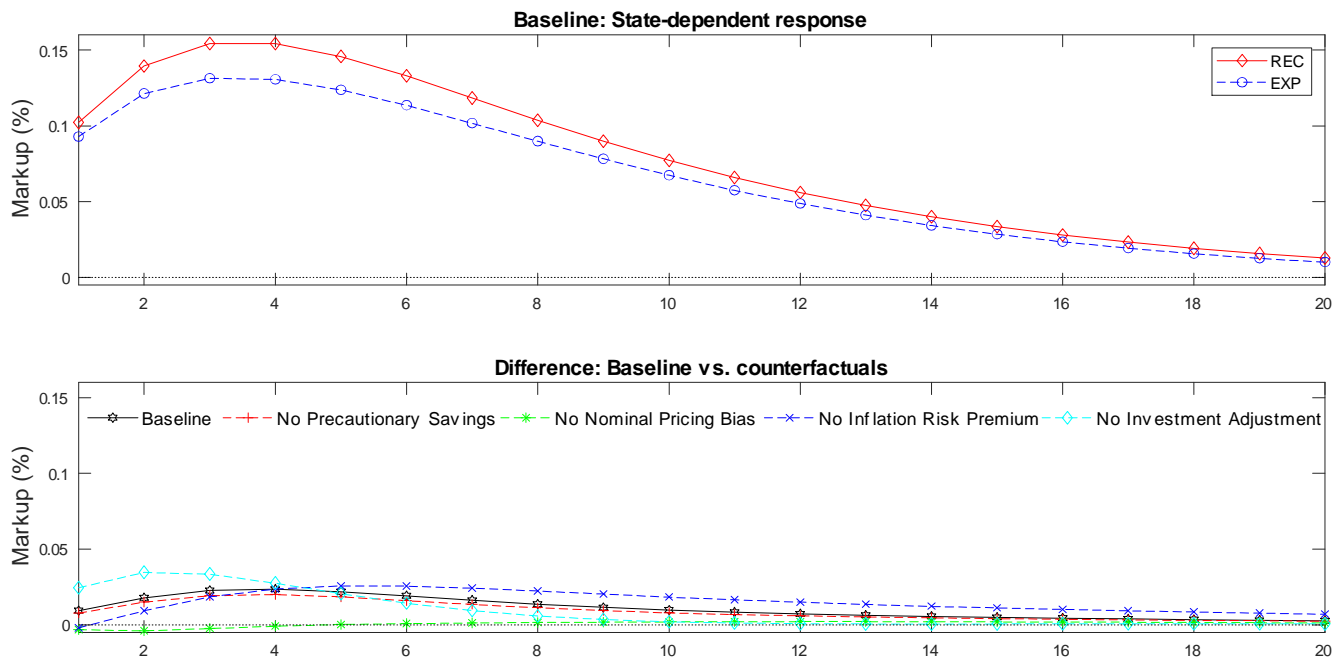


4.4 Counterfactual exercises on the drivers of the state-dependent response of the markup

We here present an additional result for Section 6.3 of the paper. We show that the only channel that eliminates the state-dependent response of the markup to an uncertainty shock is the nominal upward pricing bias channel. Results are shown in Figure 15. The upper chart in Figure 15 shows the baseline state-dependent response of the markup to an uncertainty shock. The lower chart shows the baseline difference in the impulse responses between recessions and expansions and puts it in comparison with the corresponding differences for the case we omit one at a time the uncertainty channels in the model. These results further support the importance of the nominal upward pricing bias channel in generating the stronger real effects of uncertainty shocks in recessions than expansions.

Figure 15: New Keynesian Model: Role of the uncertainty channels for the state-dependent markup response

For a positive one-standard deviation uncertainty shock, this figure shows in the upper panel the baseline state-dependent responses and in the lower panel the difference in the responses between recessions and expansions. The baseline case is when all channels for uncertainty shocks are present in the model. A given channel is removed from this baseline by solving the model using a third-order approximation at the risky steady state with the modification that the Euler-equation for a particular channel is only linearized. All responses are computed using the estimates in column (1) of Table 3 of the paper for the New Keynesian model.



References

- Adrian, T., Boyarchenko, N. & Giannone, D. (2019), ‘Vulnerable growth’, *American Economic Review* **109**(4), 1263–89.
- Alfaro, I., Bloom, N. & Lin, X. (2019), ‘The finance uncertainty multiplier’, **available at <https://nbloom.people.stanford.edu/research>**.
- Andreasen, M. M. (2012), ‘On the Effects of Rare Disasters and Uncertainty Shocks for Risk Premia in Non-Linear DSGE Models’, *Review of Economic Dynamics* **15**(3), 295–316.
- Arellano, C., Bai, Y. & Kehoe, P. J. (2019), ‘Financial markets and fluctuation in volatility’, *Journal of Political Economy* **forthcoming**.
- Basu, S. & Bundick, B. (2017), ‘Uncertainty shocks in a model of effective demand’, *Econometrica* **85**(3), 937–958.
- Basu, S. & Bundick, B. (2018), ‘Uncertainty shocks in a model of effective demand: Reply’, *Econometrica* **86**(4), 1527–1531.
- Bauer, M. D. & Rudebusch, G. D. (2016), ‘Monetary Policy Expectations at the Zero Lower Bound’, *Journal of Money, Credit and Banking* **48**(7), 1440–1465.
- Berge, T. J. & Jordà, Ò. (2011), ‘Evaluating the Classification of Economic Activity into Recessions and Expansions’, *American Economic Journal: Macroeconomics* **3**, 246–277.
- Binning, A. (2013), ‘Solving Second and Third-Order Approximations to DSGE Models: A Recursive Sylvester Equation Solution’, *Norges Bank, Working Paper 18*.
- Bloom, N. (2009), ‘The impact of uncertainty shocks’, *Econometrica* **77**(3), 623–685.
- Bloom, N. (2014), ‘Fluctuations in uncertainty’, *Journal of Economic Perspectives* **28**(2), 153–176.
- Born, B. & Pfeifer, J. (2020), ‘Uncertainty-driven business cycles: assessing the markup channel’, *Quantitative Economics* **forthcoming**.
- Caggiano, G., Castelnuovo, E., Colombo, V. & Nodari, G. (2015), ‘Estimating fiscal multipliers: News from a nonlinear world’, *Economic Journal* **125**(584), 746–776.
- Christiano, L. J., Eichenbaum, M. & Evans, C. (1999), ‘Monetary policy shocks: What have we learned and to what end?’, **In: J.B. Taylor and M. Woodford (eds.): Handbook of Macroeconomics, Elsevier Science**, 65–148.
- Collard, F. & Juillard, M. (2001a), ‘A Higher-Order Taylor Expansion Approach to Simulation of Stochastic Forward-Looking Models with an Application to a Nonlinear Phillips Curve Model’, *Computational Economics* **17**(2-3), 125–139.
- Collard, F. & Juillard, M. (2001b), ‘Accuracy of Stochastic Perturbation Methods: The Case of Asset Pricing Models’, *Journal of Economic Dynamic and Control* **25**(6-7), 979–999.
- Fernández-Villaverde, J., Guerrón-Quintana, P., Kuester, K. & Rubio-Ramírez, J. F. (2015), ‘Fiscal volatility shocks and economic activity’, *American Economic Review* **105**(11), 3352–3384.
- Fry, R. & Pagan, A. (2011), ‘Sign restrictions in structural vector autoregressions: A critical review’, *Journal of Economic Literature* **49**(4), 938–960.
- Furlanetto, F., Ravazzolo, F. & Sarferaz, S. (2019), ‘Identification of financial factors in economic fluctuations’, *Economic Journal* **129**, 311–337.
- Gilchrist, S., Sim, J. W. & Zakrajšek, E. (2014), ‘Uncertainty, financial frictions, and investment dynamics’, **Boston University and Federal Reserve Board of Governors, mimeo**.

- Gilchrist, S. & Zakrajšek, E. (2012), ‘Credit spreads and business cycle fluctuations’, *American Economic Review* **102**(4), 1692–1720.
- Kilian, L. & Vigfusson, R. (2011), ‘Are the responses of the u.s. economy asymmetric in energy price increases and decreases?’, *Quantitative Economics* **2**, 419–453.
- Klein, P. (2000), ‘Using the generalized schur form to solve a multivariate linear rational expectations model’, *Journal of Economic Dynamic and Control* **24**, 1405–1423.
- Koop, G., Pesaran, M. & Potter, S. (1996), ‘Impulse response analysis in nonlinear multivariate models’, *Journal of Econometrics* **74**(1), 119–147.
- Krippner, L. (2020), ‘A Note of Caution on Shadow Rate Estimates’, *Journal of Money, Credit and Banking* **52**(4), 951–962.
- Ludvigson, S. C., Ma, S. & Ng, S. (2019), ‘Uncertainty and business cycles: Exogenous impulse or endogenous response?’, *American Economic Journal: Macroeconomics* **forthcoming**.
- Oh, J. (2020), ‘The propagation of uncertainty shocks: Rotemberg versus Calvo’, *International Economic Review* **61**(3), 1097–1113.
- Rotemberg, J. J. (1982), ‘Monopolistic price adjustment and aggregate output’, *Review of Economic Studies* **49**, 517–531.
- Salgado, S., Guvenen, F. & Bloom, N. (2019), ‘Skewed Business Cycles’, *NBER Working Paper* (No. 26565).
- Schmitt-Grohé, S. & Uribe, M. (2004), ‘Solving Dynamic General Equilibrium Models Using a Second-Order Approximation to the Policy Function’, *Journal of Economic Dynamics and Control* **28**(4), 755–775.
- Swanson, E. (2012), ‘Risk aversion and the labor margin in dynamic equilibrium models’, *Working Paper version* .
- Swanson, E. T. (2018), ‘Risk Aversion, Risk Premia, and the Labor Margin with Generalized Recursive Preferences’, *Review of Economic Dynamics* **28**, 290–321.
- Wu, J. C. & Xia, F. D. (2016), ‘Measuring the macroeconomic impact of monetary policy at the zero lower bound’, *Journal of Money, Credit, and Banking* **48**(2-3), 253–291.